Kinetic studies on the reaction of formaldehyde with amines in the presence of sulfite

Kathryn Helen Brown

Kinetic Studies on the Reaction of Formaldehyde with Amines in the Presence of Sulfite

Kathryn Helen Brown

Thesis submitted for the qualification Doctor of Philosophy

University of Durham, Chemistry Department

October 1999

ABSTRACT

The reaction of formaldehyde with amines with and without sulfite has been studied using anilines ($RC_6H_4NH_2$) and benzylamines ($RC_6H_4CH_2NH_2$). Reaction with anilines is known to produce aminomethanesulfonates, $RC_6H_4NHCH_2SO_3^-$, which are industrially important in the azo dye industry. The kinetics and mechanism of formation of $RC_6H_4NHCH_2SO_3^-$ and $RC_6H_4CH_2NHCH_2SO_3^-$ have been studied: rate constants are quoted for the individual reaction steps in addition to the overall reaction.

The reaction of formaldehyde, HCHO, with the amine, RNH_2, gives an *N*-(hydroxymethyl)amine, $RNHCH_2OH$, via a zwitterionic intermediate. Rate constants of 8.0×10^3 to 4.3×10^6 dm^3 mol^{-1} s^{-1} have been obtained. $RNHCH_2OH$ then dehydrates in acidic conditions or loses hydroxyl ion to form an iminium ion, $[RNH{=}CH_2]^+$. This then reacts rapidly with sulfite ions to yield the product. The rate determining step was found to depend on the pH of the reaction. At low and neutral pH the reaction of HCHO with RNH_2 is the rate determining step. At high pH the rate determining step becomes dehydration of $RNHCH_2OH$ to give $[RNH{=}CH_2]^+$.

Hydroxymethanesulfonate, $CH_2(OH)(SO_3Na)$, was used to introduce HCHO and sulfite, SO_3^{2-}, into the system. This must undergo decomposition initially to yield reactive free HCHO. Above pH 3 decomposition occurs mainly through the dianion, $CH_2(O^-)(SO_3^-)$. Below pH 3, decomposition through the monoanion, $CH_2(OH)(SO_3^-)$ forms the major pathway: this may become the rate determining step in the overall reaction at low pH. Rate constants for decomposition equal to 24 ± 5 s^{-1} and 2.3×10^{-8} s^{-1} have been obtained for the dianion and monoanion respectively.

pK_a values in the range 4.9 to 5.6 have been measured for protonated adducts, $RN^+H_2CH_2SO_3^-$, formed from benzylamines. With benzylamines, reaction with another molecule of $CH_2(OH)(SO_3Na)$ can occur to produce $RN(CH_2SO_3^-)_2$ in addition to $RNHCH_2SO_3^-$.

Polymerisation of imines has also been studied: cyclic trimers and 1 : 2 HCHO : RNH_2 adducts have been synthesised.

CONTENTS

ACKNOWLEDGEMENTS

I would like to thank my supervisor, Dr. Mike Crampton, for always being so interested and willing to help. I would also like to mention my industrial supervisor, Dr. John Atherton, from Avecia, formerly Zeneca Specialities, who has made my work seem important, if only to me.

I am going to miss the rest of the lab; Linda 'Gibbo' Gibbons, Darren 'Sticky Baan' Noble, Lynsey 'Brown Owl' Rabbitt, Colin 'CG' Greenhalgh, Paul Coupe, Andy 'Taffy' Munro and also Ian 'Are You Winnin' Robotham. All I can say is it is a straight line and I didn't break it.

Finally I would especially like to thank the people without whom none of this would be worthwhile: my Mum and Dad, Tony, and my sisters Susan and Gillian.

DECLARATION

The work in this thesis was carried out in the Chemistry Department at the University of Durham between 1st October 1996 and 30th September 1999. It has not been submitted for any other degree and is the author's own work, except where acknowledged by reference.

COPYRIGHT

DEFINITIONS

HMS	hydroxymethanesulfonate, $CH_2(OH)(SO_3Na)$
HSO_3^-	bisulfite ion
SO_3^{2-}	sulfite ion
HCHO	free formaldehyde
$CH_2(OH)_2$	methylene glycol
$HCHO_{(aq)}$	aqueous formaldehyde solution, HCHO + $CH_2(OH)_2$
RNH_2	primary amine
N-(hydroxymethyl)amine	carbinolamine $R'NH_2CR_2OH$ where $R_2 = H_2$
S(IV)	sum contribution of bisulfite and sulfite ions
$S(IV)_\tau$	sum contribution of bisulfite and sulfite ions, $SO_2.H_2O$, and all other species with the sulfur in the + 4 oxidation state, such as in metal complexes
trimer	1,3,5-triphenyl-1,3,5-hexahydrotriazine
1 : 1 adduct	$RNR'CH_2SO_3^-$
1 : 2 adduct	$RN(CH_2SO_3^-)_2$
KH_2PO_4	potassium dihydrogen phosphate
KCl	potassium chloride
NaOH	sodium hydroxide
HCl	aqueous hydrochloric acid
CH_3COOH	acetic acid
CH_3COONa	aqueous sodium acetate
$Na_2B_4O_7.10H_2O$	borax
$COOH.C_6H_4.COOK$	potassium hydrogen phthalate
aqueous iodine solution	$I_2 + I_3^- + I^-$ species
$[I_2]_\tau$	$[I_2] + [I_3^-]$
ISO_3^-	iodosulfate
OH^-	hydroxide ion
H^+	hydrogen ion or proton
$[X]_{stoich}$	stoichiometric concentration of X
pH	$-\log_{10}[H^+]$
pK_i	$-\log_{10}K_i$
K_a	acid dissociation constant
K	equilibrium constant

k	rate constant
M	mol dm^{-3}
T	temperature
I	ionic strength
uv	ultraviolet
vis	visible
λ / nm	wavelength / nanometres
λ_{max}	wavelength of peak maximum
A	absorbance
ΔA	change in absorbance
A_∞	absorbance at reaction completion
ε	extinction coefficient
σ	Hammett substituent parameter
ρ	Hammett reaction parameter
^1H NMR	proton nuclear magnetic resonance
D_2O	deuterium oxide
CD_3OD	methyl-d_3 alcohol-d
CD_3CN	d_3-acetonitrile
d_6-DMSO	d_6-dimethyl sulfoxide
δ / ppm	chemical shift / parts per million
J / Hz	coupling constant / hertz
s	singlet
d	doublet
t	triplet
m	multiplet

CHAPTER 1

Introduction

CHAPTER 1: Introduction

1.1 BACKGROUND

Condensation reactions involving formaldehyde, an amine and a nucleophile, HZ, (Scheme 1.1) are potentially useful in commercial synthetic processes.

Scheme 1.1: $RNH_2 + HCHO + HZ \longrightarrow RNHCH_2Z + H_2O$

Examples include the Mannich reaction, where HZ is a compound with an acidic hydrogen, and the Strecker synthesis, where cyanide is the nucleophile.

There have been extensive studies on the reactions of amines with carbonyl compounds. However there has been little study on the kinetics and mechanisms of reactions of the type shown in Scheme 1.1, namely those involving formaldehyde, an amine and a nucleophile. This is the focus of the work here.

1.2 REACTIONS OF CARBONYL COMPOUNDS WITH AMINES

Carbonyl addition reactions involve the attack of a lone pair of electrons of a nucleophilic reagent on the carbon atom of a carbonyl group. The strong electronegativity of the oxygen polarises the double bond and leaves a partial positive charge on the carbon atom, facilitating nucleophilic attack. The attacking nucleophile approaches the carbonyl carbon perpendicular to the plane of the carbonyl group. The carbon atom of the planar carbonyl group has sp^2 hybridisation with 120° bond angles. As addition occurs, it undergoes a change in hybridisation to sp^3 and becomes tetrahedral. Steric, resonance, and inductive effects determine the rate of reaction and equilibrium constant for addition of a nucleophile to a carbonyl group.

The reactions of ketones and aldehydes with amines have been reviewed by a number of authors.[1] The products of reaction depend on whether the amine is primary, RNH_2, secondary, RR'NH, or tertiary, RR'R''N.

1.2.1 Primary amines

The reaction of a primary amine with a carbonyl compound produces an imine,[2] with the general formula RR'C=NR". The overall reaction involves nucleophilic attack by the primary amine on the carbonyl group to give a carbinolamine,[3] $RNHCR_2OH$ (**1**, Scheme 1.2). Dehydration then produces an imine, **2**.

Scheme 1.2:

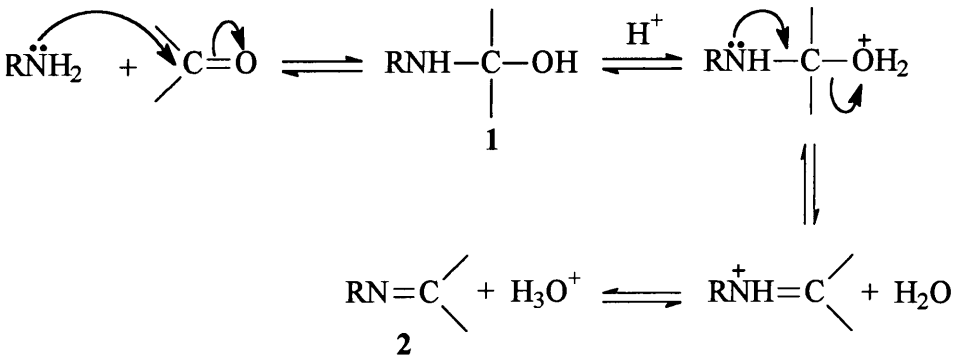

The reaction to form the carbinolamine is favourable: in concentrated solutions, virtually all of the carbonyl compound is converted to the carbinolamine.[1c] The pK_a and steric properties of the amine are principal factors in determining the equilibrium constant[4] for carbinolamine formation. The equilibrium constant[3a] for reaction of aniline with formaldehyde, HCHO, is 4.5×10^4 mol^{-1} dm^3 at 25 °C, 1.0 M ionic strength.

The pK_a of a carbinolamine is 2 to 3 pH units lower than that of the corresponding amine.[5] This has been attributed primarily to the decrease in solvation brought about by the replacement of a hydrogen atom by a hydroxymethyl group.

Imines are involved in a large number of enzymatic reactions[6] and are also thought to be important in reactions involved with the visual pigment rhodopsin.[7]

The mechanism of imine formation is discussed in detail in Section 1.3.2.

1.2.2 Secondary amines

Addition of a secondary amine to a carbonyl group gives a carbinolamine and expulsion of the hydroxyl group yields an iminium ion,[8] RR'C=N$^+$R"R'". If there is a hydrogen present on an α-carbon, elimination of this proton will yield an enamine[9] (**3**, Scheme 1.3).

Scheme 1.3:

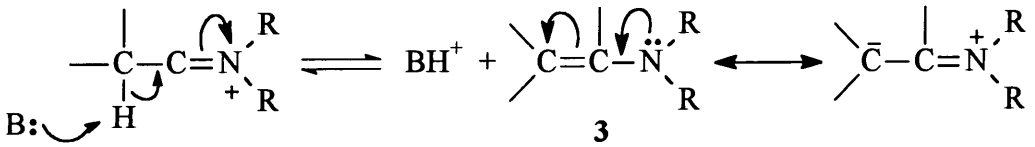

3

Imines with α-hydrogens are capable of imine - enamine tautomerism[10] (Scheme 1.4). However the imine is generally the more stable form.

Scheme 1.4:

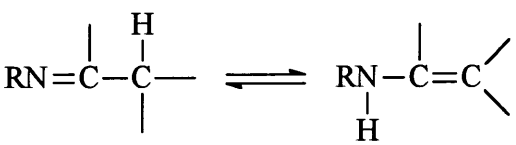

1.2.3 Tertiary amines

Addition of a tertiary amine to a carbonyl group gives an unstable ionic carbinolamine which normally reverts back to the reactants. Exceptions are where the amine and carbonyl group are in the same molecule and form a thermodynamically stable ring system, such as a six membered ring.[11]

1.3 IMINES

1.3.1 Nomenclature

Imine is the general name given to compounds containing a carbon – nitrogen double bond, C=N. Various conventions have been used in the literature to denote compounds

containing a C=N bond depending on the groups attached to the carbon and nitrogen. Table 1.1 summarises some of the terms used. Imines are often generally referred to as Schiff bases, as the reaction of aldehydes and ketones with amines was first published by Schiff[12] in 1864.

Table 1.1: Nomenclature of RR'C=NR" compounds

term	R	R'	R"
Schiff base†	aryl	H	alkyl or aryl
azomethine	aryl	H	aryl
aldimine	alkyl or aryl	H	alkyl, aryl or H
ketimine	alkyl or aryl	alkyl or aryl	alkyl, aryl or H
anil	alkyl, aryl or H	alkyl, aryl or H	phenyl
semicarbazone	alkyl, aryl or H	alkyl, aryl or H	$-NHCONH_2$
oxime	alkyl, aryl or H	alkyl, aryl or H	-OH
hydrazone	alkyl, aryl or H	alkyl, aryl or H	-NHR

† often used interchangeably with the general term imine by some authors

Here, all compounds containing a C=N bond will be referred to as imines. No distinction will be made between the different types as outlined in Table 1.1: the identity of the groups attached to the carbon and nitrogen is not significant unless specifically stated.

1.3.2 Formation of imines

There have been extensive studies on the reactions of amines with carbonyl compounds to form imines. Most of the kinetic studies have focussed on the formation of hydrazones, oximes and semicarbazones. Few studies have looked at the formation of imines of the type $RN=CH_2$, formed from formaldehyde and an amine, as these imines are very unstable. Therefore the formation can only be observed indirectly.

1.3.2.1 pH dependence

The addition of primary amines to a carbonyl group generally proceeds via a stepwise mechanism involving formation of a carbinolamine intermediate followed by dehydration to an imine. Many of these reactions exhibit bell shaped graphs[13] for rate constant against pH, with a maximum around pH 4 to 6. The position of the pH maximum occurs at a slightly higher pH for reaction with weakly basic amines than for reaction with more basic amines. The influence of structure on reactivity is different on the two sides of the pH maximum.

A number of authors[14] have attributed this pH maximum to the opposing effects of general acid catalysis and the decrease in the concentration of reactive free amine at low pH due to protonation. Later papers[15] show that the pH maximum is actually the result of a change in rate determining step with pH. Under acidic conditions the rate determining step is attack of the amine on the carbonyl group (Step 1, Scheme 1.5) as the reactive free amine becomes protonated, whereas under neutral and basic conditions the acid catalysed dehydration of the carbinolamine is rate limiting (Step 2, Scheme 1.5).

Scheme 1.5:

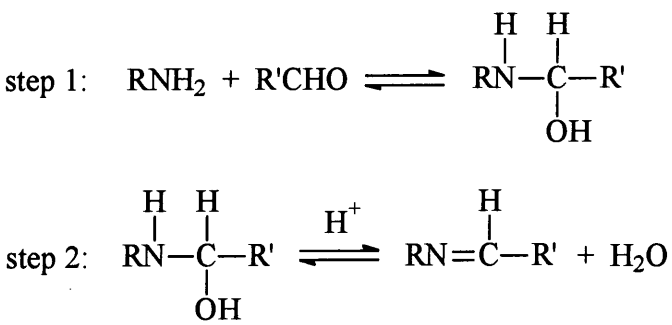

The addition step to form the carbinolamine is, in some reactions, a stepwise process itself, involving formation of a zwitterionic form[16] of the carbinolamine followed by proton transfer. This mechanism has been postulated to account for the observation of a second break in the graph of rate constant against pH at lower pH, generally around pH 1, which implies at least three sequential kinetically important steps. At very low pH the rate determining step is uncatalysed formation and breakdown of the zwitterion.

At acidic pH, the reaction can therefore be described by two separate concurrent pathways, **paths a** and **b**, Scheme 1.6.

Scheme 1.6:

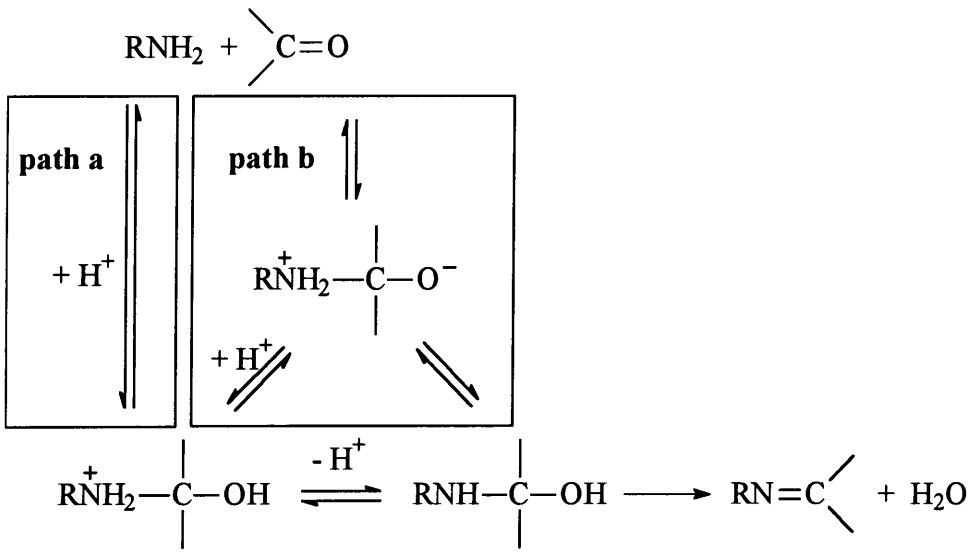

Path a involves concerted carbon – nitrogen bond formation and protonation of the carbonyl group (Scheme 1.7).

Scheme 1.7:

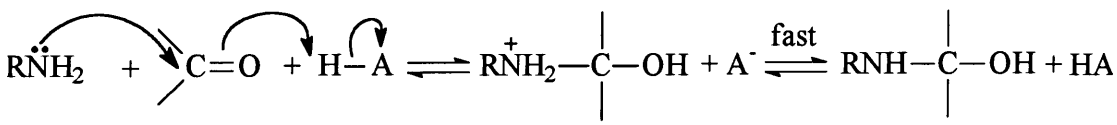

Path b is a stepwise mechanism involving initial formation of a zwitterionic form of the carbinolamine, **4**, which subsequently undergoes proton transfer to give the neutral carbinolamine (Scheme 1.8).

Scheme 1.8:

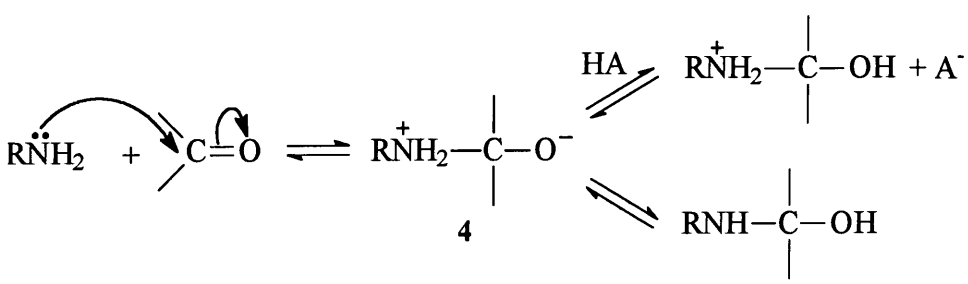

Recent theoretical studies suggest that the proton transfer to convert the zwitterion to the neutral carbinolamine proceeds through two water molecules.[17]

The steric and electronic effects of the carbonyl compound and the pK_a of the amine determine the relative contributions of each pathway.[18] It is thought that, in general, the following rules apply:[16a]

1) for weakly basic amines or carbonyl compounds for which the equilibrium constant for carbinolamine formation is small, the zwitterionic intermediate will be unstable and the reaction will proceed via **path a**.

2) for moderately basic amines and carbonyl compounds with a large equilibrium constant for carbinolamine formation, the zwitterionic intermediate will be relatively stable and **path b** is favoured.

To summarise, the rate determining step under neutral and basic conditions is generally dehydration of the carbinolamine, and under acidic conditions the rate determining step is attack of the amine on the carbonyl group. At low pH, the attack of the amine on the carbonyl group to produce the carbinolamine can occur either via a concerted mechanism or via a stepwise reaction involving formation of a carbinolamine zwitterion. The reaction pathway followed depends on the pK_a of the amine and the steric and electronic effects of the groups attached to the carbonyl compound.

Although this is generally the case, there are a number of reaction systems that have been used to form oximes, semicarbazones and hydrazones that apparently show rate limiting carbinolamine dehydration even at low pH.[19] These reactions generally involve intramolecular reactions and specifically a transition state with a cationic site on an aromatic ring. The formation of a cationic site on the substrate should increase the rate of amine attack relative to carbinolamine dehydration. This has the effect of pushing the change in rate determining step to lower pH values: the dehydration of the carbinolamine effectively becomes the rate determining step at all pH values.

1.3.2.2 General acid and base catalysis

The reaction of primary amines with carbonyl compounds is subject to general acid and base catalysis.[20] General acid catalysis probably involves concerted addition of the amine and transfer of a proton to the carbonyl group (Scheme 1.9).

Scheme 1.9:

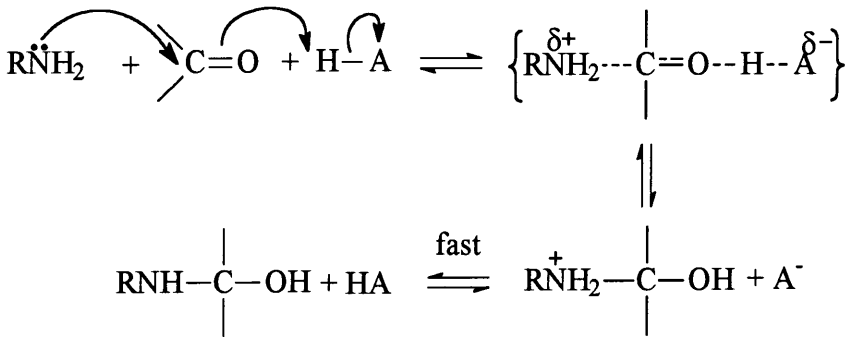

General base catalysis probably involves concerted removal of a proton from the attacking reagent to facilitate attack at the carbonyl group (Scheme 1.10).

Scheme 1.10:

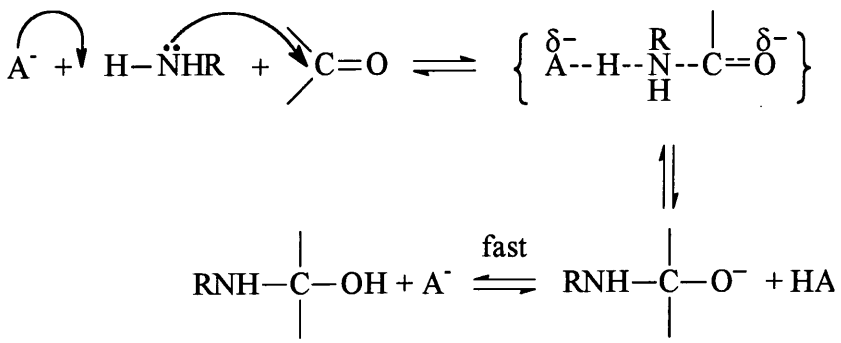

The predominant pathway[1c] in the dehydration of a carbinolamine formed from a strongly basic amine probably involves direct expulsion of a hydroxide ion: the nitrogen lone pair of electrons provides the driving force for the reaction (Scheme 1.11).

Scheme 1.11:

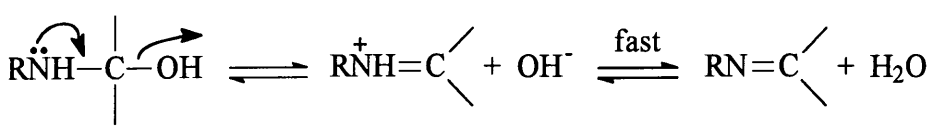

Dehydration of the carbinolamine is subject to general acid catalysis. The rate constant for the proton catalysed dehydration of the carbinolamine formed from the reaction of formaldehyde with cysteine, **5**, is equal[21] to 1.4×10^8 dm^3 mol^{-1} s^{-1} at 25 °C, 1 M ionic strength.

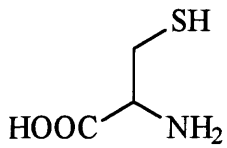

5

Semicarbazone and oxime formation, and probably formation of other imines, is catalysed by aniline and substituted anilines.[22] Catalysis by anilinium ions is much more efficient than catalysis by other acids of comparable acid strength. Aniline acts as a nucleophilic catalyst: the aniline reacts with the carbonyl compound in a rate limiting step to produce an imine, followed by fast reaction of the imine with, for example, a semicarbazide to yield the product (Scheme 1.12).

Scheme 1.12:

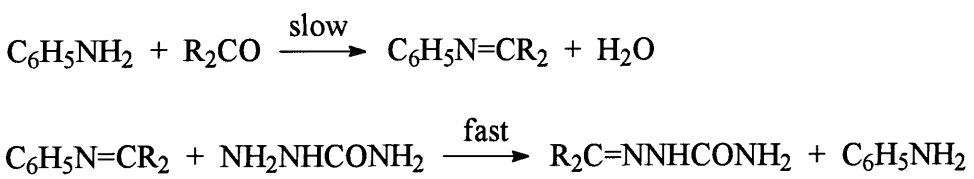

1.3.3 Stability

Iminium ions, RR'C=N$^+$HR", have a short lifetime in aqueous solution, around[23] 10^{-7} to 10^{-8} s at 25 °C. Imines are only stable and easily isolated if they contain one or more aryl groups on the carbon or nitrogen, when there is steric hindrance to further reaction, or if a hydroxy group or second nitrogen is attached to the nitrogen atom, when resonance stabilisation occurs. The most common examples are oximes (**6**), semicarbazones (**7**) and hydrazones (**8**).

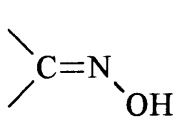

6

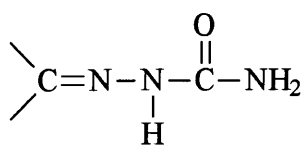

7

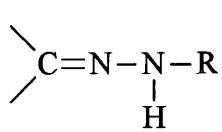

8

The imine methylene-aniline, [$C_6H_5N=CH_2$], exists in the gas phase[24] but is too unstable to be isolated in solution. The only known stable imine of the type $RN=CH_2$ is that prepared[25] using formaldehyde and 2,6-di-isopropylaniline to give the imine **9**.

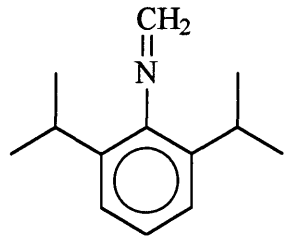

9

Some azomethines, ArN=CHAr', have recently been prepared by grinding together solid anilines and benzaldehydes.[26] These imines are probably stable due to the steric effect of the aryl groups.

1.3.4 Reactions of imines

Imines can undergo many reactions.[27] Reactions with nucleophilic reagents are very favourable, particularly when the imine is in the cationic iminium ion form. For example, the reaction of iminium ions with the nucleophile RS^- is diffusion controlled with a rate constant[23a,d] of 10^9 mol^{-1} dm^3 s^{-1} at 25 °C.

Only the main nucleophilic reactions that are of particular relevance to the present work are discussed here, namely hydrolysis, the Mannich reaction, the Strecker synthesis, and the reaction of imines with amines.

1.3.4.1 Hydrolysis

All stages in the preparation of imines from carbonyl compounds and amines are reversible. Therefore hydrolysis of imines to the starting materials is possible. The rate of hydrolysis depends on steric factors and the electron withdrawing ability of the groups on the imine. Hydrolysis occurs only on the protonated iminium ion.[28] Eldin and co-workers[23d] report a rate constant for the reaction of the iminium ion $H_2C=N^+(CH_3)(CH_2CF_3)$ with water equal to 1.8×10^7 s^{-1} at 25 °C. Values ranging from

3.1×10^6 to 1.0×10^8 s^{-1} at 25 °C are obtained for the hydrolysis of iminium ions formed from formaldehyde and *N*-methylaniline derivatives.[23a]

A bell shaped curve is observed for the graph of rate constant for hydrolysis against pH.[29] This has been interpreted as corresponding to a change in rate determining step.[30] At basic pH, the attack of hydroxide ion on the iminium ion is rate determining. The reaction is general acid catalysed[31] (Scheme 1.13).

Scheme 1.13:

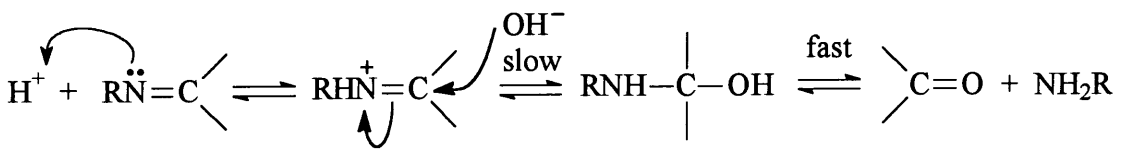

Under more acidic conditions, attack of water rather than hydroxide ion on the iminium ion becomes the predominant reaction pathway and the rate limiting step (Scheme 1.14).

Scheme 1.14:

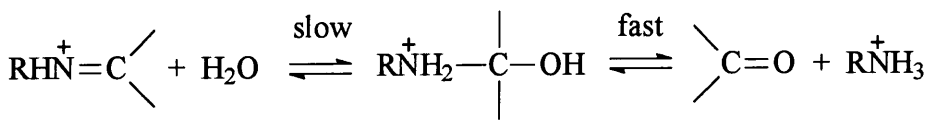

This reaction is general base catalysed: catalysis probably occurs as shown in Scheme 1.15.

Scheme 1.15:

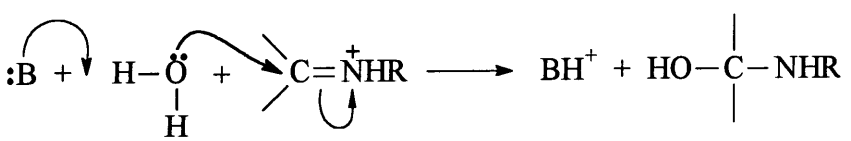

At still lower pH the rate determining step changes to rate determining loss of amine from the carbinolamine (Scheme 1.16).

Scheme 1.16:

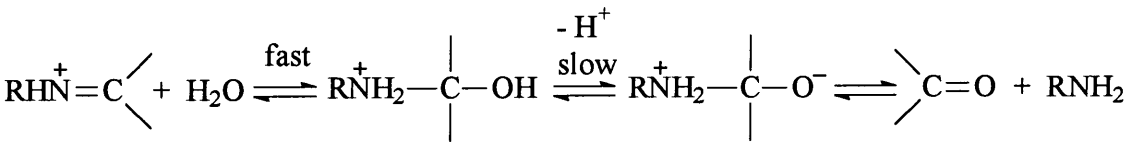

This reaction is slow at low pH as a proton has to be removed from the oxygen atom of the carbinolamine in order to obtain a sufficient driving force to expel the amine.

1.3.4.2 Mannich Reaction

The Mannich reaction involves reaction of an aldehyde, usually formaldehyde, with ammonia or a primary or secondary amine, and a compound with an easily removable, acidic hydrogen, R'H (Scheme 1.17).

Scheme 1.17: $R_2NH + HCHO + R'H \longrightarrow R_2NCH_2R' + H_2O$

R'H is usually a ketone, acid or ester. The product R_2NCH_2R' is known as a Mannich base. There have been a number of reviews published on the synthesis and reactions of Mannich bases.[32] The mechanism of the reaction has been the subject of considerable discussion[33] but kinetic studies[34] suggest the following mechanisms in acidic and basic media.

a) **acidic media:** the reaction involves electrophilic attack by an iminium ion on the enol form of R'H. Scheme 1.18 describes the reaction where R'H is cyclohexanone.[34b]

Scheme 1.18:

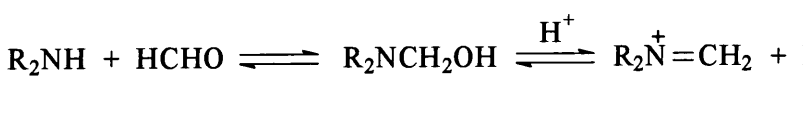

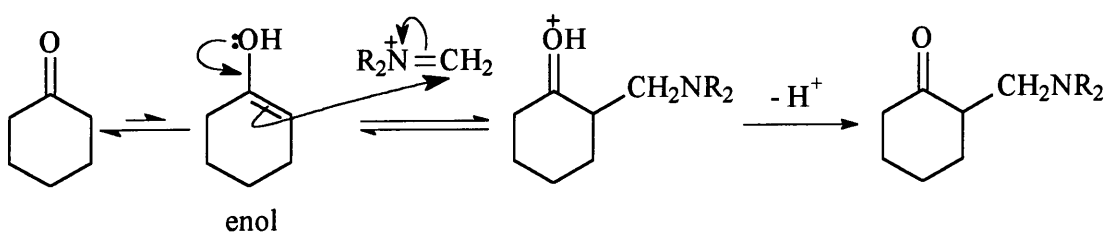

enol

b) basic media: the reaction involves electrophilic attack by an iminium ion on the enolate form of R'H (Scheme 1.19)

Scheme 1.19:

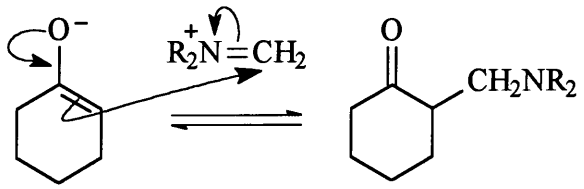

enolate

By-products can be formed by condensation of formaldehyde with the amine or R'H or by further reaction of the Mannich base.[35]

Mannich bases are used as synthetic intermediates in the synthesis of alkaloids,[36] pharmaceuticals,[37] and in the manufacture of paints.[38] There is still great interest in the Mannich reaction, with numerous papers published in the literature where the reaction is an integral part of a new synthetic process.[39]

1.3.4.3 Strecker Synthesis

The Strecker synthesis was developed[40] in 1850 and is a special case of the Mannich reaction where R'H is hydrogen cyanide, HCN. The product of reaction is an α-aminonitrile (**10**, Scheme 1.20).

Scheme 1.20: $R_2CO + NH_3 + HCN \longrightarrow H_2NCR_2CN + H_2O$

10

The reaction can also be performed using ammonium cyanide, NH_4CN, or sodium cyanide, NaCN, with ammonium chloride, NH_4Cl.[41] Salts of primary or secondary amines can also be used to obtain *N*-substituted or *N,N*-disubstituted α-aminonitriles respectively.[42]

The mechanism of reaction[43] is thought to involve reaction of the carbonyl compound with the amine to give an imine. Addition of HCN then yields the α-aminonitrile: this probably occurs via attack of cyanide ion on the protonated imine (Scheme 1.21).

Scheme 1.21:

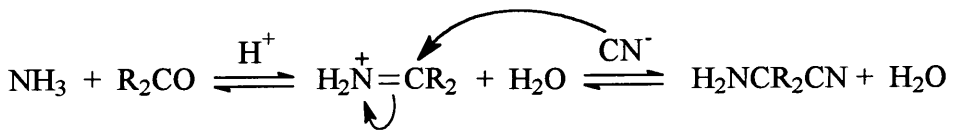

Kinetic studies[43b] show that the attack of cyanide ion is not the rate determining step therefore the reaction must proceed through rate determining formation of an intermediate, the imine, rather than via direct displacement of hydroxide by cyanide ion in the carbinolamine.

The equilibrium constant, K, for the formation of α-aminoacetonitrile[44] from free formaldehyde, ammonia and hydrogen cyanide at 25 °C is 1×10^7 mol^{-2} dm^6 (Scheme 1.22, Equation 1.1).

Scheme 1.22: $HCHO + NH_3 + HCN \xrightarrow{K} H_2NCH_2CN + H_2O$

$$K = \frac{[H_2NCH_2CN]}{[HCHO][NH_3][HCN]} \qquad \textbf{(1.1)}$$

When formaldehyde and aniline are used in the Strecker synthesis, the α-aminonitrile **11** is produced (Scheme 1.23).

Scheme 1.23:

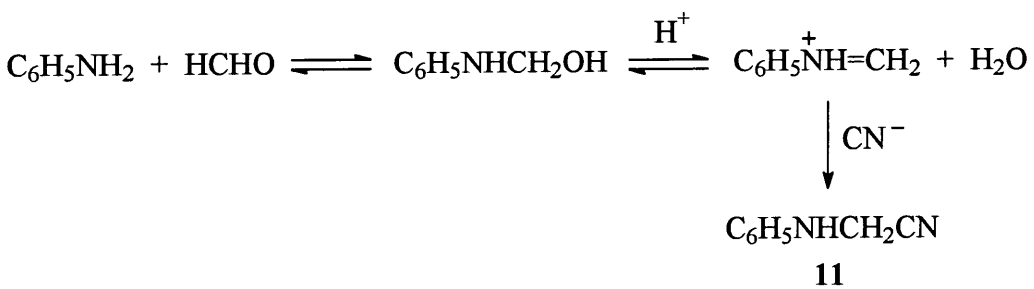

The cyanide ion can also react with formaldehyde to produce glycolonitrile (**12**, Scheme 1.24).

Scheme 1.24:

$$HCHO + CN^- \underset{k_{-GCN}}{\overset{k_{GCN}}{\rightleftharpoons}} CH_2(O^-)(CN) \overset{H^+, \text{fast}}{\rightleftharpoons} \underset{\mathbf{12}}{CH_2(OH)(CN)}$$

Schlesinger and Miller[45] determined average values of k_{GCN} and k_{-GCN} equal to 3.0×10^5 dm^3 mol^{-1} s^{-1} and 1.15×10^{-2} s^{-1} respectively at 25 °C, 0.05 M ionic strength. Glycolonitrile formation competes with α-aminonitrile formation at pH 6 and above.

The pK_a of glycolonitrile[46] is 10.7 where K_a is given by Equation 1.2.

$$K_a = \frac{[CH_2(O^-)(CN)][H^+]}{[CH_2(OH)(CN)]} \qquad \textbf{(1.2)}$$

The Strecker synthesis is used for the preparation of α-amino acids,[47] formed by hydrolysis of the α-aminonitrile (Scheme 1.25).

Scheme 1.25:

$$H_2NCR_2CN \xrightarrow{H^+, H_2O} H_2NCR_2COOH$$

α-Aminonitriles are also intermediates in the synthesis of sterically hindered amines.[48] The Strecker synthesis is still used and appears in many recent papers describing the syntheses of novel compounds.[49]

1.3.4.4 Reaction with amines

Reactions of imines with amines, or aminolysis, involves the replacement of the amine component on the imine with another amine to give the exchange products. The reaction occurs predominantly through reaction with the cationic iminium ion[50] (Scheme 1.26).

Scheme 1.26:

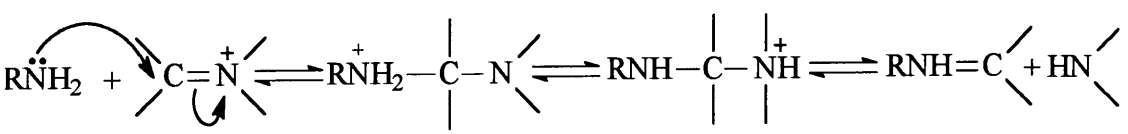

The intermediate is analogous to the carbinolamine intermediate in imine formation. Whichever step involves attack of the weaker amine on the imine containing the stronger amine is the rate determining step.[51]

1.4 1,3,5-HEXAHYDROTRIAZINES

When equimolar amounts of an amine and formaldehyde react, or when formaldehyde is present in excess, a resinous chain polymer, **13**, is formed in acidic conditions due to spontaneous polymerisation of the unstable imine [$RN{=}CH_2$] that is formed.

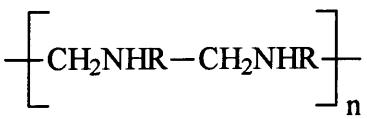

13

In neutral media, [$RN{=}CH_2$] rapidly polymerises to give a cyclic trimer, (Scheme 1.27, **14**) 1,3,5-hexahydrotriazine, also known as a hexahydro-*s*-triazine.

Scheme 1.27:

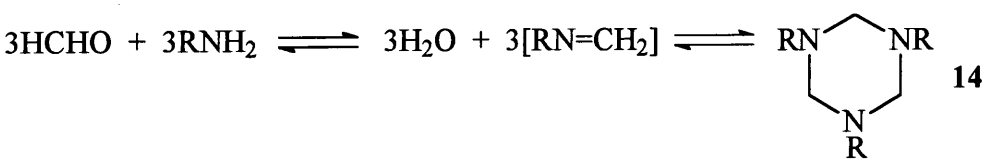

14

1,3,5-Hexahydrotriazines have been isolated as crystalline solids for both aliphatic and aromatic amines.[52] Amorphous higher polymers[53] can also form as by-products: these have been identified as cyclic tetramers.[54] For example, the tetramer 1,3,5,7-tetraazatricyclo-(3.3.1.$1^{3,7}$)-decane,[55] or hexamine, **15**, is readily formed in the reaction of equimolar formaldehyde and ammonia.

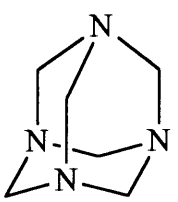

15

1,3,5-Triphenyl-1,3,5-hexahydrotriazine and other 1,3,5-triaryl-1,3,5-hexahydrotriazines have been used to promote the stabilisation of plasticised synthetic rubbers.[56]

1.5 INTRODUCTION TO FORMALDEHYDE AND SULFITE CHEMISTRY

The reactions of formaldehyde, amines and a nucleophile are important in synthetic processes. Numerous studies have examined hydrolysis of imines, the Mannich reaction and the Strecker synthesis. However only one study has looked at the reaction with sulfite as the nucleophile.

The products of reaction of formaldehyde, anilines ($RC_6H_4NH_2$) and sulfite are aminomethanesulfonates, $RC_6H_4NHCH_2SO_3^-$. These compounds are important in the azo dye industry[57] as the methanesulfonate group provides high solubility[58] and is a blocking group[59] for diazo coupling reactions. Aminomethanesulfonates are also of considerable interest for medical applications.[60]

To understand the reaction of formaldehyde, amines and sulfite, the chemistry of formaldehyde must be considered.

1.6 FORMALDEHYDE

1.6.1 Formaldehyde solution composition

Formaldehyde chemistry is complicated by the fact that formaldehyde is seldom encountered as pure HCHO, the reactive monomeric form. HCHO polymerises readily at room temperature and below and therefore can only be kept in the pure monomeric state for a very limited time. Hence formaldehyde can only be purchased in a solid polymeric form, known as paraformaldehyde, or as a solution. The most common form is a 37 % formaldehyde by weight aqueous solution containing 10 to 15 % methanol to prevent precipitation of solid polymer. This standard 37 % by weight solution was first known under the trade names[61] 'Formalin' and 'Formol'.

Formaldehyde polymers can be categorised into two main groups: linear polymers, or polyoxymethylene glycols, and cyclic polymers.

1.6.1.1 Linear polymers, or polyoxymethylene glycols, $HO(CH_2O)_nH$

Less than 0.1 % aqueous formaldehyde solution is present as monomeric formaldehyde even in concentrated solution. The formaldehyde is almost completely hydrated: the principal form is the monohydrate, methylene glycol, $CH_2(OH)_2$, with other low molecular weight polyoxymethylene glycols, $HO(CH_2O)_nH$, also present.[62] The solution composition can be described in terms of Scheme 1.28.

Scheme 1.28:

$$HCHO + H_2O \rightleftharpoons CH_2(OH)_2$$

$$2CH_2(OH)_2 \rightleftharpoons HO(CH_2O)_2H + H_2O$$

$$CH_2(OH)_2 + HO(CH_2O)_2H \rightleftharpoons HO(CH_2O)_3H + H_2O$$

etc.

The rate of formation of the higher molecular weight polyoxymethylene glycols is much slower than that of methylene glycol: the rate constants differ by a factor[63] of 100 to 1000. All of the equilibria are reversible and the different forms generally react as formaldehyde: the net effect of reactions involving aqueous formaldehyde solution is usually what would be expected if monomeric formaldehyde were employed. However the polymers differ in the readiness with which they depolymerise to yield formaldehyde in a reactive form.

Pure formaldehyde solutions are clear and colourless. Cloudiness or opalescence is caused by polymer precipitation. The degree of precipitation depends on the total formaldehyde concentration, temperature, standing time, pH and the concentration and type of solution stabiliser, if present. Each of these factors will be considered in turn.

a) Formaldehyde concentration

Iliceto and co-workers[64] have calculated the probable proportion of formaldehyde present as the various polyoxymethylene glycols at 35 °C for different aqueous

formaldehyde solution concentrations. Low formaldehyde concentrations favour methylene glycol and high concentrations favour higher polyoxymethylene glycols.[65]

b) Temperature

Polyoxymethylene glycols decrease in solubility with increasing molecular weight and can precipitate out of solution when the concentration exceeds the solubility at a particular temperature. At low temperatures,[66] formaldehyde solutions become cloudy and eventually solid hydrated polymer separates as a precipitate. Solutions in which polymer has precipitated can be clarified by warming if exposure to low temperature has been short. After long exposure, clarification is not possible. Polymer precipitation can be prevented by maintaining the solution above the minimum temperature at which precipitation is known to take place. The minimum temperature is a function of the formaldehyde concentration and the type and concentration of any solution stabilisers that may be present. Precipitation occurs below 7 °C for a 37 % by weight aqueous formaldehyde solution containing 10 % methanol.

c) Standing time

Solutions containing 37 % or more by weight formaldehyde with no stabiliser present precipitate low molecular weight polymers at room temperature. On standing, these polymers increase in molecular weight. After dilution of an aqueous formaldehyde solution to 4 % or less, higher molecular weight polymers dissociate over a period of hours at room temperature to give methylene glycol via acid or base catalysed pathways.[63a]

d) pH of the solution

In general, solutions with a pH in the range 3 to 5 are most stable with respect to polymer precipitation as the polymerisation reactions proceed at minimal rates in this range. Polymerisation becomes increasingly rapid as the pH varies from these limits.[67]

e) Solution stabilisers

A 37 % by weight formaldehyde solution usually contains 10 to 15 % methanol, CH_3OH, to prevent polymer precipitation. Methanol combines with the dissolved formaldehyde to form unstable low molecular weight compounds of high solubility. These compounds are probably hemiacetals, $HO(CH_2O)_nCH_3$, which can exist in equilibrium with polyoxymethylene glycols, as shown in Scheme 1.29.

Scheme 1.29: $CH_2(OH)_2 + CH_3OH \rightleftharpoons HOCH_2OCH_3 + H_2O$

$HO(CH_2O)_2H + CH_3OH \rightleftharpoons HO(CH_2O)_2CH_3 + H_2O$

etc.

Compounds other than alcohols that will prevent polymer precipitation by forming water soluble formaldehyde compounds include hydrogen sulfide[68] and neutral or mildly acidic nitrogen compounds such as urea[69] and melamine.[70]

To summarise, polyoxymethylene glycol polymer precipitation in a formaldehyde solution can be avoided, or kept to a minimum, by adding a stabiliser to the solution, storing above 7 °C at pH 3 to 5, and diluting the solution and leaving to stand prior to use to ensure depolymerisation of higher molecular weight polymers to methylene glycol.

Formaldehyde can also be purchased in a solid polymeric form, known as paraformaldehyde. This contains a mixture of low molecular weight polyoxymethylene glycols containing 8 to 100 formaldehyde units per molecule.[71]

1.6.1.2 Cyclic polymers

Trioxane, **16**, or alpha-trioxymethylene is the cyclic trimer of formaldehyde. **16** is a stable chemical compound with unique, well defined properties. Tetraoxane, **17**, is the cyclic tetramer of formaldehyde. Neither of these compounds is present in significant quantities in formaldehyde solutions.[72]

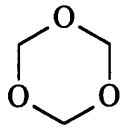

16

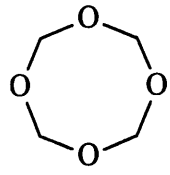

17

1.6.1.3 Other reactions that can occur in formaldehyde solution

Whilst the principal change that can take place in formaldehyde solution is polymerisation and polymer precipitation, other reactions may also occur. These, in order of relative importance, are:

1) Cannizzaro reaction

This reaction, shown in Scheme 1.30, proceeds most rapidly in alkaline conditions and is accelerated by high temperatures and the catalytic effect of trace metallic impurities such as iron and aluminium.

Scheme 1.30: $2HCHO + H_2O \longrightarrow HCOOH + CH_3OH$

2) methylal, $CH_2(OCH_3)_2$, formation

This reaction (Scheme 1.31) occurs in 37 % by weight aqueous formaldehyde solution containing methanol as a stabiliser and is catalysed by acidic conditions and the presence of metallic salts such as iron, zinc and aluminium formates.

Scheme 1.31: $HCHO + 2CH_3OH \longrightarrow CH_2(OCH_3)_2 + H_2O$

3) oxidation to formic acid

The pH of pure aqueous formaldehyde lies in the range 2.5 to 3.5 due to the presence of traces of formic acid[73] (Scheme 1.32). Neutral or basic formaldehyde solutions can be

The pK_a of methylene glycol[77] to give $CH_2(OH)(O^-)$ is 13.27 at 25 °C in aqueous solution.

Funderburk and co-workers[78] studied the reaction of formaldehyde dehydration with respect to pH and determined that the pseudo first order, buffer independent rate constant can be described by Equation 1.3.

$$k_{deh} = k_o + k_H[H^+] + k_{OH}[OH^-] \qquad \textbf{(1.3)}$$

At 25 °C, 1.0 M ionic strength, the values of k_H, k_{OH} and k_o are equal to 2.84 mol^{-1} dm^3 s^{-1}, 2.1×10^3 mol^{-1} dm^3 s^{-1} and 4×10^{-3} s^{-1} respectively. Between pH 4 and 7 the dehydration is approximately pH independent.

1.6.3 Detection of formaldehyde

The HCHO content of pure aqueous formaldehyde solutions or solutions containing only small quantities of impurities can be determined accurately using specific gravity or refractivity methods. Chemical procedures are also often used because of their simplicity. There are a number of methods available although none are specific to formaldehyde. 'Formaldehyde' by Walker[66] gives a detailed description of all the tests and Büchi[79] has published a comprehensive review of the various methods. Büchi concludes that the sodium sulfite method[80] is the most satisfactory. This can be used to detect any ketone or aldehyde but is sensitive to formaldehyde because of its high reactivity. Impurities commonly present have little effect on the results, as do the presence of methanol and methylal.[81] The test is based on the detection of sodium hydroxide liberated quantitatively when formaldehyde reacts with sodium sulfite to form hydroxymethanesulfonate, $CH_2(OH)(SO_3Na)$ (Scheme 1.35). The sodium hydroxide is titrated against a strong acid.

Scheme 1.35: $HCHO + Na_2SO_3 + H_2O \rightleftharpoons NaOH + CH_2(OH)(SO_3Na)$

This is a simple and sensitive method that can be used to detect and approximate the presence of small quantities of formaldehyde.

1.7 HYDROXYMETHANESULFONATE, $CH_2(OH)(SO_3Na)$

1.7.1 Introduction

Hydroxymethanesulfonate, or HMS, $CH_2(OH)(SO_3Na)$, is the adduct of formaldehyde and sodium sulfite. HMS dissociates in aqueous solution and therefore is a convenient method of producing formaldehyde and sulfite *in situ* in equimolar amounts. Of particular interest here is the reaction of HMS with amines, as this is effectively a reaction involving formaldehyde, an amine and a nucleophile, namely sulfite. The formation of HMS is utilised in the formaldehyde clock reaction demonstration. HMS is present in the atmosphere and has been detected in beer. These factors will also be discussed.

1.7.2 Reaction with ammonia

There has been only one previous study reported in the literature on the reaction of hydroxymethanesulfonate, $CH_2(OH)(SO_3Na)$, with an amine: Le Hénaff[82] studied the reaction with ammonia. The products obtained are the 1 : 1 and 1 : 2 ammonia : $CH_2(OH)(SO_3^-)$ adducts $H_2NCH_2SO_3^-$ and $HN(CH_2SO_3^-)_2$. The reactions are shown in Scheme 1.36. Concentrations of the intermediates are small. The rate and equilibrium constants obtained at 20 °C are shown in Table 1.2.

Table 1.2: Literature values[82] for the rate and equilibrium constants at 20 °C

constant	value
k_{-6}	6.8×10^{-5} s^{-1}
k_{-3} / k_6	40.5
k_{-5} / k_6	2.7×10^{-4} mol dm^{-3}
$K = [NH_3][CH_2(OH)(SO_3^-)] / [H_2NCH_2SO_3^-]$	1.4×10^{-3} mol dm^{-3}
k'_{-6}	2.0×10^{-5} s^{-1}
k'_{-3} / k'_6	320
k'_{-5} / k'_6	2.4×10^{-3} mol dm^{-3}
$K' = [H_2NCH_2SO_3^-]][CH_2(OH)(SO_3^-)] / [HN(CH_2SO_3^-)_2]$	2.6×10^{-3} mol dm^{-3}

Scheme 1.36:

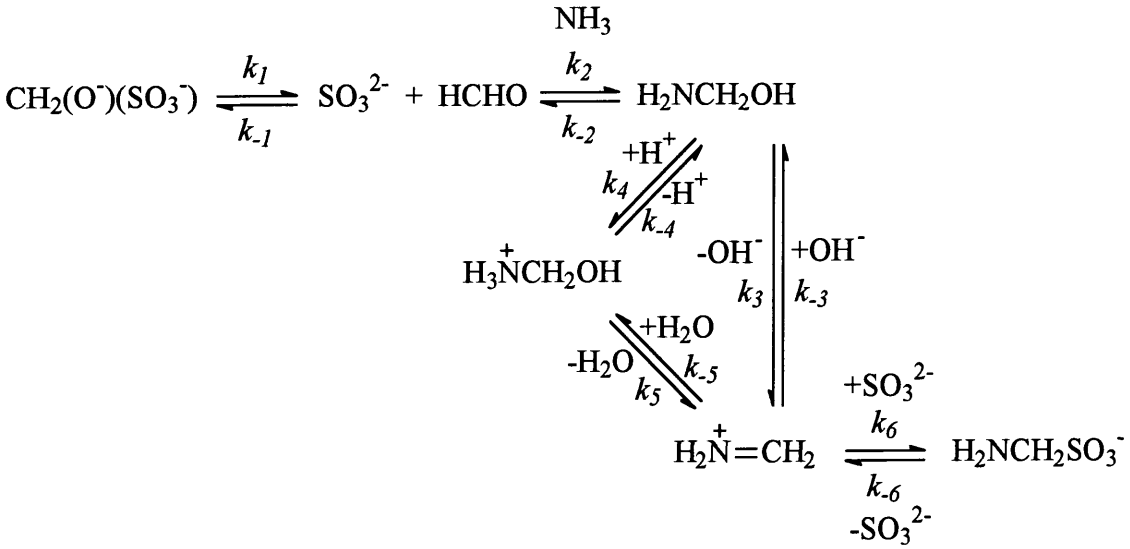

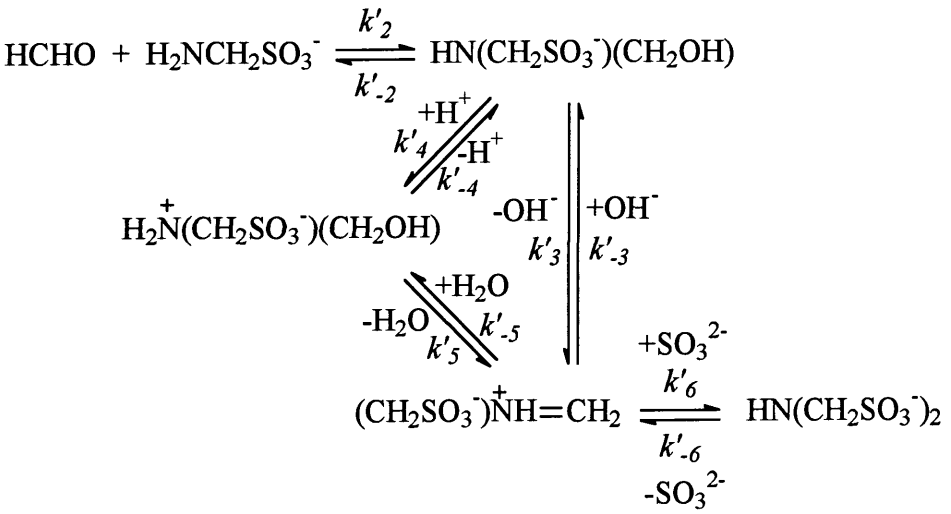

Le Hénaff states that the reaction is greatly retarded by the presence of free sulfite in the system and suggests that formation of the 1 : 3 adduct, $N(CH_2SO_3^-)_3$, may also be possible.

1.7.3 Occurrence

Several authors have postulated,[83] and later studies have confirmed,[84] that HMS can exist in cloud water. For example, concentrations in excess of 3×10^{-4} M have been measured in fog water in California.[84e] For HMS to be formed in cloud water it is necessary that either low concentrations of oxidants or very high concentrations of

HCHO and $S(IV)_\tau$ species[†] be present, such as is the case near combustion sources. There must be low concentrations of oxidants as the formation of HMS from HCHO and $S(IV)_\tau$ is slow relative to the oxidation of $S(IV)_\tau$ by hydrogen peroxide, H_2O_2, also present in the atmosphere.

HMS is not oxidised by H_2O_2 or ozone.[85] It is thought that once HMS is present in cloud droplets it will persist until the cloud precipitates or evaporates. HMS has recently been detected in atmospheric aerosol samples[86] indicating that it can also exist outside of clouds.

HMS and other aldehyde – bisulfite adducts can inhibit free radical reactions in beer. The acetaldehyde – bisulfite adduct has been detected during fermentation and in commercial beers[87] and has been shown to inhibit haze formation and flavour staling of beer during storage.[88] It has been postulated that aldehyde – bisulfite adducts such as HMS have a radical scavenging activity and can prevent free radical oxidation chain reactions during beer storage, leading to better stability of beer quality.

1.7.4 Formaldehyde clock reaction

Clock reactions involve the sudden appearance of a product some time after the initial mixing of reagents. The term clock arises from the fact that at fixed concentrations and constant temperature the appearance of the product occurs at a definite time after the initial mixing. Reactions of this type are frequently used as demonstrations as the endpoint is usually visually interesting.

The formaldehyde clock reaction forms the basis of several demonstrations and student experiments. Aqueous solutions of formaldehyde and bisulfite / sulfite ions are mixed, resulting in a dramatic rise in pH when the reaction nears completion. Any pH indicator in the pH range 7 to 11, such as phenolphthalein, can be used to show the endpoint.

Many authors[89] have interpreted the reaction on the basis of a mechanism originally suggested by Wagner[90] in 1929. He suggested that the reaction primarily being followed

[†] $S(IV)_\tau = HSO_3^- + SO_3^{2-} + SO_2.H_2O$ + all other species where sulfur is in the +4 oxidation state, such as in metal complexes

was the reaction of HCHO with bisulfite ions, HSO_3^-, to give HMS which was then superseded by the reaction of HCHO with sulfite ions, SO_3^{2-}, when all of the HSO_3^- had reacted (Scheme 1.37).

Scheme 1.37:

$$HCHO + HSO_3^- \rightleftharpoons CH_2(OH)(SO_3^-)$$

$$HCHO + SO_3^{2-} \rightleftharpoons CH_2(O^-)(SO_3^-)$$

These reactions are slow compared to the reaction of bisulfite ions with hydroxide ions, OH^-, to give sulfite ions and water, which is virtually instantaneous. When all of the bisulfite ions have reacted, the OH^- concentration will rise rapidly and the pH change can be observed with a suitable indicator.

The colour change does coincide with the completion of bisulfite consumption.[91] However more recent research[92] suggests that above pH 4 the reaction is carried primarily by sulfite ions as opposed to bisulfite ions. In aqueous solution formaldehyde occurs mainly as the hydrate, methylene glycol, $CH_2(OH)_2$. The rate of HMS formation is so much faster than the rate of dehydration of methylene glycol that the rate determining step must be the latter under the usual formaldehyde clock laboratory conditions.[93] To support this, the reaction is first order in free formaldehyde and zero order in the combined initial bisulfite and sulfite ion concentration. Therefore the rate constant associated with the formaldehyde clock reaction actually corresponds to the dehydration of methylene glycol to give free formaldehyde, HCHO.

Burnett[93] laid out certain precautionary guidelines required in the choice of concentrations and experimental procedures to follow for a successful formaldehyde clock reaction. The ease of preparation of the reagents and the reproducibility of the results make this experiment popular for demonstrations and basic chemistry classes.

1.8 AIMS

This work concerns the reaction of formaldehyde with amines with and without the presence of sulfite, utilising anilines and benzylamines ($RC_6H_4CH_2NH_2$) as the amines. The reaction with anilines produces aminomethanesulfonates which are industrially important: the use of benzylamines provides a means of comparing aromatic versus aliphatic systems using amines of similar structure. This work aims to:

- investigate the individual steps in the reaction
- study the reaction of formaldehyde with amines to give carbinolamines
- indirectly study the formation of imines of the type $RN{=}CH_2$ by trapping the imine with a nucleophile
- examine the possibility of polymerisation of $RN{=}CH_2$ imines to give, for example, 1,3,5-hexahydrotriazines, and study the stability of these polymers in solution
- study the reaction of formaldehyde with amines in the presence of sulfite and determine the effects of pH and structure of the amine
- study the decomposition of the aminomethanesulfonate products
- determine the overall rate determining step in the reaction of formaldehyde with amines in the presence of sulfite

Formaldehyde and sulfite can be introduced into the system using hydroxymethanesulfonate, $CH_2(OH)(SO_3Na)$. This has the advantage of avoiding the use of aqueous formaldehyde solution, where formaldehyde is predominantly in the form of methylene glycol rather than the reactive free HCHO form. As the kinetics and mechanism of the decomposition of $CH_2(OH)(SO_3Na)$ has not previously been reported in detail, it has been investigated here.

1.9 REFERENCES

1. (a) B. Capon, *Org. React. Mech.*, 1975, 1; (b) M. M. Sprung, *Chem. Rev.*, 1940, **26**, 297; (c) W. P. Jencks, *Progr. Phys. Org. Chem.*, 1964, **2**, 63; (d) R. Bonnett, 'The Chemistry of the Carbon Nitrogen Double Bond', Ed. S. Patai, Interscience, London, 1970, pp. 64

2. R. W. Layer, *Chem. Rev.*, 1963, **63**, 489

3. (a) W. R. Abrams and R. G. Kallen, *J. Am. Chem. Soc.*, 1976, **98**, 7777; (b) *ibid.*, 7789

4. (a) R. G. Kallen, R. O. Viale and L. K. Smith, *J. Am. Chem. Soc.*, 1972, **94**, 576; (b) I. M. C. Brighente, L. R. Vottero, A. J. Terezani and R. A. Yunes, *J. Phys. Org. Chem.*, 1991, **4**, 107; (c) I. M. C. Brighente and R. A. Yunes, *J. Braz. Chem. Soc.*, 1997, **8**, 549; (d) R. Wolfenden and W. P. Jencks, *J. Am. Chem. Soc.*, 1961, **83**, 2763

5. R. G. Kallen and W. P. Jencks, *J. Biol. Chem.*, 1966, **241**, 5864

6. (a) E. E. Snell and W. T. Jenkins, *J. Cell. Comp. Physiol.*, 1959, **54**, 161; (b) D. E. Metzler, M. Ikawa and E. E. Snell, *J. Am. Chem. Soc.*, 1954, **76**, 648; (c) G. A. Hamilton and F. H. Westheimer, *ibid.*, 1959, **81**, 6332; (d) W. P. Jencks, 'Catalysis in Chemistry and Enzymology', Dover, New York, 1987; (e) A. E. Braunstein. 'The Enzymes', Vol. 2, Eds. P. D. Boyer, H. Lardy and K. Myrback, Academic Press, Inc., New York, 1960, p. 113; (f) E. E. Snell, 'The Mechanism of Action of Water-soluble Vitamins', Little, Brown And Co., Boston, Mass., 1961, p. 18; (g) I. Fridovich and F. H. Westheimer, *J. Am. Chem. Soc.*, 1962, **84**, 3208; (h) E. Grazi, T. Cheng and B. L. Horecker, *Biochem. Biophys. Res. Commun.*, 1962, **7**, 250; (i) E. Grazi, P. T. Rowley, T. Cheng, O. Tchola and B. L. Horecker, *ibid.*, **9**, 38

7. (a) R. A. Morton and G. A. J. Pitt, *Prog. Chem. Org. Nat. Prod.*, 1957, **14**, 244; (b) R. Hubbard, *Proc. Natl. Phys. Lab., London, Symp. No. 8*, 1958, 151

8. (a) S. J. Benkovic, P. A. Benkovic and D. R. Comfort, *J. Am. Chem. Soc.*, 1969, **91**, 1860; (b) J. W. Stanley, J. G. Beasley and I. W. Mathison, *J. Org. Chem.*, 1972, **37**, 3746

9. S. F. Dyke, 'The Chemistry of Enamines', Cambridge University Press, London, 1973

10. (a) D. Craig, L. Schaefgen and W. P. Tyler, *J. Am. Chem. Soc.*, 1948, **70**, 1624; (b) G. O. Dudek and R. H. Holm, *ibid.*, 1961, **83**, 3914; (c) T. M. Patrick, Jr., *ibid.*, 1952, **74**, 2984; (d) M. Saunders and E. H. Gold, *J. Org. Chem.*, 1962, **27**, 1439

11. R. McGrindle and A. J. McAlees, *J. Chem. Soc., Chem. Commun.*, 1983, 61

12. H. Schiff, *Ann.*, 1864, **131**, 118

13. (a) E. Barrett and A. Lapworth, *J. Chem. Soc.*, 1908, **93**, 85; (b) J. B. Conant and P. D. Bartlett, *J. Am. Chem. Soc.*, 1932, **54**, 2881; (c) F. H. Westheimer, *ibid.*, 1934, **56**, 1962; (d) A. Ölander, *Z. Physik. Chem.*, 1927, **129**, 1; (e) W. P. Jencks, *J. Am. Chem. Soc.*, 1959, **81**, 475; (f) E. H. Cordes and W. P. Jencks, *ibid.*, 1962, **84**, 832; (g) J. E. Reimann, W. P. Jencks, *ibid.*, 1966, **88**, 3973; (h) L. do Amaral, W. A. Sandstrom and E. H. Cordes, *ibid.*, 2225; (i) B. M. Anderson and W. P. Jencks, *ibid.*, 1960, **82**, 1773; (j) A. V. Willi, *Helv. Chim. Acta*, 1956, **39**, 1193; (k) J. M. Sayer and W. P. Jencks, *J. Am. Chem. Soc.*, 1973, **95**, 5637; (l) A. Williams and M. L. Bender, *J. Am. Chem. Soc.*, 1966, **88**, 2508

14. (a) L. P. Hammett, 'Physical Organic Chemistry', McGraw-Hill Book Co. Inc., New York, 1940, p. 333; (b) G. H. Stempel, Jr., and G. S. Schaffel, *J. Am. Chem. Soc.*, 1944, **66**, 1158; (c) Ref. 13b

15. (a) Ref. 13e – i; (b) A. S. Stachissini and L. do Amaral, *J. Org. Chem.*, 1991, **56**, 1419; (c) Ref. 1c

16. (a) J. M. Sayer, B. Pinsky, A. Schonbrunn and W. Washtein, *J. Am. Chem. Soc.*, 1974, **96**, 7998; (b) S. Rosenberg, S. M. Silver, J. M. Sayer and W. P. Jencks, *J. Am. Chem. Soc.*, 1974, **96**, 7986; (c) J. Hine, F. A. Via, J. K. Gotkis and J. C. Craig, Jr., *ibid.*, 1970, **92**, 5186; (d) J. M. Sayer and W. P. Jencks, *J. Am. Chem. Soc.*, 1972, **94**, 3262; (e) H. Diebler and R. N. F. Thorneley, *ibid.*, 1973, **95**, 896

17. (a) N. E. Hall and B. J. Smith, *J. Phys. Chem.*, 1998, **102A**, 4930; (b) I. H. Williams, *J. Am. Chem. Soc.*, 1987, **109**, 6299

18. (a) R. Fett, E. L. Simionatto and R. A. Yunes, *J. Phys. Org. Chem.*, 1990, **3**, 620; (b) I. M. C. Brighente, R. M. Budal and R. A. Yunes, *J. Chem. Soc., Perkin Trans 2*, 1991, 861; (c) Ref. 16a

19. (a) M. Calzadilla, A. Malpica and P. M. Diaz, *Int. J. Chem. Kinetics*, 1996, **28**, 687; (b) A. Malpica, M. Calzadilla, J. Baumrucker, J. Jiménez, L. López, G. Escobar and C. Montes, *J. Org. Chem.*, 1994, **59**, 3398; (c) P. Sojo, F. Viloria, L. Malave, R. Possamia, M. Calzadilla, J. Baumrucker, A. Malpica, R. Moscovici and L. do Amaral, *J. Am. Chem. Soc.*, 1976, **98**, 4519

20. (a) Ref. 13a, b, e, f, h, l; (b) E. H. Cordes and W. P. Jencks, *J. Am. Chem. Soc.*, 1962, **84**, 4319; (c) D. H. R. Barton, R. E. O'Brien and S. Sternhall, *J. Chem. Soc.*, 1962, 470

21. R. G. Kallen, *J. Am. Chem. Soc.*, 1971, **93**, 6236

22. E. H. Cordes and W. P. Jencks, *J. Am. Chem. Soc.*, 1962, **84**, 826

23. (a) S. Eldin and W. P. Jencks, *J. Am. Chem. Soc.*, 1995, **117**, 4851; (b) *ibid.*, 9415; (c) W. P. Jencks, *J. Phys. Org. Chem.*, 1996, **9**, 337; (d) S. Eldin, J. A. Digits, S.-T. Huang and W. P. Jencks, *J. Am. Chem. Soc.*, 1995, **117**, 6631; (e) C. K. Kim, I. Y. Lee, C. K. Kim and I. Lee, *J. Phys. Org. Chem.*, 1999, **12**, 479

24. G. Distefano, A. G. Giumanini, A. Modelli and G. Poggi, *J. Chem. Soc., Perkin Trans. 2*, 1985, 1623

25. G. Verardo, S. Cauci and A. G. Giumanini, *J. Chem Soc., Chem. Commun.*, 1985, **24**, 1787

26. J. Schmeyers, F. Toda, J. Boy and G. Kaupp, *J. Chem. Soc., Perkin Trans. 2*, 1998, 989

27. R. Bonnett, 'The Chemistry of the Carbon Nitrogen Double Bond', Ed. S. Patai, Interscience, London, 1970, pp. 255

28. J. Hine, J. C. Craig, Jr., J. G. Underwood and F. A. Via, *J. Am. Chem. Soc.*, 1970, **92**, 5194

29. (a) Ref. 13f, k; (b) K. Koehler, W. Sandstrom and E. H. Cordes, *J. Am. Chem. Soc.*, 1964, **86**, 2413

30. (a) W. P. Jencks, 'Catalysis in Chemistry and Enzymology', Dover, New York, 1987, pp. 490 – 496; (b) M. A. E. D. ElTaher, *J. Solution. Chem.*, 1996, **25**, 401; (c) M. Brault, R. M. Pollack and C. L. Bevins, *J. Org. Chem.*, 1976, **41**, 346; (d) E. H. Cordes and W. P. Jencks, *J. Am. Chem. Soc.*, 1963, **85**, 2843; (e) Ref. 13f; (f) Ref. 29b

31. (a) Ref. 13k; (b) R. L. Reeves, *J. Am. Chem. Soc.*, 1962, **84**, 3332

32. (a) M. Tramontini and L. Angiolini, *Tetrahedron*, 1990, **46**, 1791; (b) F. F. Blicke, *Organic Reactions*, 1942, **1**, 303; (c) H. O. House, 'Modern Synthetic Reactions', 2nd Ed., W. A. Benjamin, Inc., Philippines, 1972, pp 654 – 660

33. (a) K. Bodendorf and G. Koralewski, *Arch. Pharm.*, 1933, **271**, 101; (b) S. V. Lieberman and E. C. Wagner, *J. Org. Chem.*, 1949, **14**, 1001

34. (a) E. R. Alexander and E. J. Underhill, *J. Am. Chem. Soc.*, 1949, **71**, 4014; (b) T. F. Cummings and J. R. Shelton, *J. Org. Chem.*, 1960, **25**, 419; (c) J. E. Fernandez and J. S. Fowler, *ibid.*, 1964, **29**, 402; (d) J. E. Fernandez, J. S. Fowler and S. J. Glaros, *ibid.*, 1965, **30**, 2787; (e) D. N. Kirk and V. Petrow, *J. Chem. Soc.*, 1962, 1091; (f) M. Masui, K. Fujita and H. Ohmori, *Chem. Commun.*, 1970, **13**, 182; (g) H. Volz and H. H. Kiltz, *Tetrahedron Letters*, 1970, **22**, 1917

35. J. March, 'Advanced Organic Chemistry', Wiley-Interscience, New York, 1992, 4th Ed., p. 901

36. R. Robinson, *J. Chem. Soc.*, 1917, **111**, 762

37. For example: (a) H. Bungaard, *Methods in Enzymology*, 1985, **112**, 347; (b) J. R. Dimmock, S. K. Raghavan, B. M. Logan and G. E. Bigam, *Eur. J. Med. Chem.*, 1983, **18**, 249

38. M. Tramontini, L Angiolini and N. Ghedini, *Polymer*, 1988, **29**, 771

39. Recent examples include: (a) M. Przeslawska, A. Koll and M. Witanowski, *J. Phys. Org. Chem.*, 1999, **12**, 486; (b) M. Arend and N. Risch, *Tet. Letters*, 1999, **40**, 6205;

(c) N. Su, J. S. Bradshaw, P. B. Savage, K. E. Krakowiak, R. M. Izatt, S. L. DeWall and G. W. Gokel, *Tet.*, 1999, **55**, 9737; (d) F. P. Tseng, F. C. Chang, S. F. Lin and J. J. Lin, *J. Appl. Poly. Sci.*, 1999, **71**, 2129; (e) I. Ripoche, J. L. Canet, B. Aboab, J. Gelas and Y. Troin, *J. Chem. Soc., Perkin Trans. 1*, 1998, **20**, 3485

40. A. Strecker, *Liebigs Ann. Chem.*, 1850, **75**, 27

41. (a) J. March, 'Advanced Organic Chemistry', Wiley-Interscience, New York, 1992, 4th Ed., p. 965; (b) D.K. Crump, for The Dow Chemical Company, E. P. 0 481 394 B1; (c) K. Mai and G. Patil, *Synth. Commun.*, 1985, **15**, 157; (d) *Tetrahedron Letts.*, 1984, **25**, 4583

42. D. B. Luten, *J. Org. Chem.*, 1938, **3**, 588

43. (a) Y. Ogata and A. Kawasaki, *J. Chem. Soc., B*, 1971, 325; (b) T. D. Stewart and C. Li, *J. Am. Chem. Soc.*, 1938, **60**, 2782; (c) J. Taillades and A. Commeyras, *Tetrahedron*, 1974, **30**, 2493; (d) Ref. 8b

44. G. Moutou, J. Taillades, S. Bénefice-Malouet, A. Commeyras, G. Messina and R. Mansani, *J. Phys. Org. Chem.*, 1995, **8**, 721

45. G. Schlesinger and S. L. Miller, *J. Am. Chem. Soc.*, 1973, **95**, 3729

46. W. Reenstra, R. H. Abeles and W. P. Jencks, *J. Am. Chem. Soc.*, 1982, **104**, 1019

47. (a) M. Béjaud, L. Mion, J. Taillades and A. Commeyras, *Tetrahedron*, 1975, **31**, 403; (b) R. M. Williams, 'Synthesis of Optically Active α-Amino Acids', Pergamon Press, New York, 1989, p. 208

48. (a) J. Sansoulet and C. Tackx, *C. R. Acad. Sci.*, 1960, **250**, 4370; (b) W. H. Taylor and C. R. Hauser, *J. Am. Chem. Soc.*, 1960, **82**, 1960

49. Recent examples include: (a) R. H. Dave and B. D. Hosangadi, *Tet.*, 1999, **55**, 11295; (b) P. Portonovo, B. Liang and M. M. Joullie, *Tet.-Asymmetry*, 1999, **10**, 1451; (c) K. P. Fondekar, F. J. Volk and A. W. Frahm, *ibid.*, 727; (d) M. BoisChoussy and J. P. Zhu, *J. Org. Chem.*, 1998, **63**, 5662; (e) J. T. Edward and F. L. Chubb, *Proc. R. Ir. Acad.*, 1983, **83B**, 57

50. W. P. Jencks, 'Catalysis in Chemistry and Enzymology', Dover, New York, 1987, p. 505 - 506

51. (a) B. A. Porai-Koshits and A. L. Remizov, *Prob. Mekhanizma Org. Reaktsii, Akad. Nauk Ukr. SSR, Otdel Fizmat. i Khim. Nauk*, 1953, 238; *Chem. Abstr.*, 1956, **50**, 16686; (b) Ref. 50; (c) Ref. 2

52. (a) J. Graymore, *J. Chem. Soc.*, 1932, 1353; (b) J. G. Miller and E. C. Wagner, *J. Am. Chem. Soc.*, 1932, **54**, 3698; (c) E. Zangrando, G. Poggi, A. G. Giumanini and G. Verardo, *J. f. prakt. Chem.*, 1987, **329**, 195

53. (a) Ref 52b; (b) H. Krassig and H. Ringsdorf, *Makromol. Chem.*, 1957, **22**, 163; (c) R. Carpignano, V. Bersano and A. Recorsio, *Ann. Chim., Rome*, 1959, **49**, 1593

54. L. Randaccio, E. Zangrando, M. H. Gei and A. G. Giumanini, *J. f. prakt. Chem.*, 1987, **329**, 187

55. (a) J. F. Walker, 'Formaldehyde', American Chemical Society Monograph, Reinhold Publishing, New York, 1964, 3rd Ed., pp 511 – 551; (b) E. M. Smolin and L. Rapoport, 'The Chemistry of Heterocyclic Compounds: *s*-Triazines and Derivatives', Interscience Publishers Ltd., London, 1959, pp 545 – 596; (d) H. H. Richmond, G. S. Myers and G. F. Wright, *J. Am. Chem. Soc.*, 1948, **70**, 3659; (e) A. T. Nielsen, D. W. Moore, M. D. Ogan and R. L. Atkins, *J. Org. Chem.*, 1979, **44**, 1678

56. E. Gartner and A. Kock, U.S. Patent 2365405, 1944

57. (a) Ciba Ltd., Swiss Patent, 1953, 294228; (b) H. Berthold, M. Fedke and W. Pritakow, Germ. (East) Patent, 1971, 94397

58. M. G. Neumann and R. A. M. C. De Groote, *J. Pharm. Sci.*, 1978, **67**, 1283

59. R. A. M. C. De Groote, and M. G. Neumann, *Ciencia e Cultura*, 1977, **D2.3**, 63

60. (a) Y. Kurono, K. Ikeda and K. Uekama, *Chem. Pharm. Bull.*, 1975, **23**, 409; (b) W. Ackerman, *Proc. Soc. Expt. Biol. Med.*, 1952, **80**, 362; (c) R. L. Thompson, *J. Immun.*, 1947, **55**, 347; (d) L. Neelakantan and W. H. Hartung, *J. Org. Chem.*, 1959, **24**, 1943

61. J. E. Orloff, 'Formaldehyde', 1909, Liebzig, Barth, p. 45

62. (a) T. M. Gorrie, S. K. Raman, H. K. Rouette and H. Zollinger, *Helv. Chim. Acta*, 1973, **56**, 175; (b) P. Skell and H. Suhr, *Ber.*, 1961, **94**, 3317

63. (a) M. Wadano, C. Trogus and K. Hess, *Chem. Ber.*, 1934, **67**, 174; (b) A. Skarbal and R. Leutner, *Oesterr. Chem. Z.*, 1937, **40**, 235; (c) H. Hasse and G. Maurer, *Ind. Eng. Chem. Res.*, 1991, **30**, 2195; (d) H. C. Sutton and T. M. Downes, *J. Chem. Soc., Chem. Comm.*, 1972, 1

64. A. Iliceto, S. Bezzi, N. Dallaporta and G. Giacommetti, *Gazz. Chim. Ital.*, 1951, **81**, 915

65. M. Baccaredda, *Gazz. Chim. Ital.*, 1947, **78**, 735

66. J. F. Walker, 'Formaldehyde', American Chemical Society Monograph, Reinhold Publishing, New York, 1964, 3rd Ed.

67. (a) R. Bieber and G. Trümpler, *Helv. Chim. Acta*, 1947, **30**, 706; (b) Ref. 63a

68. W. S. Hinegardner, E. I. du Pont de Nemours & Co., Inc., U. S. Patent 2002243, 1935

69. (a) H. M. Kvalnes, E. I. du Pont de Nemours & Co., Inc., U. S. Patent 2476212, 1949; Reissue 23, 174, 1949; (b) J. F. Walker, E. I. du Pont de Nemours & Co., Inc., U. S. Patent 2488363, 1949

70. R. C. Swain and P. Adams, American Cyanamid Co., U. S. Patent 2237092, 1942

71. (a) M. Delépine, *Compt. Rend.*, 1897, **124**, 1528; (b) H. Staudinger, R. Signer, H. Johner, M. Luthy, W. Kern, D. Russidis and O. Schweitzer, *Ann.*, 1929, **474**, 241

72. K. Moedritzer and J. R. van Wazer, *J. Phys. Chem.*, 1966, **70**, 2025

73. M. Wadano, *Ber.*, 1934, **67**, 191

74. R.P.Bell, *Adv. Phys. Org. Chem.*, 1966, 1

75. P. Valenta, *Coll. Czech. Chem. Commun.*, 1960, **25**, 853

76. (a) R. P. Bell and W. C. E. Higginson, *Proc. Roy. Soc.*, 1949, **197A**, 141; (b) M. Eigen, *Discuss. Faraday Soc.*, 1965, **39**, 7; (c) R. P. Bell and P. G. Evans, *Proc. Roy. Soc. London, Ser. A*, 1966, **291**, 297; (d) Ref. 74

77. R. P. Bell and D. P. Onwood, *Trans. Faraday Soc.*, 1962, **58**, 1557

78. L. H. Funderburk, L. Aldwin and W. P. Jencks, *J. Am. Chem. Soc.*, 1978, **100**, 5444

79. J. Büchi, *Pharm. Acta Helv.*, 1931, **6**, 1

80. (a) G. Lemme, *Chem. Ztg.*, 1903, **27**, 896; (b) S. S. Sadtler, *Am. J. Pharm.*, 1904, **76**, 84; (c) A. Seyewetz and H. Gibello, *Bull. Soc. Chim.*, 1904, **31**, 691

81. P. Borgstrom, *J. Am. Chem. Soc.*, 1923, **45**, 2150

82. Le Hénaff, *C. R. Acad. Sci.*, 1963, **256**, 3090

83. (a) Y. Katagiri, N. Sawaki, Y. Arai, H. Okochi and M. Igawa, *Chem. Letts.*, 1996, **3**, 197; (b) J. W. Munger, D. J. Jacob and M. R. Hoffmann, *J. Atmos. Chem.*, 1984, **1**, 335; (c) J. W. Munger, D. J. Jacob, J. M. Waldman and M. R. Hoffmann, *J. Geophys. Res.*, 1983, **88**, 5109; (d) L. W. Richards, J. A. Anderson, D. L. Blumenthal, J. A. McDonald, G. L. Kok and A. L. Lazrus, *Atmos. Environ.*, 1983, **17**, 911

84. (a) X. Rao and J. L. Collett, *Environ. Sci. and Technol.*, 1995, **29**, 1023; (b) E. G. Chapman, C. J. Barinaga, H. R. Udseth and R. D. Smith, *Atmos. Environ., A*, 1990, **24**, 2951; (c) J. W. Munger, C. Tiller and M. R. Hoffmann, *Science*, 1990, **86**, 545; (d) C. C. Ang, F. Lipari and S. J. Swarin, *Environ. Sci. Technol.*, 1987, **21**, 102; (e) J. W. Munger, C. Tiller and M. R. Hoffmann, *Science*, 1986, **231**, 247

85. (a) G. L. Kok, S. N. Gitlin and A. L. Lazrus, *J. Geophys. Res.*, 1986, **91**, 2801; (b) J. Hoigne, H. Bader, W. R. Haag and J. Staehelin, *Water Res.*, 1985, **19**, 993

86. (a) R. W. Dixon and H. Aasen, *Atmos. Environ.*, 1999, **33**, 2023; (b) K. R. Neubauer, S. T. Sum, M. V. Johnston and A. S. Wexler, *J. Geophys. Res., D*, 1996, **101**, 18701

87. (a) H. Kaneda, M. Takashio, T. Osawa, S. Kawakishi, S. Koshino and T. Tamaki, *J. Food Science*, 1996, **61**, 105; (b) H. Kaneda, M. Takashio, T. Osawa, S. Kawakishi and T. Tamaki, *J. Am. Soc. Brewing Chemists*, 1996, **54**, 115

88. H. Kaneda, T. Osawa, S. Kawakishi, M. Munekata and S. Koshino, *J. Agricultural and Food Chem.*, 1994, **42**, 2428

89. (a) D. O. Cooke, 'Inorganic Reaction Mechanisms', The Chemical Society, London, 1979, p. 71; (b) T. Cassen, *J. Chem. Educ.*, 1976, **53**, 197; (c) P. Jones and K. B. Oldham, *J. Chem. Educ.*, 1963, **40**, 366; (d) D. G. Chisman, *Sch. Sci. Rev.*, 1956, **38**, 100

90. C. Wagner, *Ber.*, 1929, **62**, 2873

91. P. Warneck, *J. Chem. Educ.*, 1989, **66**, 334

92. S. D. Boyce, M. R. Hoffmann, *J. Phys. Chem.*, 1984, **88**, 4740

93. M. G. Burnett, *J. Chem. Educ.*, 1982, **59**, 160

CHAPTER 2

Reaction of formaldehyde with aniline and aniline derivatives

CHAPTER 2: Reaction of formaldehyde with aniline and aniline derivatives

2.1 INTRODUCTION

The condensation of formaldehyde with aniline has been examined by a number of authors, mainly from a synthetic viewpoint. The products of the reaction depend on the pH of the reaction medium.

The reactions that occur in neutral media are shown in Scheme 2.1. Either path **a** or path **b** occurs: the reaction proceeds via path **a** when the reagents are present in equimolar amounts and via path **b** when aniline is present in at least 2 : 1 excess.

Scheme 2.1:

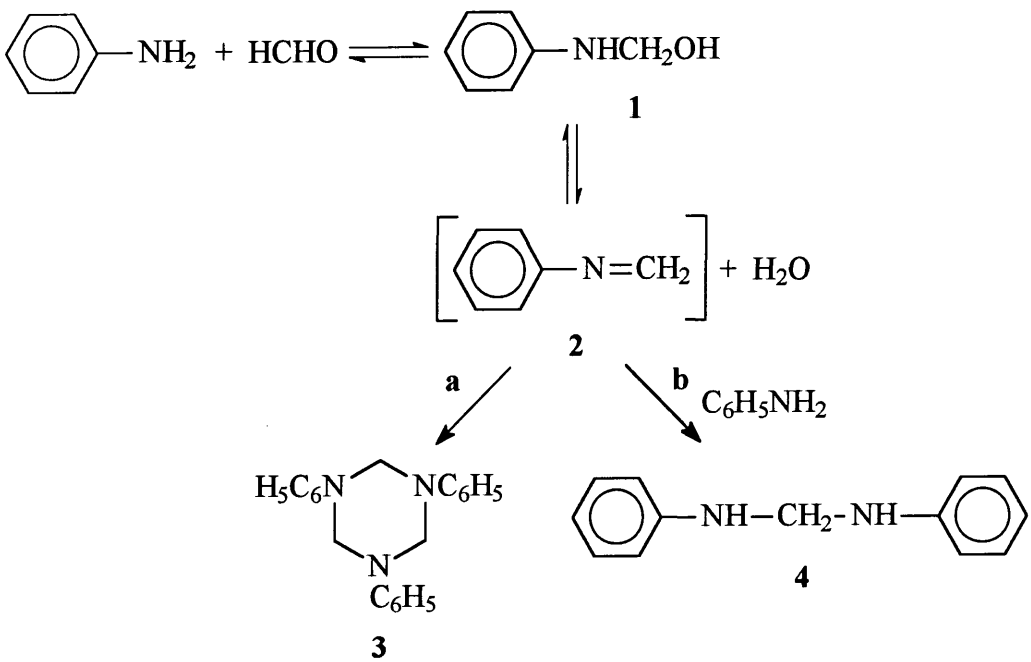

Initially an *N*-(hydroxymethyl)amine, or carbinolamine, **1** is formed. This then dehydrates to give an unstable imine, **2**, which immediately polymerises to give a cyclic trimer (**3**, path **a**) or reacts with another amine molecule to give a dinuclear species (**4**, path **b**).

In acidic media the reaction scheme is different from that in neutral media. In strongly acidic media the formaldehyde molecule is made more electrophilic by protonation (Scheme 2.2).

Scheme 2.2:

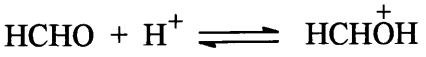

The concentration of free amine, the reactive species, is considerably lowered by protonation in acidic media (Scheme 2.3).

Scheme 2.3:

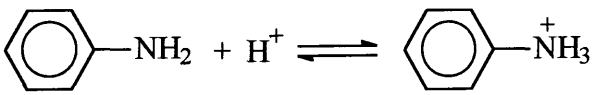

The pK_a of the anilinium ion[1] is 4.60, therefore aniline will be present mainly in the protonated form in acidic media but reaction will occur through the free base form of the amine rather than the protonated form. The anilinium ion is stabilised by efficient hydration in water: the solvation energy of a protonated cationic amine is larger than that of the free amine therefore it will be less favourable for the protonated form to add a hydroxymethyl group. Although the electron withdrawing effect of the hydroxymethyl group, $-CH_2OH$, is not much greater than that of hydrogen,[2] the addition of one hydroxymethyl group lowers the pK_a value of an amine by two to three units.[3] This has been attributed primarily to the decrease in solvation energy brought about by the replacement of a hydrogen atom by a hydroxymethyl group.

The reactions that occur in acidic media are shown in Scheme 2.4. Either path **c** or path **d** occurs: the reaction proceeds via path **c** when the reagents are present in equimolar amounts and via path **d** when aniline is present in at least 2 : 1 excess.

Scheme 2.4:

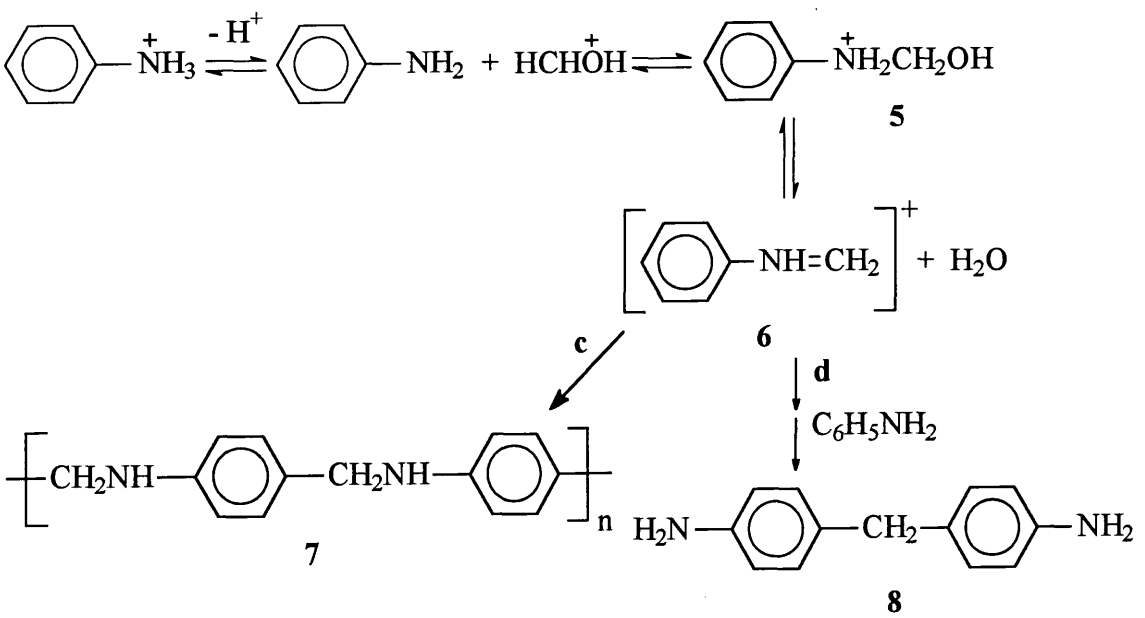

Initially a cationic *N*-(hydroxymethyl)amine, **5**, is formed. This then loses water to give an unstable iminium ion, **6**, which immediately polymerises to form a chain polymer (**7**, path **c**) or reacts with another amine molecule to give a dinuclear species (**8**, path **d**). Although **8** is the final product in the presence of excess aniline, initially the product with the amino nitrogens directly attached to the $-CH_2$ group, **4**, forms. **4** rapidly decomposes in acid solution[4] to regenerate the reactants, the amine and the iminium ion. These react more slowly to give **8** via a series of protonation / intermolecular rearrangement steps as described by Santhanalakshmi[4b]: it is not formed by intramolecular rearrangement of **4** as suggested by some authors.[5]

There are a number of papers in the literature[4c,6] that suggest that the initial products of reaction of formaldehyde with aniline and aniline derivatives in the presence of acid are 4-aminobenzyl alcohol, **9**, and *N*-(4-aminobenzyl)aniline, **10**. These studies were carried out at 40 – 80 °C, much higher temperatures than other studies.

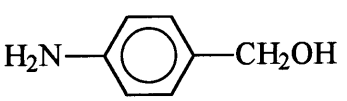

9

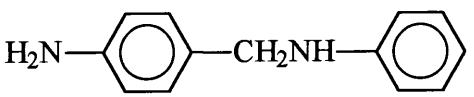

10

9 is formed by attack of formaldehyde at the para position of the aniline molecule. **10** is said to be unstable in the presence of acid and reverts instantaneously back into the reactants, aniline and **9**. Product **8** forms at a later stage in the reaction by attack of the iminium ion derived from **9** on the para position of the aniline molecule.[4c] However, the amino nitrogen is more electron rich than the other positions in the aniline molecule, therefore reaction at the nitrogen leading to formation of *N*-(hydroxymethyl)amine will occur faster.

The product of reaction of aniline with formaldehyde therefore depends on the pH of the system and the molar ratio of amine to formaldehyde. **3**, **4**, and **8** can be isolated as solids and **7** as an insoluble thermosetting polymer.[4b] The products formed in neutral media, **3** and **4**, are unstable in acidic solutions and convert to **7** and **8** respectively via intermolecular rearrangement.

A major difference between reactions in neutral and acidic media is that under neutral conditions reaction occurs through the nitrogen centre of aniline whilst in acidic solution reaction occurs through the para ring carbon. This may indicate that the nucleophilicity of the para ring carbon is reduced to a lesser extent by protonation than that of the nitrogen atom. A further possibility is that electrophilic attack is possible at the para carbon atom of the protonated anilinium ion.

The mechanism of the reaction of formaldehyde with aniline and aniline derivatives has not been studied comprehensively, especially in neutral and alkaline conditions. Only Ogata et al[7] and Abrams and Kallen[8] have reported kinetic data for the reaction.

Ogata et al[7] examined the effect of substituents on the aniline ring on the rate constant for reaction with formaldehyde to give dinuclear products **10** in the pH range 0.7 to 1.6 at 25 °C. They suggested that electrophilic attack of the iminium ion on the amine is the rate determining step in the formation of dinuclear products.

Abrams and Kallen[8] studied the reaction of formaldehyde with aniline and aniline derivatives in the pH range 0 to 14 at 25 °C and 1.0 M ionic strength, with formaldehyde present in large excess relative to the amine. The products were *N*-(hydroxymethyl)amines rather than imines. When formaldehyde is in excess, a second formaldehyde molecule can add to *N*-(hydroxymethyl)amines formed from primary amines to give *N,N*-(dihydroxymethyl)amines (**11**, Scheme 2.5).

Scheme 2.5: $RNHCH_2OH + HCHO_{(aq)} \rightleftharpoons RN(CH_2OH)_2$

11

Table 2.1 describes the equilibrium constants K_1, K_2 and K_3 obtained by Abrams and Kallen[8] for formation of the *N*-(hydroxymethyl)amine, the cationic *N*-(hydroxymethyl)amine formed from the protonated form of the amine, and the *N,N*-(dihydroxymethyl)amine respectively, described in Scheme 2.6 and Equations 2.1 to 2.3. It is thought that the cationic *N*-(hydroxymethyl)amine only forms directly when formaldehyde is present in such large excess that the protonated amine also reacts.[3]

Scheme 2.6:

$$RNH_2 + HCHO_{(aq)} \overset{K_1}{\rightleftharpoons} RNHCH_2OH$$

$$\overset{+}{R}NH_3 + HCHO_{(aq)} \overset{K_2}{\rightleftharpoons} \overset{+}{R}NH_2CH_2OH$$

$$RNHCH_2OH + HCHO_{(aq)} \overset{K_3}{\rightleftharpoons} RN(CH_2OH)_2$$

$$K_1 = \frac{[RNHCH_2OH]}{[RNH_2][HCHO_{(aq)}]} \qquad (2.1)$$

$$K_2 = \frac{[\overset{+}{R}NH_2CH_2OH]}{[\overset{+}{R}NH_3][HCHO_{(aq)}]} \qquad (2.2)$$

$$K_3 = \frac{[RN(CH_2OH)_2]}{[RNHCH_2OH][HCHO_{(aq)}]} \qquad (2.3)$$

Table 2.1: Results reported by Abrams and Kallen[8] for the equilibrium constants for formation of *N*-(hydroxymethyl)amine, K_1, the cationic *N*-(hydroxymethyl)amine, K_2, and *N*,*N*-(dihydroxymethyl)amine, K_3, for aniline and its derivatives at 25 °C, I = 1 M

amine	pK_a	equilibrium constant / $dm^3\ mol^{-1}$			pK_a ref.
		K_1	K_2	K_3	
aniline	4.60	22.3	0.10	-	1
4-methoxyaniline	5.36	23.2	0.30	-	1
4-methylaniline	5.08	22.7	0.30	-	1
4-chloroaniline	4.15	26.0	0.30	-	1
4-cyanoaniline	1.71	27.2	-	-	1
4-nitroaniline	1.02	27.3	0.85	-	1
3-fluoro-4-nitroaniline	-0.30	20.0	-	-	8
3,5-dinitroaniline	0.23	23.0	-	1.4	1
N-methylaniline	4.85	13.2	0.55		1
4-methoxy-*N*-methylaniline	5.78	18.6	0.85	-	9
4-methyl-*N*-methylaniline	5.54	16.2	0.20	-	9
4-chloro-*N*-methylaniline	4.21	10.6	0.45	-	9
4-nitro-*N*-methylaniline	0.55	2.8	-	-	1

N-(Hydroxymethyl)amine, **1**, and its protonated cationic form, **5**, are related by an acid - base equilibrium. Using the cycle shown in Scheme 2.7, the value of $K_{a(5)}$, the acid dissociation constant for **5**, can be calculated using Equation 2.4.

Scheme 2.7:

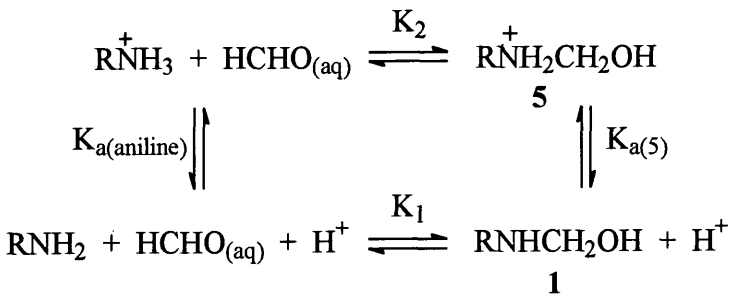

$$K_{a(5)} = K_{a(aniline)} \bullet \frac{K_1}{K_2} \qquad (2.4)$$

The K_1 and K_2 values for aniline given in Table 2.1 give a value for $K_{a(5)}$ of 5.6×10^{-3} which corresponds to a $pK_{a(5)}$ of 2.25.

The equilibrium constants in Table 2.1 show a relatively small dependence on basicity. K_1 values for *N*-methylanilines are smaller than those for anilines. K_3 values are smaller than K_1: the authors attributed this to steric, solvation and orbital electronegativity factors. They also state *N*-(hydroxymethyl)amine formation occurs by general acid and general base catalysed pathways in addition to a pH independent pathway. They obtained catalytic constants for a range of general acids and bases, including the species present in phosphate buffers, $H_2PO_4^-$ and HPO_4^{2-}, for three aniline derivatives (Table 2.2).

Table 2.2: Catalytic constants determined by Abrams and Kallen[8] at 25 °C, I = 1.0 M

catalyst	catalytic constant / $dm^6\ mol^{-2}\ s^{-1}$		
	3-fluoro-4-nitroaniline	4-nitroaniline	4-cyanoaniline
$H_2PO_4^-$	1.15	6.31	-
HPO_4^{2-}	0.52	4.57	14.5

For comparison, Kallen and Jencks[3] obtained equilibrium constants for the reaction of five primary aliphatic amines with formaldehyde to give the *N*-(hydroxymethyl)amine and *N,N*-(dihydroxymethyl)amine products. They obtained values for K_1 and K_3 and for K_4, described by Scheme 2.8 and Equation 2.5.

Scheme 2.8:

$$RNH_2 + 2HCHO_{(aq)} \overset{K_4}{\rightleftharpoons} RN(CH_2OH)_2$$

$$K_4 = \frac{[RN(CH_2OH)_2]}{[RNH_2][HCHO_{(aq)}]^2} \qquad (2.5)$$

They found that K_3 is always much smaller than K_1 and K_4, but the relative values of K_1 and K_4 depend on the amine used. They obtained K_1 values in the range 6 - 55 $dm^3\ mol^{-1}$, K_3 = 0.3 - 2 $dm^3\ mol^{-1}$ and K_4 = 2 - 110 $dm^6\ mol^{-2}$ for aliphatic amines.

There has previously been little study on the kinetics of the reaction of formaldehyde with aniline and its derivatives. The reaction of aqueous formaldehyde with aniline and seven aniline derivatives was therefore investigated here in the pH range 6 to 8 to gain information on the rate constants and mechanism involved. The reaction was studied under conditions with formaldehyde present in large excess. This excludes the possibility of formation of dinuclear species **4** and **8**. However it does facilitate the formation of the *N,N*-(dihydroxymethyl)amine. For kinetic measurements the contribution due to formation of the *N,N*-(dihydroxymethyl)amine was minimised by using sufficiently low formaldehyde concentrations. The concentration of aqueous formaldehyde is given as $[HCHO_{(aq)}]$, which includes both hydrated and unhydrated formaldehyde. The amines studied are shown in Table 2.3.

Table 2.3: Amines studied in the reaction with aqueous formaldehyde

amine	pK_a[†]	amine	pK_a[†]
aniline 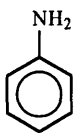	4.60	3-chloroaniline 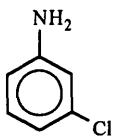	3.46
4-methylaniline[‡] 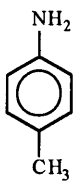	5.08	3-cyanoaniline[¶] 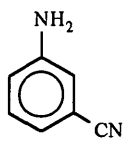	2.75
4-dimethylaminoaniline[§] 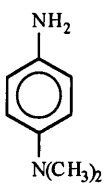	6.59	3-nitroaniline 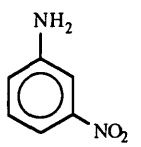	2.47
4-chloroaniline 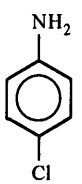	4.15	*N*-methylaniline 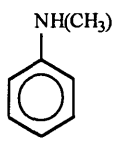	4.85

[†] pK_a values correspond to dissociation of the protonated amines at 25 °C, reference 1

[‡] also known as *p*-toluidine

[§] also known as *N*,*N*-dimethyl-1,4-phenylenediamine

[¶] also known as 3-aminobenzonitrile

This range of anilines was chosen so that factors such as effects of pK_a, the presence of electron donating and withdrawing groups and the effect of substitution on the amino nitrogen could be investigated.

2.2 RESULTS AND DISCUSSION

2.2.1 Reaction of aqueous formaldehyde with aniline, $C_6H_5NH_2$

2.2.1.1 Absorbance against wavelength spectra and absorbance against time plots

The reaction of 5.3×10^{-3} to 0.10 M aqueous formaldehyde with 1.0×10^{-4} M aniline at 25 °C in the pH range 5.8 to 7.9 was investigated.

Absorbance against wavelength spectra were obtained over time for 1.0×10^{-4} M aniline with and without the presence of 0.05 or 0.10 M aqueous formaldehyde. The spectra with aqueous formaldehyde added show a shift to higher wavelength. The higher the concentration of aqueous formaldehyde, the greater the change in spectrum observed. All reactions are complete by the first spectrum (Figure 2.1).

Figure 2.1: Effect of adding 0.05 and 0.1 M aqueous formaldehyde on the uv / vis spectrum of 1.0×10^{-4} M aniline at 25 °C, unbuffered, in aqueous solution

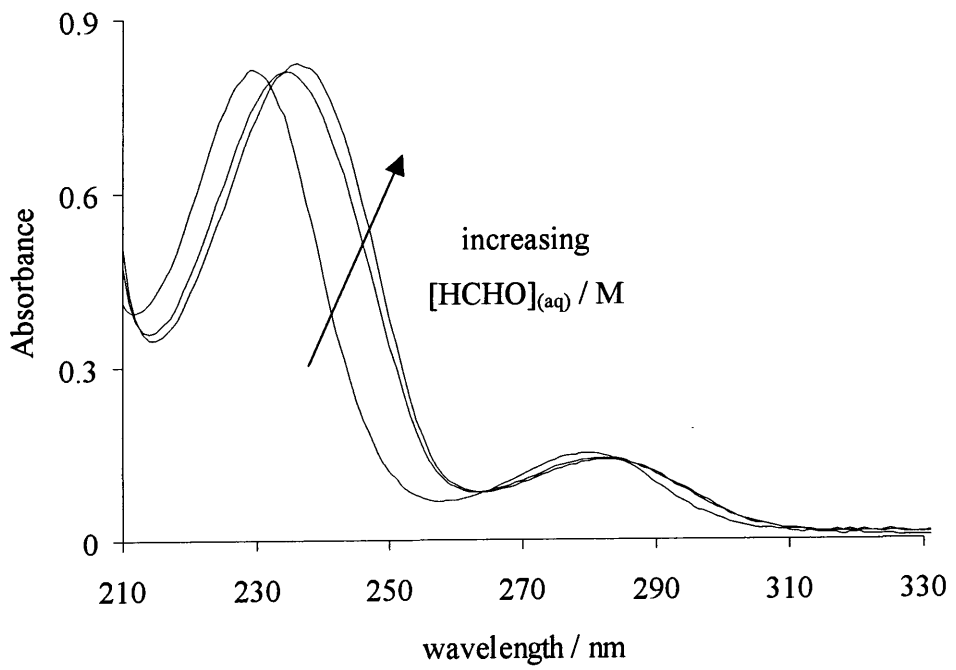

Plots of absorbance against time were obtained for the reaction of 1.0×10^{-4} M aniline and 5.3×10^{-3} to 0.053 M aqueous formaldehyde at pH 5.8 to 7.9, using a potassium dihydrogen phosphate / sodium hydroxide buffer system with $[KH_2PO_4]_{stoich} = 0.05$ M,

and maintaining a constant ionic strength, I, of 1.0 M using potassium chloride. Formation of the product at 245 nm was followed. Plots were first order and were fitted using a single exponential equation to obtain k_{obs} / s^{-1} values (Figure 2.2, Table 2.4).

Figure 2.2: Absorbance against time plot at 245 nm with single exponential fit superimposed for the reaction of 1.0×10^{-4} M aniline with 0.011 M aqueous formaldehyde at pH 5.8, $[KH_2PO_4]_{stoich}$ = 0.05 M, I = 1 M

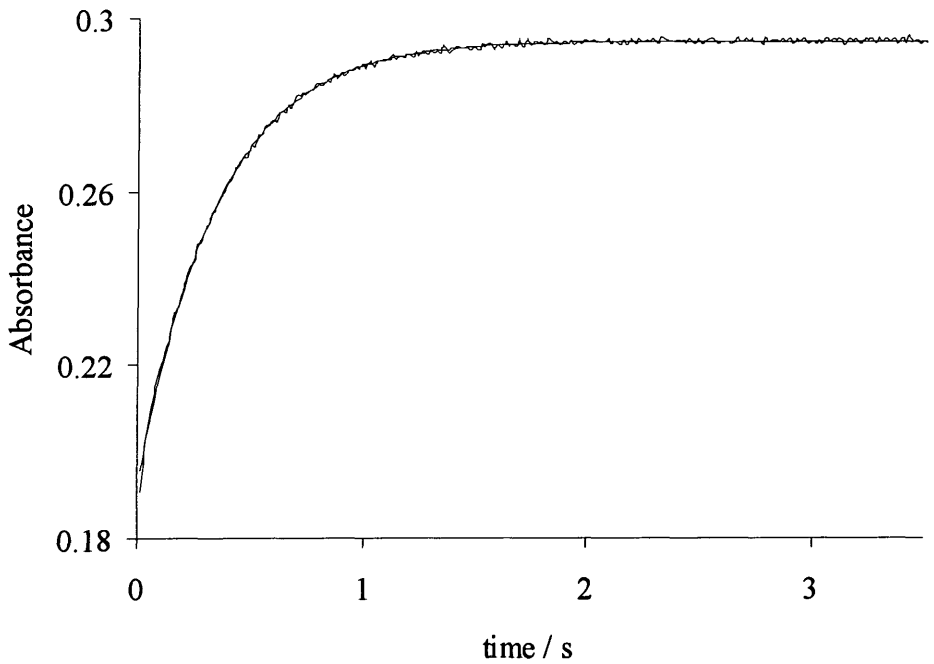

Table 2.4: k_{obs} / s^{-1} values for 1.0×10^{-4} M aniline with varied aqueous formaldehyde concentration, pH 5.8 to 7.9, 25 °C, aqueous solution, $[KH_2PO_4]_{stoich}$ = 0.05 M, I = 1 M

$[HCHO_{(aq)}]$ / M	pH 5.8		pH 6.9		pH 7.9	
	k_{obs} / s^{-1}	ΔA	k_{obs} / s^{-1}	ΔA	k_{obs} / s^{-1}	ΔA
5.3×10^{-3}	2.61 ± 0.10	0.06	3.08 ± 0.29	0.07	2.97 ± 0.17	0.09
0.011	2.84 ± 0.06	0.11	3.47 ± 0.06	0.11	3.40 ± 0.07	0.16
0.021	3.53 ± 0.16	0.17	4.34 ± 0.11	0.18	4.42 ± 0.25	0.24
0.035	4.22 ± 0.11	0.22	5.27 ± 0.07	0.23	5.42 ± 0.07	0.30
0.053	5.16 ± 0.07	0.28	6.62 ± 0.09	0.28	6.84 ± 0.09	0.37

The reaction followed is an equilibrium as the change in absorbance over time, ΔA, increases with increasing aqueous formaldehyde concentration.

Although *N*-(hydroxymethyl)amines formed from aromatic amines and formaldehyde have not been isolated,[10] the data obtained by Abrams and Kallen[8] indicate that the major product of interaction of formaldehyde and anilines in aqueous solution is the *N*-(hydroxymethyl)amine. Spectral shifts and the magnitude of the equilibrium constants indicate that, as with aliphatic amines,[3] the formaldehyde adducts of aromatic amines are *N*-(hydroxymethyl)amines and not imines.[11]

Plotting k_{obs} / s^{-1} against aqueous formaldehyde concentration allowed the determination of the forward and back rate constants, k_f / dm^3 mol^{-1} s^{-1} and k_b / s^{-1}, given in Scheme 2.9 where $HCHO_{(aq)}$ is the sum contribution from hydrated and unhydrated formaldehyde. k_f / dm^3 mol^{-1} s^{-1} and k_b / s^{-1} are equal to the gradient and intercept respectively (Appendix 1). Linear regression yielded correlation coefficients between 0.997 and 0.999 (Figure 2.3).

Scheme 2.9: $RNH_2 + HCHO_{(aq)} \underset{k_b}{\overset{k_f}{\rightleftharpoons}} RNHCH_2OH$

Figure 2.3: k_{obs} / s^{-1} against $[HCHO_{(aq)}]$ / M at pH 6.9, 25 °C, in aqueous solution, with $[KH_2PO_4]_{stoich}$ = 0.05 M, I = 1 M

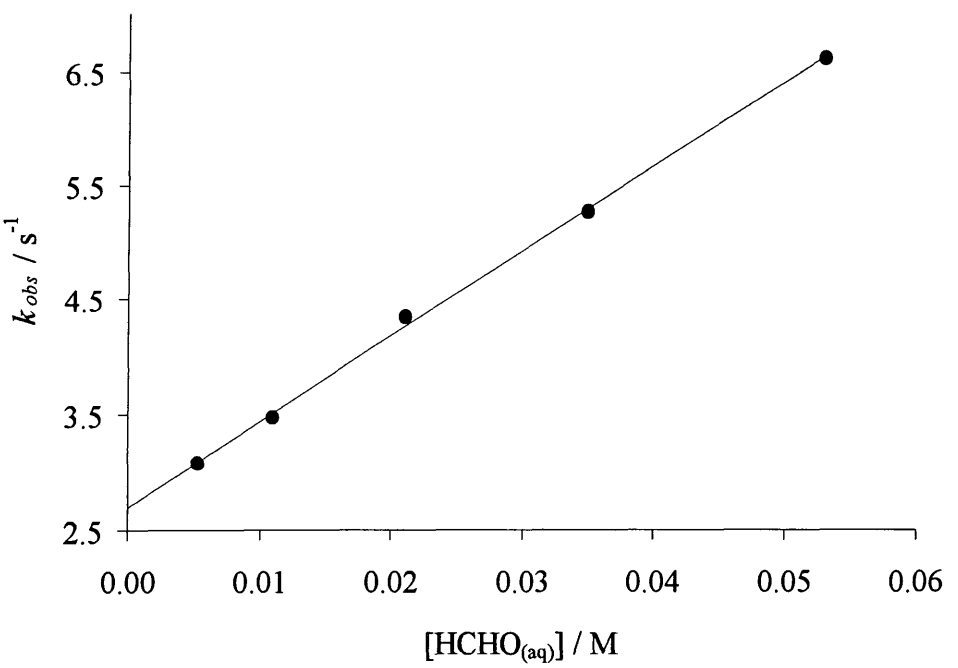

The values obtained for k_f / dm^3 mol^{-1} s^{-1} and k_b / s^{-1} and the calculated equilibrium constant K / dm^3 mol^{-1}, where K = k_f / k_b, are given in Table 2.5.

Table 2.5: Values of k_f and k_b and the equilibrium constant, K, for the reaction of aniline with aqueous formaldehyde, pH 5.8 to 7.9, 25 °C, aqueous solution, I = 1 M

pH	k_f / dm^3 mol^{-1} s^{-1}	k_b / s^{-1}	K / dm^3 mol^{-1}
5.8	53.9 ± 1.7	2.33 ± 0.05	23 ± 1
7.0	73.9 ± 1.5	2.71 ± 0.04	27 ± 1
7.9	80.9 ± 2.4	2.59 ± 0.07	31 ± 1

Since none of the reactants will be appreciably protonated in the pH range used, the value of the equilibrium constant, K, would be expected to be independent of pH. The slight increase observed in the values in Table 2.5 may therefore be within experimental error: the average value of K is 27 ± 4 dm^3 mol^{-1}. This is in good agreement with the value of 22.3 dm^3 mol^{-1} obtained by Abrams and Kallen[8] from equilibrium spectrophotometric measurements.

The rate constant for the formation of the *N*-(hydroxymethyl)amine, k_f, shows a real increase with increasing pH and this was investigated further.

2.2.1.2 General acid and base catalysis

To determine whether the buffer concentration has any effect on the value of k_{obs} / s^{-1} obtained, the reaction was studied using a constant aqueous formaldehyde concentration and varying the buffer concentration whilst retaining the buffer ratio and maintaining the ionic strength at 1.0 M using potassium chloride.

Initially the reaction of 0.053 M aqueous formaldehyde with 1.0 × 10^{-4} M aniline in the pH range 5.8 to 7.9 using potassium dihydrogen phosphate / sodium hydroxide buffers with a stoichiometric potassium dihydrogen phosphate concentration of 0.050 to 0.144 M was studied. The k_{obs} / s^{-1} values obtained are shown in Table 2.6.

Table 2.6: k_{obs} / s^{-1} values for 1.0×10^{-4} M aniline and 0.053 M aqueous formaldehyde with varied buffer concentration at pH 5.8 to 7.9, aqueous solution, 25 °C, I = 1 M

$[KH_2PO_4]_{stoich}$ / M	pH 5.8		pH 6.9		pH 7.9	
	k_{obs} / s^{-1}	ΔA	k_{obs} / s^{-1}	ΔA	k_{obs} / s^{-1}	ΔA
0.050	4.76 ± 0.02	0.32	7.41 ± 0.08	0.33	8.25 ± 0.12	0.28
0.080	6.07 ± 0.12	0.32	9.11 ± 0.08	0.33	9.90 ± 0.28	0.28
0.100	6.93 ± 0.14	0.32	10.2 ± 0.1	0.33	11.1 ± 0.2	0.28
0.120	7.96 ± 0.13	0.32	11.2 ± 0.1	0.33	12.1 ± 0.2	0.28
0.144	8.81 ± 0.19	0.32	12.6 ± 0.1	0.33	13.3 ± 0.2	0.28

The k_{obs} values obtained show a dependence on $[KH_2PO_4]_{stoich}$: plotting k_{obs} / s^{-1} against $[KH_2PO_4]_{stoich}$ / M gives linear plots. Linear regression yielded correlation coefficients between 0.998 and 0.999 (Figure 2.4). The values obtained for the gradient and intercept of the plots are given in Table 2.7.

Figure 2.4: k_{obs} / s^{-1} against $[KH_2PO_4]_{stoich}$ / M at pH 5.8, 6.9 and 7.9 at 25 °C in aqueous solution with $[HCHO_{(aq)}]$ = 0.053 M, I = 1 M

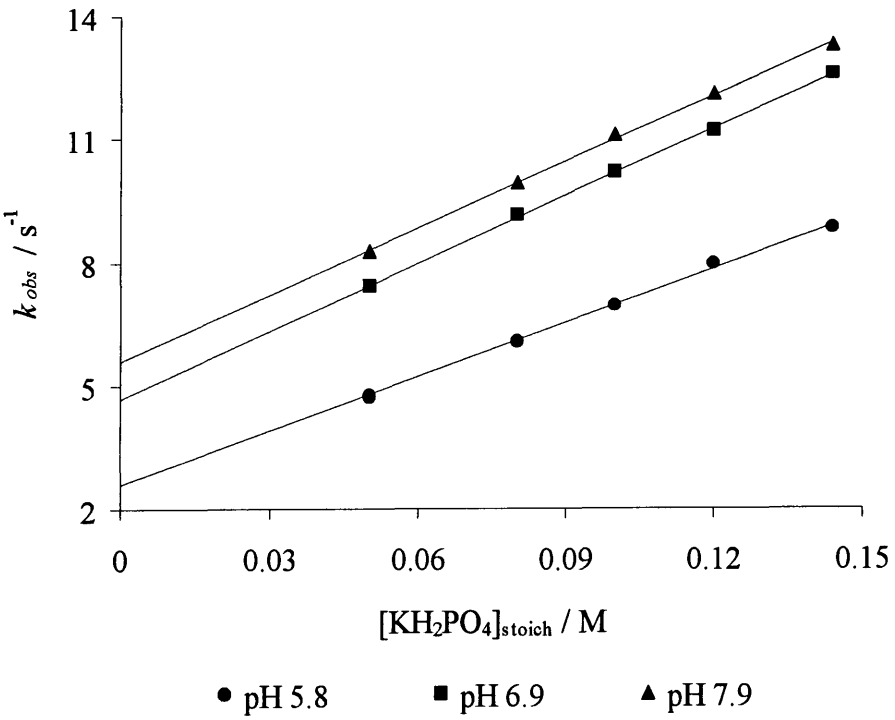

Table 2.7: Gradients and intercepts obtained for k_{obs} / s^{-1} against $[KH_2PO_4]_{stoich}$ / M with 0.053 M aqueous formaldehyde at pH 5.8 to 7.9, 25 °C, aqueous solution, I = 1 M

pH	gradient / $dm^3\ mol^{-1}\ s^{-1}$	intercept / s^{-1}
5.8	43.8 ± 1.2	2.58 ± 0.13
6.9	53.0 ± 1.1	4.84 ± 0.11
7.9	53.8 ± 1.2	5.61 ± 0.12

The intercept obtained increases with increasing pH and the gradient shows a slight variation with pH. The dependence of k_{obs} on $[KH_2PO_4]_{stoich}$ at constant pH implies general catalysis: if it was merely specific there would be no dependence on $[KH_2PO_4]_{stoich}$. Plotting k_{obs} against $[KH_2PO_4]_{stoich}$ at different pH gives an indication of whether the catalysis is due to one or both buffer components: if the lines are parallel, this implies catalysis by either the acid or base form of the buffer whereas non-parallel lines implies catalysis by both buffer components. The gradients do show a slight dependence on pH (Figure 2.3): combining this with the results reported by Abrams and Kallen[8] it is probable that the reaction is both acid and base catalysed. There is very little change in the gradients at different pH, which implies that the catalytic constants for the buffer components are approximately equal.

The intercept obtained in Table 2.7 describes the non-buffer catalysed pathway. The variation of the intercept with pH describes the contribution to the rate constant of the hydronium ion, hydroxide ion and solvent catalysed terms in the rate equation.

As the reaction is subject to general acid and general base catalysis in addition to a pH independent pathway, k_{obs} can be expressed in terms of Equation 2.6. k_w is the rate constant for the uncatalysed, or solvent catalysed, reaction, k_{H+} and k_{OH-} are the rate constants due to catalysis by protons and hydroxide ions respectively, and k_{H2PO4-} and k_{HPO42-} the general acid and base rate constants due to the buffer components. Each of these terms contains contributions to both the forward and reverse rate coefficients, k_f and k_b.

$$k_{obs} = k_w + k_{H^+}[H^+] + k_{OH^-}[OH^-] + k_{H2PO4^-}[H_2PO_4^-] + k_{HPO42^-}[HPO_4^{2-}] \quad \textbf{(2.6)}$$

The first three terms of Equation 2.6 are constant at a given buffer ratio and constant ionic strength. Therefore at constant pH, Equation 2.6 simplifies to Equation 2.7.

$$k_{obs} = \text{constant} + k_{H2PO4^-}[H_2PO_4^-] + k_{HPO4^{2-}}[HPO_4^{2-}] \quad \textbf{(2.7)}$$

The separate buffer component concentrations may be expressed in terms of a fraction of $[KH_2PO_4]_{stoich}$ as in Equations 2.8 and 2.9.

$$[H_2PO_4^-] = x[KH_2PO_4]_{stoich} \quad \textbf{(2.8)}$$

$$[HPO_4^{2-}] = (1 - x)[KH_2PO_4]_{stoich} \quad \textbf{(2.9)}$$

Substituting these into Equation 2.6 gives Equation 2.10.

$$k_{obs} = \text{constant} + x\,k_{H2PO4^-}[KH_2PO_4]_{stoich} + (1 - x)k_{HPO4^{2-}}[KHPO_4]_{stoich} \quad \textbf{(2.10)}$$

Therefore plotting k_{obs} / s^{-1} against $[KH_2PO_4]_{stoich}$ / M should give a linear plot, as obtained, with a gradient equal to $\{x\ k_{H2PO4^-} + (1\text{-}x)\ k_{HPO4^{2-}}\}$ and intercept equal to $\{k_w + k_{H^+}[H^+] + k_{OH^-}[OH^-]\}$. Therefore the values obtained for the gradient at different pH in Table 2.7 can be used to calculate values of k_{H2PO4^-} and $k_{HPO4^{2-}}$. The values of x and (1-x), the fraction of buffer present as $H_2PO_4^-$ and HPO_4^{2-} respectively, are given in Table 2.8.

Table 2.8: Buffer component ratios at the different pH values used

pH	$[H_2PO_4^-] : [HPO_4^{2-}]$	x	1-x
5.8	0.89 : 0.11	0.89	0.11
7.0	0.42 : 0.58	0.42	0.58
7.9	0.07 : 0.93	0.07	0.93

As the gradient obtained is equal to $\{x\ k_{H2PO4^-} + (1\text{-}x)\ k_{HPO4^{2-}}\}$, plotting the values for the gradient given in Table 2.7 against x should give a linear plot with a gradient equal to $\{k_{H2PO4^-} - k_{HPO4^{2-}}\}$ and an intercept equal to $k_{HPO4^{2-}}$. Using this method, values for

k_{H2PO4^-} and k_{HPO42^-} of 43 ± 13 and 56 ± 3 $dm^6\ mol^{-2}\ s^{-1}$ respectively are obtained. These values indicate that both buffer components contribute extensively to catalysis of the reaction. Abrams and Kallen[8] obtained catalytic constants in the range 1 to 15 $dm^6\ mol^{-2}\ s^{-1}$ for substituted anilines.

The reaction was also studied using a lower aqueous formaldehyde concentration of 0.011 M at pH 6.9 using a potassium dihydrogen phosphate / sodium hydroxide buffer with a stoichiometric potassium dihydrogen phosphate concentration of 0.050 to 0.144 M. The ionic strength was maintained at 1.0 M using potassium chloride. An aniline concentration of 1.0×10^{-4} M was used throughout. The results are shown in Table 2.9.

Table 2.9: k_{obs} / s^{-1} values for 1.0×10^{-4} M aniline and 0.011 M aqueous formaldehyde with varied buffer concentration at pH 6.9, aqueous solution, 25 °C, I = 1 M

$[KH_2PO_4]_{stoich}$ / M	pH 6.9	
	k_{obs} / s^{-1}	ΔA
0.050	3.40 ± 0.05	0.12
0.080	4.46 ± 0.19	0.12
0.100	5.40 ± 0.26	0.12
0.120	5.89 ± 0.23	0.12
0.144	6.77 ± 0.36	0.12

Plotting k_{obs} / s^{-1} against $[KH_2PO_4]_{stoich}$ / M gives a linear plot. The values obtained for the gradient and intercept are given in Table 2.10. Linear regression gave a correlation coefficient of 0.994.

Table 2.10: Gradient and intercept obtained for k_{obs} / s^{-1} against $[KH_2PO_4]_{stoich}$ / M with 0.011 M aqueous formaldehyde at pH 6.9, 25 °C, aqueous solution, I = 1 M

pH	gradient / $dm^3\ mol^{-1}\ s^{-1}$	intercept / s^{-1}
6.9	36.4 ± 1.7	1.57 ± 0.17

Using this lower aqueous formaldehyde concentration, the major reaction being followed is the reverse reaction, described by k_b.

2.2.2 Reaction of aqueous formaldehyde with 4-methylaniline

2.2.2.1 Absorbance against wavelength spectra and absorbance against time plots

The reaction of 5.3×10^{-3} to 0.10 M aqueous formaldehyde with 1.0×10^{-4} M 4-methylaniline at 25 °C in the pH range 5.8 to 7.9 was investigated.

Absorbance against wavelength spectra were obtained over time for 1.0×10^{-4} M 4-methylaniline with and without the presence of 0.05 or 0.10 M aqueous formaldehyde. The spectra with aqueous formaldehyde added show a shift to higher wavelength with a corresponding increase in absorbance as compared to the spectrum of 1.0×10^{-4} M 4-methylaniline alone. The higher the concentration of aqueous formaldehyde, the greater the change in spectrum observed. All reactions are complete by the first spectrum (Figure 2.5).

Figure 2.5: Effect of adding 0.05 and 0.1 M aqueous formaldehyde on the uv / vis spectrum of 1.0×10^{-4} M 4-methylaniline at 25 °C, pH 7, in aqueous solution

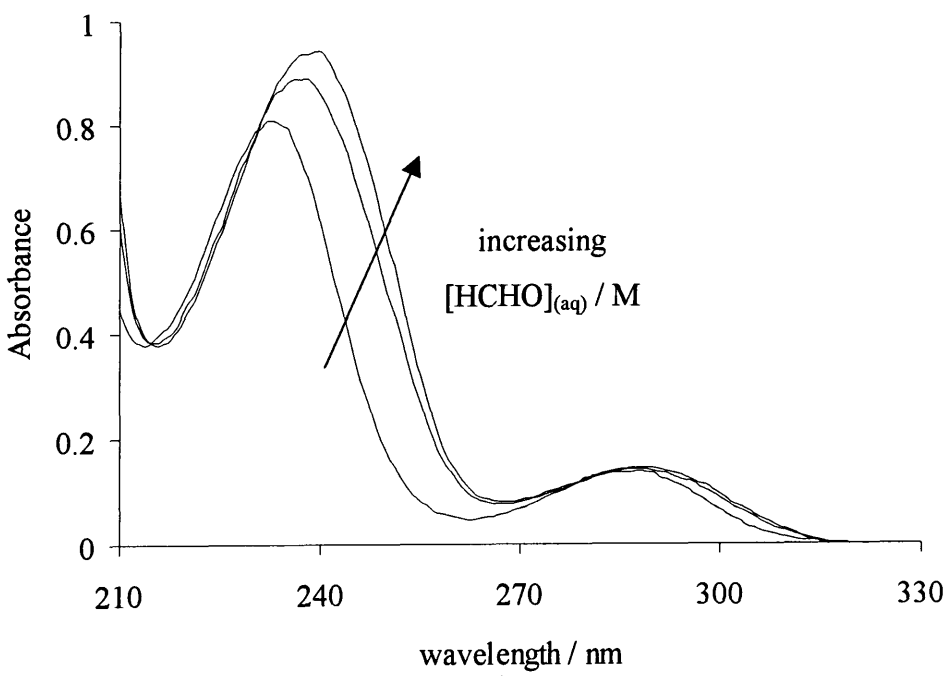

Plots of absorbance against time were obtained for the reaction of 1.0×10^{-4} M 4-methylaniline and 5.3×10^{-3} to 0.053 M aqueous formaldehyde at pH 5.8 to 7.9, using a potassium dihydrogen phosphate / sodium hydroxide buffer system with $[KH_2PO_4]_{stoich}$ = 0.05 M, and maintaining a constant ionic strength, I, of 1.0 M using potassium chloride. Formation of the product at 245 nm was followed. Plots were first order and were fitted using a single exponential equation to obtain k_{obs} / s^{-1} values (Table 2.11).

Table 2.11: k_{obs} / s^{-1} for 1.0×10^{-4} M 4-methylaniline, varied aqueous formaldehyde concentration, pH 5.8 to 7.9, 25 °C, aqueous solution, $[KH_2PO_4]_{stoich}$ = 0.05 M, I = 1 M

$[HCHO_{(aq)}]$ / M	pH 5.8		pH 6.9		pH 7.9	
	k_{obs} / s^{-1}	ΔA	k_{obs} / s^{-1}	ΔA	k_{obs} / s^{-1}	ΔA
5.3×10^{-3}	3.59 ± 0.61	0.01	4.05 ± 0.64	0.01	3.86 ± 0.28	0.02
0.011	3.92 ± 0.29	0.02	4.60 ± 0.31	0.02	4.40 ± 0.19	0.03
0.021	4.26 ± 0.31	0.03	5.70 ± 0.31	0.03	5.83 ± 0.25	0.05
0.035	5.20 ± 0.15	0.04	7.44 ± 0.31	0.04	7.86 ± 0.27	0.06
0.053	6.34 ± 0.25	0.05	9.65 ± 0.41	0.05	10.2 ± 0.2	0.07

The reaction is an equilibrium as the change in absorbance over time, ΔA, increases with increasing aqueous formaldehyde concentration. Plotting k_{obs} / s^{-1} against aqueous formaldehyde concentration gives values for k_f / dm^3 mol^{-1} s^{-1} and k_b / s^{-1} as shown in Table 2.12. Linear regression yielded correlation coefficients between 0.998 and 0.999.

Table 2.12: k_f, k_b and the equilibrium constant, K, for the reaction of 4-methylaniline with aqueous formaldehyde, pH 5.8 to 7.9, 25 °C, aqueous solution, I = 1 M

pH	k_f / dm^3 mol^{-1} s^{-1}	k_b / s^{-1}	K / dm^3 mol^{-1}
5.8	73.9 ± 1.5	2.71 ± 0.04	27 ± 1
6.9	118 ± 3	3.34 ± 0.08	35 ± 1
7.9	136 ± 3	3.05 ± 0.10	45 ± 2

The rate constant for the formation of the *N*-(hydroxymethyl)amine, k_f, shows an increase with increasing pH whereas the rate constant for dissociation of the *N*-(hydroxymethyl)amine, k_b, shows no real dependence on pH. Consequently the equilibrium constant, K, increases with increasing pH.

2.2.2.2 General acid and base catalysis

To determine whether the buffer concentration has any effect on the value of k_{obs} / s^{-1} obtained, the reaction was studied using a constant aqueous formaldehyde concentration and varying the buffer concentration whilst retaining the buffer ratio and maintaining the ionic strength at 1.0 M using potassium chloride.

Initially the reaction of 0.053 M aqueous formaldehyde with 1.0×10^{-4} M 4-methylaniline at pH 7.9 using a potassium dihydrogen phosphate / sodium hydroxide buffer with a stoichiometric potassium dihydrogen phosphate concentration of 0.050 to 0.144 M was studied. The k_{obs} / s^{-1} values obtained are shown in Table 2.13.

Table 2.13: k_{obs} / s^{-1} for 1.0×10^{-4} M 4-methylaniline and 0.053 M aqueous formaldehyde, varied buffer concentration, pH 7.9, aqueous solution, 25 °C, I = 1 M

$[KH_2PO_4]_{stoich}$ / M	pH 7.9	
	k_{obs} / s^{-1}	ΔA
0.050	11.8 ± 0.4	0.05
0.080	14.8 ± 0.8	0.05
0.100	16.8 ± 0.6	0.05
0.120	19.3 ± 0.6	0.05
0.144	20.8 ± 0.6	0.05

Plotting k_{obs} / s^{-1} against $[KH_2PO_4]_{stoich}$ / M gives a linear plot. The values obtained for the gradient and intercept are given in Table 2.14. Linear regression yielded a correlation coefficient of 0.992.

Table 2.14: Gradient and intercept obtained for k_{obs} / s^{-1} against $[KH_2PO_4]_{stoich}$ / M with 0.053 M aqueous formaldehyde at pH 7.9, 25 °C, aqueous solution, I = 1 M

pH	gradient / dm^3 mol^{-1} s^{-1}	intercept / s^{-1}
7.9	98.8 ± 5.2	6.94 ± 0.54

The values obtained for aniline at pH 7.9 were 53.8 ± 1.2 dm^3 mol^{-1} s^{-1} and 5.61 ± 0.12 s^{-1} for the gradient and intercept respectively.

The reaction was then studied using a lower aqueous formaldehyde concentration of 0.011 M at pH 6.9 using a potassium dihydrogen phosphate / sodium hydroxide buffer with a stoichiometric potassium dihydrogen phosphate concentration of 0.050 to 0.144 M. The ionic strength was maintained at 1.0 M using potassium chloride. A constant 4-methylaniline concentration of 1.0×10^{-4} M was used throughout. The results are shown in Table 2.15.

Table 2.15: k_{obs} / s^{-1} values for 1.0×10^{-4} M 4-methylaniline and 0.011 M $[HCHO_{(aq)}]$ with varied buffer concentration at pH 6.9, aqueous solution, 25 °C, I = 1 M

$[KH_2PO_4]_{stoich}$ / M	pH 6.9	
	k_{obs} / s^{-1}	ΔA
0.050	4.39 ± 0.27	0.02
0.080	5.77 ± 0.23	0.02
0.100	7.11 ± 0.49	0.02
0.120	7.71 ± 0.53	0.02
0.144	9.37 ± 0.84	0.02

Plotting k_{obs} / s^{-1} against $[KH_2PO_4]_{stoich}$ / M gives a linear plot. The values obtained for the gradient and intercept are given in Table 2.16. Linear regression gave a correlation coefficient of 0.990. The analogous reaction with aniline yielded a gradient and intercept of 36.4 ± 1.7 dm^3 mol^{-1} s^{-1} and 1.57 ± 0.17 s^{-1} respectively.

Table 2.16: Gradient and intercept obtained for k_{obs} / s^{-1} against $[KH_2PO_4]_{stoich}$ / M with 0.011 M aqueous formaldehyde at pH 6.9, 25 °C, aqueous solution, I = 1 M

pH	gradient / dm^3 mol^{-1} s^{-1}	intercept / s^{-1}
6.9	52.2 ± 3.0	1.72 ± 0.31

The results obtained for the reaction of 4-methylaniline with aqueous formaldehyde solution again clearly indicate that buffer catalysis is occurring. Ideally values for all of the catalytic species involved in the reaction should be obtained. For each catalytic species the relation K = k_f / k_b will hold so that catalytic coefficients for forward and reverse reactions are related by the equilibrium constant for the reaction. However in order to obtain reliable values of all catalytic coefficients experiments that facilitate plots of k_{obs} / s^{-1} against buffer concentration at a variety of pH values would be required. It was decided to make measurements using a standard set of conditions with a variety of aniline derivatives in order to examine aniline substituent effects.

2.2.3 Reaction of aqueous formaldehyde with 4-dimethylaminoaniline

The reaction of 5.3 × 10^{-3} to 0.10 M aqueous formaldehyde with 1.0 × 10^{-4} M 4-dimethylaminoaniline, 4-$N(CH_3)C_6H_4NH_2$, at pH 6.9, 25 °C was investigated. 4-Dimethylaminoaniline was found to be sparingly soluble in water but readily soluble in acetonitrile, therefore a stock solution in acetonitrile was prepared, to give a final solvent composition of 2 % acetonitrile / 98 % water by volume.

Absorbance against wavelength spectra were obtained over time for 1.0 × 10^{-4} M 4-dimethylaminoaniline with and without the presence of 0.05 or 0.10 M aqueous formaldehyde. The spectra with aqueous formaldehyde added show a shift to higher wavelength with a corresponding increase in absorbance as compared to the spectrum of 1.0 × 10^{-4} M 4-dimethylaminoaniline alone. The higher the concentration of aqueous formaldehyde, the greater the change in spectrum observed. All reactions are complete by the first spectrum (Figure 2.6).

Figure 2.6: Effect of adding 0.05 and 0.1 M aqueous formaldehyde on the spectrum of 1.0×10^{-4} M 4-dimethylaminoaniline at 25 °C, pH 7, 2 % acetonitrile / 98 % water

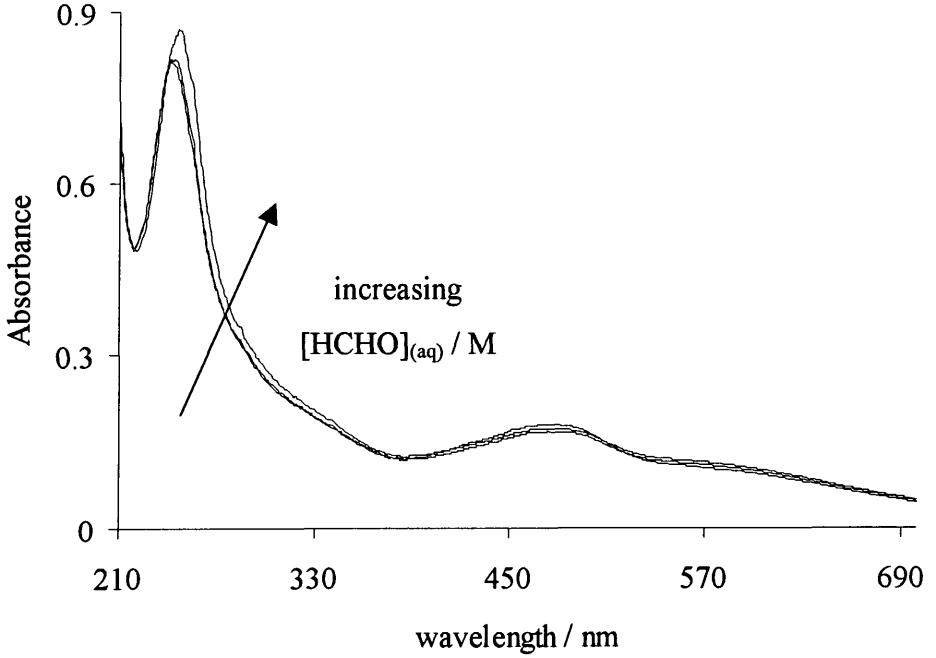

Plots of absorbance against time were obtained for the reaction of 1.0×10^{-4} M 4-dimethylaminoaniline and 5.3×10^{-3} to 0.053 M aqueous formaldehyde at pH 6.9 using a potassium dihydrogen phosphate / sodium hydroxide buffer system with $[KH_2PO_4]_{stoich}$ = 0.05 M, and maintaining a constant ionic strength, I, of 1.0 M using potassium chloride. Formation of the product at 260 nm was followed. Plots were first order: the k_{obs} / s^{-1} values obtained are shown in Table 2.17.

Table 2.17: k_{obs} / s^{-1} for 1.0×10^{-4} M 4-dimethylaminoaniline with varied $[HCHO_{(aq)}]$, pH 6.9, 25 °C, 2 % acetonitrile / 98 % water, $[KH_2PO_4]_{stoich}$ = 0.05 M, I = 1 M

$[HCHO_{(aq)}]$ / M	pH 6.9	
	k_{obs} / s^{-1}	ΔA
5.3×10^{-3}	4.86 ± 0.26	0.03
0.011	5.63 ± 0.14	0.05
0.021	7.01 ± 0.27	0.07
0.035	8.43 ± 0.17	0.09
0.053	10.6 ± 0.9	0.12

The reaction is an equilibrium as the change in absorbance over time, ΔA, increases with increasing aqueous formaldehyde concentration. Plotting k_{obs} / s^{-1} against aqueous formaldehyde concentration gives a linear plot: k_f / dm^3 mol^{-1} s^{-1} and k_b / s^{-1} are equal to the gradient and intercept respectively (Table 2.18). Linear regression gave a correlation coefficient of 0.997. The equilibrium constant K, is equal to k_f / k_b.

Table 2.18: k_f and k_b and the equilibrium constant, K, for 4-dimethylaminoaniline with aqueous formaldehyde, pH 6.9, 25 °C, 2 % acetonitrile / 98 % water, I= 1 M

pH	k_f / dm^3 mol^{-1} s^{-1}	k_b / s^{-1}	K / dm^3 mol^{-1}
6.9	119 ± 3	4.34 ± 0.09	27 ± 1

2.2.4 Reaction of aqueous formaldehyde with 4-chloroaniline

The reaction of 5.3 × 10^{-3} to 0.10 M aqueous formaldehyde with 1.0 × 10^{-4} M 4-chloroaniline, 4-$ClC_6H_4NH_2$, at pH 6.9, 25 °C was investigated. 4-Chloroaniline was found to be sparingly soluble in water but readily soluble in methanol, therefore a stock solution in methanol was prepared, to give a final solvent composition of 2 % methanol / 98 % water by volume.

Absorbance against wavelength spectra were obtained over time for 1.0 × 10^{-4} M 4-chloroaniline with and without the presence of 0.05 or 0.10 M aqueous formaldehyde. The spectra with aqueous formaldehyde added show a shift to higher wavelength with a corresponding increase in absorbance as compared to the spectrum of 1.0 × 10^{-4} M 4-chloroaniline alone. The higher the concentration of aqueous formaldehyde, the greater the change in spectrum observed. All reactions are complete by the first spectrum (Figure 2.7).

Figure 2.7: Effect of adding 0.05 and 0.1 M aqueous formaldehyde on the uv / vis spectrum of 1.0×10^{-4} M 4-chloroaniline at 25 °C, pH 7, in 2 % methanol / 98 % water

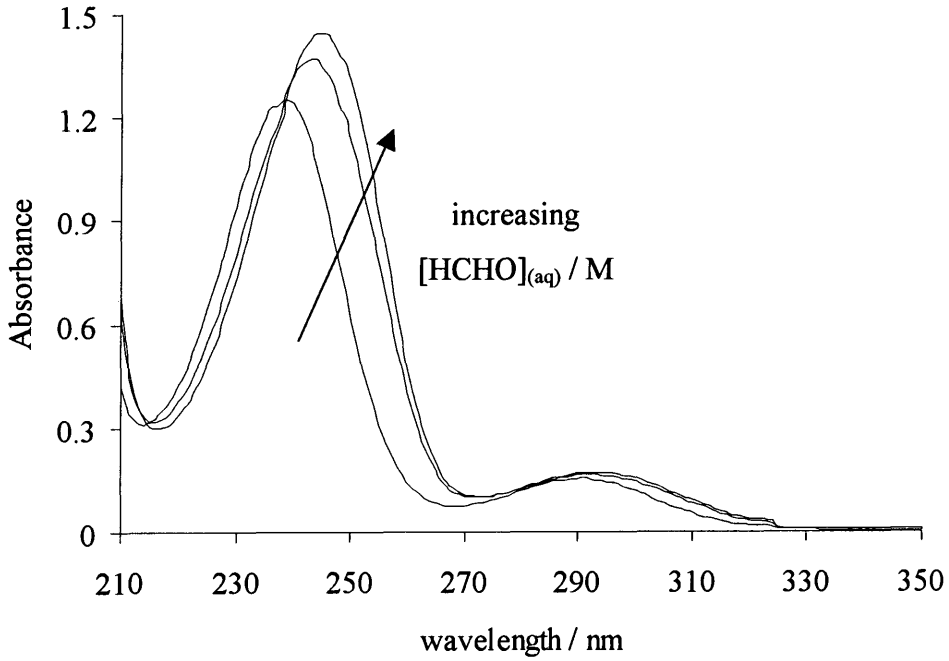

Plots of absorbance against time were obtained for the reaction of 1.0×10^{-4} M 4-chloroaniline and 5.3×10^{-3} to 0.053 M aqueous formaldehyde at pH 6.9 where $[KH_2PO_4]_{stoich}$ = 0.05 M, and I = 1.0 M using potassium chloride. Formation of the product at 250 nm was followed. Plots were first order: the k_{obs} / s^{-1} values obtained are shown in Table 2.19.

Table 2.19: k_{obs} / s^{-1} for 1.0×10^{-4} M 4-chloroaniline with varied $[HCHO_{(aq)}]$ at pH 6.9, 25 °C, 2 % methanol / 98 % water, $[KH_2PO_4]_{stoich}$ = 0.05 M, I= 1 M

$[HCHO_{(aq)}]$ / M	pH 6.9	
	k_{obs} / s^{-1}	ΔA
5.3×10^{-3}	1.72 ± 0.02	0.09
0.011	1.94 ± 0.01	0.15
0.021	2.41 ± 0.02	0.25
0.035	3.02 ± 0.02	0.32

The reaction is an equilibrium as the change in absorbance over time, ΔA, increases with increasing aqueous formaldehyde concentration. Plotting k_{obs} / s^{-1} against aqueous formaldehyde concentration gives a linear plot: k_f / dm^3 mol^{-1} s^{-1} and k_b / s^{-1} are equal to the gradient and intercept respectively (Table 2.20). Linear regression yielded a correlation coefficient of 0.999. The equilibrium constant K, is equal to k_f / k_b.

Table 2.20: k_f and k_b and the equilibrium constant, K, for the reaction of 4-chloroaniline with aqueous formaldehyde, pH 6.9, 25 °C, 2 % methanol / 98 % water, I = 1 M

pH	k_f / dm^3 mol^{-1} s^{-1}	k_b / s^{-1}	K / dm^3 mol^{-1}
6.9	44.1 ± 0.8	1.48 ± 0.02	30 ± 1

2.2.5 Reaction of aqueous formaldehyde with 3-chloroaniline

The reaction of 5.3 × 10^{-3} to 0.10 M aqueous formaldehyde with 1.0 × 10^{-4} M 3-chloroaniline, 3-$ClC_6H_4NH_2$, at pH 6.9, 25 °C was investigated.

Absorbance against wavelength spectra were obtained over time for 1.0 × 10^{-4} M 3-chloroaniline with and without the presence of 0.05 or 0.10 M aqueous formaldehyde. The spectra with aqueous formaldehyde added show a shift to higher wavelength with a corresponding increase in absorbance as compared to the spectrum of 1.0 × 10^{-4} M 3-chloroaniline alone. The higher the concentration of aqueous formaldehyde, the greater the change in spectrum observed. All reactions are complete by the first spectrum (Figure 2.8).

Plots of absorbance against time were obtained for the reaction of 1.0 × 10^{-4} M 3-chloroaniline and 5.3 × 10^{-3} to 0.053 M aqueous formaldehyde at pH 6.9 where $[KH_2PO_4]_{stoich}$ = 0.05 M, and I = 1.0 M using potassium chloride. Formation of the product at 245 nm was followed. Plots were first order: the k_{obs} / s^{-1} values obtained are shown in Table 2.21.

Figure 2.8: Effect of adding 0.05 and 0.1 M aqueous formaldehyde on the uv / vis spectrum of 1.0×10^{-4} M 3-chloroaniline at 25 °C, pH 7, in aqueous solution

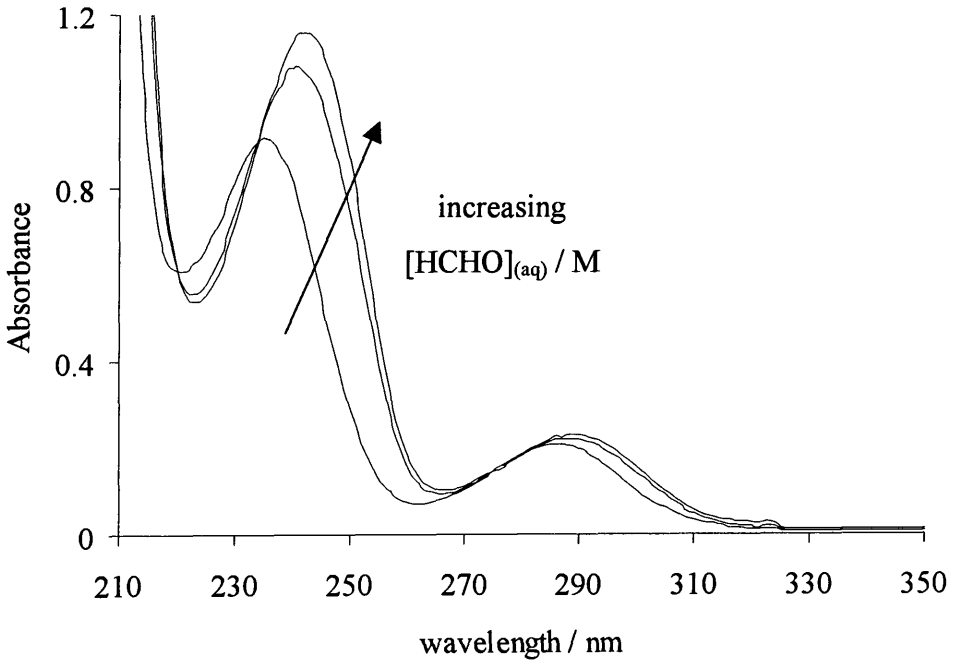

Table 2.21: k_{obs} / s^{-1} for 1.0×10^{-4} M 3-chloroaniline with varied aqueous formaldehyde concentration, pH 6.9, 25 °C, aqueous solution, $[KH_2PO_4]_{stoich}$ = 0.05 M, I = 1 M

$[HCHO_{(aq)}]$ / M	pH 6.9	
	k_{obs} / s^{-1}	ΔA
5.3×10^{-3}	0.89 ± 0.01	0.07
0.011	1.02 ± 0.02	0.13
0.021	1.26 ± 0.01	0.21
0.035	1.54 ± 0.01	0.27
0.053	1.92 ± 0.01	0.33

The reaction is an equilibrium as the change in absorbance over time, ΔA, increases with increasing aqueous formaldehyde concentration. Plotting k_{obs} / s^{-1} against aqueous formaldehyde concentration gives a linear plot: k_f / dm^3 mol^{-1} s^{-1} and k_b / s^{-1} are equal to the gradient and intercept respectively (Table 2.22). Linear regression gave a correlation coefficient of 0.997. The equilibrium constant K, is equal to k_f / k_b.

Table 2.22: Values of k_f and k_b and the equilibrium constant, K, for the reaction of 3-chloroaniline with aqueous formaldehyde, pH 6.9, 25 °C, aqueous solution, I= 1 M

pH	k_f / dm^3 mol^{-1} s^{-1}	k_b / s^{-1}	K / dm^3 mol^{-1}
6.9	21.4 ± 0.3	0.79 ± 0.01	27 ± 1

2.2.6 Reaction of aqueous formaldehyde with 3-cyanoaniline

The reaction of 5.3 × 10^{-3} to 0.10 M aqueous formaldehyde with 1.0 × 10^{-4} M 3-cyanoaniline, 3-$CNC_6H_4NH_2$, at pH 6.9, 25 °C was investigated. 3-Cyanoaniline was found to be sparingly soluble in water but readily soluble in methanol, therefore a stock solution in methanol was prepared, to give a final solvent composition of 2 % methanol / 98 % water by volume.

Absorbance against wavelength spectra were obtained over time for 1.0 × 10^{-4} M 3-cyanoaniline with and without the presence of 0.05 or 0.10 M aqueous formaldehyde. The spectra with aqueous formaldehyde added show a shift to higher wavelength with a corresponding increase in absorbance as compared to the spectrum of 1.0 × 10^{-4} M 3-cyanoaniline alone. The higher the concentration of aqueous formaldehyde, the greater the change in spectrum observed. All reactions are complete by the first spectrum (Figure 2.9).

Plots of absorbance against time were obtained for the reaction of 1.0 × 10^{-4} M 3-cyanoaniline and 5.3 × 10^{-3} to 0.053 M aqueous formaldehyde at pH 6.9 where $[KH_2PO_4]_{stoich}$ = 0.05 M, and I = 1.0 M using potassium chloride. Formation of the product at 330 nm was followed. Plots were first order: the k_{obs} / s^{-1} values obtained are shown in Table 2.23.

Figure 2.9: Effect of adding 0.05 and 0.1 M aqueous formaldehyde on the uv / vis spectrum of 1.0×10^{-4} M 3-cyanoaniline, 25 °C, pH 7, 2 % methanol / 98 % water

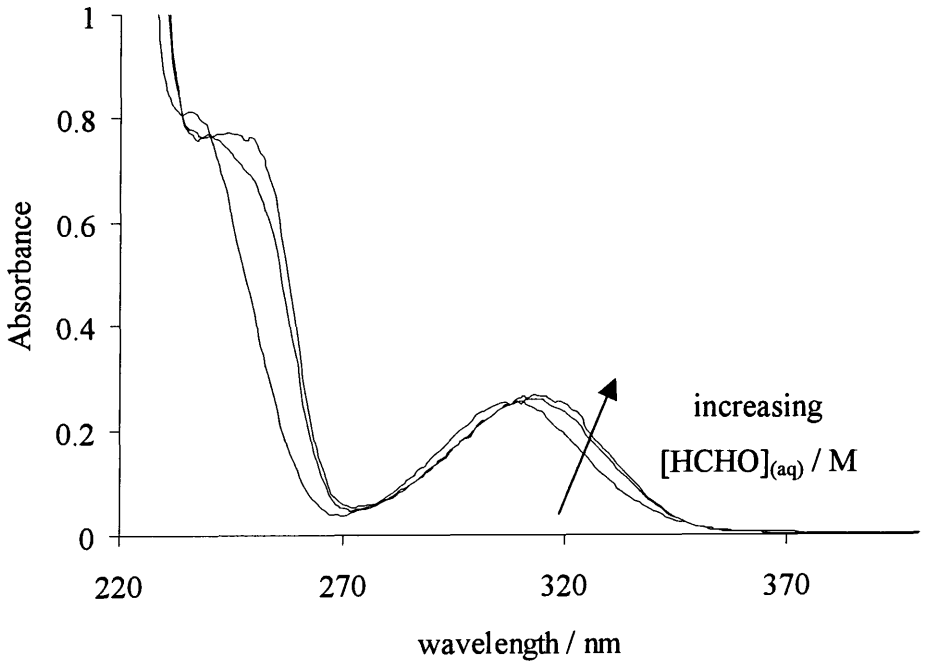

Table 2.23: k_{obs} / s^{-1} for 1.0×10^{-4} M 3-cyanoaniline with varied $[HCHO_{(aq)}]$ at pH 6.9, 25 °C, 2 % methanol / 98 % water, $[KH_2PO_4]_{stoich}$ = 0.05 M, I= 1 M

$[HCHO_{(aq)}]$ / M	pH 6.9	
	k_{obs} / s^{-1}	ΔA
5.3×10^{-3}	0.32 ± 0.04	0.007
0.011	0.37 ± 0.02	0.01
0.021	0.45 ± 0.02	0.02
0.035	0.54 ± 0.01	0.03
0.053	0.68 ± 0.02	0.04

The reaction is an equilibrium as the change in absorbance over time, ΔA, increases with increasing aqueous formaldehyde concentration. Plotting k_{obs} / s^{-1} against aqueous formaldehyde concentration gives a linear plot: k_f / dm^3 mol^{-1} s^{-1} and k_b / s^{-1} are equal to the gradient and intercept respectively (Table 2.24). Linear regression gave a correlation coefficient of 0.999. The equilibrium constant K, is equal to k_f / k_b.

Table 2.24: k_f and k_b and the equilibrium constant, K, for 3-cyanoaniline with aqueous formaldehyde, pH 6.9, 25 °C, 2 % methanol / 98 % water, I= 1 M

pH	k_f / dm^3 mol^{-1} s^{-1}	k_b / s^{-1}	K / dm^3 mol^{-1}
6.9	7.36 ± 0.12	0.28 ± 0.01	26 ± 1

2.2.7 Reaction of aqueous formaldehyde with 3-nitroaniline

The reaction of 5.3 × 10^{-3} to 0.10 M aqueous formaldehyde with 1.0 × 10^{-4} M 3-nitroaniline, 3-$NO_2C_6H_4NH_2$, at pH 6.9, 25 °C was investigated. 3-Nitroaniline was found to be sparingly soluble in water but readily soluble in methanol, therefore a stock solution in methanol was prepared, to give a final solvent composition of 2 % methanol / 98 % water by volume.

Absorbance against wavelength spectra were obtained over time for 1.0 × 10^{-4} M 3-nitroaniline with and without the presence of 0.05 or 0.10 M aqueous formaldehyde. The spectra with aqueous formaldehyde added show a shift to higher wavelength with a corresponding increase in absorbance as compared to the spectrum of 1.0 × 10^{-4} M 3-nitroaniline alone. The higher the concentration of aqueous formaldehyde, the greater the change in spectrum observed. All reactions are complete by the first spectrum (Figure 2.10).

Plots of absorbance against time were obtained for the reaction of 1.0 × 10^{-4} M 3-nitroaniline and 5.3 × 10^{-3} to 0.053 M aqueous formaldehyde at pH 6.9 where $[KH_2PO_4]_{stoich}$ = 0.05 M, and I = 1.0 M using potassium chloride. Formation of the product at 245 nm was followed. Plots were first order: the k_{obs} / s^{-1} values obtained are shown in Table 2.25.

Figure 2.10: Effect of adding 0.05 and 0.1 M aqueous formaldehyde on the uv / vis spectrum of 1.0×10^{-4} M 3-nitroaniline at 25 °C, pH 7, in 2 % methanol / 98 % water

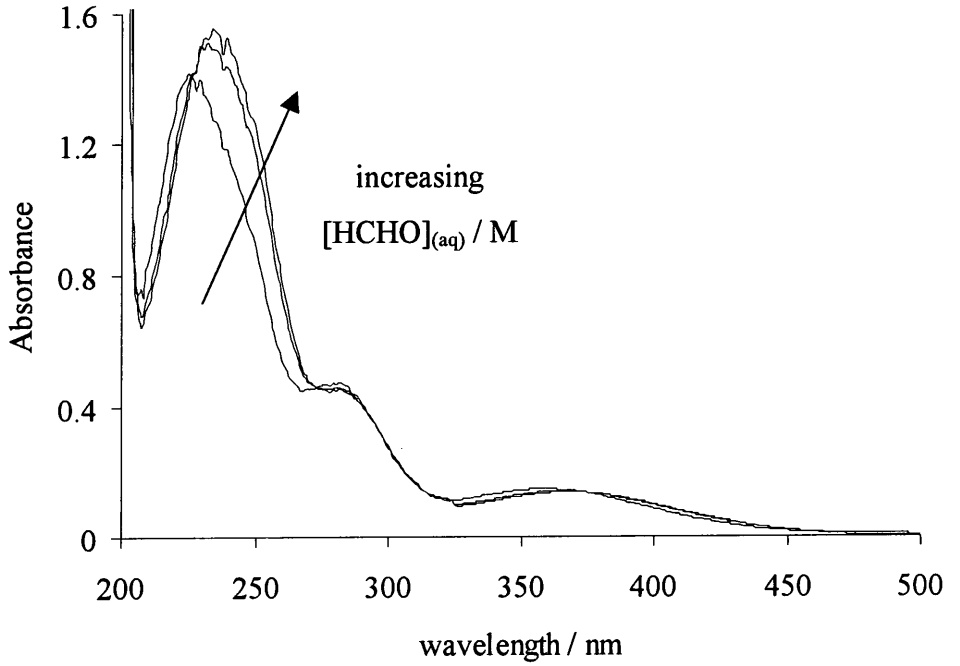

Table 2.25: k_{obs} / s^{-1} for 1.0×10^{-4} M 3-nitroaniline with varied [$HCHO_{(aq)}$] at pH 6.9, 25 °C, 2 % methanol / 98 % water, $[KH_2PO_4]_{stoich}$ = 0.05 M, I= 1 M

[$HCHO_{(aq)}$] / M	pH 6.9	
	k_{obs} / s^{-1}	ΔA
5.3×10^{-3}	0.16 ± 0.01	0.04
0.011	0.18 ± 0.02	0.08
0.021	0.21 ± 0.01	0.12
0.035	0.28 ± 0.01	0.16
0.053	0.35 ± 0.01	0.20

The reaction is an equilibrium as the change in absorbance over time, ΔA, increases with increasing aqueous formaldehyde concentration. Plotting k_{obs} / s^{-1} against aqueous formaldehyde concentration gives a linear plot: k_f / dm^3 mol^{-1} s^{-1} and k_b / s^{-1} are equal to the gradient and intercept respectively (Table 2.26). Linear regression gave a correlation coefficient of 0.997. The equilibrium constant K, is equal to k_f / k_b.

Table 2.26: k_f and k_b and the equilibrium constant, K, for the reaction of 3-nitroaniline with aqueous formaldehyde, pH 6.9, 25 °C, 2 % methanol / 98 % water, I= 1 M

pH	k_f / dm^3 mol^{-1} s^{-1}	k_b / s^{-1}	K / dm^3 mol^{-1}
6.9	4.01 ± 0.13	0.13 ± 0.01	31 ± 3

2.2.8 Reaction of aqueous formaldehyde with *N*-methylaniline

The reaction of 5.3 × 10^{-3} to 0.10 M aqueous formaldehyde with 1.0 × 10^{-4} M *N*-methylaniline, $C_6H_5NH(CH_3)_2$, at pH 6.9, 25 °C was investigated.

Absorbance against wavelength spectra were obtained over time for 1.0 × 10^{-4} M *N*-methylaniline with and without the presence of 0.05 or 0.10 M aqueous formaldehyde. The spectra with aqueous formaldehyde added show a shift to higher wavelength with a corresponding increase in absorbance as compared to the spectrum of 1.0 × 10^{-4} M *N*-methylaniline alone. The higher the concentration of aqueous formaldehyde, the greater the change in spectrum observed. All reactions are complete by the first spectrum (Figure 2.11).

Figure 2.11: Effect of adding 0.05 and 0.1 M aqueous formaldehyde on the uv / vis spectrum of 1.0 × 10^{-4} M *N*-methylaniline at 25 °C, pH 7, in aqueous solution

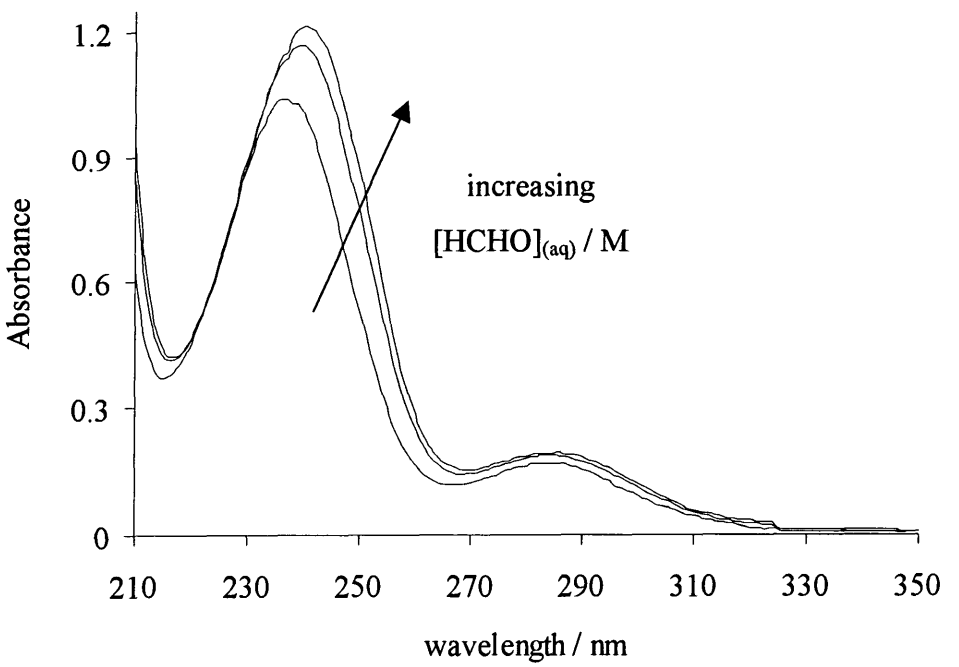

Plots of absorbance against time were obtained for the reaction of 1.0×10^{-4} M *N*-methylaniline and 5.3×10^{-3} to 0.053 M aqueous formaldehyde at pH 6.9 where $[KH_2PO_4]_{stoich}$ = 0.05 M, and I = 1.0 M using potassium chloride. Formation of the product at 245 nm was followed. Plots were first order: the k_{obs} / s^{-1} values obtained are shown in Table 2.27.

Table 2.27: k_{obs} / s^{-1} values 1.0×10^{-4} M *N*-methylaniline with varied $[HCHO_{(aq)}]$ at pH 6.9, 25 °C, aqueous solution, $[KH_2PO_4]_{stoich}$ = 0.05 M, I = 1 M

$[HCHO_{(aq)}]$ / M	pH 6.9	
	k_{obs} / s^{-1}	ΔA
5.3×10^{-3}	7.18 ± 0.40	0.02
0.011	7.72 ± 0.16	0.03
0.021	8.91 ± 0.18	0.05
0.035	10.2 ± 0.2	0.07
0.053	12.4 ± 0.5	0.10

The reaction is an equilibrium as the change in absorbance over time, ΔA, increases with increasing aqueous formaldehyde concentration. Plotting k_{obs} / s^{-1} against aqueous formaldehyde concentration gives a linear plot: k_f / dm^3 mol^{-1} s^{-1} and k_b / s^{-1} are equal to the gradient and intercept respectively (Table 2.28). Linear regression gave a correlation coefficient of 0.998. The equilibrium constant K, is equal to k_f / k_b.

Table 2.28: Values of k_f and k_b and the equilibrium constant, K, for the reaction of *N*-methylaniline with aqueous formaldehyde, pH 6.9, 25 °C, aqueous solution, I = 1 M

pH	k_f / dm^3 mol^{-1} s^{-1}	k_b / s^{-1}	K / dm^3 mol^{-1}
6.9	108 ± 3	6.58 ± 0.09	16 ± 1

2.2.9 Comparison of results: Hammett plot

Table 2.29 summarises the results obtained for the reaction of 1.0×10^{-4} M amine with an aqueous formaldehyde concentration of 5.3×10^{-3} to 0.053 M at 25 °C, 1.0 M ionic strength and pH 6.9 where $[KH_2PO_4]_{stoich} = 0.05$ M. Hammett substituent parameters, σ, are quoted for the 4- and 3- substituted anilines.

Table 2.29: Summary of rate and equilibrium constants obtained experimentally, and pK_a values[1] and σ values,[12] for RC_6H_4NHR'

R	R'	pK_a	σ	k_f / $dm^3\ mol^{-1}\ s^{-1}$	k_b / s^{-1}	K / $dm^3\ mol^{-1}$
H	H	4.60	0	73.9	2.71	27
4-CH_3	H	5.08	-0.17	118	3.34	35
4-$N(CH_3)_2$	H	6.59	-0.12	119	4.34	27
4-Cl	H	4.15	0.23	44.1	1.48	30
3-Cl	H	3.46	0.37	21.4	0.79	27
3-CN	H	2.75	0.61	7.36	0.28	26
3-NO_2	H	2.47	0.71	4.01	0.13	31
H	CH_3	4.85	-	108	6.58	16

The reaction of formaldehyde with amines involves nucleophilic attack of the amine on the carbonyl group. Therefore the relative reactivities of the amines can be rationalised in terms of their pK_a values: electron donating groups on the amine such as 4-CH_3 and 4-$N(CH_3)_2$, will make the amino group a better nucleophile and so the reaction will occur faster. Conversely amines with electron withdrawing groups such as 3-NO_2, 3-CN, 3-Cl and 4-Cl, will have lower pK_a values and the reaction will be slower.

Figure 2.12 shows a Hammett plot of log (k_f / k_o) against σ, where k_o is the forward rate constant for the parent compound, aniline. The gradient of the line gives a Hammett reaction parameter, ρ, equal to -1.6 ± 0.1. Linear regression gives a correlation coefficient of 0.978. A similar plot using the rate constant for the back reaction, k_b, gives a ρ value of -1.7 ± 0.1 and a correlation coefficient of 0.961.

Figure 2.12: Hammett plot for the forward rate constant, k_f

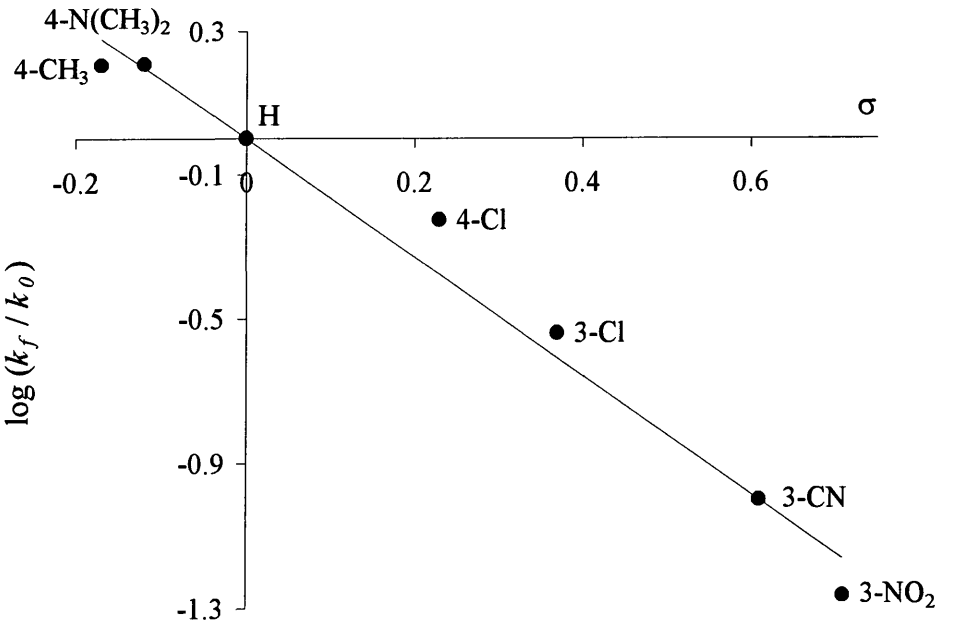

The formation of *N*-(hydroxymethyl)amines is likely to involve at least two steps as shown in Scheme 2.10.

Scheme 2.10:

$$RNH_2 + HCHO \underset{k_{-N}}{\overset{k_N}{\rightleftharpoons}} R\overset{+}{N}H_2CH_2O^- \overset{K}{\rightleftharpoons} RNHCH_2OH$$

The first step, involving nucleophilic attack by the amine, is likely to be rate limiting. The second step is a rapid proton transfer: the positively charged nitrogen becomes unprotonated and the negatively charged oxygen protonated. The ρ value of -1.6 for the forward reaction is consistent with accumulation of positive charge on the nitrogen atom during nucleophilic attack, corresponding to k_N.

The ρ value for the reverse reaction is -1.7. The major substituent effect here will be on the value of the equilibrium constant K. Since this step involves loss of a proton from the anilinium nitrogen atom, values of K should give a positive value of ρ. However if the proton transfer step is rapid then the rate constant in the reverse direction, k_b, will be equal to k_{-N} / K. The inverse dependence on K will lead to a negative value of ρ: the concentration of zwitterionic intermediate will be higher for anilines containing electron releasing groups than for anilines with electron withdrawing groups.

The values of k_f and k_b used to construct the Hammett plot are composites containing contributions to reaction by uncatalysed, acid catalysed and base catalysed pathways. However the values given in Table 2.29 were obtained under identical experimental conditions and it is likely that they reflect the true overall reactivity of the aniline derivatives.

The stoichiometric concentration of aqueous formaldehyde solution was used to calculate k_f and k_b. However, in aqueous solution formaldehyde will be largely present as the hydrated form, $CH_2(OH)_2$. Bell[13] reports that the most probable value[14] of the equilibrium constant for dehydration, K_{deh}, at 25 °C is 5×10^{-4}. Therefore in aqueous solution formaldehyde will be largely present in the hydrated form. This will affect the k_f value obtained although will not affect k_b as the value of this rate constant does not depend on the formaldehyde concentration. K_{deh} is equal to k_{deh} / k_{hyd} where k_{deh} and k_{hyd} are the rate constants corresponding to dehydration and hydration respectively (Scheme 2.11).

Scheme 2.11:

$$CH_2(OH)_2 \underset{k_{hyd}}{\overset{k_{deh}}{\rightleftharpoons}} HCHO + H_2O$$

The reaction with amines will almost certainly involve the free dehydrated form of formaldehyde: studies of nucleophilic reactions with carbonyl compounds of varying fractions of hydration have repeatedly shown that the unhydrated carbonyl compound is the reactive species.[15] Hence it is necessary to consider the possibility that dehydration of $CH_2(OH)_2$ is kinetically significant (Scheme 2.12).

Scheme 2.12:

$$RNH_2 + CH_2(OH)_2 \underset{k_{hyd}}{\overset{k_{deh}}{\rightleftharpoons}} RNH_2 + HCHO + H_2O \underset{k_{-4}}{\overset{k_4}{\rightleftharpoons}} RNHCH_2OH + H_2O$$

Bernasconi[16] describes a general analysis of competitive equilibria. There are two possible cases that may occur. Both involve treating HCHO as a steady state intermediate which leads to Equation 2.11, where $[CH_2(OH)_2]$ is approximated to $[HCHO_{(aq)}]$.

$$\text{rate} = -\frac{d[RNH_2]}{dt} = \frac{k_{deh}[HCHO_{(aq)}]k_4[RNH_2]}{k_4[RNH_2] + k_{hyd}} - \frac{k_{-4}[RNHCH_2OH]k_{hyd}}{k_4[RNH_2] + k_{hyd}} \qquad \textbf{(2.11)}$$

Case 1: $k_{hyd} >> k_4.[RNH_2]$

Here the assumption is that the formaldehyde hydration / dehydration equilibrium is rapid compared to reaction with aniline. Therefore Equation 2.11 reduces to:

$$\text{rate} = \frac{k_{deh}[HCHO_{(aq)}]k_4[RNH_2]}{k_{hyd}} - k_{-4}[RNHCH_2OH] \quad \textbf{(2.12)}$$

$$\text{But } [RNH_2]_{stoich} = [RNH_2] + [RNHCH_2OH] \quad \textbf{(2.13)}$$

$$\therefore \text{rate} = \frac{k_{deh}[HCHO_{(aq)}]k_4([RNH_2]_{stoich} - [RNHCH_2OH])}{k_{hyd}} - k_{-4}([RNH_2]_{stoich} - [RNH_2]) \quad \textbf{(2.14)}$$

Using the equilibrium condition that the rate at equilibrium is equal to zero leads to:

$$\text{rate} = \left(\frac{k_{deh}\, k_4[HCHO_{(aq)}]}{k_{hyd}} - k_{-4} \right) [RNH_2]_{stoich} \quad \textbf{(2.15)}$$

$$k_{obs} = k_4 K_{deh}[HCHO_{(aq)}] - k_{-4} \quad \textbf{(2.16)}$$

This predicts a first order reaction with respect to aniline with a rate constant that increases linearly with aqueous formaldehyde concentration. Equation 2.16 shows that the values of k_4 can be obtained from the values in Table 2.29 by multiplying the values of k_f by a factor of $1 / K_{deh} = 2000$ to account for the hydration of formaldehyde.

The values of k_4 and k_{-4} for the reaction of amine with free formaldehyde, HCHO, are shown in Table 2.30. The values of k_4 are calculated by multiplying k_f by 2000: $k_{-4} = k_b$ as the reverse reaction does not depend on the formaldehyde concentration. Values of K_4, where $K_4 = k_4 / k_{-4}$, are also shown.

Table 2.30: Summary of rate and equilibrium constants obtained

amine	k_4 / $dm^3\ mol^{-1}\ s^{-1}$	k_{-4} / s^{-1}	K_4 / $dm^3\ mol^{-1}$
aniline	1.5×10^5	2.71	5.5×10^4
4-methylaniline	2.4×10^5	3.34	7.1×10^4
4-dimethylaminoaniline	2.4×10^5	4.34	5.5×10^4
4-chloroaniline	8.8×10^4	1.48	6.0×10^4
3-chloroaniline	4.3×10^4	0.79	5.4×10^4
3-cyanoaniline	1.5×10^4	0.28	5.2×10^4
3-nitroaniline	8.0×10^3	0.13	6.2×10^4
N-methylaniline	2.2×10^5	6.58	3.3×10^4

Case 2: $k_4 >> k_{hyd.}[RNH_2]$

Here the assumption is that dehydration of formaldehyde is rate limiting. Therefore Equation 2.11 reduces to:

$$-\frac{d[RNH_2]}{dt} = k_{deh}[HCHO_{(aq)}] - \frac{k_{-4}[RNHCH_2OH]k_{hyd}}{k_4[RNH_2]} \qquad \textbf{(2.17)}$$

This predicts a more complex dependence on the amine concentration. However at high aqueous formaldehyde concentrations the reaction will go largely to completion and the forward rate term will dominate. Therefore:

$$-\frac{d[RNH_2]}{dt} = k_{deh}[HCHO_{(aq)}] \qquad \textbf{(2.18)}$$

This predicts a zero order dependence with respect to the amine concentration.

The work here used conditions where the concentration of aqueous formaldehyde solution is in large excess of amine concentrations. Disappearance of the amine was followed and good first order plots were observed for all amines: this implies Case 1 rather than Case 2. Furthermore the Hammett plot in Figure 2.12 indicates that the values of k_f depend on the nature of the aniline derivative: this would not be expected if formaldehyde dehydration were rate limiting.

It is possible to calculate an approximate value for k_{deh} using information reported by Funderburk and co-workers[17] who studied the rate of formaldehyde dehydration with respect to pH and determined rate constants for buffer independent and buffer dependent rate equations (Equation 2.19).

$$k_{deh} = k_o + k_{H^+}[H^+] + k_{OH^-}[OH^-] + k_{HA}[HA] + k_{A^-}[A^-] \qquad \textbf{(2.19)}$$

The values at 1.0 M ionic strength, 25 °C, are quoted as $k_o = 4.2 \times 10^{-3}$ s^{-1}, $k_{H^+} = 2.84$ M^{-1} s^{-1}, and $k_{OH^-} = 2.1 \times 10^{-3}$ M^{-1} s^{-1}. Bell and Evans[15c] report general acid and base catalysis rate constants k_{HA} and k_{A^-} equal to 8.8×10^{-2} M^{-1} s^{-1} and 0.39 M^{-1} s^{-1} respectively for a phosphate buffer at 25 °C. At pH 7, $[H_2PO_4^-] = 0.02$ mol dm^{-3} and $[HPO_4^{2-}] = 0.03$ mol dm^{-3} under the experimental conditions used. Therefore the calculated value of k_{deh} using Equation 2.19 is 0.018 s^{-1}. As k_{hyd} is equal to k_{deh} divided by K_{deh}, $k_{hyd} = 35$ s^{-1}.

For aniline, k_4 is equal to $k_f \times 2000 = 1.5 \times 10^5$ dm^3 mol^{-1} s^{-1} under the conditions employed here. 1.0×10^{-4} mol dm^{-3} aniline was used therefore the value of $k_4.[RNH_2]$ is 15 s^{-1}.

This analysis indicates that k_{hyd} is larger, although not greatly larger, than k_4 and is probably sufficient for the condition $k_{hyd} >> k_4$ to be valid and for the kinetic expressions shown in Case 1 to hold. For amines less reactive than aniline the condition $k_{hyd} >> k_4$ will also apply. However for more reactive amines the condition is less likely to be valid. This may account for some curvature in the Hammett plot (Figure 2.12) where, for the more reactive amines, dehydration of formaldehyde may become partially rate limiting.

2.3 CONCLUSION

The reaction of formaldehyde with aniline and substituted anilines to produce *N*-(hydroxymethyl)amines was investigated in the pH range 6 to 8. The rate and equilibrium constants determined in this study are shown in Table 2.31.

Table 2.31: Summary of rate and equilibrium constants obtained at 25 °C

amine	k_f / dm^3 mol^{-1} s^{-1}	k_b / s^{-1}	K / dm^3 mol^{-1}	k_4 / dm^3 mol^{-1} s^{-1}	k_{-4} / s^{-1}	K_4 / dm^3 mol^{-1}
aniline	73.9	2.71	27	1.5×10^5	2.71	5.5×10^4
4-methylaniline	118	3.34	35	2.4×10^5	3.34	7.1×10^4
4-dimethylaminoaniline	119	4.34	27	2.4×10^5	4.34	5.5×10^4
4-chloroaniline	44.1	1.48	30	8.8×10^4	1.48	6.0×10^4
3-chloroaniline	21.4	0.79	27	4.3×10^4	0.79	5.4×10^4
3-cyanoaniline	7.36	0.28	26	1.5×10^4	0.28	5.2×10^4
3-nitroaniline	4.01	0.13	31	8.0×10^3	0.13	6.2×10^4
N-methylaniline	108	6.58	16	2.2×10^5	6.58	3.3×10^4

The k_f, k_b and K values refer to the reaction with aqueous formaldehyde solution whereas k_4, k_{-4} and K_4 refer to the values calculated for reaction with free formaldehyde, HCHO, alone. It has been shown that dehydration of $CH_2(OH)_2$ to give free formaldehyde, the reactive species, is not rate limiting in these systems as the value of k_{hyd} is generally sufficiently greater than k_4 for the condition $k_{hyd} >> k_4$ to hold. Values of K obtained are in good agreement with literature values available for aniline, 4-methylaniline, 4-chloroaniline and *N*-methylaniline equal to 22.3, 22.7, 26.0 and 13.2 dm^3 mol^{-1} respectively.

Although *N*-(hydroxymethyl)amines formed from aromatic amines and formaldehyde have not been isolated,[10] the data obtained by Abrams and Kallen[8] indicate that the major product of interaction of formaldehyde and anilines in aqueous solution is the *N*-(hydroxymethyl)amine. Spectral shifts and the magnitude of the equilibrium constants indicate that, as with aliphatic amines,[3] the formaldehyde adducts of aromatic

amines are *N*-(hydroxymethyl)amines and not imines.[11] Spectra of aqueous solutions of amine with aqueous formaldehyde show a shift in wavelength to longer wavelengths with increased absorbance relative to the parent amine spectra. Abrams and Kallen[8] observed the same spectral characteristics for *N*-(hydroxymethyl)amines.

On the basis of observations with aliphatic amines and aliphatic aldehydes[18] and with aliphatic or aromatic amines with aromatic aldehydes,[19] it is expected that the spectral properties of imines produced from the reaction of anilines with formaldehyde would be substantially different from that of the parent amine. For example, with *N*-methylaniline the resulting imine would be cationic. Consequently the nitrogen could not conjugate with the aromatic system: the iminium ion would be expected to exhibit significantly different spectral characteristics.

The reaction was studied under conditions with formaldehyde in excess to prevent formation of dinuclear species, whilst using sufficiently low aqueous formaldehyde concentrations to exclude the possibility of *N,N*-(dihydroxymethyl)amine formation.

The formation of *N*-(hydroxymethyl)amines is likely to involve at least two steps, the first being formation of a zwitterionic compound, **12**, Scheme 2.13.

Scheme 2.13: $RNH_2 + HCHO \rightleftharpoons R\overset{+}{N}H_2CH_2O^- \rightleftharpoons RNHCH_2OH$

12

Reaction parameters, ρ, equal to −1.6 and −1.7 were obtained from the Hammett plots for the forward and back reactions respectively. These values are consistent with accumulation of positive charge on the nitrogen atom during nucleophilic attack in the forward direction and an inverse dependence on the equilibrium constant in the reverse direction.

The reaction is subject to general acid and base catalysis. Buffer catalytic constants, k_{H2PO4^-} and k_{HPO42^-}, equal to 43 ± 13 and 56 ± 3 $dm^6\ mol^{-2}\ s^{-1}$ respectively were obtained: both buffer components contribute extensively to the catalysis of the reaction. Abrams and Kallen[8] obtained catalytic constants in the range 1 to 15 $dm^6\ mol^{-2}\ s^{-1}$ for substituted anilines.

The mechanism of general acid / base catalysis in the reaction of amines with formaldehyde has been discussed in detail by Abrams and Kallen.[8] They state that the most likely explanation is a stepwise pre-association mechanism as shown in Scheme 2.14.

Scheme 2.14:

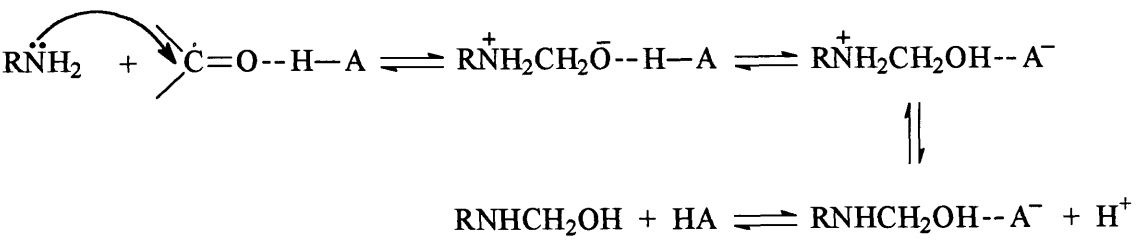

Initial interaction of the acid with the carbonyl group aids nucleophilic attack by the amine. This step is likely to be rate limiting except in the case of very weakly acidic catalysts where the proton transfer to oxygen may be the slow step.

2.4 EXPERIMENTAL

2.4.1 Absorbance against wavelength spectra of formaldehyde with aniline and aniline derivatives

Absorbance against wavelength spectra were obtained for the amine alone and with 0.05 and 0.10 M aqueous formaldehyde solution added at pH 7, or unbuffered in the case of aniline. The reactions of aniline and the 4-CH_3, 3-Cl and *N*-CH_3 aniline derivatives were carried out in 100 % aqueous solution, the 4-Cl, 3-NO_2 and 3-CN aniline derivatives in 2 % methanol / 98 % water by volume, and the 4-$N(CH_3)_2$ aniline derivative in 2 % acetonitrile / 98 % water by volume. Mixed solvent systems were used where the aniline derivative was only sparingly soluble in water at the concentration required.

Spectra were obtained using a Perkin – Elmer Lambda 2 or 12 uv / vis spectrometer at 25 °C with 1 cm pathlength stoppered quartz cuvettes, taking scans every 15 minutes for up to an hour using a scan speed of 480 nm min^{-1}. The cuvettes were left in the spectrometer for at least 10 minutes prior to use to allow the temperature to equilibrate to 25 °C. Addition of the amine solution was used to initiate the reaction. In all experiments the reaction was complete by the time the first spectrum was taken and there was no further change in the spectrum over the timescale used.

For the experiments performed at pH 7 a potassium dihydrogen phosphate / sodium hydroxide buffer was employed, with stoichiometric concentrations of 0.19 M potassium dihydrogen phosphate and 0.11 M sodium hydroxide.

2.4.2 Absorbance against time plots

The reaction of aqueous formaldehyde at concentrations ranging from 5.3×10^{-3} to 0.053 M with 1×10^{-4} M amine in the pH range 5.8 to 7.9 was investigated. The reactions of aniline and the 4-CH_3, 3-Cl and *N*-CH_3 aniline derivatives were carried out in 100 % aqueous solution, the 4-Cl, 3-NO_2 and 3-CN aniline derivatives in 2 % methanol / 98 % water by volume, and the 4-$N(CH_3)_2$ aniline derivative in 2 % acetonitrile / 98 % water by volume. Mixed solvent systems were used where the aniline derivative was only sparingly soluble in water at the concentration required.

Plots of absorbance against time were obtained: formation of the product was followed. The wavelengths used for the different amines are shown in Table 2.31.

Table 2.31: Wavelengths used to study the amines

amine	wavelength / nm
$C_6H_5NH_2$	245
$4\text{-}CH_3C_6H_4NH_2$	260
$4\text{-}N(CH_3)_2C_6H_4NH_2$	260
$4\text{-}ClC_6H_4NH_2$	250
$3\text{-}ClC_6H_4NH_2$	245
$3\text{-}CNC_6H_4NH_2$	330
$3\text{-}NO_2C_6H_4NH_2$	245
$C_6H_5NH(CH_3)$	245

245 nm would have been a more suitable wavelength to study 4-methylaniline, $4\text{-}CH_3C_6H_4NH_2$, as this would have given a larger absorbance change than that obtained at 260 nm.

Initially experiments at constant buffer concentration and altered aqueous formaldehyde concentration were performed: 0.05 M $[KH_2PO_4]_{stoich}$ was used as this gives the minimum buffer catalysis whilst still retaining sufficient buffer capacity. The reaction was also followed using a constant aqueous formaldehyde concentration and altered buffer concentration.

Absorbance against time plots were recorded using an Applied Photophysics DX.17MV BioSequential Stopped – flow ASVD Spectrometer at 24.9 – 25.2 °C with a cell of 1 cm path length. Ten averages were obtained, each the average of three runs of 1 to 10 seconds depending on the aqueous formaldehyde or buffer concentration employed, except for 3-nitroaniline where only five averages were obtained, each the average of three runs of 50 seconds.

The appropriate aqueous formaldehyde solution was placed in one syringe and the amine solution with the appropriate buffer solution and potassium chloride in the other. The amine / buffer / KCl solutions were made just prior to use. The averages were fitted to obtain first order rate constants, k_{obs} / s^{-1}, using the single exponential fit function on the !SX.17MV program installed on the spectrometer. Values of k_{obs} / s^{-1} are quoted to two decimal places, or three significant figures if $k_{obs} \geq 10$ s^{-1}. Only the initial data was used to fit the results for 4-chloroaniline as a true first order plot was not obtained for the whole set of results. This may be due to formation of the *N,N*-(dihydroxymethyl)amine.

Solid KCl was placed in a volumetric flask, the appropriate buffer added, and the KCl dissolved using an ultrasonic bath. The amine was added just prior to use and the solution made to the line using distilled water. For the amines where a mixed solvent system was required, a final composition of 2 % methanol / acetonitrile by volume was obtained by using 2 cm^3 of the stock amine in methanol / acetonitrile in 50 cm^3 total volume.

For certain reactions, a change in ionic strength caused by the addition of inert ions can greatly affect the rate constant. In the reactions studied here, there is formation of a charged transition state. This species will have a denser ionic atmosphere than the reactants and therefore increasing the ionic strength will increase the rate constant as formation of the transition state will be favoured. Therefore potassium chloride was used to keep the ionic strength constant at 1.0 M. For experiments at constant pH and varied [$HCHO_{(aq)}$] where the ionic strength was not kept constant, plots of k_{obs} / s^{-1} against [$HCHO_{(aq)}$] / M did not give linear plots.

A stock solution of pH 6 buffer consisting of KH_2PO_4 and NaOH with stoichiometric concentrations of 0.30 and 0.034 mol dm^{-3} respectively was prepared. The concentration of HPO_4^{2-} will approximately be equal to that of $[NaOH]_{stoich}$ and therefore $[HPO_4^{2-}]$ = 0.034 mol dm^{-3}. Hence the amount of KH_2PO_4 present in the $H_2PO_4^-$ form will be equal to $[KH_2PO_4]_{stoich}$ minus $[HPO_4^{2-}]$, therefore $[H_2PO_4^-]$ = 0.266 mol dm^{-3}. Hence at pH 6, $H_2PO_4^-$ will be the predominant form, therefore only this species was used to calculate the ionic strength of the buffer. This approximation is sufficiently accurate when calculating the ionic strength. Equations 2.20 to 2.23 show the method

used to calculate the ionic strength, I, at pH 6, where c is equal to $[KH_2PO_4]_{stoich}$ / M and z is the charge on the ion. Strictly speaking the molality should be considered, but under the conditions used the molarity approximates to the molality.

$$I = \tfrac{1}{2} \Sigma c_i z_i^2 \qquad \textbf{(2.20)}$$

$$= \tfrac{1}{2} [c(1)^2 + c(-1)^2] \qquad \textbf{(2.21)}$$

$$= c \qquad \textbf{(2.22)}$$

$$\therefore \; I = [KH_2PO_4]_{stoich} \qquad \textbf{(2.23)}$$

Therefore at pH 6 the ionic strength of the buffer is equal to $[KH_2PO_4]_{stoich}$. For example when $[KH_2PO_4]_{stoich}$ = 0.05 M, I = 0.05 M. Therefore [KCl] = 1 - 0.05 = 0.95 M.

A stock solution of pH 8 buffer consisting of KH_2PO_4 and NaOH with stoichiometric concentrations of 0.30 and 0.28 mol dm^{-3} respectively was prepared. Therefore $[HPO_4^{2-}]$ = 0.28 mol dm^{-3} and $[H_2PO_4^-]$ = 0.02 mol dm^{-3}. Hence at pH 8, HPO_4^{2-} will be the predominant form, therefore only this species was used to calculate the ionic strength of the buffer. Applying Equation 2.20, the ionic strength of the buffer at pH 8 is equal to 3 × $[KH_2PO_4]_{stoich}$.

A stock solution of pH 7 buffer consisting of KH_2PO_4 and NaOH with stoichiometric concentrations of 0.30 and 0.175 mol dm^{-3} respectively was prepared. Therefore $[HPO_4^{2-}]$ = 0.175 mol dm^{-3} and $[H_2PO_4^-]$ = 0.125 mol dm^{-3}. Therefore at pH 7, $HPO4^{2-}$ and $H_2PO_4^-$ will be present in approximately equal amounts. Hence at pH 7 the ionic strength of the buffer is equal to 2 × $[KH_2PO_4]_{stoich}$.

For the experiments where the concentration of the aqueous formaldehyde was altered, the buffer concentration and potassium chloride concentration were kept constant at each pH. The buffers employed and the corresponding stoichiometric buffer concentrations and potassium chloride concentrations in the final reaction mixtures are shown in Table 2.33.

Table 2.33: Buffer and potassium chloride concentrations for the reactions with altered aqueous formaldehyde concentration

pH	component A	$[A]_{stoich}$ / M	component B	$[B]_{stoich}$ / M	[KCl] / M
5.8	KH_2PO_4	0.050	NaOH	5.6×10^{-3}	0.96
7.0	KH_2PO_4	0.050	NaOH	0.029	0.90
7.9	KH_2PO_4	0.050	NaOH	0.047	0.85

For the experiments where the concentration of the aqueous formaldehyde was kept constant, the buffer concentration and potassium chloride concentration were altered whilst ensuring the same buffer component ratio was retained and the ionic strength was kept constant at 1.0 M. The buffers employed and the corresponding stoichiometric buffer concentrations and potassium chloride concentrations in the final reaction mixtures are shown in Table 2.34.

Table 2.34: Buffer and potassium chloride concentrations for the reactions with altered buffer concentration

$[KH_2PO_4]_{stoich}$ / M	pH 5.8		pH 6.9		pH 7.9	
	$[NaOH]_{stoich}$ / M	[KCl] / M	$[NaOH]_{stoich}$ / M	[KCl] / M	$[NaOH]_{stoich}$ / M	[KCl] / M
0.050	5.6×10^{-3}	0.96	0.029	0.90	0.047	0.85
0.080	8.9×10^{-3}	0.92	0.046	0.84	0.075	0.76
0.100	0.011	0.90	0.058	0.80	0.094	0.70
0.120	0.013	0.88	0.070	0.76	0.112	0.64
0.144	0.016	0.858	0.084	0.714	0.134	0.566

The pH values of all solutions were determined using a Jenway 3020 pH meter calibrated using pH 7 and pH 10 buffers. pH values are quoted to one decimal place.

Linear regression within Microsoft Excel was used to calculate k_f and k_b values. Values of k_f are quoted to three significant figures and values of k_b to two decimal places. For 4-chloroaniline the 0.053 M aqueous formaldehyde solution gave an anomalously high result therefore this was not included in the data analysis. The equilibrium constant, K, is quoted to two significant figures. The percentage error in K was calculated using Equation 2.24. The percentage error was then converted to an absolute value of K.

$$\% \text{ error in K} = \sqrt{[(\% \text{ error in } k_f)^2 + (\% \text{ error in } k_b)^2]} \qquad \textbf{(2.24)}$$

Linear regression on Microsoft Excel was used to calculate ρ values: the linear plots were fitted through the origin. ρ values are quoted to one decimal place.

2.4.3 Aqueous formaldehyde solution

The aqueous formaldehyde solutions were prepared by diluting, with distilled water, the purchased 37 % by weight aqueous formaldehyde solution. These solutions were left to stand at room temperature for at least 2½ hours, more usually 4 – 4½ hours, to ensure depolymerisation. In concentrated solutions the amount of free formaldehyde available is less than the stoichiometric amount of formaldehyde in solution as a significant fraction of the total formaldehyde exists as polyoxymethylene polymers (Chapter 1, Section 1.6).

The concentration of $HCHO_{(aq)}$ was calculated assuming complete depolymerisation: it was assumed that $[HCHO_{(aq)}]$ = [aqueous formaldehyde]$_{stoich}$ and $HCHO_{(aq)}$ refers to unhydrated and hydrated formaldehyde. The uv / vis spectrum of a 0.1 M aqueous formaldehyde solution did not show any significant absorbance above 230 nm. Therefore the spectrum due to aqueous formaldehyde will not interfere significantly with the spectra or plots obtained here.

Concentrations of aqueous formaldehyde above 0.053 M were not used for kinetic studies as above this concentration the results obtained were not a single exponential plot. Plots consisting of two consecutive first order processes were obtained, but the two processes were not sufficiently well separated to study both independently. These

processes are likely to be formation of the *N*-(hydroxymethyl)amine followed by formation of an *N,N*-(dihydroxymethyl)amine. Abrams and Kallen[8] also observed *N,N*-(dihydroxymethyl)amine formation with high formaldehyde concentrations.

2.5 REFERENCES

1. D. D. Perrin, 'Dissociation constants of organic bases in aqueous solution', Butterworths, London, 1965 and 1972 Supplement

2. J. Hine and R. D. Weimar, Jr., *J. Am. Chem. Soc.*, 1965, **87**, 3387

3. R. G. Kallen and W. P. Jencks, *J. Biol. Chem.*, 1966, **241**, 5864

4. (a) E. C. Wagner, *J. Org. Chem.*, 1954, **19**, 1862; (b) J. Santhanalakshmi, *Thermochim. Acta.*, 1988, **127**, 369; (c) M. R. G. Nayar and J. D. Francis, *Makromol. Chem.*, 1978, **179**, 1783; (d) I. Wiesner and L. Wiesnerov, *Int. Polymer Sci. Tech.*, 1974, **1**, 107

5. (a) I. Wiesner, *Collect. Czech. Chem. Commun.*, 1973, **38**, 1473; (b) O. Y. Fedotova, M. A. Askarov and A. B. Kucharev, *Dokl. Akad. Nauk Uzb. SSR*, 1958, **6**, 31; *Chem. Abstr.*, 1959, **53**, 7092h

6. (a) M. R. G. Nayar and J. D. Francis, *Ind. J. Chem.*, 1983, **22B**, 776; (b) Y. Ogata and M. Okano, *J. Am. Chem. Soc.*, 1950, **72**, 1459

7. Y. Ogata, M. Okano and M. Sugawara, *J. Am. Chem. Soc.*, 1951, **73**, 1715

8. W. R. Abrams and R. G. Kallen, *J. Am. Chem. Soc.*, 1976, **98**, 7777

9. L. D. Kershner and R. L. Schowen, *J. Am. Chem. Soc.*, 1971, **93**, 2014

10. (a) W. P. Jencks, *Prog. Phys. Org. Chem.*, 1964, **2**, 63; (b) J. F. Walker, 'Formaldehyde', 3rd Ed., American Chemical Society Monograph Series, Reinhold, New York, 1964; (c) P. Y. Sollenberg and R. B. Martin, 'The Chemistry of the Amino Group', Ed. S. Patai, Interscience, New York, 1968, pp 349 – 406

11. J. De Luis, Ph.D. Thesis, 'Chemistry of Formaldehyde Amine Condensation Products', Pennsylvania State University, University Park, 1964; *Chem. Abstr.*, 1965, **63**, 8184d

12. D. D. Perrin and G. B. Barlin, *Quarterly Reviews, Chem. Soc. London*, 1966, **20**, 75

13. R. P. Bell, *Adv. Phys. Org. Chem.*, 1966, 1

14. P. Valenta, *Coll. Czech. Chem. Comm.*, 1960, **25**, 853

15. (a) R. G. Kallen, *J. Am. Chem. Soc.*, 1971, **93**, 6236; (b) G. E. Lienhard and W. P. Jencks, *ibid.*, 1966, **88**, 3982; (c) R. P. Bell and P. G. Evans, *Proc. R. Soc. London, Ser. A.*, 1966, **291**, 297; (d) P. Le Hénaff, *C. R. Acad. Sci., Paris*, 1963, **256**, 1752; (e) Ref. 10a

16. C. F. Bernasconi, 'Relaxation Kinetics', Academic Press, Inc., London, 1976

17. L. H. Funderburk, L. Aldwin and W. P. Jencks, *J. Am. Chem. Soc.*, 1978, **100**, 5444

18. (a) J. Hine and C. Y. Yeh, *J. Am. Chem. Soc.*, 1967, **89**, 2669; (b) A. Williams and M. L. Bender, *ibid.*, 1966, **88**, 2508; (c) J. Hine, J. C. Craig, Jr., J. G. Underwood, II, and F. A. Via, *ibid.*, 1970, **92**, 5194; (d) J. Hine, F. A. Via, J. K. Gotkis and J. C. Craig, Jr., *ibid.*, 5186; (e) J. Hine, C. Y. Yeh and F. C. Schmalstieg, *J. Org. Chem.*, 1970, **35**, 340; (f) E. M. Kosower and T. S. Sorensen, *ibid.*, 1963, **28**, 692

19. (a) E. H. Cordes and W. P. Jencks, *J. Am. Chem. Soc.*, 1962, **84**, 832; (b) *ibid.*, 1963, **85**, 2843

CHAPTER 3

Polymerisation of $RC_6H_4N{=}CH_2$ imines

CHAPTER 3: Polymerisation of $RC_6H_4N=CH_2$ imines

3.1 INTRODUCTION

Under neutral conditions, the reaction of aniline and formaldehyde in equimolar amounts results in the formation of 1,3,5-triphenyl-1,3,5-hexahydrotriazine, or 1,3,5-triphenylhexahydro-*s*-triazine (Scheme 3.1, **1**). Initially an *N*-(hydroxymethyl)amine is formed. This then dehydrates to give an unstable imine, $[C_6H_5N=CH_2]$, which rapidly polymerises to give the cyclic trimer **1**.

Scheme 3.1:

1,3,5-Triphenyl-1,3,5-hexahydrotriazine is a white, crystalline solid with a melting point[1] of 141 °C. X-ray diffraction techniques show it exists in the chair conformation.[2] It is capable of dissociating at high temperatures: it is thought that the vapour consists mainly of the monomeric imine.[3]

1,3,5-Triphenyl-1,3,5-hexahydrotriazine is unstable under acidic conditions and converts to a chain polymer, **2**, via intermolecular rearrangement.[4]

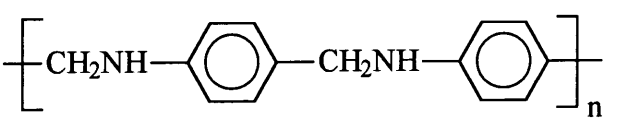

2

Other 1,3,5-triaryl-1,3,5-hexahydrotriazines have been synthesised using the amines 4-methylaniline,[1] and 2,6- and 3,5- dimethylaniline.[3] The analogous trimer formed from the reaction of formaldehyde with ammonia has also been prepared. The ^1H NMR

spectrum[5] of this trimer shows a sharp singlet at δ 3.95 ppm in deuterated water, D_2O, corresponding to the -NCH_2N- group hydrogens.

1,3,5-Triphenyl-1,3,5-hexahydrotriazine was prepared here using the literature method.[1] The novel syntheses of [4-$RC_6H_4N{=}CH_2$] imine polymers were attempted using the amines 4-dimethylaminoaniline, 4-aminobenzoic acid, 4-nitroaniline and sulfanilic acid, where R = -NMe_2, -COOH, -NO_2, and -SO_3H respectively. These amines were chosen to see if the presence of electron withdrawing or donating groups on the amine has any effect on the reaction.

The work described in Chapter 2 studied the formation of the *N*-(hydroxymethyl)amine. The stability of 1,3,5-triphenyl-1,3,5-hexahydrotriazine in solution and the mechanism of formation of this trimer were studied here to attempt to determine under what conditions the *N*-(hydroxymethyl)amine reacts further to give the cyclic imine trimer 1,3,5-triphenyl-1,3,5-hexahydrotriazine.

3.2 RESULTS AND DISCUSSION

3.2.1 Preparation of 4-$RC_6H_4N{=}CH_2$ imine polymers

3.2.1.1 Preparation of 1,3,5-triphenyl-1,3,5-hexahydrotriazine

1,3,5-Triphenyl-1,3,5-hexahydrotriazine was synthesised using the method reported by Miller and Wagner.[1] A mixture of 9.71g aniline (0.10 mol) and 100 cm^3 distilled water was chilled in ice and 11.18g 37 % weight aqueous formaldehyde solution (0.14 mol) added with stirring. The hard, cream coloured solid produced was collected by filtration after five hours and washed with distilled water. The product was extracted using boiling ethanol and the filtrate immediately chilled in ice with stirring. Approximately 10 cm^3 water was added gradually to hasten the separation and decrease the conversion of the trimer to a higher polymer. The white solid produced had a melting point of 139 - 141 °C: the literature value[1] is 141 °C.

The ^1H NMR spectrum of aqueous formaldehyde solution in deuterated dimethyl sulfoxide, d_6-DMSO, shows peaks at δ 4.48 to 4.73 ppm due to methylene glycol and other linear polyoxymethylene glycols and a peak around δ 3.2 ppm due to the presence of methanol stabiliser (Chapter 1, Section 1.6). ^1H NMR spectra in d_6-DMSO were also obtained for aniline, **3**, and 1,3,5-triphenyl-1,3,5-hexahydrotriazine, **1** (Figures 3.1 and 3.2 respectively). Tables 3.1 and 3.2 summarise the two spectra.

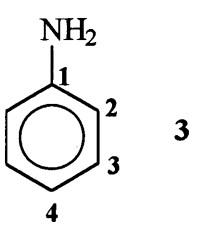

3

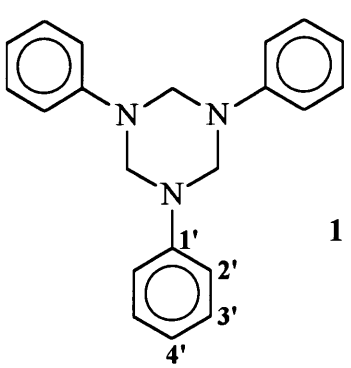

1

Figure 3.1: ^{1}H NMR spectrum of aniline in d_6-DMSO

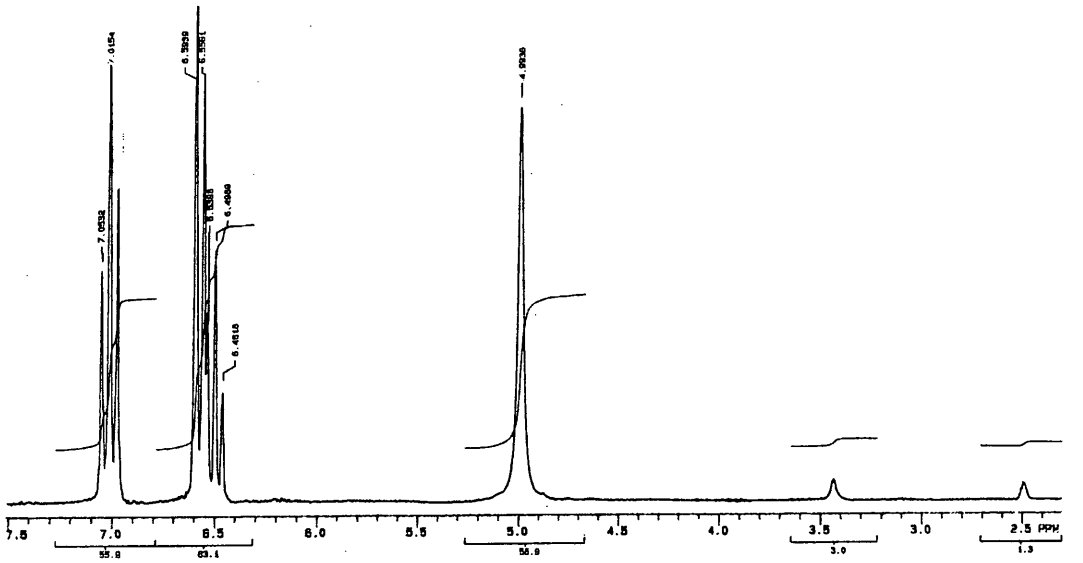

Table 3.1: ^{1}H NMR spectrum of aniline in d_6-DMSO: peak assignments

δ / ppm	integral ratio	multiplicity	J / Hz	assignment
2.49	-	-	-	DMSO
3.43	-	-	-	H_2O
4.99	2	s	-	-NH_2
6.50	3	t	8	Ar-**H4**
6.57		d	8	Ar-**H2**
7.02	2	t	8	Ar-**H3**

Table 3.2: ^{1}H NMR spectrum of 1,3,5-triphenyl-1,3,5-hexahydrotriazine in d_6-DMSO: peak assignments

δ / ppm	integral ratio	multiplicity	J / Hz	assignment
2.49	-	-	-	DMSO
3.34	-	-	-	H_2O
4.90	2	s	-	-NCH_2N-
6.78	1	t	8	Ar-**H4'**
7.06	2	d	8	Ar-**H2'**
7.17	2	t	8	Ar-**H3'**

Figure 3.2: ^{1}H NMR spectrum of 1,3,5-triphenyl-1,3,5-hexahydrotriazine in d_6-DMSO

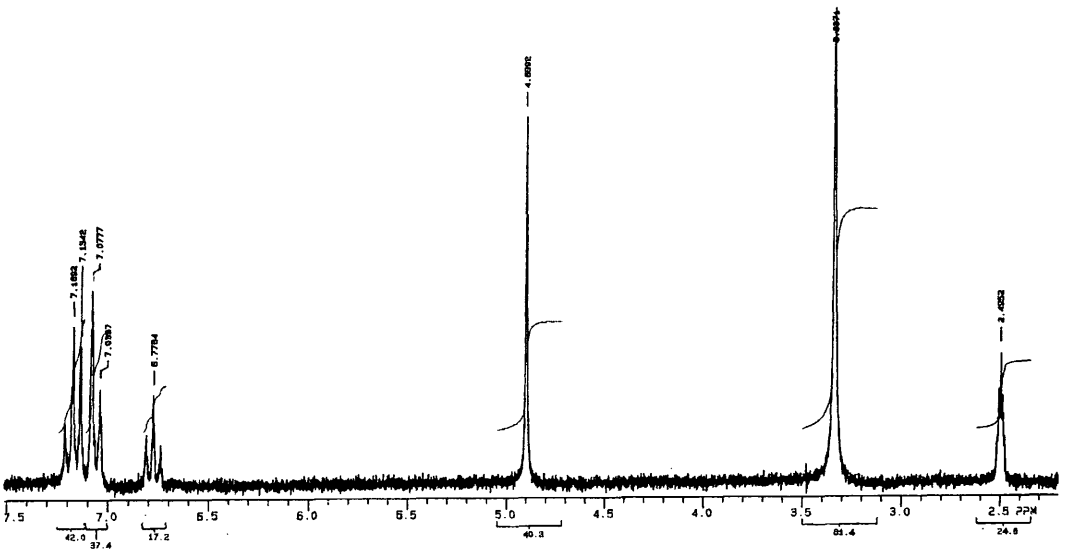

The melting point and ^{1}H NMR spectrum are consistent with the structure being that of 1,3,5-triphenyl-1,3,5-hexahydrotriazine.

3.2.1.2 Synthesis using 4-dimethylaminoaniline

A method based on that used by Miller and Wagner[1] for the preparation of the imine polymer formed from formaldehyde with 4-methylaniline, or *p*-toluidine, 4-$CH_3C_6H_4NH_2$, was used to attempt the novel synthesis of an imine polymer using the amine 4-dimethylaminoaniline, **4**, also known as *N,N*-dimethyl-1,4-phenylenediamine.

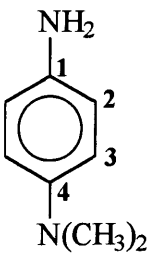

4

6.74 g (0.05 mol) **4**, a black / purple crystalline solid, was dissolved in 30 cm^3 of ethanol, this solution chilled in ice, and 7.5 cm^3 (0.10 mol) 37 % weight aqueous formaldehyde solution added with vigorous stirring. A dark brown solid formed within minutes: the solid was collected by filtration after thirty minutes and washed with copious amounts of ice cold ethanol (~ 400 cm^3). The resulting pink / brown solid was left to dry overnight on filter paper open to the air. A yield of 55 % was obtained, based on quantitative formation of a trimer.

Recrystallisation of the product using boiling ethanol or hot 60 - 80° petroleum ether was unsuccessful: little solid was produced and that obtained was virtually identical to the crude product when analysed using ^{1}H NMR.

^{1}H NMR spectra in d_6-DMSO were obtained for the starting material, 4-dimethylaminoaniline, and the product (Figures 3.3 and 3.4 respectively). Tables 3.3 and 3.4 summarise the two spectra. The ^{1}H NMR spectrum is consistent with the structure being that of a trimer, **5**.

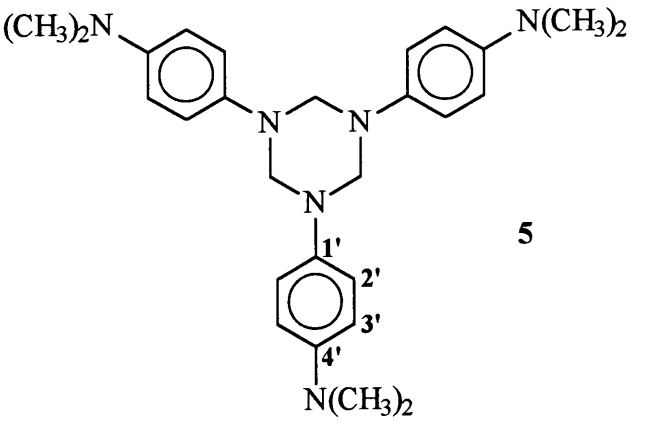

5

Figure 3.3: ^{1}H NMR spectrum of 4-dimethylaminoaniline in d_6-DMSO

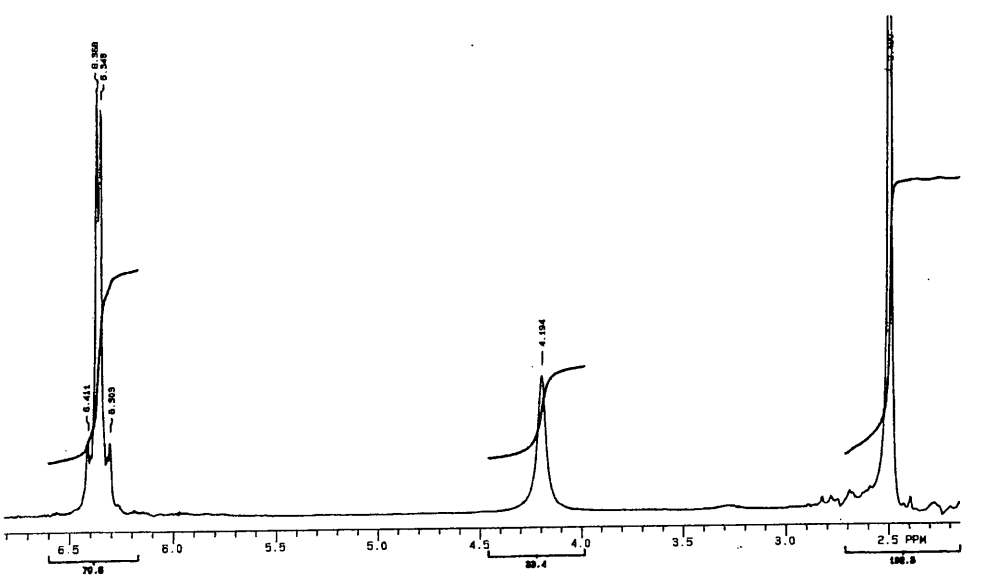

Table 3.3: ^{1}H NMR spectrum of 4-dimethylaminoaniline in d_6-DMSO: peak assignments

δ / ppm	integral ratio	multiplicity	J / Hz	assignment
2.49	3	s	-	DMSO and -N(CH_3)$_2$
4.19	1	s	-	-NH_2
6.36	2	m	-	Ar-**H2**, Ar-**H3**

Figure 3.4: ^{1}H NMR spectrum of the product in d_6-DMSO

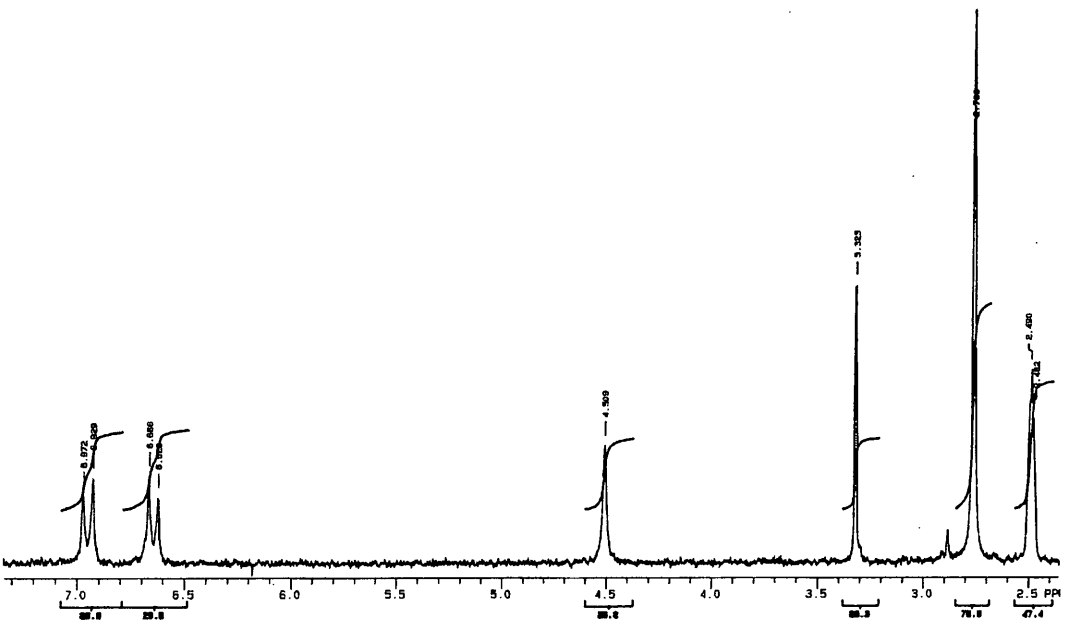

Table 3.4: ^{1}H NMR spectrum of the product in d_6-DMSO: peak assignments

δ / ppm	integral ratio	multiplicity	J / Hz	assignment
2.49	-	-	-	DMSO
2.77	3	s	-	-N(CH_3)$_2$
3.32	-	-	-	H_2O
4.51	1	s	-	-NCH_2N-
6.64	1	d	9	Ar-**H2'**
6.95	1	d	9	Ar-**H3'**

Absorbance against wavelength spectra were obtained for 2.0×10^{-5} M starting material and product in acetonitrile. The product is insoluble in acetonitrile therefore a stock solution in dioxan was prepared, giving a final solvent composition of 2 % dioxan / 98 % acetonitrile by volume. The spectrum of 4-dimethylaminoaniline shows peaks at 257 and 326 nm with extinction coefficients, ε, of 11000 and 2700 mol^{-1} dm^3 cm^{-1} respectively. The spectrum of the product changed over time: the initial and final spectrum after 6 hours are shown in Figure 3.5. Table 3.5 summarises the peak positions and ε for the two spectra.

Figure 3.5: Absorbance against wavelength spectrum of 2.0×10^{-5} M product in 2 % dioxan / 98 % acetonitrile by volume and the change over time

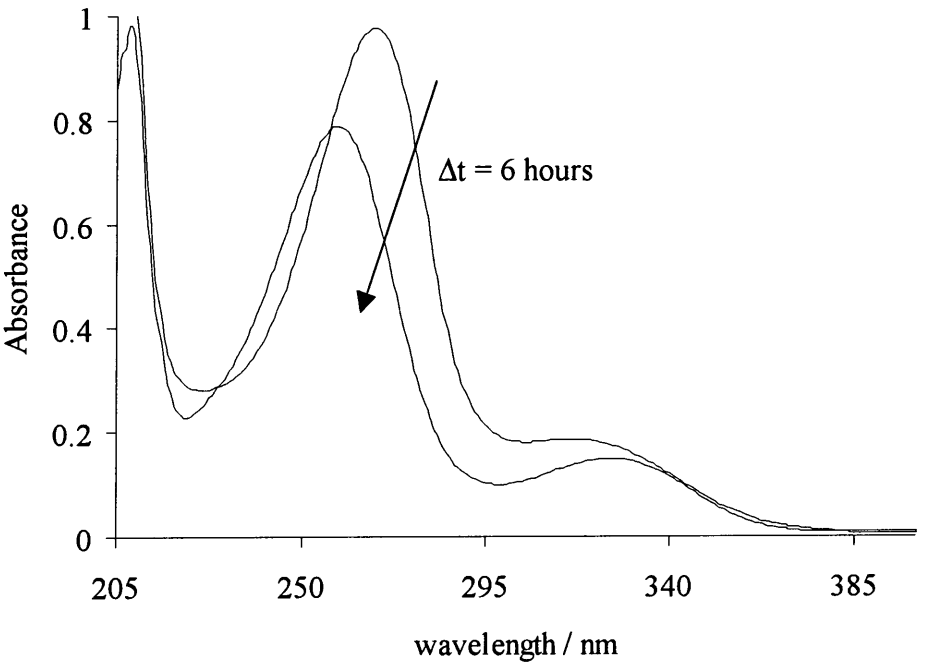

Table 3.5: Spectral appearance of 2.0×10^{-5} M product in 2 % dioxan / 98 % acetonitrile by volume: initial and final spectrum after 6 hours

spectrum	λ_{max} / nm (ε / mol^{-1} dm^3 cm^{-1})
initial	267 (47000); 316 (9000)
after 6 hours	259 (38000); 326 (7200)

The final spectrum of the product after 6 hours is the same as the spectrum of the starting material, 4-dimethylaminoaniline, except that the apparent extinction coefficient is approximately three times larger. This implies the product is the trimer **5** and in solution this decomposes over time to give three equivalents of the starting material, 4-dimethylaminoaniline.

3.2.1.3 Synthesis using 4-aminobenzoic acid

The novel synthesis of an imine polymer prepared using the amine 4-aminobenzoic acid, **6**, was attempted.

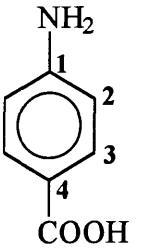

6

6.84 g (0.05 mol) **6**, a white powder, was dissolved in 60 cm^3 of ethanol: the yellow solution produced was then chilled in ice. 7.5 cm^3 (0.10 mol) 37 % weight aqueous formaldehyde solution was added with vigorous stirring. A thick white solid formed within seconds: the solid was collected by filtration after thirty minutes and washed with ice cold ethanol. The white powder was left to dry overnight on filter paper open to the air. Recrystallisation of the product using boiling ethanol or hot 60 - 80° petroleum ether was unsuccessful: little solid was produced.

^{1}H NMR spectra in d_6-DMSO were obtained for the starting material, 4-aminobenzoic acid, and the product (Figures 3.6 and 3.7 respectively). Tables 3.6 and 3.7 summarise the two spectra. The ^{1}H NMR spectrum is not consistent with the structure being that of a trimer: the ratios of the peak intensities show the product is probably a 1 : 2 formaldehyde : amine adduct, **7**. A yield of 75 % was obtained based on quantitative formation of **7**.

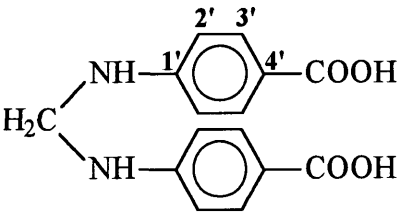

7

Figure 3.6: ^{1}H NMR spectrum of 4-aminobenzoic acid in d_6-DMSO

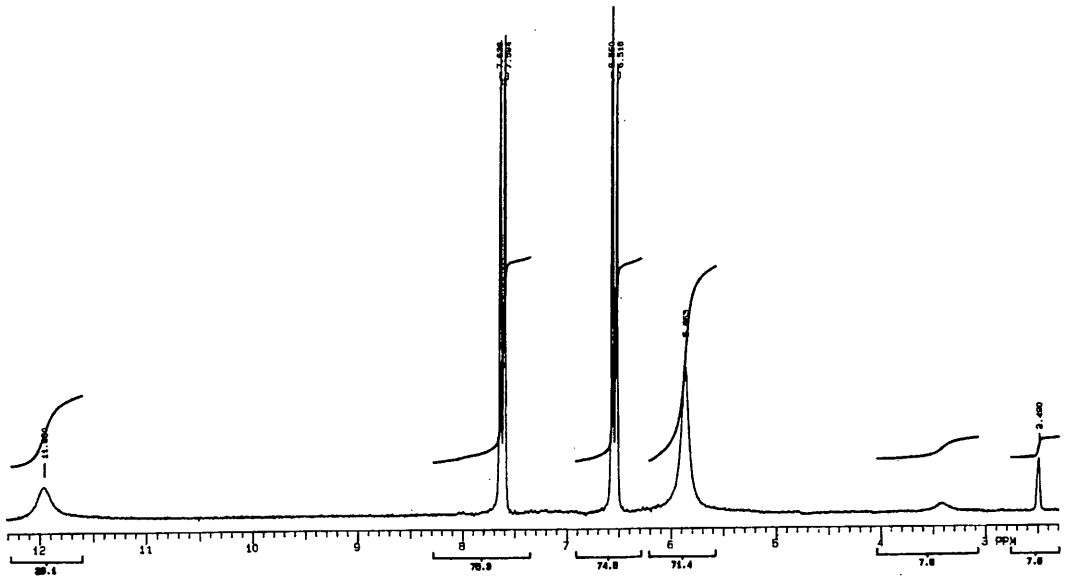

Table 3.6: ^{1}H NMR spectrum of 4-aminobenzoic acid in d_6-DMSO: peak assignments

δ / ppm	integral ratio	multiplicity	J / Hz	assignment
2.49	-	-	-	DMSO
5.86	2	s	-	-NH_2
6.54	2	d	9	Ar-**H2**
7.62	2	d	9	Ar-**H3**
11.96	1	broad s	-	-COOH

Figure 3.7: ^{1}H NMR spectrum of the product in d_6-DMSO

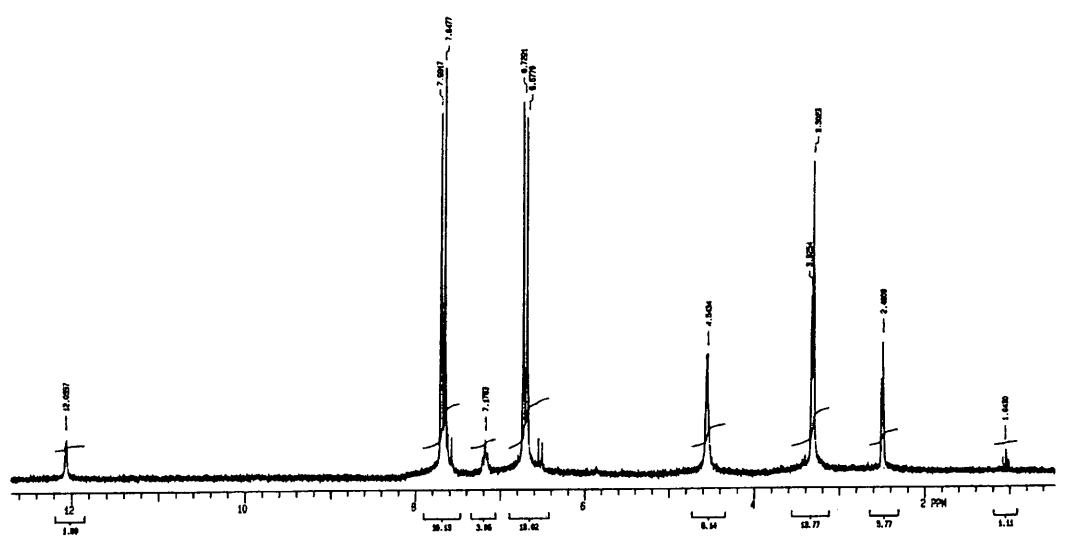

Table 3.7: ^{1}H NMR spectrum of the product in d_6-DMSO: peak assignments

δ / ppm	integral ratio	multiplicity	J / Hz	assignment
1.04	-	-	-	ethanol
2.49	-	-	-	DMSO
3.30	-	-	-	H_2O
4.54	3	s	-	-NC**H**$_2$N-
6.70	6	d	9	Ar-**H2'**
7.18	1	s	-	-
7.67	6	d	9	Ar-**H3'**
12.06	1	s	-	-COO**H**

3.2.1.4 Synthesis using 4-nitroaniline

The novel synthesis of an imine polymer prepared using the amine 4-nitroaniline, **8**, was attempted.

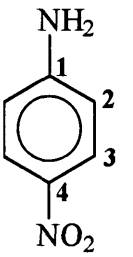

8

6.89 g (0.05 mol) **8**, a yellow / brown solid, was dissolved in 150 cm^3 of ethanol: this yellow solution was then chilled in ice. 7.5 cm^3 (0.10 mol) 37 % weight aqueous formaldehyde solution was added with vigorous stirring. After approximately 10 minutes a yellow solid began to form: the solid was collected by filtration after 1 hour and washed with a small amount of ice cold ethanol. The yellow solid was left to dry overnight on filter paper open to the air.

^{1}H NMR spectra in deuterated acetonitrile, CD_3CN, were obtained for the starting material, 4-nitroaniline, and the product (Figures 3.9 and 3.9 respectively). Tables 3.8 and 3.9 summarise the two spectra. The ^{1}H NMR spectrum is not consistent with the structure being that of a trimer: the ratios of the peak intensities show the product is

probably a 1 : 2 formaldehyde : amine adduct, **9**. A yield of 10 % was obtained based on quantitative formation of **9**. This yield is very low, however a considerable amount of solid dissolved when washed with ethanol. Therefore this yield could be improved.

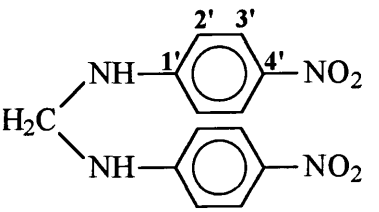

9

Figure 3.8: ^{1}H NMR spectrum of 4-nitroaniline in CD_3CN

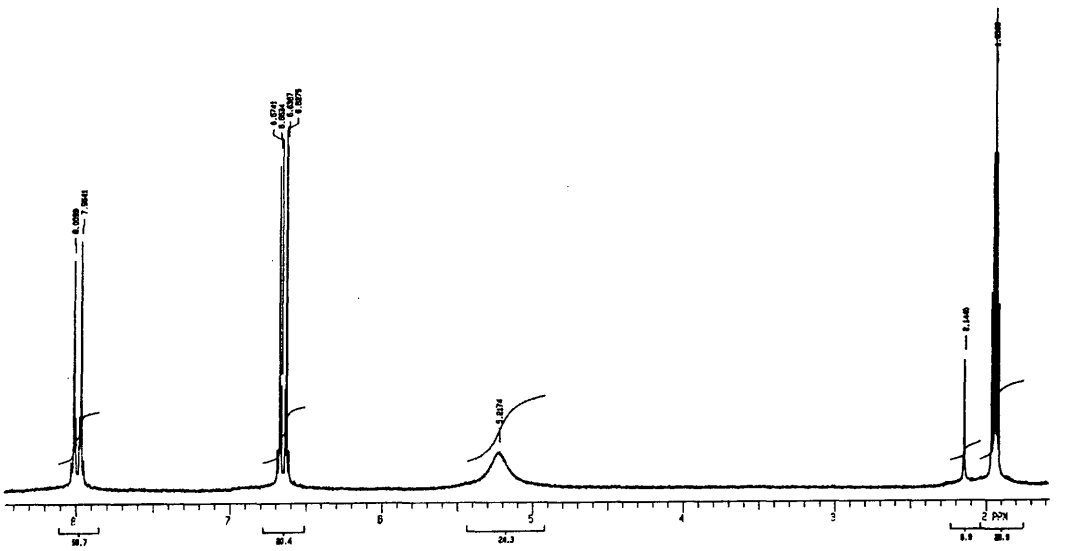

Table 3.8: ^{1}H NMR spectrum of 4-nitroaniline in CD_3CN: peak assignments

δ / ppm	integral ratio	Multiplicity	J / Hz	assignment
1.94	-	-	-	CHD_2CN
2.14	-	-	-	-
5.22	1	broad s	-	$-NH_2$
6.66	1	d	9	Ar-**H2**
7.99	1	d	9	Ar-**H3**

Figure 3.9: ^{1}H NMR spectrum of the product in CD_3CN

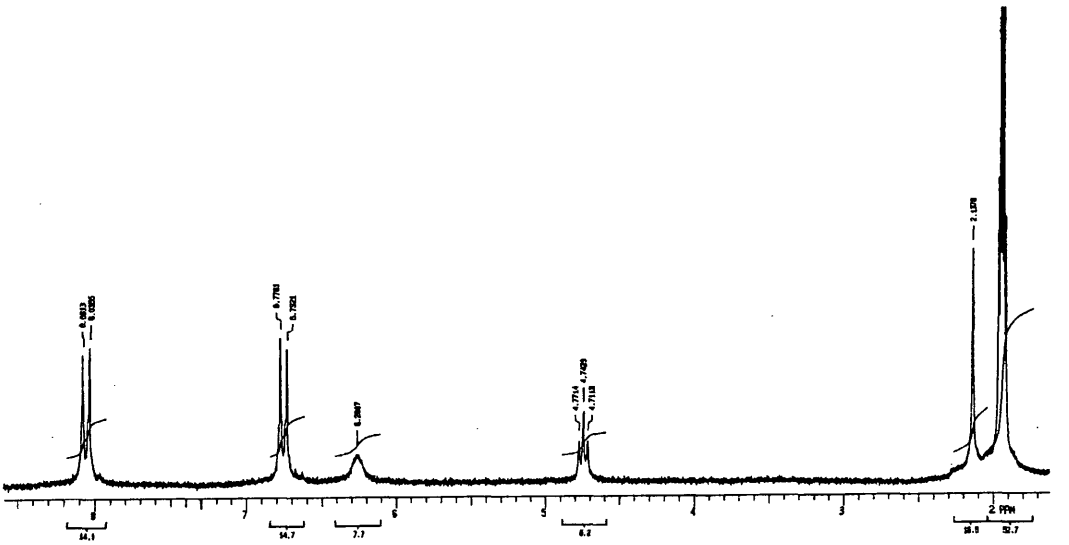

Table 3.9: ^{1}H NMR spectrum of the product in CD_3CN: peak assignments

δ / ppm	integral ratio	multiplicity	J / Hz	assignment
1.94	-	-	-	CHD_2CN
2.14	-	-	-	-
4.74	1	t	-	-NCH_2N-
6.26	1	broad s	-	-NH-
6.76	2	d	9	Ar-**H2'**
8.06	2	d	9	Ar-**H3'**

Absorbance against wavelength spectra were obtained for 2.0×10^{-5} M starting material and product in acetonitrile. The spectrum of 4-nitroaniline shows peaks at 226 and 365 nm with ε values of 8100 and 19000 mol^{-1} dm^3 cm^{-3} respectively. The spectrum of the product is shown in Figure 3.10: there was no change over time.

Figure 3.10: Absorbance against wavelength spectrum of 2.0×10^{-5} M product in acetonitrile

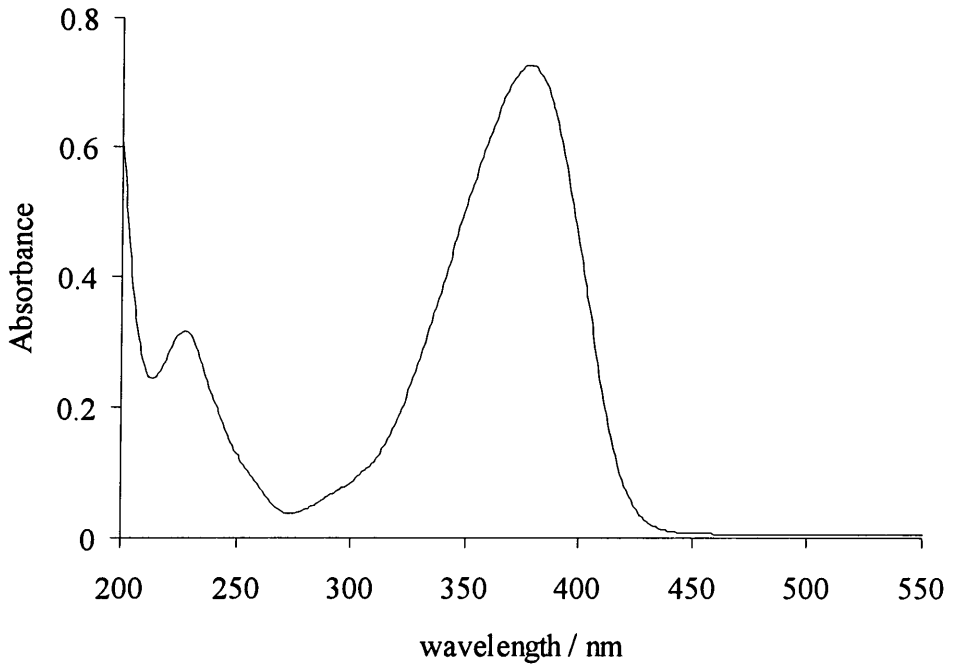

The spectrum of the product shows peaks at 227 and 387 nm with ε values of 17000 and 38000 mol^{-1} dm^3 cm^{-3} respectively. The spectrum is similar to the spectrum of the starting material, 4-nitroaniline, except that the apparent extinction coefficient is approximately two times larger. This implies the product consists of two equivalents of amine, as in the adduct **9**, and in solution this decomposes to give two equivalents of the starting material, 4-nitroaniline.

3.2.1.5 Synthesis using sulfanilic acid

The novel synthesis of an imine polymer prepared using the amine sulfanilic acid, **10**, was attempted.

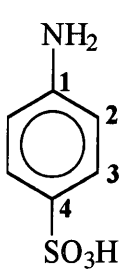

10

4.09 g (0.024 mol) **10**, a white solid, was added slowly with stirring to 300 cm^3 distilled water. When all the solid had dissolved, 3 cm^3 (0.05 mol) 37 % weight aqueous formaldehyde solution was added with vigorous stirring and the solution immediately chilled in ice. The peach / white solid was collected by filtration after 2 hours and left to dry overnight on filter paper open to the air.

^1H NMR spectra in d_6-DMSO were obtained for the starting material, sulfanilic acid, and the product (Figures 3.11 and 3.12 respectively). Tables 3.10 and 3.11 summarise the two spectra. The ^1H NMR spectrum is not consistent with the structure being that of a trimer. It is difficult to interpret the spectrum as the DMSO peak masks any peak due to the $-NCH_2N-$ group. However the product is probably a 1 : 2 formaldehyde : amine adduct, **11**, as obtained previously. A yield of 12 % was obtained based on quantitative formation of **11**. This yield is very low, however sulfanilic acid is not particularly soluble in water. Therefore this yield could be probably be improved by using a different solvent.

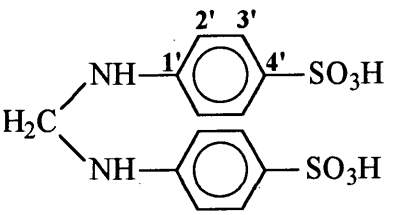

11

Figure 3.11: ^1H NMR spectrum of sulfanilic acid in d_6-DMSO

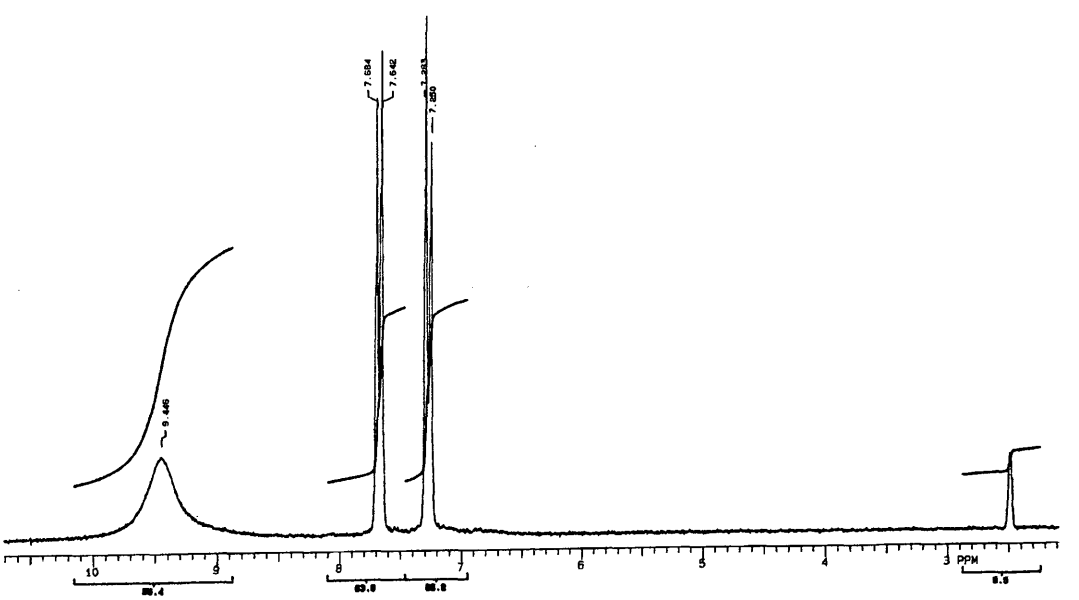

Table 3.10: ^{1}H NMR spectrum of sulfanilic in d_6-DMSO: peak assignments

δ / ppm	integral ratio	multiplicity	J / Hz	assignment
2.49	-	-	-	DMSO
7.27	2	d	9	Ar-**H2**
7.66	2	d	9	Ar-**H3**
9.45	3	broad s	-	-SO_3**H** and -NH_2

Figure 3.12: ^{1}H NMR spectrum of the product in d_6-DMSO

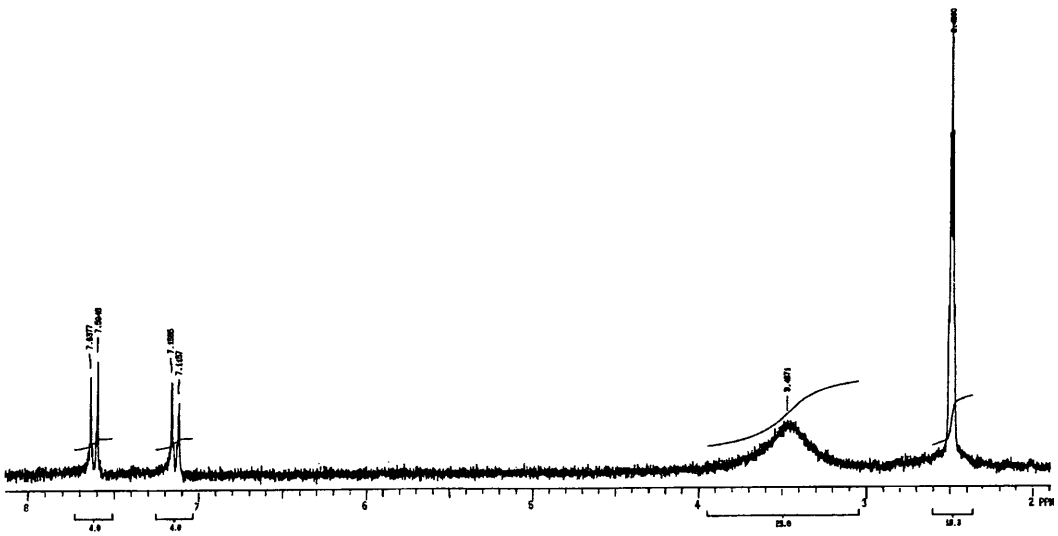

Table 3.11: ^{1}H NMR spectrum of the product in d_6-DMSO: peak assignments

δ / ppm	integral ratio	multiplicity	J / Hz	assignment
2.49	-	-	-	DMSO and -NC**H**$_2$N-
3.47	6	broad s	-	H_2O and -N**H**-
7.14	1	d	9	Ar-**H2'**
7.62	1	d	9	Ar-**H3'**

3.2.1.6 Summary

The [4-$RC_6H_4N{=}CH_2$] imine trimers **12** have been prepared for the amines where R = H and -$N(CH_3)_2$. These were shown to be the trimers from ^1H NMR and uv / vis spectral evidence. However the products where R = -COOH, -NO_2 and -SO_3H appear to be 1 : 2 formaldehyde : amine adducts with the general structure **13**. This is evident from ^1H NMR and uv / vis spectral results.

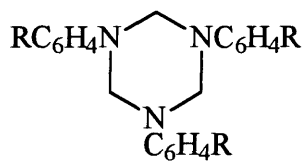

12

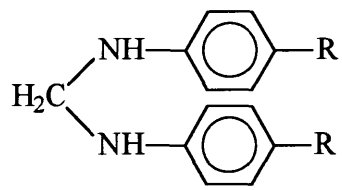

13

3.2.1.7 Mechanisms

The mechanism of formation of the trimer has not been determined. A proposed mechanism is shown in Scheme 3.2.

Scheme 3.2:

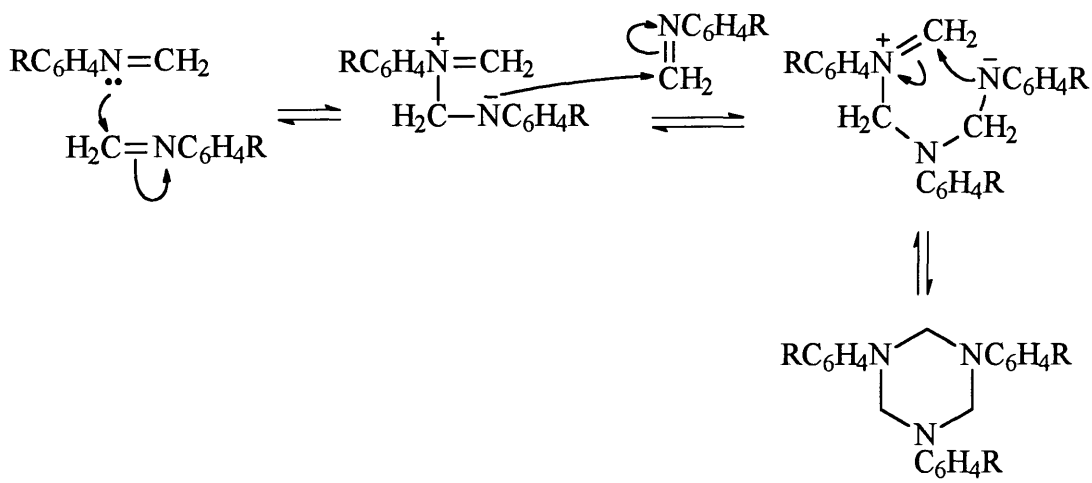

The nitrogen atom of one imine molecule acts as a nucleophile attacking the δ positively charged -CH_2 carbon of another. The negatively charged nitrogen produced will then

readily react with another imine molecule to give the trimer, a six membered ring. The trimer rather than a dimer, **14**, is produced as the six membered ring will be more thermodynamically stable than the four membered ring of the dimer. Imine dimers have not been isolated.[2]

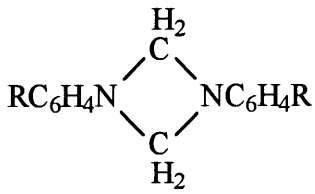

14

A 1 : 2 formaldehyde : amine product is produced when the amine has an electron withdrawing group on the aromatic ring, such as -COOH, $-NO_2$ and $-SO_3H$. These groups will make the nitrogen of the imine less nucleophilic. A possible pathway for formation would involve reaction of amine with the imine or even with the *N*-(hydroxymethyl)amine formed from the reaction of formaldehyde with the amine (Chapter 2). These pathways are shown in Scheme 3.3.

Scheme 3.3:

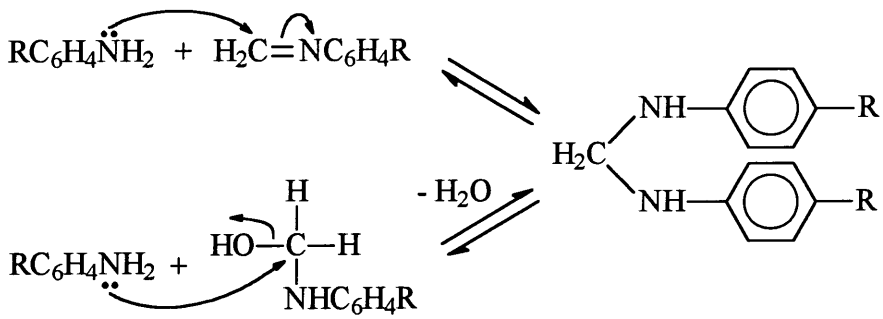

These mechanisms involve nucleophilic attack of the amine on the imine or *N*-(hydroxymethyl)amine: the amine will act as the nucleophile in preference to the less nucleophilic imine.

3.2.2 1,3,5-Triphenyl-1,3,5-hexahydrotriazine, the $C_6H_5N=CH_2$ trimer

3.2.2.1 Stability of the trimer in solution

The stability in solution of 1,3,5-triphenyl-1,3,5-hexahydrotriazine, synthesised in Section 3.2.1.1, was investigated.

3.2.2.1.1 Effect of solvent composition

1,3,5-Triphenyl-1,3,5-hexahydrotriazine, the trimer, has low solubility in water but was found to be soluble in dioxan. The absorbance against wavelength spectrum in dioxan shows a peak at 251 and a shoulder at 277 nm with extinction coefficients of 43000 and 9000 mol^{-1} dm^3 cm^{-1} respectively (Figure 3.13).

Figure 3.13: Absorbance against wavelength spectrum of the trimer in dioxan

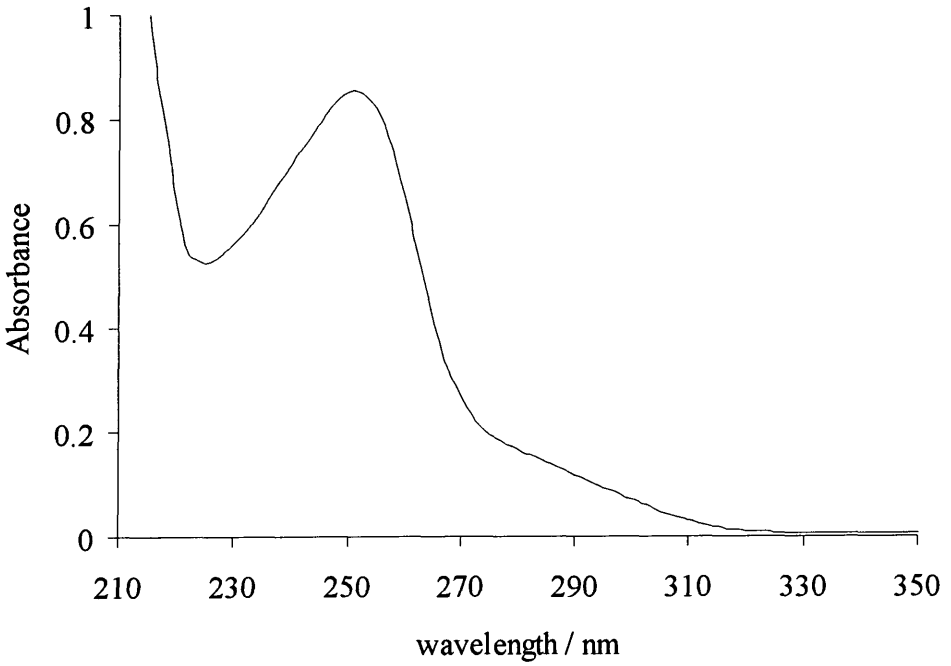

By observing the spectrum of the trimer in different solvents, it was determined that in a mixed dioxan / water solvent system with 20 % or less dioxan by volume, the spectrum obtained can be assumed to be like that in 100 % water.

The absorbance against wavelength spectrum of the trimer changes when in a mixed dioxan / water solvent containing over 20 % dioxan by volume. The same trend is observed when using acetonitrile instead of dioxan. Figure 3.14 shows the initial spectra obtained for 2×10^{-5} mol dm^{-3} trimer in mixed acetonitrile / water solvents. The trimer has limited solubility in acetonitrile therefore a concentrated stock solution in dioxan was used. All solutions therefore contain < 1 % dioxan by volume.

Figure 3.14: Absorbance against wavelength spectra for 2×10^{-5} mol dm^{-3} trimer in mixed acetonitrile / water solvents†: initial spectra

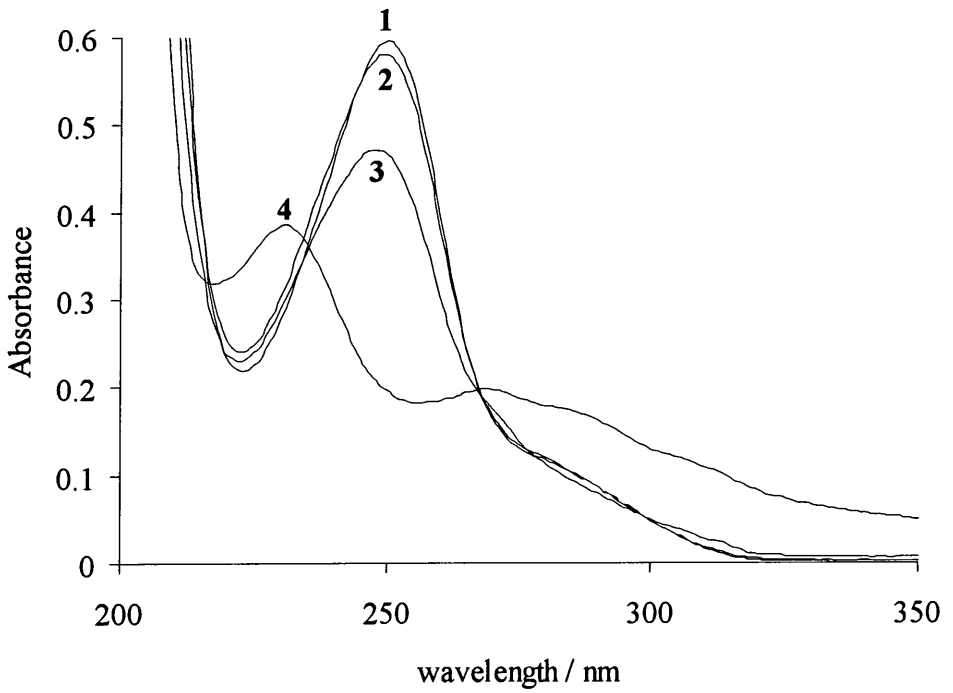

1 = 100 % acetonitrile; **2** = 60 % acetonitrile / 40 % water by volume;
3 = 40 % acetonitrile / 60 % water by volume; **4** = 100 % water

† all solutions also contain < 1 % dioxan by volume

The spectrum in ~ 100 % acetonitrile showed no change over time. However the other spectra showed a decrease in absorbance over time followed by an increase in absorbance and a peak shift to shorter wavelength. The reactions are complete within 24 hours. Figure 3.15 shows the change over time for 2×10^{-5} mol dm^{-3} trimer in a 60 % acetonitrile / 40 % water solvent by volume.

Figure 3.15: Absorbance against wavelength spectrum and change over time for 2×10^{-5} mol dm^{-3} trimer in 60 % acetonitrile / 40 % water by volume solvent†

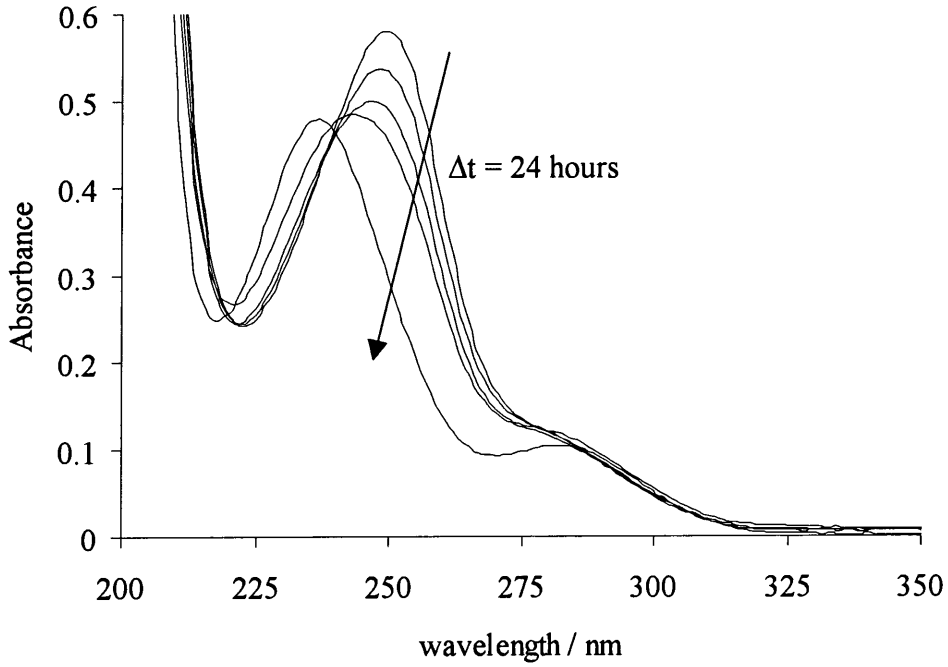

† solutions also contain < 1 % dioxan by volume

For comparison, the absorbance against wavelength spectrum of aniline in mixed dioxan / water and acetonitrile / water solvents was obtained. The initial spectrum of the trimer is different from that of the corresponding aniline spectrum although the similarities increase as the water content of the solvent increases. Over time, the spectrum of the trimer becomes very similar to that of aniline with an apparent extinction coefficient equal to approximately three times that of aniline. This corresponds to decomposition of the trimer which will produce three moles of aniline.

Absorbance against time plots were obtained for 2×10^{-5} mol dm^{-3} trimer in 30 % acetonitrile / 70 % water and 40 % acetonitrile / 60 % water by volume solvents. Decomposition of the trimer at 248 nm was followed. The effect of the presence of 0.01 to 0.03 mol dm^{-3} aqueous sodium sulfite solution, Na_2SO_3, was also investigated at pH 9.5 and in unbuffered solution. The pH of an unbuffered system was found to be pH 6.5. The plots were first order: k_{obs} / s^{-1} values obtained are shown in Table 3.12.

Table 3.12: k_{obs} / s^{-1} values obtained for the decomposition of 2×10^{-5} mol dm^{-3} trimer and the effect of the presence of aqueous sulfite solution

% solvent by volume		pH†	$[Na_2SO_3]$ / M	k_{obs} / s^{-1}
acetonitrile	water			
30	70	-	0	$1.27 \times 10^{-4} \pm 4 \times 10^{-7}$
40	60	-	0	$7.21 \times 10^{-5} \pm 1 \times 10^{-7}$
40	60	-	0.01	$4.80 \times 10^{-5} \pm 2 \times 10^{-7}$
40	60	9.5	0.02	$9.73 \times 10^{-6} \pm 2 \times 10^{-7}$
40	60	9.5	0.03	$6.43 \times 10^{-6} \pm 8 \times 10^{-8}$

† no value quoted for unbuffered solutions where pH ~ 6.5, higher in the presence of Na_2SO_3

The rate constant for decomposition increases as the proportion of water in the solvent system increases. The rate constant decreases on addition of sulfite: the higher the concentration of sulfite the greater the decrease. The solutions containing sulfite will be alkaline so the decrease possibly reflects a pH effect.

3.2.2.1.2 pH effects

The effect of pH on the absorbance against wavelength spectrum of 2×10^{-5} mol dm^{-3} trimer was studied in a 20 % dioxan / 80 % water by volume solvent at pH 1.1, 4.3, 6.9 and 10.7 were obtained. The spectra showed little change over time. All the spectra have the same general profile, as shown in Figure 3.13, except at pH 1 where the spectrum showed very little absorbance. This is probably due to protonation of the trimer or the decomposition product, aniline, as the spectral appearance of the trimer returned on basification to pH 6.9.

Absorbance against time plots were obtained for 2×10^{-5} mol dm^{-3} trimer in a 40 % acetonitrile / 60 % water by volume solvent at nine pH values in the range 4.9 to 11.1 using conventional uv / vis spectrometry. Decomposition of the trimer at 248 nm was followed.

The plots are not simple first order. Two rate processes are involved in the decomposition: an initial fast reaction followed by a slower reaction (Figure 3.16).

Figure 3.16: Absorbance against time plots for the decomposition of 2×10^{-5} mol dm^{-3} trimer in 40 % acetonitrile / 60 % water by volume solvent at pH 5.5 and 6.0, 25 °C

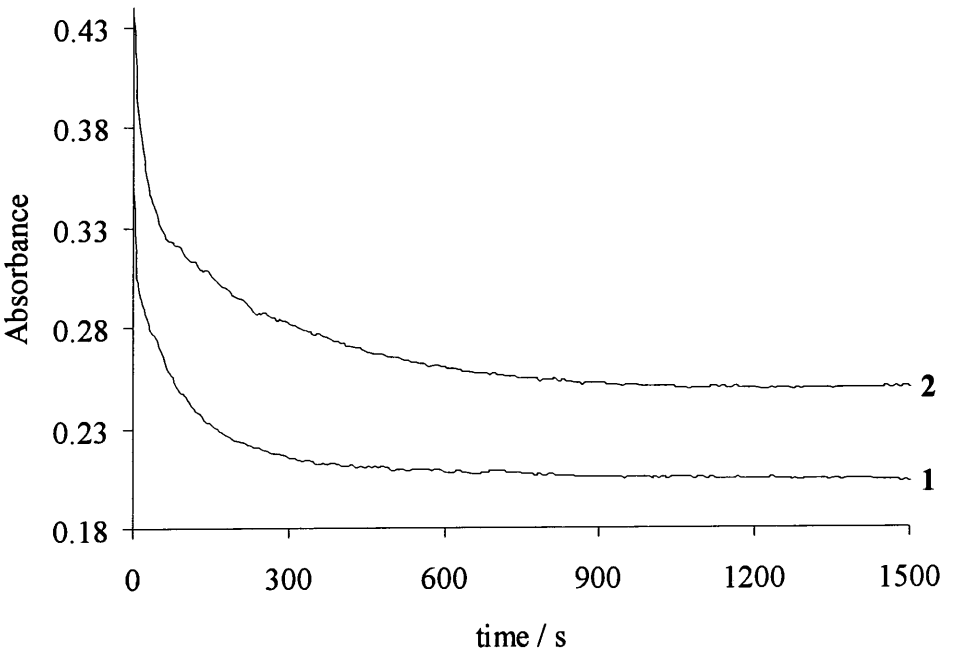

1 = pH 5.5; **2** = pH 6.0

Both processes visibly decrease in rate as the pH increases implying the reaction is acid catalysed.

Stopped flow spectrophotometry was used to obtain absorbance against time plots for 1×10^{-5} mol dm^{-3} trimer in a 40 % acetonitrile / 60 % water by volume solvent at twelve pH values in the range 1.1 to 4.5. Decomposition of the trimer at 248 nm was followed.

The plots are again not simple first order. As before, two rate processes are observed in the decomposition: an initial fast reaction followed by a slower reaction. The initial absorbances of the absorbance against time plots show a general decrease as the solution becomes more acidic (Table 3.13). This indicates rapid protonation of the trimer.

Table 3.13: Initial absorbances in the absorbance against time plots for the decomposition of 1.0×10^{-5} mol dm^{-3} trimer, pH 1.1 to 4.8.

pH	initial absorbance	pH	initial absorbance
1.1	0.122	2.2	0.215
1.2	0.132	2.6	0.225
1.3	0.137	3.0	0.232
1.5	0.156	3.2	0.233
1.8	0.189	3.7	0.238
2.0	0.205	4.8	0.235

Plotting initial absorbance against pH gives a sigmoidal curve from which a pK_a of around 1 to 2 can be obtained for the trimer (Figure 3.17). The value of the absorbance corresponding to complete protonation is not known, hence a precise value of the pK_a is not obtainable.

Figure 3.17: Plot of initial absorbance against pH

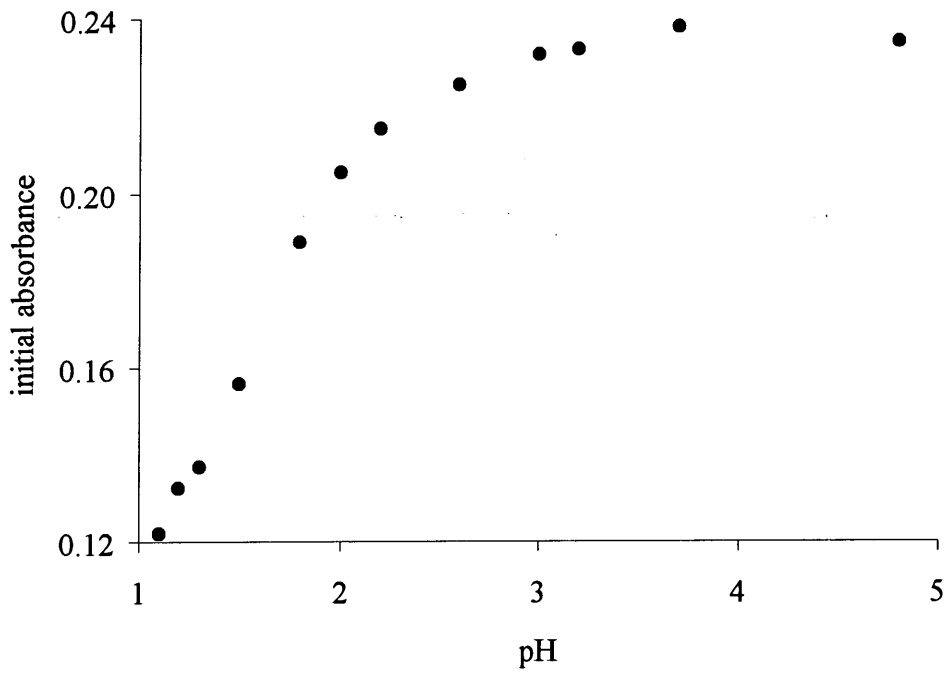

The pK_a of aniline[6] is 4.60. The pK_a of the trimer would be expected to be lower than this due to the presence of other electron withdrawing nitrogen atoms in the six membered ring.

3.2.2.2 Formation of the trimer

3.2.2.2.1 ^{1}H NMR studies

^{1}H NMR spectroscopy was used to attempt to follow the formation of the trimer. Initially the spectra of the starting materials, 0.2 M aniline and 0.2 M aqueous formaldehyde solution, in deuterated acetonitrile, CD_3CN, were obtained for comparison. Figures 3.18 and 3.19 and Tables 3.14 and 3.15 describe the ^{1}H NMR spectra obtained.

Figure 3.18: ^{1}H NMR spectrum of aniline in CD_3CN

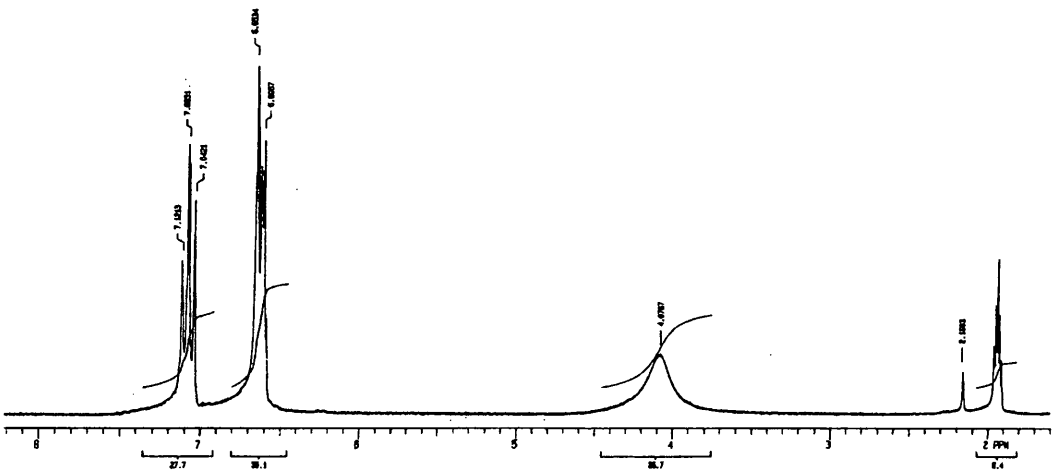

Table 3.14: ^{1}H NMR spectrum of aniline in CD_3CN: peak assignments

δ / ppm	integral ratio	multiplicity	J / Hz	assignment
1.94	-	-	-	CHD_2CN
2.16	-	-	-	-
4.08	2	broad s	-	$-NH_2$
6.61	3	t	8	Ar-**H4**
6.63		d	8	Ar-**H2**
7.08	2	t	8	Ar-**H3**

Figure 3.19: ^{1}H NMR spectrum of aqueous formaldehyde solution in CD_3CN

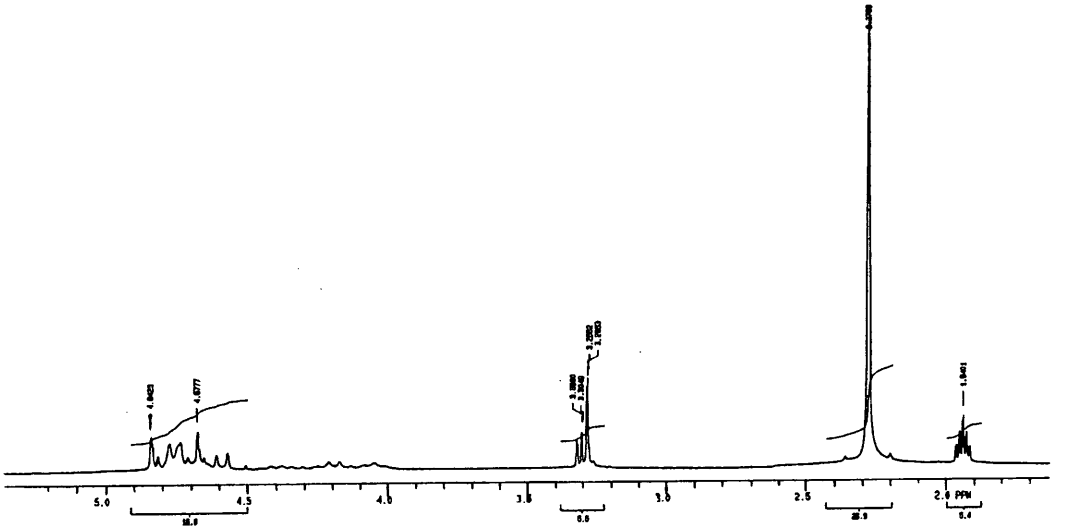

Table 3.15: ^{1}H NMR spectrum of aqueous formaldehyde solution in CD_3CN: peak assignments

δ / ppm	integral ratio	multiplicity	J / Hz	assignment
1.94	-	-	-	CHD_2CN
2.28	-	s	-	CH_3OH
3.29 – 3.31	1	-	-	-CH_2 in $CH_2(OH)_2$ and other
4.5 – 4.8	3	-	-	polyoxymethylene glycols

There is no peak in the spectrum due to water: the equilibrium constants for formation of $CH_2(OH)_2$ and other polyoxymethylene glycols are so large that, under the conditions used, the water will be predominantly in this form rather than as free water. The peak at δ 2.28 ppm is probably due to methanol present as a stabiliser in the aqueous formaldehyde solution. As methanol is present, the formation of methyl substituted products, such as $RNHCH_2OCH_3$, must also be considered.

The reaction of 0.20 M aniline and 0.21 M aqueous formaldehyde solution was followed over time. A spectrum was recorded 15 minutes after addition of the aniline then again after 2, 4 and 6 hours, and 3 and 4 days. After 4 days, white crystals had formed in the sample. ^{1}H NMR identified this as the trimer. Figure 3.20 shows the spectrum obtained 15 minutes after mixing. There was no change in the spectrum over time. Table 3.16 summarises the information obtained from the spectrum.

Figure 3.20: 0.20 M aniline and 0.21 M aqueous formaldehyde solution: 15 minutes after mixing

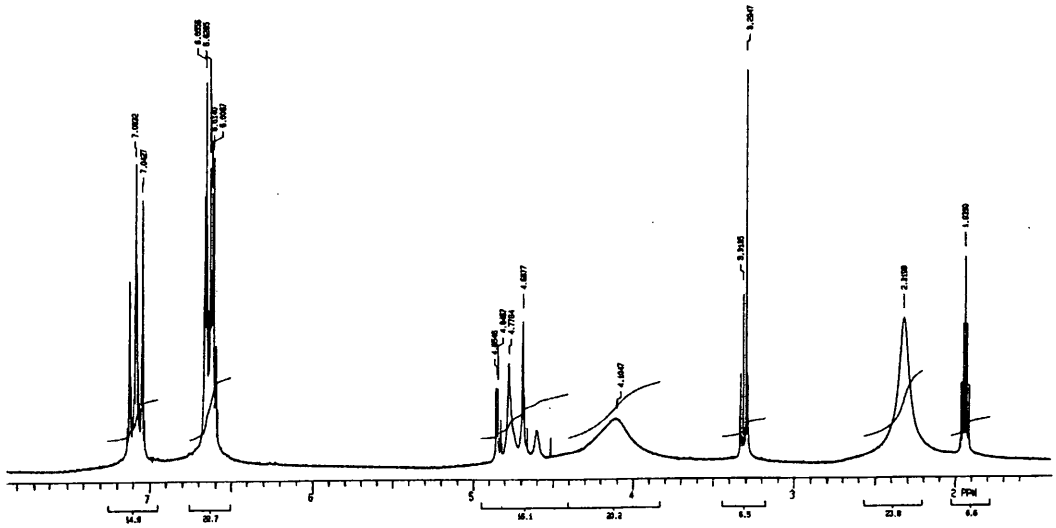

Table 3.16: Peak assignments: 15 minutes after mixing

δ / ppm	integral ratio	multiplicity	J / Hz	assignment
1.94	-	-	-	CHD_2CN
2.32	-	-	-	CH_3OH
3.29	1	m	-	H_2O
3.32				$C_6H_5NHCH_2OH$
4.10	3	broad s	-	-N**H**
4.6 – 4.9	2	-	-	aq. formaldehyde
~ 6.61	3	t	8	Ar-**H4** in product
6.61		t	8	Ar-**H4**
6.63		d	8	Ar-**H2**
6.66		d	8	Ar-**H2** in product
~ 7.07	2	t	8	Ar-**H3** in product
7.08		t	8	Ar-**H3**

The spectrum does not show evidence of the trimer. Instead another species is observed, probably the *N*-(hydroxymethyl)amine, $C_6H_5NHCH_2OH$. The trimer does form over time but precipitates out of solution as white crystals.

To see whether a similar product could be observed using another amine, the reaction was repeated using benzylamine. Initially the spectra of the starting material, 0.20 M benzylamine, **15**, in CD_3CN was obtained for comparison. Figure 3.21 and Table 3.17 describe the ^1H NMR spectrum obtained.

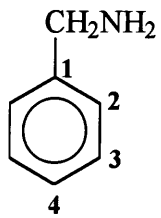

15

Figure 3.21: ^1H NMR spectrum of benzylamine in CD_3CN

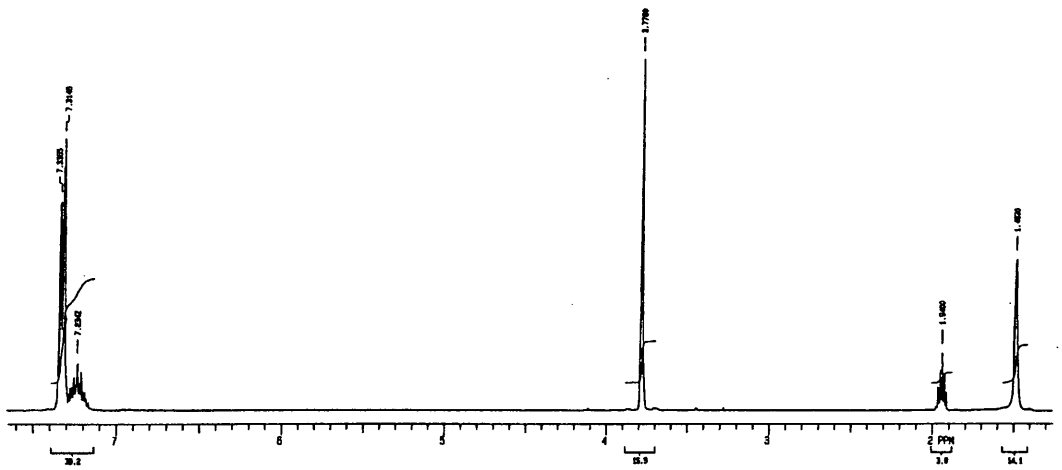

Table 3.17: ^1H NMR spectrum of benzylamine in CD_3CN: peak assignments

δ / ppm	integral ratio	multiplicity	J / Hz	assignment
1.84	2	s	-	-
1.94	-	-	-	CHD_2CN
3.78	2	s	-	$-CH_2NH_2$
7.23	5	m	-	Ar-**H3**
7.33		d	5	Ar-**H2**, **H4**

It is not clear what the peak at δ 1.84 ppm is due to: it may be due to an impurity in the benzylamine stock. This peak does not appear in any subsequent spectra.

The reaction of 0.20 M benzylamine and 0.20 M aqueous formaldehyde solution was followed over time. A spectrum was recorded 10 minutes after addition of the benzylamine then again after 1, 2, and 3 hours, and 1 and 2 days. There was no precipitation of any solid.

Figures 3.22 and 3.23 show the spectra obtained 10 minutes and 1 day after mixing respectively. There was no further change in the spectrum. Tables 3.18 and 3.19 summarise the information obtained from the two spectra.

Figure 3.22: 0.20 M benzylamine and 0.21 M aqueous formaldehyde solution: 10 minutes after mixing

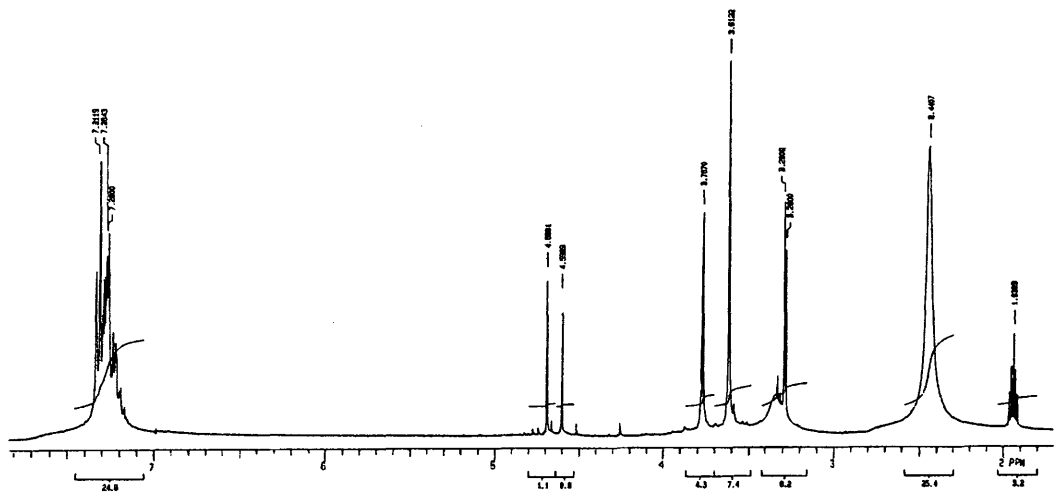

Table 3.18: Peak assignments: 10 minutes after mixing

δ / ppm	integral ratio	multiplicity	J / Hz	assignment
1.94	-	-	-	CHD_2CN
2.44	-	broad s	-	$\mathbf{CH_3}OH$
3.28	2	s	-	$C_6H_5CH_2NHC\mathbf{H_2}OH$
3.29		s	-	H_2O
~ 3.3		broad s	-	-N**H**
3.61	2	s	-	$C_6H_5C\mathbf{H_2}NHCH_2OH$
3.77	1	s	-	$C_6H_5C\mathbf{H_2}NH_2$
4.6 – 4.8	1	-	-	aqueous formaldehyde
~ 7.26	6	m	-	Ar-**H3**, **H4** in amine and product
7.33		d	-	Ar-**H2** in amine and product

Figure 3.23: 0.20 M benzylamine and 0.21 M aqueous formaldehyde solution: 1 day after mixing

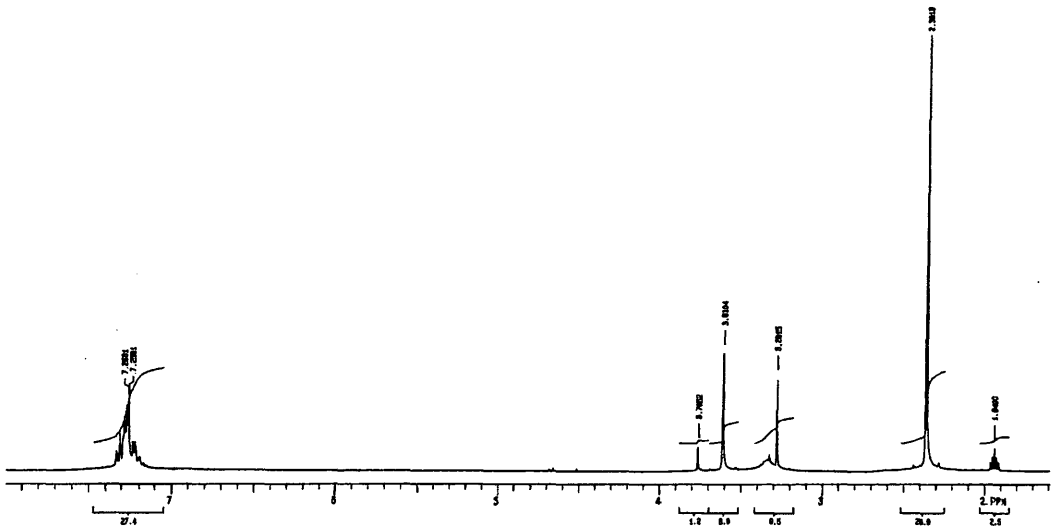

Table 3.19: Peak assignments: 1 day after mixing

δ / ppm	integral ratio	multiplicity	J / Hz	assignment
1.94	-	-	-	CHD_2CN
2.36	-	s	-	$\mathbf{CH_3}OH$
3.28	2	s	-	$C_6H_5CH_2NHC\mathbf{H_2}OH$
~ 3.3		broad s	-	-N**H**
3.61	2	s	-	$C_6H_5C\mathbf{H_2}NHCH_2OH$
3.77	1	s	-	$C_6H_5C\mathbf{H_2}NH_2$
~ 7.26	6	m	-	Ar-**H3**, **H4** in amine and product
7.33		m	-	Ar-**H2** in amine and product

After 1 day all the aqueous formaldehyde has reacted: there are no peaks due to water, methanol or the $-CH_2$ groups of methylene glycol and other linear polyoxymethylene glycols remaining. There is only a relatively small amount of unreacted benzylamine after this time.

The experiment was repeated using a 90 % CD_3CN / 10 % D_2O solvent by volume. The same product was observed, but the reaction occurred much faster: the reaction was complete within 1 hour. There was no evidence of any other product.

There is no evidence of a trimeric species in the spectra. The product is probably the *N*-(hydroxymethyl)amine, $C_6H_5CH_2NHCH_2OH$, rather than the imine as -CHN=C- bands are usually observed around δ 7.5 to 8.0 ppm.[7] There was no evidence of such bands in the spectra obtained here.

3.2.2.2.2 Uv / vis spectroscopy studies

As the trimer has a distinctive uv spectrum, the possibility of following the formation of the trimer by observing the change over time of the uv spectrum of a solution of aniline and formaldehyde was investigated. However the reaction of 5.0×10^{-5} M aniline with 1×10^{-4} to 0.1 M aqueous formaldehyde solution in a 10 % dioxan / 90 % water solvent by volume solvent showed no change in the spectrum over time: the spectrum was merely that of aniline. Acid was added to try to catalyse the reaction, but very poor spectra were obtained, probably due to protonation of the aniline. Base catalysis was not effective either: the spectrum remained unchanged after 17 hours.

The reaction may not be observed due to the low concentrations used or may be limited by the rate of dehydration of the aqueous formaldehyde solution to give free formaldehyde, HCHO, the reactive form.

3.3 CONCLUSION

The [4-$RC_6H_4N{=}CH_2$] imine trimers were prepared for the amines where R = H and -$N(CH_3)_2$. The products when R = -COOH, -NO_2 and -SO_3H appear to be 1 : 2 formaldehyde : amine adducts. These can form via reaction of the amine with the imine or *N*-(hydroxymethyl)amine.

The stability in solution of the imine trimer formed from aqueous formaldehyde solution and aniline was studied. The trimer decomposes in solution to give as the eventual products aniline and, by inference, aqueous formaldehyde. The results show that the reaction is acid catalysed and involves at least two measurable processes. These acid catalysed reactions could be as shown in Scheme 3.4.

Scheme 3.4:

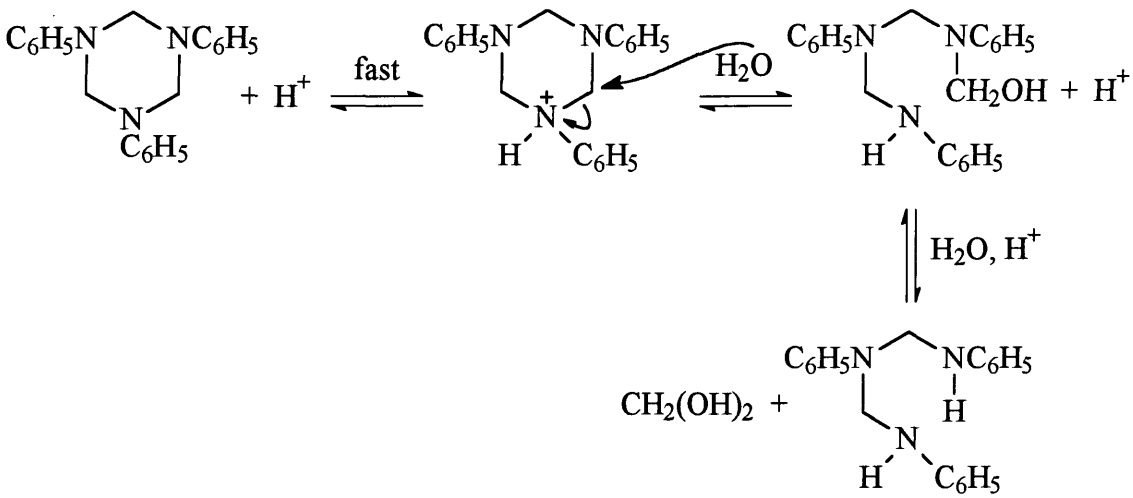

These reactions involve rapid protonation of the trimer followed by rate determining attack of water with carbon – nitrogen bond cleavage. Acid catalysed decomposition of the *N*-(hydroxymethyl)amine then yields an aniline derivative and aqueous formaldehyde. Further analogous decomposition will yield aniline.

Formation of the *N*-(hydroxymethyl)amines $C_6H_5NHCH_2OH$ and $C_6H_5CH_2NHCH_2OH$ was observed using ^1H NMR spectroscopy for the reaction of aqueous formaldehyde solution with aniline and benzylamine respectively in equimolar amounts. The trimer

formed over time for the reaction with aniline and precipitated out of solution as white crystals.

The *N*-(hydroxymethyl)amine is therefore the major product in the reaction of aqueous formaldehyde solution with amines in equimolar concentrations: the trimer only forms over a long period of time, over days under the conditions used. Dehydration of the *N*-(hydroxymethyl)amine is therefore likely to be rate limiting. Formation of cyclic imines is accelerated by the presence of an electron withdrawing group on the aniline such as 4-$N(CH_3)_2$.

The 1 : 2 formaldehyde : amine adducts produced with 4-$RC_6H_4NH_2$ amines, where R = -COOH, -NO_2 and -SO_3H, form much faster, generally within seconds or minutes under the conditions used. This suggests that these products form predominantly via reaction of the amine with the *N*-(hydroxymethyl)amine, as opposed to reaction of the amine with the imine, as the imine will probably not form this rapidly.

3.4 EXPERIMENTAL

3.4.1 Preparation of 4-$RC_6H_4N{=}CH_2$ imine polymers

The imine polymers were prepared as described in the text.

Recrystallisation was attempted for the 4-dimethylaminoaniline imine trimer using boiling ethanol or hot 60 - 80° petroleum ether. 50 cm^3 boiling ethanol or 60 - 80° petroleum ether heated to 50 °C was added to 1 g of product. This was then filtered rapidly through oven-hot apparatus and the filtrate cooled rapidly in ice. For the ethanol recrystallisation, 20 cm^3 distilled water was then added gradually over approximately 5 minutes. Solid began to form within a few minutes, forming faster on the addition of water. The solution was left stirring in ice for 1 hour. The solution was then filtered and the solid collected. For the recrystallisation involving petroleum ether, the filtrate was cooled in ice for 10 minutes then left at room temperature for 24 hours. The solid produced over this time was filtered and washed with cold 60 - 80° petroleum ether. Both these methods were unsuccessful: little solid was produced and that obtained was virtually identical to the crude product when analysed using uv / vis and ^1H NMR spectroscopy.

Recrystallisation was also attempted for the 4-aminobenzoic acid product using boiling ethanol or hot 60 - 80° petroleum ether. 50 cm^3 boiling ethanol or 100 cm^3 60 - 80° petroleum ether heated to 50 °C was added to 1 g of product. This was then filtered rapidly through oven-hot apparatus and the filtrate cooled rapidly in ice. For the ethanol recrystallisation, 20 cm^3 distilled water was then added gradually over approximately 5 minutes. The solution was left stirring in ice for 2½ hours. No solid formed. For the recrystallisation involving petroleum ether, the filtrate was cooled in ice for 10 minutes then left at room temperature for 24 hours. Little solid was produced. The solution was cooled in ice for a further 6 hours: no further solid was produced. Both these methods were therefore unsuccessful: little solid was produced.

Recrystallisation of the aniline, 4-nitroaniline and sulfanilic acid products was not attempted.

Sulfanilic acid is relatively soluble in water therefore the preparation was performed in aqueous solution. However lower concentrations had to be used due to the limited solubility. The aqueous sulfanilic acid solution was chilled in ice after addition of aqueous formaldehyde solution to prevent sulfanilic acid from precipitating out of solution. The product obtained has limited solubility in d_6-DMSO: the ^{1}H NMR sample was left overnight to dissolve.

CD_3CN was used as the ^{1}H NMR solvent for the 4-nitroaniline product as in d_6-DMSO the -NCH_2N- peak is masked by the solvent peak: d_6-DMSO is a good hydrogen bond donor therefore the spectra are shifted downfield in this solvent. The -NCH_2N- peak in the sulfanilic acid product is also masked, however it is not soluble in CD_3CN therefore this could not be used to obtain a spectrum.

^{1}H NMR spectra were recorded using a 200 MHz Varian Mercury – 200, VXR 200 or Gemini 200 spectrometer. The peak due to residual protons in the deuterated solvent was used for locking purposes and as the reference peak for spectra. Chemical shifts are quoted to 2 decimal places. Coupling constants are given where the multiplicity is greater than a singlet and are quoted to the nearest whole number.

Absorbance against wavelength spectra were obtained for 4-dimethylaminoaniline and 4-nitroaniline and the respective imine polymers formed. Spectra were obtained using a Perkin – Elmer Lambda 2 uv / vis spectrometer at 25 °C with 1 cm stoppered quartz cuvettes, taking scans every 5 or 10 minutes for up to 4 hours using a scan speed of 480 nm min^{-1}. The cuvettes were left in the spectrometer for at least 10 minutes prior to use to allow the temperature to equilibrate to 25 °C. Extinction coefficients are quoted to 2 or 3 significant figures and were calculated using only one spectrum in most cases.

3.4.2 Stability of 1,3,5-triphenyl-1,3,5-hexahydrotriazine

3.4.2.1 Conventional uv / vis spectroscopy studies

Absorbance against wavelength spectra were obtained for the trimer and for aniline in < 1 % dioxan / > 99 % water by volume to 100 % acetonitrile or dioxan solvents and for the trimer in a 20 % dioxan / 80 % water by volume solvent at pH 1.1 to 10.7.

Absorbance against wavelength spectra were obtained using a Perkin – Elmer Lambda 2 uv / vis spectrometer at 25 °C with 1 cm stoppered quartz cuvettes, taking scans every minute for up to 2 hours using a scan speed of 480 nm min^{-1}. The cuvettes were left in the spectrometer for at least 10 minutes prior to use to allow the temperature to equilibrate to 25 °C. Extinction coefficients are quoted to 2 or 3 significant figures and were calculated using only one spectrum in some cases.

Plots of absorbance against time were obtained for 2×10^{-5} mol dm^{-3} trimer in 30 % acetonitrile / 70 % water and 40 % acetonitrile / 60 % water by volume solvents, with and without the presence of aqueous sulfite solution, and in a 20 % dioxan / 80 % water by volume solvent at nine pH values in the range 4.9 to 11.1 at 25 °C.

Plots were recorded using a Perkin – Elmer Lambda 2 uv / vis spectrometer at 25 °C with 1 cm stoppered quartz cuvettes. The data interval ranged from 5 seconds to 3 minutes and the overall reaction time from 2 to 15 hours depending on the pH, the solvent system used and whether aqueous sodium sulfite was present. The cuvettes were left in the spectrometer for at least 10 minutes prior to use to allow the temperature to equilibrate at 25 °C. The decomposition of the trimer was followed at 248 nm. The reaction was initiated by adding a small volume of a concentrated solution of trimer in dioxan.

Sulfite ions absorb in the region studied: spectra of 0.01, 0.05 and 0.10 M aqueous sodium sulfite solution were obtained and showed high absorbance around 250 nm and to shorter wavelength. For example, the extinction coefficient of sulfite ions at 245 nm was found to be 50 dm^3 mol^{-1} cm^{-1}. Therefore when aqueous sodium sulfite solution was added, the appropriate concentration was also added to the reference in order to subtract the absorbance due to the presence of sulfite from the absorbance against time plots.

First order kinetics were fitted using the PECCS program installed on the Perkin – Elmer Lambda 2 spectrometer. Rate constants are quoted to 2 decimal places.

The buffers employed and the corresponding stoichiometric buffer concentrations in the final solutions are shown in Table 3.20. Where buffers were used, the appropriate volume of buffer was also present in the reference cuvette.

Table 3.20: Final buffer concentrations

pH	component A	$[A]_{stoich}$ / M	component B	$[B]_{stoich}$ / M
1.1	HCl	0.027	KCl	0.010
4.3	CH_3COOH	0.020	CH_3COONa	4.0×10^{-3}
4.9	CH_3COOH	0.050	CH_3COONa	0.020
5.3	CH_3COOH	0.050	CH_3COONa	0.050
5.5	CH_3COOH	0.030	CH_3COONa	0.050
6.0	CH_3COOH	0.010	CH_3COONa	0.050
6.9	CH_3COOH	0.010	CH_3COONa	0.056
9.5	$Na_2B_4O_7.10H_2O$	6.3×10^{-3}	HCl	0.010
10.2	$Na_2B_4O_7.10H_2O$	6.3×10^{-3}	HCl	2.3×10^{-3}
10.7	$Na_2B_4O_7.10H_2O$	2.5×10^{-3}	NaOH	3.7×10^{-3}
11.1	$Na_2B_4O_7.10H_2O$	6.3×10^{-3}	NaOH	9.2×10^{-3}

The pH values of all solutions were determined using a Jenway 3020 pH meter calibrated using pH 7 and pH 10 (for alkaline solutions) or pH 4 (for acidic solutions) buffers. pH values are quoted to one decimal place.

3.4.2.2 Stopped flow spectrophotometry studies

The decomposition of 1×10^{-5} mol dm^{-3} trimer in a 40 % acetonitrile / 60 % water by volume solvent at twelve pH values in the range 1.1 to 4.5 was studied using stopped flow spectrophotometry. Decomposition of the trimer at 248 nm was followed. Plots were recorded using an Applied Photophysics DX.17MV BioSequential Stopped – flow ASVD Spectrometer at 25.0 – 25.3 °C with a cell of 2 mm path length. Ten averages were obtained, each the average of three runs of 50 to 100 seconds depending on the pH value. The trimer solution in 40 % acetonitrile / 60 % water by volume was placed in

one syringe and the aqueous buffer solution with 40 % acetonitrile by volume added in the other.

Aqueous hydrochloric acid, HCl, was used to control the pH. The final HCl concentrations in the solutions at each pH are shown in Table 3.21.

Table 3.21: Final aqueous hydrochloric acid concentrations

pH	[HCl] / M	pH	[HCl] / M
1.1	0.050	2.2	4.0×10^{-3}
1.2	0.040	2.6	2.0×10^{-3}
1.3	0.030	3.0	1.0×10^{-3}
1.5	0.020	3.2	7.0×10^{-4}
1.8	0.010	3.7	5.0×10^{-4}
2.0	7.0×10^{-3}	4.8	3.0×10^{-4}

For the experiments at pH 3.2 to 4.8, where very low HCl concentrations were used, purified water was used throughout to minimise carbon dioxide concentration effects. The purified water was prepared by using an isomantle to heat distilled water in a round bottomed flask. After boiling for 10 minutes, a soda lime drying tube was attached and all joints sealed.

The pH values of all solutions were determined using a Jenway 3020 pH meter calibrated using pH 7 and pH 10 (for alkaline solutions) or pH 4 (for acidic solutions) buffers. pH values are quoted to one decimal place.

3.4.2.3 ^{1}H NMR studies

The reactions of aniline and of benzylamine with aqueous formaldehyde solution were followed using ^{1}H NMR spectroscopy. Initially the spectrum of 0.20 M amine alone was obtained, then the spectrum in the presence of equimolar aqueous formaldehyde solution. The solutions were made immediately prior to use. The aqueous formaldehyde was placed in the NMR tube, 1 cm^3 CD_3CN, or 0.9 cm^3 CD_3CN and 0.1 cm^3 D_2O,

added followed by the neat amine which was added at the NMR machine side. The ^1H NMR spectrum of 0.20 M aqueous formaldehyde solution was also obtained for comparison.

Spectra were recorded 10 to 15 minutes after mixing, then regularly until there was no further change in the spectrum. The time of mixing refers to the time at which the amine was added to the NMR tube. The time of each spectrum was taken as the time when the spectrometer started to acquire the spectrum.

^1H NMR spectra were recorded using a 200 MHz Varian Mercury – 200 or Gemini 200 spectrometer. The δ 1.94 ppm singlet due to residual protons in the deuterated solvent, CD_3CN, was used for locking purposes and as the reference peak for all spectra. Chemical shifts are quoted to 2 decimal places. Coupling constants are given where the multiplicity is greater than a singlet and are quoted to the nearest whole number.

3.5 REFERENCES

1. J. G. Miller and E. C. Wagner, *J. Am. Chem. Soc.*, 1932, **54**, 3698

2. A. G. Giumanini, G. Verardo, L. Randaccio, N. Bresciani-Pahor and P. Traldi, *J. f. prakt. Chem.*, 1985, **327**, 739

3. G. Distefano, A. G. Giumanini, A. Modelli and G. Poggi, *J. Chem. Soc., Perkin Trans. 2*, 1985, 1623

4. J. Santhanalakshmi, *Thermochim. Acta.*, 1988, **127**, 369

5. A. T. Nielsen, D. W. Moore, M. D. Ogan and R. L. Atkins, *J. Org. Chem.*, 1979, **44**, 1678

6. D. D. Perrin, 'Dissociation constants of organic bases in aqueous solution', Butterworths, London, 1965 and 1972 Supplement

7. M. R. Crampton, S. D. Lord and R. Millar, *J. Chem. Soc., Perkin Trans. 2*, 1997, 909

CHAPTER 4

Decomposition of hydroxymethanesulfonate, $CH_2(OH)(SO_3Na)$

CHAPTER 4: Decomposition of hydroxymethanesulfonate, $CH_2(OH)(SO_3Na)$

4.1 INTRODUCTION

The formaldehyde sodium bisulfite addition compound $CH_2(OH)(SO_3Na)$, also known as hydroxymethanesulfonate (HMS), is the salt of a strong acid and so is assumed to exist in solution as the singly charged anion (Scheme 4.1, **1**). This anion is itself a weak acid and will be in equilibrium with a doubly charged anion (**2**). Over time, equilibrium will be established with free bisulfite, HSO_3^-, or sulfite ions, SO_3^{2-}, and free formaldehyde, HCHO.

Scheme 4.1:

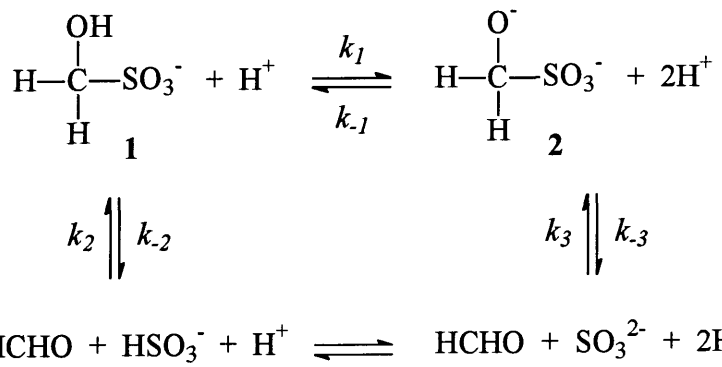

The kinetics of HMS formation and decomposition have been examined previously by a number of authors. Table 4.1 summarises the rate and equilibrium constants reported in the literature.

Table 4.1: Literature values of rate and equilibrium constants

constant	value	experimental conditions		reference
		pH	T / °C	
$K_a = k_1 / k_{-1}$	2.0×10^{-12} mol dm^{-3}	9 - 12	25	1
pK_a	11.7	9 - 12	25	1
k_2	7.90×10^2 mol^{-1} dm^3 s^{-1}	0 – 3.5	25	2
k_3	2.48×10^7 mol^{-1} dm^3 s^{-1}	0 – 3.5	25	2
k_3	9.5×10^6 mol^{-1} dm^3 s^{-1}	9 - 12	25	1
k_{-3}	43 s^{-1}	9 - 12	25	1
$K_3 = k_3 / k_{-3}$	2.2×10^5 mol^{-1} dm^3	9 - 12	25	1

The literature value of the acid dissociation constant, K_a, of $CH_2(OH)(SO_3^-)$ suggests that below pH 11.7 the equilibrium lies in favour of the monoanion as opposed to the dianion. The quoted rate constant for formation of the monoanion, k_2, is smaller than that for the dianion, k_3. This is in agreement with the greater nucleophilicity expected for sulfite than for bisulfite. The rate constant for decomposition of the dianion, k_{-3}, is relatively large, however there is no literature value for the rate constant for decomposition of the monoanion, k_{-2}.

Several authors have considered merely the overall reaction shown in Scheme 4.2, where S(IV) is equal to the sum contributions of bisulfite and sulfite ions.

Scheme 4.2: $\mathrm{HCHO + S(IV) \underset{k_b}{\overset{k_f}{\rightleftharpoons}} HMS}$

Table 4.2 summarises the literature values reported for k_f, k_b and the equilibrium constant K where $K = k_f / k_b$.

Table 4.2: Literature values of k_f, k_b and the equilibrium constant K

k_f / mol^{-1} dm^3 s^{-1}	k_b / s^{-1}	K / mol^{-1} dm^3	experimental conditions		reference
			pH	T / °C	
-	-	8.5×10^6	4.0	20	3
1.94	4.8×10^{-7}	4.0×10^6	4.0	25	4
-	5.5×10^{-6}	-	5.0	20	5
12.6	3.5×10^{-6}	3.6×10^6	5.0	25	4
42	1.1×10^{-5}	3.8×10^6	5.6	25	6

The values reported in the literature are relatively consistent. Both k_f and k_b are dependent on pH. The rate constant for formation increases approximately six times and the decomposition rate constant increases approximately one order of magnitude per pH unit. The equilibrium constant is of the order 10^6, hence it may be assumed that in aqueous solution, at pH 4 to 6 at least, the equilibrium will lie in favour of the adduct, HMS.

The actual pathway followed in the formation and decomposition of HMS, namely either predominantly via bisulfite or sulfite ions, has been the subject of great debate. The relative contributions of bisulfite and sulfite ions to the observed reaction with HCHO may be expected to depend on the equilibrium concentrations of bisulfite and sulfite ions as determined by the pH, and the intrinsic nucleophilicity of each species. Some workers[7] have suggested bisulfite is the only reactant to undergo reaction with HCHO, whereas others[1,8] have obtained evidence that the reactivity of sulfite ions is much greater than bisulfite ions. Stewart and Donnally[9] studied the analogous reaction involving benzaldehyde rather than formaldehyde, to give the adduct $C_6H_5CH(OH)(SO_3^-)$, and proposed that in the pH range 3 to 13 practically all of the formation reaction involves sulfite and not bisulfite ions. Bell and Evans[10] proposed that formation of HMS occurs via rapid nucleophilic addition of sulfite ions to HCHO following rate limiting dehydration of methylene glycol, $CH_2(OH)_2$, the principal species of formaldehyde in aqueous solution.

It can be seen from the literature values given in Tables 4.1 and 4.2 that the formation and decomposition of HMS has not been studied comprehensively over a wide pH range. Therefore the rate of decomposition of HMS was investigated here in a pH range of 1 to 8 by reacting liberated bisulfite and sulfite ions with added aqueous iodine solution. Aqueous iodine solution exists as a number of species, primarily I_3^- with I_2 and I^-. The equilibrium constant for the formation of I_3^- from I_2 and I^- is approximately[11] 720 mol^{-1} dm^3 at 25 °C. Second order rate constants for the reactions of I_3^- and I_2 with HSO_3^- and SO_3^{2-} at 25 °C have been reported in the literature.[12] The reactions are shown in Scheme 4.3.

Scheme 4.3:

$$I_3^- + HSO_3^- \xrightarrow{k_1} ISO_3^- + 2I^- + H^+$$

$$I_2 + HSO_3^- \xrightarrow{k_2} ISO_3^- + I^- + H^+$$

$$I_3^- + SO_3^{2-} \xrightarrow{k_3} ISO_3^- + 2I^-$$

$$I_2 + SO_3^{2-} \xrightarrow{k_4} ISO_3^- + I^-$$

The second order rate constants are quoted as $k_1 = 1.5 \times 10^7$, $k_2 = 1.7 \times 10^9$, $k_3 = 2.9 \times 10^8$ and $k_4 = 3.1 \times 10^9$ mol^{-1} dm^3 s^{-1}. The relative values of the rate constants are $k_2 > k_1$, $k_4 > k_3$, $k_3 > k_1$ and $k_4 > k_2$, showing that sulfite is a stronger nucleophile than bisulfite and I_2 is a stronger electrophile than I_3^-. The iodosulfate, ISO_3^-, that is formed rapidly hydrolyses with a first order rate constant of 298 s^{-1} at 25 °C, according to Scheme 4.4.

Scheme 4.4: $ISO_3^- + H_2O \longrightarrow I^- + SO_4^{2-} + 2H^+$

These reactions of sulfite and bisulfite with iodine are irreversible. The bisulfite / sulfite equilibrium[13] has a pK_a of 7.2 therefore at pH values below 7 the bisulfite form predominates whereas at pH values above 7 sulfite will be the major form. Hydrogen ions are produced during the reactions therefore reaction mixtures of sufficiently high buffer capacity are needed to maintain the correct pH. High buffer concentrations were therefore used.

If the reaction of HMS with aqueous iodine solution is written in terms of Scheme 4.5, where S(IV) is the sum contribution from both sulfite and bisulfite ions and $[I_2]_\tau$ is the sum of $[I_2]$ plus $[I_3^-]$, then the rate expression for the reaction can be derived as shown below (Equations 4.1 and 4.2).

Scheme 4.5: $\text{HMS} \underset{k_f}{\overset{k_b}{\rightleftharpoons}} \text{HCHO} + \text{S(IV)} \xrightarrow[k_4]{\text{iodine}_{(aq)}} \text{products}$

Assuming S(IV) is a steady state intermediate:

$$[\text{S(IV)}] = \frac{k_b[\text{HMS}]}{k_f[\text{HCHO}] + k_4[I_2]_\tau} \qquad \textbf{(4.1)}$$

$$-\frac{d[I_2]_\tau}{dt} = \frac{k_4 k_b[\text{HMS}][I_2]_\tau}{k_f[\text{HCHO}] + k_4[I_2]_\tau} \qquad \textbf{(4.2)}$$

It is expected that the rate of reaction of S(IV) with the aqueous iodine solution will be much faster than the reaction of S(IV) with HCHO and therefore $k_4 >> k_f$. Hence the rate equation reduces to Equation 4.3.

$$- \frac{d[I_2]_\tau}{dt} = k_b[HMS] \qquad \textbf{(4.3)}$$

Therefore the reaction should be zero order with respect to total aqueous iodine solution concentration. In support of this, the rate of decomposition of aldehyde – bisulfite adducts has previously been shown to be independent of the concentration of iodine.[14]

The uv / vis spectrum of a standardised aqueous iodine solution with added potassium iodide was found to show peaks at 287 and 350 nm with extinction coefficients of 19600 ± 300 and 13400 ± 300 mol^{-1} dm^3 cm^{-1} respectively (Appendix 2).

Initially the reaction of aqueous iodine solution with aqueous sulfite solution was investigated to observe the change in spectrum obtained. Then the reaction of HMS with aqueous iodine solution was investigated in the pH range 1 to 8 to examine the decomposition of HMS to gain a better understanding of the mechanism involved.

4.2 RESULTS AND DISCUSSION

4.2.1 Reaction of aqueous sulfite solution with aqueous iodine solution

The reaction of 4×10^{-4} M aqueous iodine solution with solutions of 1.0×10^{-3} to 0.03 M aqueous sodium sulfite solution in the pH range 3.5 to 5.2 was investigated. Decomposition was followed at 300 or 350 nm. The results are shown in Table 4.3.

Table 4.3: k_{obs} / s^{-1} values for the reaction of aqueous sulfite solution with 4×10^{-4} M aqueous iodine solution at pH 3.5 to 5.2, 25 °C

pH	$[Na_2SO_3]$ / M	k_{obs} / s^{-1}
3.0	1.0×10^{-3}	275 ± 3
3.0	0.01	271 ± 3
3.5	1.0×10^{-3}	274 ± 3
3.5	0.01	271 ± 3
5.1	5.2×10^{-3}	272 ± 6
5.1	0.01	271 ± 6
5.1	0.02	268 ± 5
5.2	0.03	269 ± 5

The reaction of aqueous iodine solution with aqueous sodium sulfite solution was found to be a first order reaction, the rate constant of which is independent of pH, at least in the pH range 3 to 5. The bisulfite / sulfite equilibrium[13] has a pK_a of 7.2, therefore in this pH range the bisulfite form will predominate.

The independence of the measured rate constant on the concentration of aqueous sodium sulfite solution is unexpected if following the reaction of HSO_3^- and SO_3^{2-} with aqueous iodine solution. However the reaction being observed may be the hydrolysis of ISO_3^- (Scheme 4.4) if this also absorbs around 350 nm. This species is formed rapidly from the reactants and the hydrolysis is quoted in the literature[12] as having a first order rate constant of 298 s^{-1} at 25 °C which is similar to values obtained here. The results

indicate that the decolourisation of iodine by aqueous sodium sulfite solution is a very rapid reaction under the conditions used.

4.2.2 Decomposition of hydroxymethanesulfonate, $CH_2(OH)(SO_3Na)$

The reaction of aqueous $CH_2(OH)(SO_3Na)$ at concentrations of 5.0×10^{-3} to 0.03 M with 2×10^{-4} M aqueous iodine solution at 25 °C in the pH range 1 to 8 was investigated. The disappearance of the iodine peak at 350 nm was followed. As predicted from Equation 4.6, the reaction was found to be zero order with respect to iodine concentration. Hence plots of absorbance against time were linear, the gradient of the line being dependent on the concentration of $CH_2(OH)(SO_3Na)$. Figures 4.1 and 4.2 show results for the reaction at pH 5.0.

Figure 4.1: Change over time in the uv / vis spectrum of 0.010 M $CH_2(OH)(SO_3Na)$ with 2×10^{-4} M aqueous iodine solution at pH 5.0, 25 °C

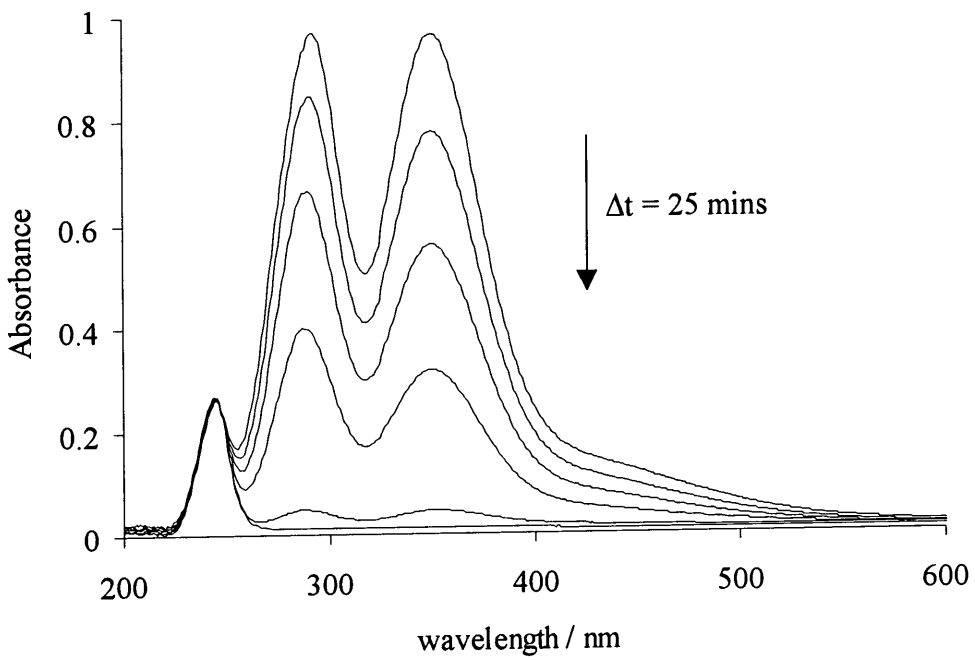

Figure 4.2: Zero order plots for varying $CH_2(OH)(SO_3Na)$ concentration with 2×10^{-4} M aqueous iodine solution at pH 5.0, 25 °C.

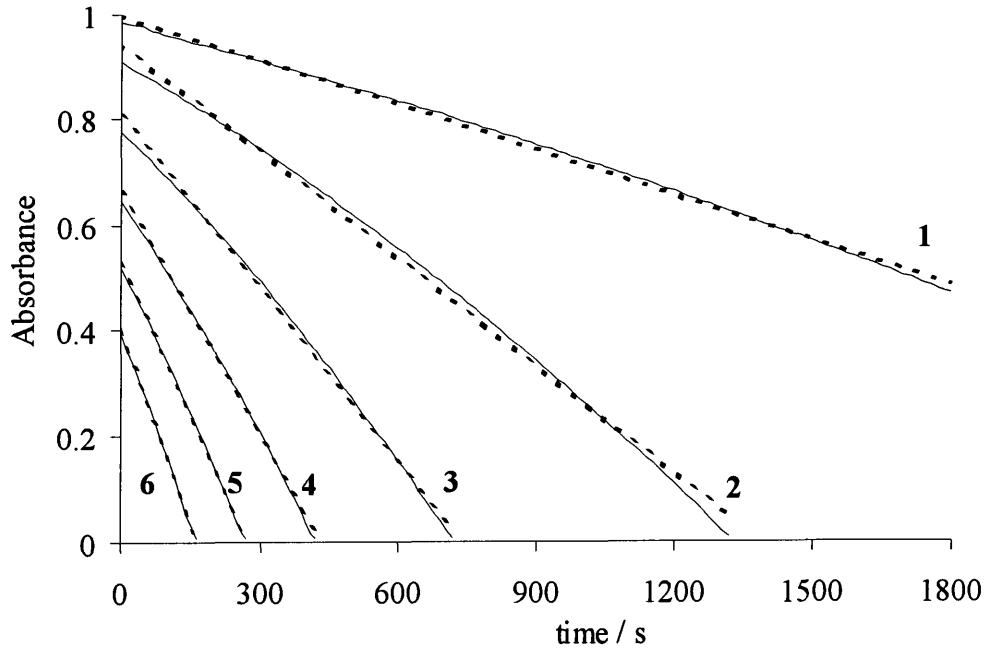

1 = 5.0×10^{-3} M $CH_2(OH)(SO_3Na)$; **2** = 0.010 M; **3** = 0.015 M; **4** =0.020 M; **5** = 0.025 M; **6** = 0.030 M. Solid line = data; dashed line = linear fit.

As zero order plots were obtained, k_{obs} / mol dm^{-3} s^{-1} was determined by dividing the gradient of the plot by 13400 mol^{-1} dm^3 cm^{-1}, the extinction coefficient of iodine at 350 nm. The results are shown in Table 4.4.

Plotting k_{obs} / mol dm^{-3} s^{-1} against $CH_2(OH)(SO_3Na)$ concentration facilitated the calculation of the first order rate constant defined in Scheme 4.5, k_b, equal to the gradient (Figure 4.3).

Table 4.4: k_{obs} / mol dm^{-3} s^{-1} obtained at different pH with varied HMS concentration and 2×10^{-4} M aqueous iodine solution

[HMS] / M	k_{obs} / mol dm^{-3} s^{-1}							
	pH 1.2	pH 2.0	pH 3.1	pH 3.9	pH 5.0	pH 5.9	pH 7.0	pH 7.9
5.0×10^{-3}	-	-	-	1.49×10^{-9}	2.13×10^{-8}	1.70×10^{-7}	1.82×10^{-6}	1.66×10^{-5}
0.010	-	-	9.70×10^{-10}	2.69×10^{-9}	5.08×10^{-8}	3.45×10^{-7}	4.04×10^{-6}	3.62×10^{-5}
0.015	2.52×10^{-10}	1.30×10^{-10}	1.14×10^{-9}	4.31×10^{-9}	8.06×10^{-8}	5.23×10^{-7}	6.22×10^{-6}	5.68×10^{-5}
0.020	3.41×10^{-10}	2.04×10^{-10}	1.39×10^{-9}	5.68×10^{-9}	1.14×10^{-7}	7.35×10^{-7}	8.33×10^{-6}	7.65×10^{-5}
0.025	4.72×10^{-10}	3.19×10^{-10}	1.68×10^{-9}	7.17×10^{-9}	1.45×10^{-7}	9.70×10^{-7}	-	9.37×10^{-5}
0.030	5.87×10^{-10}	4.67×10^{-10}	2.00×10^{-9}	8.96×10^{-9}	1.79×10^{-7}	1.20×10^{-6}	1.30×10^{-5}	1.16×10^{-4}

Figure 4.3: k_{obs} / mol dm^{-3} s^{-1} against $[CH_2(OH)(SO_3Na)]$ / M at pH 5.0, 25 °C.

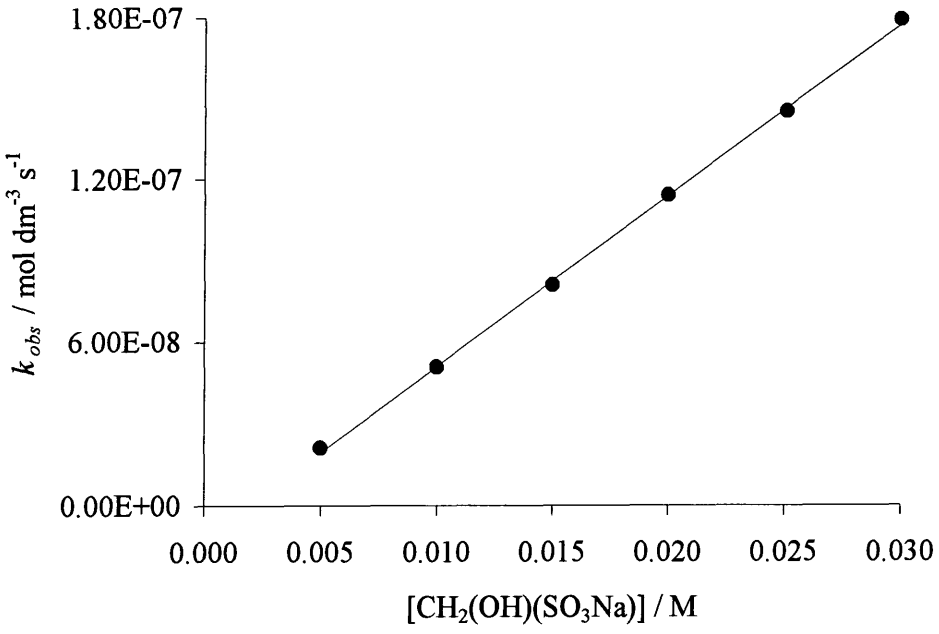

The values obtained for k_b are given in Table 4.5. Linear regression yielded correlation coefficients between 0.979 and 0.999.

Table 4.5: Calculated values of k_b, the first order rate constant for the decomposition of HMS to HCHO + S(IV), at different pH

pH	k_b / s^{-1}
1.2	$2.27 \times 10^{-8} \pm 1.2 \times 10^{-9}$
2.0	$2.25 \times 10^{-8} \pm 2.3 \times 10^{-9}$
3.1	$5.19 \times 10^{-8} \pm 3.4 \times 10^{-9}$
3.9	$2.98 \times 10^{-7} \pm 8.0 \times 10^{-9}$
5.0	$6.30 \times 10^{-6} \pm 8.3 \times 10^{-8}$
5.9	$4.14 \times 10^{-5} \pm 1.4 \times 10^{-6}$
7.0	$4.64 \times 10^{-4} \pm 5.0 \times 10^{-6}$
7.9	$3.94 \times 10^{-3} \pm 5.3 \times 10^{-5}$

The first order rate constant for the decomposition of HMS, k_b, increases with increasing pH above pH 3. At pH 1 and 2 there is little change in k_b. These values of k_b are in good agreement with the corresponding literature values determined at pH 4.0, 5.0 and 5.6 given in Table 4.2.

At pH ≥ 3, the increase in value of the rate constant with increasing pH is likely to indicate reaction via a deprotonated form of the substrate. Since the pK_a of sulfurous acid[15] is 1.8, the sulfite group will be anionic in this pH range. Hence the pH dependence indicates that path **b** in Scheme 4.6, involving decomposition to sulfite ions, will be dominant. Paths **a** and **b** are shown as irreversible as the sulfite and bisulfite ions will be removed irreversibly when reacted with aqueous iodine solution.

Scheme 4.6:

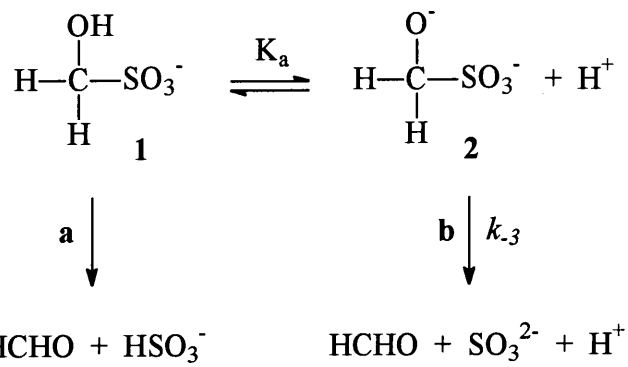

The values of k_b are given in terms of the stoichiometric concentration of $CH_2(OH)(SO_3Na)$, $[HMS]_{stoich}$. If the dianion $CH_2(O^-)(SO_3^-)$ is the reactive form then it is possible to evaluate a rate constant for its decomposition, k_{-3}, in the following way, where K_a is the acid dissociation constant of the monoanion $CH_2(OH)(SO_3^-)$ (Equations 4.4 to 4.7).

$$[CH_2(O^-)(SO_3^-)] = [HMS]_{stoich} \cdot \frac{K_a}{K_a + [H^+]} \qquad \textbf{(4.4)}$$

$$-\frac{d[HMS]_{stoich}}{dt} = k_b[HMS]_{stoich} \qquad \textbf{(4.5)}$$

$$= k_{-3}[CH_2(O^-)(SO_3^-)] \qquad \textbf{(4.6)}$$

$$\therefore\ k_{-3} = k_b \cdot \frac{K_a + [H^+]}{K_a} \qquad (4.7)$$

The value of K_a has been reported in the literature[1] as 2.0×10^{-12} mol dm^{-3}. Values of k_{-3} can therefore be calculated (Table 4.6) using the k_b values given in Table 4.5. The values at pH 1.2 and 2.0 have not been calculated as the rate constant levels off below around pH 3.

Table 4.6: Calculated k_{-3} values, the first order rate constant for the decomposition of the dianion $CH_2(O^-)(SO_3^-)$ to HCHO + SO_3^{2-}, in the pH range 3.1 to 7.9

pH	k_{-3} / s^{-1}
3.1	20.6 ± 1.3
3.9	18.8 ± 0.5
5.0	31.5 ± 0.4
5.9	26.1 ± 0.9
7.0	22.3 ± 0.2
7.9	24.8 ± 0.3

The average value of k_{-3} obtained is 24 ± 5 s^{-1}. Sørensen and Andersen[1] report a value of 43 s^{-1} in media in the pH range 9 to 12.

If the reaction is written in terms of the three possible species of HMS (Scheme 4.7), namely the neutral species $CH_2(OH)(SO_3H)$, **3**, the monoanion $CH_2(OH)(SO_3^-)$, **1**, and the dianion $CH_2(O^-)(SO_3^-)$, **2**, then the overall rate may be determined as in Equations 4.8 to 4.19. K_{SO3H} is the acid dissociation constant of the neutral species **3** to the monoanion **1** and K_a is the acid dissociation constant of the monoanion **1** to the dianion **2**.

Scheme 4.7:

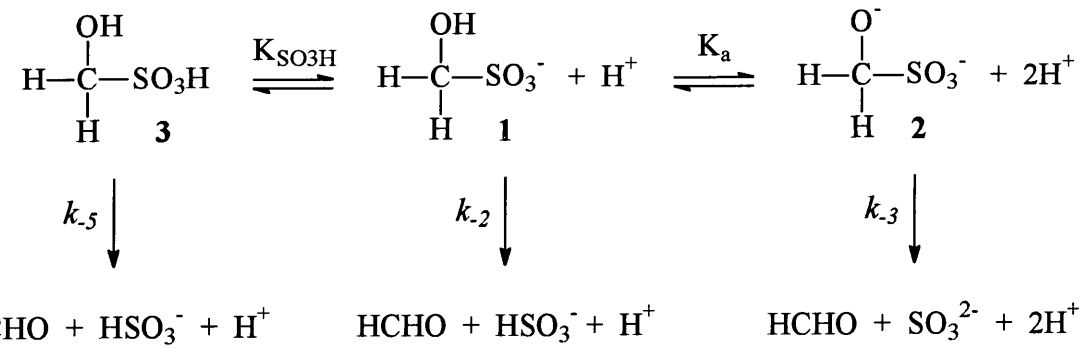

$$\text{rate} = k_{-5}[\mathbf{3}] + k_{-2}[\mathbf{1}] + k_{-3}[\mathbf{2}] \qquad \textbf{(4.8)}$$

$$[\text{HMS}]_{\text{stoich}} = [\mathbf{3}] + [\mathbf{1}] + [\mathbf{2}] \qquad \textbf{(4.9)}$$

[1], **[2]** and **[3]** are related by the equilibrium constants K_{SO3H} and K_a shown in Equations 4.10 and 4.11.

$$K_{SO3H} = \frac{[\mathbf{1}][H^+]}{[\mathbf{3}]} \qquad \textbf{(4.10)}$$

$$K_a = \frac{[\mathbf{2}][H^+]}{[\mathbf{1}]} \qquad \textbf{(4.11)}$$

Rearranging Equations 4.10 and 4.11 in terms of **[1]** gives:

$$[\mathbf{3}] = \frac{[\mathbf{1}][H^+]}{K_{SO3H}} \qquad \textbf{(4.12)}$$

$$[\mathbf{2}] = \frac{K_a[\mathbf{1}]}{[H^+]} \qquad \textbf{(4.13)}$$

Substituting Equations 4.12 and 4.13 into Equation 4.9 gives:

$$[\text{HMS}]_{\text{stoich}} = \frac{[\mathbf{1}][H^+]}{K_{SO3H}} + [\mathbf{1}] + \frac{K_a[\mathbf{1}]}{[H^+]} \qquad \textbf{(4.14)}$$

$$[HMS]_{stoich} = \frac{[\mathbf{1}][H^+]^2 + [\mathbf{1}][H^+]K_{SO3H} + [\mathbf{1}]K_aK_{SO3H}}{[H^+]K_{SO3H}} \quad \textbf{(4.15)}$$

$$\therefore\ [\mathbf{1}] = \frac{K_{SO3H}[H^+][HMS]_{stoich}}{[H^+]^2 + [H^+]K_{SO3H} + K_aK_{SO3H}} \quad \textbf{(4.16)}$$

Equation 4.16 may be simplified by assuming that $[H^+] >> K_a$. This assumption will hold under the experimental conditions used, as $K_a = 2.0 \times 10^{-12}$ mol dm^{-3} and $[H^+] = 1 \times 10^{-8}$ to 0.1 M. Hence Equation 4.16 reduces to:

$$[\mathbf{1}] = \frac{K_{SO3H}[HMS]_{stoich}}{[H^+] + K_{SO3H}} \quad \textbf{(4.17)}$$

Similar treatment on **[2]** and **[3]** yields Equations 4.18 and 4.19.

$$[\mathbf{2}] = \frac{K_aK_{SO3H}[HMS]_{stoich}}{[H^+]([H^+] + K_{SO3H})} \quad \textbf{(4.18)}$$

$$[\mathbf{3}] = \frac{[H^+][HMS]_{stoich}}{[H^+] + K_{SO3H}} \quad \textbf{(4.19)}$$

Substituting Equations 4.17, 4.18 and 4.19 into Equation 4.8 gives:

$$\text{rate} = \frac{k_{-5}[H^+][HMS]_{stoich}}{[H^+] + K_{SO3H}} + \frac{k_{-2}K_{SO3H}[HMS]_{stoich}}{[H^+] + K_{SO3H}} + \frac{k_{-3}K_aK_{SO3H}[HMS]_{stoich}}{[H^+]([H^+] + K_{SO3H})} \quad \textbf{(4.20)}$$

$$\text{rate} = k_{obs}[HMS]_{stoich} \quad \textbf{(4.21)}$$

$$k_{obs} = \frac{k_{-5}[H^+]}{[H^+] + K_{SO3H}} + \frac{k_{-2}K_{SO3H}}{[H^+] + K_{SO3H}} + \frac{k_{-3}K_aK_{SO3H}}{[H^+]([H^+] + K_{SO3H})} \quad \textbf{(4.22)}$$

k_{obs} is the first order rate constant for the decomposition of HMS to HCHO and S(IV) so is equivalent to the k_b values given in Table 4.5.

At pH ≥ 3, a linear increase in $\log(k_{obs} / s^{-1})$ with pH was observed. As stated previously, this will be due to an increase in the concentration of the dianion and implies that decomposition of HMS occurs virtually entirely through the dianion $CH_2(O^-)(SO_3^-)$ at pH ≥ 3. Hence at pH ≥ 3 the value of k_{obs} will depend primarily on the final term in Equation 4.22.

At pH values below 3 the value of $\log(k_{obs} / s^{-1})$ becomes constant. In this pH region there are two possible pathways through which decomposition could predominantly occur: either via the neutral form **3** (Case 1) or via the monoanion **1** (Case 2). Both of these cases will be considered in turn.

Case 1: Decomposition via the neutral form **3** is dominant at low pH

This requires that $[H^+] >> K_{SO3H}$ in this pH range, so that Equation 4.22 reduces to:

$$k_{obs} = k_{-5} + \frac{k_{-2}K_{SO3H}}{[H^+]} + \frac{k_{-3}K_aK_{SO3H}}{[H^+]^2} \qquad \textbf{(4.23)}$$

From this equation it can be seen that only the k_{-5} term is independent of $[H^+]$. Therefore when $\log(k_{obs} / s^{-1})$ becomes constant as the pH is varied between 1 and 3, k_{-5} must become the dominant term. Therefore k_{-5} can be assigned a value of 2.3×10^{-8} s^{-1}.

Making the assumption that decomposition via the monoanion makes a negligible contribution and using values of $k_{-5} = 2.3 \times 10^{-8}$ s^{-1} and $k_{-3} = 24$ s^{-1} together with Sørensen and Anderson's value[1] of $K_a = 2.0 \times 10^{-12}$ mol dm^{-3}, the best value of K_{SO3H} was determined using the MicroMath Scientist package. A good fit for the experimental data was obtained with a K_{SO3H} value of 1×10^{-3}, corresponding to a pK_{SO3H} value of 3 (Figure 4.4).

Figure 4.4: Graph of log (k_b / s^{-1}) against pH with the theoretical plot superimposed calculated using a pK_{SO3H} value of 3

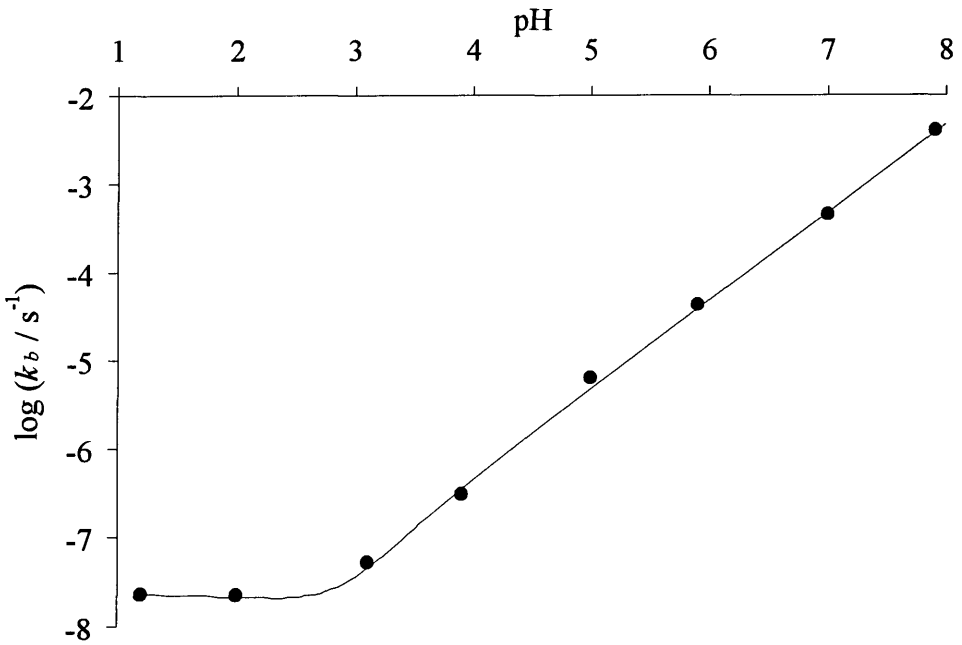

The pK_{SO3H} of sulfurous[15] acid, H_2SO_3, is 1.8. Therefore Case 1 suggests that $CH_2(OH)(SO_3H)$ is less acidic than sulfurous acid. This is unlikely since the hydroxymethyl group, $-CH_2OH$, is electron withdrawing relative to hydrogen and should be acid strengthening. Hence the pK_{SO3H} value for $CH_2(OH)(SO_3H)$ will be expected to be less 1.8, the value for sulfurous acid. Stewart and Donnally[9] estimated the analogous first dissociation constant of the adduct $C_6H_5CH(OH)(SO_3H)$ to be around 4×10^{-2} with a corresponding pK_{SO3H} of 1.4. The second dissociation constant, K_a, for this compound is reported as 7.0×10^{-10}, corresponding to a pK_a of 9.2.

Case 2: Decomposition via the monoanion **1** is dominant at low pH

This requires that $K_{SO3H} >> [H^+]$ in this pH range so that equation 4.22 reduces to:

$$k_{obs} = \frac{k_{-5}[H^+]}{K_{SO3H}} + k_{-2} + \frac{k_{-3}K_a}{[H^+]} \qquad \textbf{(4.24)}$$

The value of $\log(k_{obs} / s^{-1})$ at the plateau between pH 1 and 3 would therefore correspond to the value of k_{-2}, the pH independent term, and hence k_{-2} could be assigned a value of 2.3×10^{-8} s^{-1}.

In order to see whether this is a reasonable value for k_{-2}, it is possible to calculate a value of k_{-2} from the literature values given in Table 4.1 by considering the equilibria in Scheme 4.1. Equilibrium constants can be written for each step as shown in Equations 4.25 to 4.28.

$$K_2 = \frac{[1]}{[HCHO][HSO_3^-]} \qquad (4.25)$$

$$K_a = \frac{k_1}{k_{-1}} = \frac{[2][H^+]}{[1]} \qquad (4.26)$$

$$K_3 = \frac{[2]}{[HCHO][SO_3^{2-}]} \qquad (4.27)$$

$$K_{HSO3^-} = \frac{[SO_3^{2-}][H^+]}{[HSO_3^-]} \qquad (4.28)$$

Substituting Equations 4.26 to 4.28 into Equation 4.25 gives:

$$K_2 = \frac{K_3 K_{HSO3^-}}{K_a} \qquad (4.29)$$

Literature values[1] of K_3 and K_a are 2.2×10^5 mol^{-1} dm^3 and 2.0×10^{-12} mol dm^{-3} respectively. K_{HSO3^-} is equal[13] to 6.3×10^{-8} mol dm^{-3}. Using these values, a value of 6.9×10^9 mol^{-1} dm^3 can be calculated for K_2. The literature value[2] of k_2 is quoted as 7.90×10^2 mol^{-1} dm^3 s^{-1}. Using this and the calculated K_2 value, a value of k_{-2} equal to 1×10^{-7} s^{-1} is obtained. Given that this value has been calculated using more than one literature source under different experimental conditions with variable reliability, this is in reasonable agreement with the experimental value obtained here of 2.3×10^{-8} s^{-1}.

Hence it seems probable that at pH values below 3, decomposition through the monoanion forms the major pathway.

The pathway for decomposition of the monoanion **1** is likely to involve two steps, with the first being rate limiting (Scheme 4.8).

Scheme 4.8:

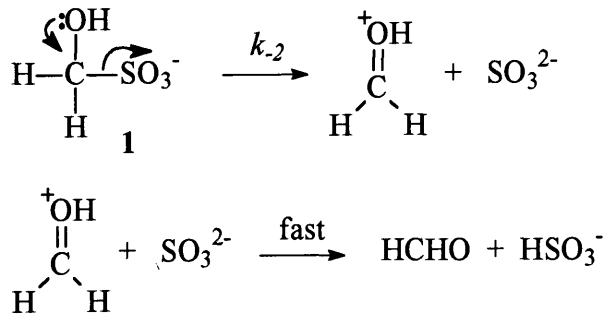

The first step involves expulsion of sulfite from the monoanion and results in separation of positive and negative charges. The rate constant k_{-2} corresponds to this step. Rapid proton transfer will follow this to give bisulfite ions. The value of k_{-2} is therefore expected to be considerably lower than the value for k_{-3}, which involves expulsion of sulfite from the dianion to give HCHO directly.

Making the assumption that decomposition via the neutral form makes a negligible contribution and using values of $k_{-2} = 2.3 \times 10^{-8}$ s^{-1} and $k_{-3} = 24$ s^{-1} together with Sørensen and Anderson's value[1] of $K_a = 2.0 \times 10^{-12}$ mol dm^{-3}, the best value of K_{SO3H} was determined using the MicroMath Scientist package. A reasonable fit for the experimental data was obtained with a K_{SO3H} value of 0.32, corresponding to a pK_{SO3H} value of 0.5 (Figure 4.5).

Figure 4.5: Graph of log (k_b / s^{-1}) against pH with the theoretical plot superimposed calculated using a pK_{SO3H} value of 0.5

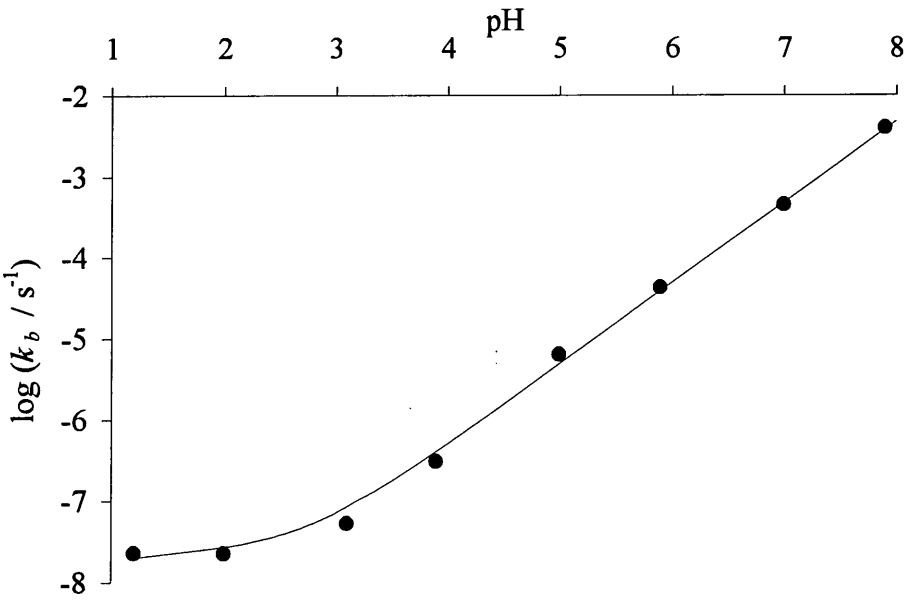

The pK_{SO3H} value for $CH_2(OH)(SO_3Na)$ is expected to be less than 1.8, the pK_{SO3H} for sulfurous acid, due to the electron withdrawing effect of the hydroxymethyl group, $-CH_2OH$. The value of 0.5 obtained here conforms to this prediction whereas for Case 1 the pK_{SO3H} value for HMS had to be assumed to be greater than the pK_{SO3H} for sulfurous acid to obtain a good fit for the experimental data.

4.3 CONCLUSION

The reaction of aqueous sodium sulfite solution with aqueous iodine solution was investigated. It appeared that the hydrolysis of iodosulfate, formed from reaction of HSO_3^- and SO_3^{2-} with I_3^- and I_2, was the process observed rather than the actual reaction of HSO_3^- and SO_3^{2-} with I_3^- and I_2. A first order rate constant of 271 ± 2 s^{-1} at 25 °C was obtained. This compares well with the literature value of 298 s^{-1} at 25 °C.

The decomposition of HMS was investigated in the pH range 1 to 8. The rate constants determined in this study are summarised in Table 4.7.

Table 4.7: Rate constants obtained at 25 °C

pH	constant	value / s^{-1}
-	k_{-2}	2.3×10^{-8}
-	k_{-3}	24 ± 5
1.2	k_b	$2.27 \times 10^{-8} \pm 1.2 \times 10^{-9}$
2.0	k_b	$2.25 \times 10^{-8} \pm 2.3 \times 10^{-9}$
3.1	k_b	$5.19 \times 10^{-8} \pm 3.4 \times 10^{-9}$
3.9	k_b	$2.98 \times 10^{-7} \pm 8.0 \times 10^{-9}$
5.0	k_b	$6.30 \times 10^{-6} \pm 8.3 \times 10^{-8}$
5.9	k_b	$4.14 \times 10^{-5} \pm 1.4 \times 10^{-6}$
7.0	k_b	$4.64 \times 10^{-4} \pm 5.0 \times 10^{-6}$
7.9	k_b	$3.94 \times 10^{-3} \pm 5.3 \times 10^{-5}$

Values of k_b, the first order rate constant for decomposition of HMS to S(IV) and HCHO, are in good agreement with literature values at pH 4.0, 5.0 and 5.6. An average value of k_{-3} of 24 ± 5 s^{-1} was obtained for the rate constant for decomposition of the dianion to give SO_3^{2-} and HCHO. This is of the same order as the value of 43 s^{-1} reported in the literature for the pH range 9 to 12. A value of 2.3×10^{-8} s^{-1} was determined for k_{-2}, the first order rate constant for decomposition of the monoanion to give HSO_3^- and HCHO.

To summarise, this work has determined that the decomposition of HMS occurs virtually entirely through the dianion $CH_2(O^-)(SO_3^-)$ at pH values above 3. Below this pH, decomposition through the monoanion $CH_2(OH)(SO_3^-)$ forms the major pathway, although the reaction is considerably slower than when it occurs through the dianion.

The pathway for decomposition of the monoanion is likely to involve two steps, the first being rate limiting. Initially sulfite will be expelled from the monoanion resulting in separation of positive and negative charges, followed by rapid proton transfer to give the final species, bisulfite and HCHO. The value of k_{-2} is therefore expected to be considerably lower than the value for k_{-3}, which involves direct expulsion of sulfite, the final species, from the dianion.

4.4 EXPERIMENTAL

4.4.1 Reaction of aqueous sulfite solution with aqueous iodine solution

The reaction of aqueous sulfite solution at concentrations ranging from 1.0×10^{-3} to 0.03 M with 4×10^{-4} M aqueous iodine solution in the pH range 3.0 to 5.2 was investigated.

Plots of absorbance against time were obtained. The disappearance of the aqueous iodine solution peak at 300 or 350 nm was followed. Aqueous sulfite solution does not absorb strongly in this region. The plots were recorded using an Applied Photophysics DX.17MV BioSequential Stopped – flow ASVD Spectrometer at 25.0 – 25.1 °C with a cell of 1 cm path length. Ten averages were obtained, each the average of three runs of 0.05 seconds. The appropriate aqueous sulfite solution was placed in one syringe and the aqueous iodine solution with the appropriate buffer solution, if used, in the other. The averages were fitted to obtain first order rate constant values, k_{obs}, using the single exponential fit function on the !SX.17MV program installed on the spectrometer. Rate constants are quoted to one decimal place.

Experiments performed at pH 3.5 were unbuffered. At pH 5 an acetate / acetic acid buffer was used, with stoichiometric concentrations of 0.12 M sodium acetate and 0.05 M acetic acid. At pH 3.0, 0.01 M $HCl_{(aq)}$ was added for the 0.01 M sulfite experiment and 1.0×10^{-3} M $HCl_{(aq)}$ for the 1.0×10^{-3} M sulfite experiment to control the pH.

4.4.2 Decomposition of hydroxymethanesulfonate, $CH_2(OH)(SO_3Na)$

The reaction of aqueous $CH_2(OH)(SO_3Na)$ at six concentrations ranging from 5.0×10^{-3} to 0.03 M with 2×10^{-4} M aqueous iodine solution in the pH range 1.2 to 7.9 was investigated.

Absorbance against wavelength spectra were obtained for three $CH_2(OH)(SO_3Na)$ concentrations at pH 5.0 using a Perkin – Elmer Lambda 2 uv / vis spectrometer at

25 °C with 1 cm stoppered quartz cuvettes, taking scans every 5 minutes using a scan speed of 480 nm min^{-1}.

Plots of absorbance against time were obtained at all pH values. The disappearance of the aqueous iodine solution peak at 350 nm was followed. The experiments at pH 1.2 to 5.0 and the three lower concentrations at pH 5.9 were carried out using conventional uv / vis spectrometry. The plots were recorded on a Perkin – Elmer Lambda 2 or Lambda 12 uv / vis spectrometer at 25 °C using 1 cm stoppered quartz cuvettes. The data interval ranged from 15 to 90 seconds and the overall time from 15 minutes to 16 hours depending on the pH used. At pH 3.1 the lowest $CH_2(OH)(SO_3Na)$ concentration and at pH 1.2 and 2.0 the lowest two concentrations were not used to obtain k_b values as the reactions were deemed too slow to obtain reliable rate constants.

For all uv / vis work the cuvettes were left in the spectrometer for at least 10 minutes prior to use to allow the temperature to equilibrate to 25 °C. Addition of the aqueous iodine solution was used to initiate the reaction. Zero order kinetics were observed and linear regression on Microsoft Excel was used to calculate k_b values. Rate constants are quoted to three significant figures.

The three higher concentrations at pH 5.9 and the experiments at pH 7.0 and 7.9 were performed using stopped - flow spectrophotometry at 25.0 – 25.1 °C using an Applied Photophysics DX.17MV BioSequential Stopped – flow ASVD Spectrometer with a 1 cm path length. Ten averages were obtained, each the average of three runs of 0.2 to 50 seconds depending on the $CH_2(OH)(SO_3Na)$ concentration and the pH used. The appropriate aqueous $CH_2(OH)(SO_3Na)$ solution was placed in one syringe and the aqueous iodine solution with the appropriate buffer solution in the other. The averages were fitted using linear regression on the !SX.17MV program installed on the spectrometer. Rate constants are quoted to three significant figures. The 0.025 M $CH_2(OH)(SO_3Na)$ solution at pH 7.0 gave an anomalously high result therefore this was not included in the data analysis.

The MicroMath Scientist package for Microsoft Windows, Version 2.0 was used to fit the data to obtain the best K_{SO3H} value.

The buffers employed and the corresponding stoichiometric buffer concentrations in the final reaction mixture are shown in Table 4.8.

Table 4.8: Buffer concentrations, in aqueous solution

pH	component A	$[A]_{stoich}$ / M	component B	$[B]_{stoich}$ / M
1.2	KCl	0.019	HCl	0.20
2.0	KCl	0.019	HCl	0.020
3.1	$COOH.C_6H_4.COOK$	0.075	HCl	0.033
3.9	$COOH.C_6H_4.COOK$	0.075	HCl	1.5×10^{-4}
5.0	CH_3COONa	0.12	CH_3COOH	0.050
5.9	KH_2PO_4	0.13	NaOH	0.015
7.0	KH_2PO_4	0.13	NaOH	0.076
7.9	KH_2PO_4	0.13	NaOH	0.12

The pH values of all solutions were determined using a Jenway 3020 pH meter calibrated using pH 7 and pH 10 (for alkaline solutions) or pH 4 (for acidic solutions) buffers. pH values are quoted to one decimal place.

4.5 REFERENCES

1. P. E. Sørensen and V. S. Andersen, *Acta Chem. Scand.*, 1970, **24**, 1301

2. S. D. Boyce and M. R. Hoffmann, *J. Phys. Chem.*, 1984, **88**, 4740

3. S. Dong and P. K. Dasgupta, *Atmos. Environ.*, 1986, **20**, 1635

4. G. L. Kok, S. N. Gitlin and A. L. Lazrus, *J. Geophys. Res., D*, 1986, **91**, 2801

5. D. A. Blackadder and C. Hinshelwood, *J. Chem. Soc.*, 1958, 2720

6. U. Deister, R. Neeb, G. Helas and P. Warneck, *J. Phys. Chem.*, 1986, **90**, 3213

7. (a) P. Jones and K. B. Oldham, *J. Chem. Educ.*, 1963, **40**, 366; (b) C. Wagner, *Ber.*, 1929, **69**, 2873

8. (a) E. A. Betterton and M. R. Hoffmann, *J. Phys. Chem.*, 1987, **91**, 3011; (b) A. Skrabal and R. Skrabal, *Sitz. Akad. Wirs. Wien*, 1936, **145**, 617

9. T. D. Stewart and L. H. Donnally, *J. Am. Chem. Soc.*, 1932, **54**, 3559

10. R. P. Bell and P. G. Evans, *Proc. R. Soc. London, Ser. A*, 1966, **291**, 297

11. (a) D. A. Palmer, R. W. Ramette and R. E. Mesmer, *J. Solution Chem.*, 1984, **13**, 637; (b) R. W. Ramette and R. W. Sandford, *J. Am. Chem. Soc.*, 1965, **87**, 5001

12. B. S. Yiin and D. W. Margerum, *Inorg. Chem.*, 1990, **29**, 1559

13. (a) E. Hayon, A. Treinin and J. Wilf, *J. Am. Chem. Soc.*, 1972, **94**, 47; (b) H. V. Tartar and H. H. Garretson, *J. Am. Chem. Soc.*, 1941, **63**, 808

14. T. D. Stewart and L. H. Donnally, *J. Am. Chem. Soc.*, 1932, **54**, 2333

15. 'CRC Handbook of Chemistry and Physics', CRC Press, Florida, 1982, 63rd Ed., D173

CHAPTER 5

Reaction of hydroxymethanesulfonate, $CH_2(OH)(SO_3Na)$, with aniline and aniline derivatives

CHAPTER 5: Reaction of hydroxymethanesulfonate, $CH_2(OH)(SO_3Na)$, with aniline and aniline derivatives

5.1 INTRODUCTION

There have been no studies reported in the literature on the reaction of hydroxymethanesulfonate, $CH_2(OH)(SO_3Na)$, with aniline and aniline derivatives. There has only been one previous study performed in this area, which used ammonia as the amine[1] (Chapter 1, Section 1.7.2). The reaction of $CH_2(OH)(SO_3Na)$ with aniline and two aniline derivatives was therefore investigated here using ^1H NMR and uv / vis spectroscopy to gain a better understanding of the reaction kinetics and mechanism. The amines studied are shown in Table 5.1.

Table 5.1: Amines studied in the reaction with $CH_2(OH)(SO_3Na)$

amine			pK_a[†]
aniline	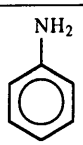	**5.1**	4.60
4-methylaniline	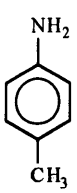	**5.2**	5.08
4-dimethylaminoaniline[§]	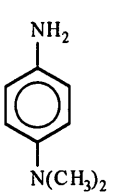	**5.3**	6.59

[†] pK_a values correspond to dissociation of the protonated amines at 25 °C, reference 2

[§] also known as *N,N*-dimethyl-1,4-phenylenediamine

The reaction of aniline and 4-methylaniline with $CH_2(OH)(SO_3Na)$ was followed using ^1H NMR spectroscopy. The spectrum of the amine alone was obtained, then in the

presence of equimolar $CH_2(OH)(SO_3Na)$, then with each reagent in excess. The kinetics of the reaction with all three amines was studied using uv / vis spectroscopy. The effect of the presence of added sulfite ions in the system was also investigated.

The results indicate that aminomethanesulfonates, $XC_6H_4NHCH_2SO_3^-$, are the major products of these reactions. Attempts were made to study the decomposition of the aniline product, $C_6H_5NHCH_2SO_3^-$, to the iminium ion, $[C_6H_5NH{=}CH_2]^+$, by reacting pre-formed $C_6H_5NHCH_2SO_3^-$ with aqueous iodine solution to trap sulfite / bisulfite ions formed on decomposition. It is important to note that both of the starting materials used to prepare $C_6H_5NHCH_2SO_3^-$ react with iodine. The reaction of $CH_2(OH)(SO_3Na)$ with iodine has already been studied here (Chapter 4). Aniline is known to react with iodine via electrophilic aromatic substitution. The kinetics in aqueous solution have been studied by Berliner[3] who determined that the reaction is subject to general base catalysis and that the mechanism is likely to involve I^+ as the iodinating agent.

The reaction of aniline with aqueous iodine solution at pH 5.0 was investigated here. The reaction of $C_6H_5NHCH_2SO_3^-$ with aqueous iodine solution in the pH range 4.1 to 5.2 was then investigated. The reaction in the presence of residual aniline was also studied.

5.2 RESULTS AND DISCUSSION

5.2.1 Reaction of $CH_2(OH)(SO_3Na)$ with aniline

5.2.1.1 ^1H NMR studies

Initially the ^1H NMR spectra of the starting materials $CH_2(OH)(SO_3Na)$ and aniline were obtained. Figure 5.1 and Table 5.2 describe the ^1H NMR spectrum of 0.20 M $CH_2(OH)(SO_3Na)$ in D_2O.

Figure 5.1: ^1H NMR spectrum of $CH_2(OH)(SO_3Na)$ in D_2O

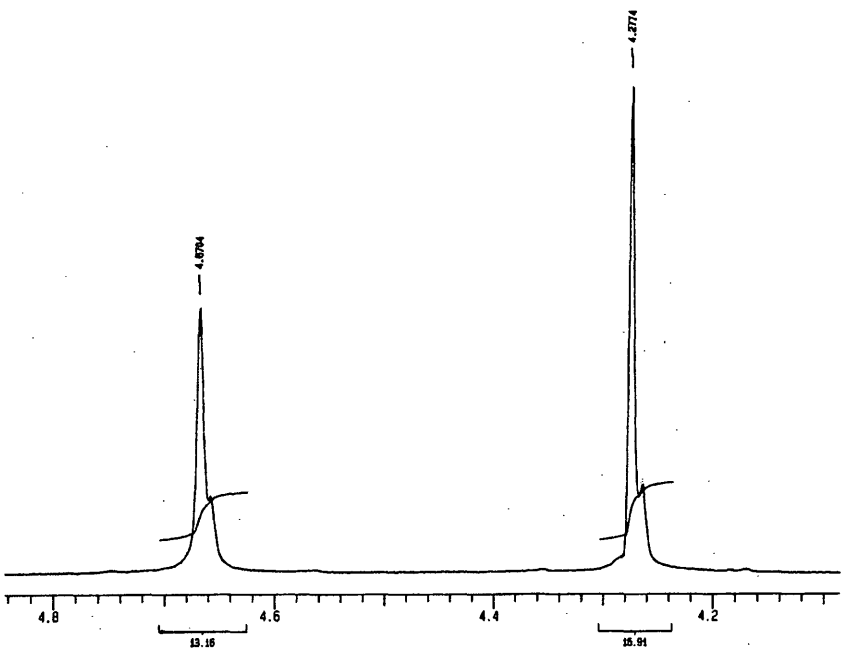

Table 5.2: ^1H NMR spectrum of $CH_2(OH)(SO_3Na)$ in D_2O: peak assignments

δ / ppm	integral ratio	multiplicity	J / Hz	assignment
4.28	-	s	-	$CH_2(OH)(SO_3Na)$
4.67	-	-	-	D_2O

Figure 5.2 and Table 5.3 describe the ^{1}H NMR spectrum of 0.23 M aniline (**5.1**) in D_2O.

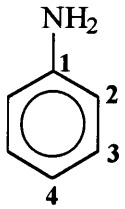

5.1

Figure 5.2: ^{1}H NMR spectrum of aniline in D_2O

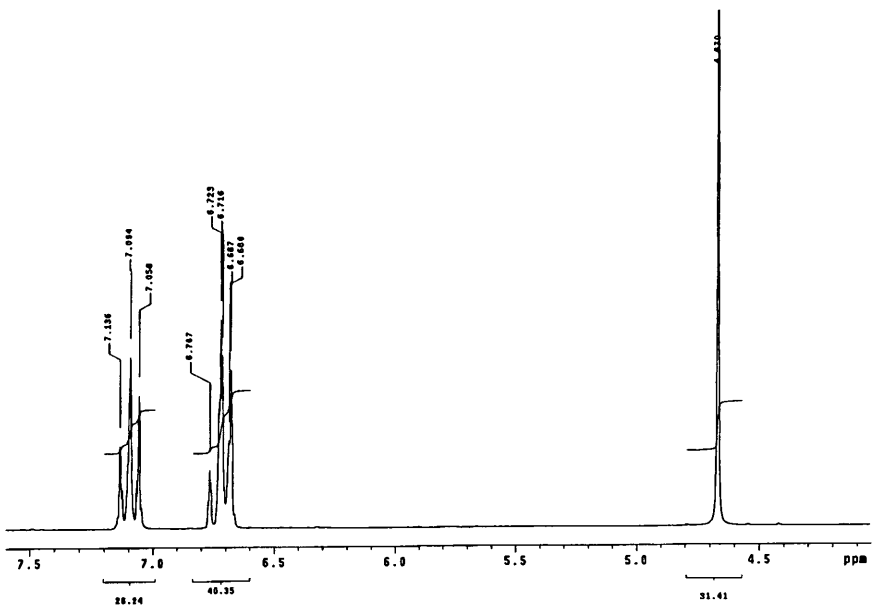

Table 5.3: ^{1}H NMR spectrum of aniline in D_2O: peak assignments

δ / ppm	integral ratio	multiplicity	J / Hz	assignment
4.67	-	-	-	D_2O, -NH_2
6.70	3	d	8	Ar-H2
6.72		t	8	Ar-H4
7.09	2	t	8	Ar-H3

The spectrum of 0.20 M aniline and 0.20 M $CH_2(OH)(SO_3Na)$ was obtained, then with each reagent in excess: 0.20 M aniline with 0.40 M $CH_2(OH)(SO_3Na)$ and 0.21 M aniline with 0.10 M $CH_2(OH)(SO_3Na)$. A spectrum was recorded immediately (3 to 5 minutes) after addition of the $CH_2(OH)(SO_3Na)$, then again after approximately 30 minutes, 1 hour and 2 or 5 hours, and continued until there was no further change in the spectrum.

There are two possible products that may form in the reaction. Firstly, a 1 : 1 aniline : $CH_2(OH)(SO_3Na)$ adduct $C_6H_5NHCH_2SO_3^-$, **5.4**, can form. In the presence of excess $CH_2(OH)(SO_3Na)$, a second molecule may react to give a 1 : 2 aniline : $CH_2(OH)(SO_3Na)$ adduct, $C_6H_5N(CH_2SO_3^-)_2$, **5.5**.

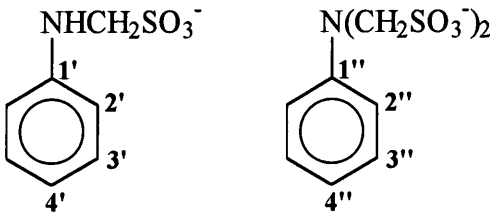

5.4 **5.5**

5.2.1.1.1 Equimolar aniline and $CH_2(OH)(SO_3Na)$

The results obtained for the reaction of equimolar 0.20 M aniline and $CH_2(OH)(SO_3Na)$ are shown in Figures 5.3, 5.4 and 5.5 which show the spectra obtained 4 minutes, 38 minutes and 5 hours after mixing respectively. There was no further change in the spectrum over time. Tables 5.4, 5.5 and 5.6 summarise the information obtained from the three spectra.

Figure 5.3: 0.20 M aniline and 0.20 M $CH_2(OH)(SO_3Na)$: 4 minutes after mixing

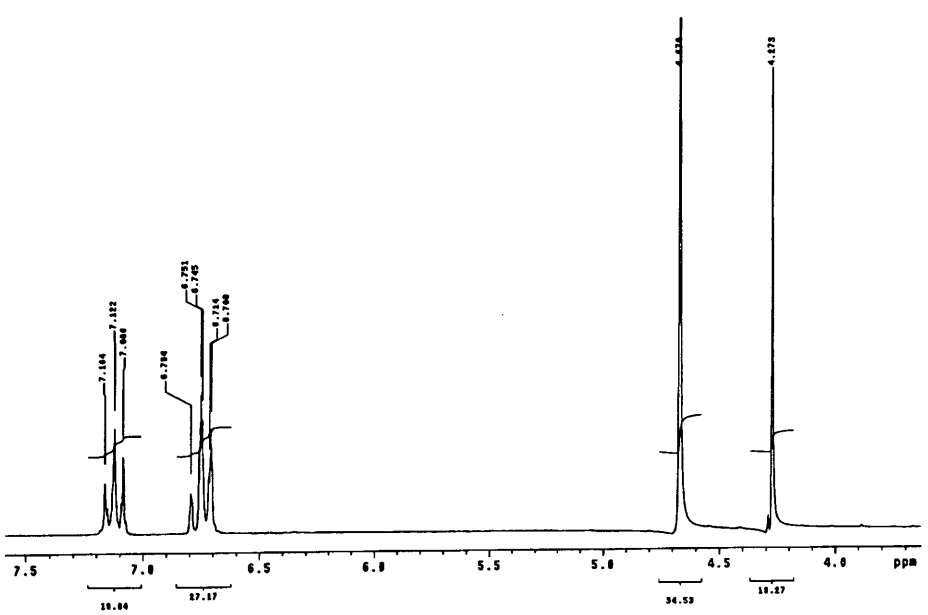

Table 5.4: Peak assignments: 4 minutes after mixing

time after mixing	δ / ppm	integral ratio	multiplicity	J / Hz	assignment
4 minutes	4.27	2	s	-	$CH_2(OH)(SO_3Na)$
	~ 4.3		s	-	$-NHCH_2SO_3^-$
	4.67	-	-	-	D_2O, $-NH_2$
	6.73	3	d	8	Ar-H2
	6.75		t	8	Ar-H4
	7.12	2	t	8	Ar-H3

Table 5.5: Peak assignments: 38 minutes after mixing

time after mixing	δ / ppm	integral ratio	multiplicity	J / Hz	assignment
38 minutes	4.28	2	s	-	$CH_2(OH)(SO_3Na)$
	4.30		s	-	$-NHCH_2SO_3^-$
	4.67	-	-	-	D_2O, $-NH_2$
	6.72	3	d	8	Ar-H2
	~ 6.72		d	8	Ar-H4'
	6.75		t	8	Ar-H4
	6.78		t	8	Ar-H2'
	7.13	2	t	8	Ar-H3
	~ 7.15		t	8	Ar-H3'

Figure 5.4: 0.20 M aniline and 0.20 M $CH_2(OH)(SO_3Na)$: 38 minutes after mixing

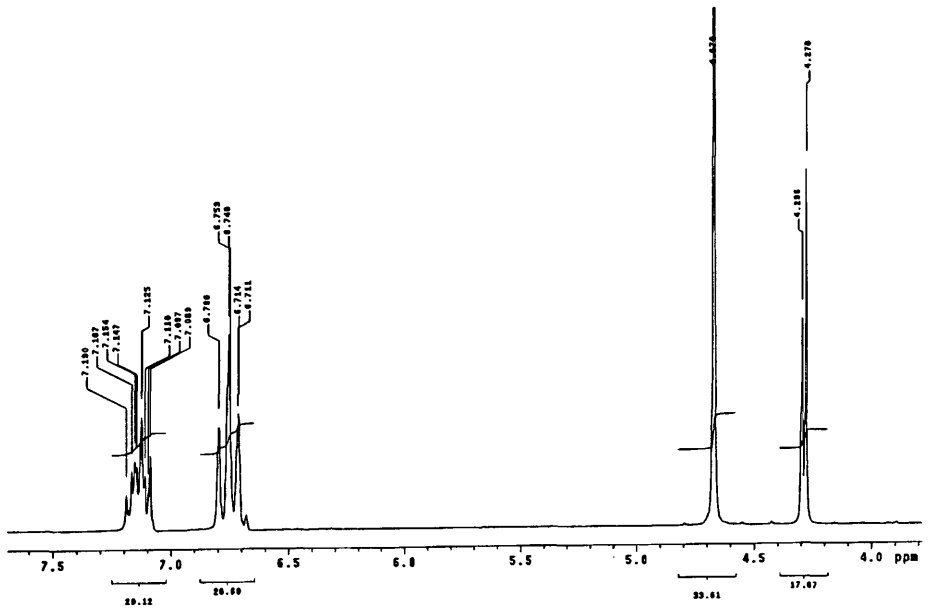

Figure 5.5: 0.20 M aniline and 0.20 M $CH_2(OH)(SO_3Na)$: 5 hours after mixing

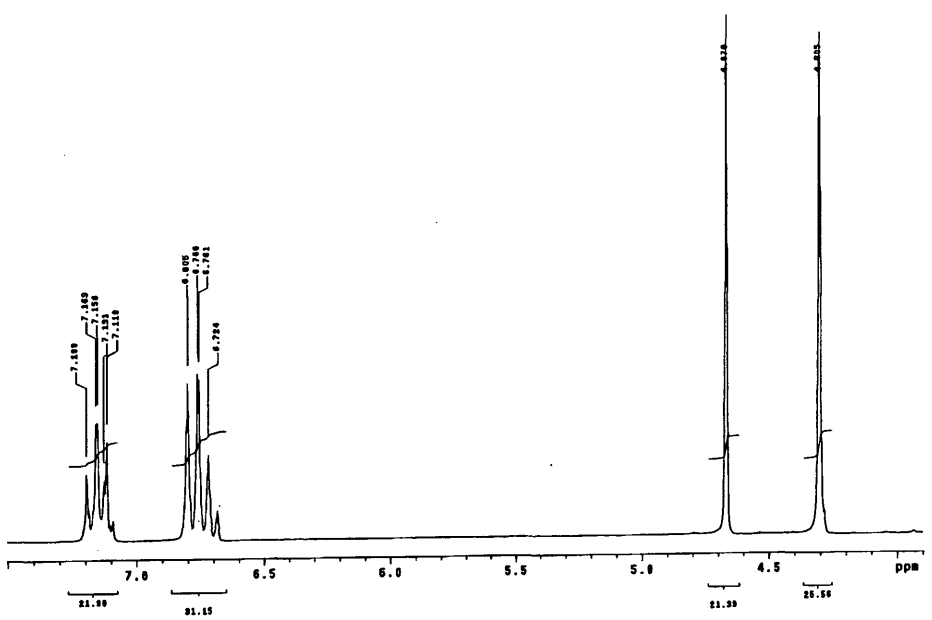

Table 5.6: Peak assignments: 5 hours after mixing

time after mixing	δ / ppm	integral ratio	multiplicity	J / Hz	assignment
5 hours	4.31	2	s	-	$-NHCH_2SO_3^-$
	4.67	-	-	-	D_2O, $-NH_2$
	~ 6.72	3	d	-	Ar-H2
	6.72		t	-	Ar-H4'
	~ 6.76		t	8	Ar-H4
	6.79		d	8	Ar-H2'
	~ 7.13	2	t	-	Ar-H3
	7.16		t	8	Ar-H3'

The spectra show the formation of the 1 : 1 adduct $C_6H_5NHCH_2SO_3^-$ over time. After 4 minutes the spectrum shows the presence of a small amount of $C_6H_5NHCH_2SO_3^-$ with a small peak around δ 4.3 ppm: there is no obvious change in the aromatic region in this spectrum. Over time the δ 4.30 ppm peak increases in intensity and the δ 4.27 ppm $CH_2(OH)(SO_3Na)$ peak decreases: after 5 hours all of the $CH_2(OH)(SO_3Na)$ is converted to the product. Over time there is also a visible change in the peaks in the aromatic region: peaks due to the 1 : 1 adduct $C_6H_5NHCH_2SO_3^-$ appear and those due to the parent compound, aniline, decrease in intensity.

There is no evidence of formation of the 1 : 2 adduct $C_6H_5N(CH_2SO_3^-)_2$. The presence of the $-CH_2SO_3^-$ electron withdrawing group on aniline will make the nitrogen less nucleophilic than that in aniline therefore reducing the tendency to add a second $CH_2(OH)(SO_3Na)$ molecule. Hence no 1 : 2 adduct is observed.

5.2.1.1.2 $CH_2(OH)(SO_3Na)$ in excess

The spectra obtained for the reaction of 0.20 M aniline and 0.40 M $CH_2(OH)(SO_3Na)$ also show formation of only the 1 : 1 adduct $C_6H_5NHCH_2SO_3^-$. There is no evidence of formation of the 1 : 2 adduct $C_6H_5N(CH_2SO_3^-)_2$ even though $CH_2(OH)(SO_3Na)$ is present in excess. Table 5.7 summarises the spectra obtained 3 minutes and 2 hours after mixing. There was no further change in the spectrum over time.

Table 5.7: 0.20 M aniline and 0.40 M $CH_2(OH)(SO_3Na)$: peak assignments

time after mixing	δ / ppm	integral ratio	multiplicity	J / Hz	assignment
3 minutes	4.26	3	s	-	$CH_2(OH)(SO_3Na)$
	4.67	-	-	-	D_2O, -NH_2
	6.71	3	d	8	Ar-H2
	6.73		t	8	Ar-H4
	7.10	2	t	8	Ar-H3
2 hours	4.31	3	s	-	$CH_2(OH)(SO_3Na)$
	4.33		s	-	-$NHCH_2SO_3^-$
	4.67	-	-	-	D_2O, -NH_2
	6.72	3	t	8	Ar-H4'
	~ 6.73		d	8	Ar-H2
	~ 6.74		t	8	Ar-H4
	6.80		d	8	Ar-H2'
	~ 7.14	2	t	8	Ar-H3
	7.18		t	8	Ar-H3'

After 3 minutes there is little evidence of the product. However after 36 minutes there are peaks present due to the 1 : 1 adduct $C_6H_5NHCH_2SO_3^-$ and the reaction is complete within 2 hours. After this time the peaks due to the -CH_2- groups in the $CH_2(OH)(SO_3Na)$ and product are approximately equal in intensity and the aromatic peaks due to aniline relatively small, implying the equilibrium lies in favour of the product, $C_6H_5NHCH_2SO_3^-$.

5.2.1.1.3 Aniline in excess

The spectra obtained for the reaction of 0.21 M aniline and 0.10 M $CH_2(OH)(SO_3Na)$ show formation of the 1 : 1 adduct $C_6H_5NHCH_2SO_3^-$. Table 5.8 summarises the spectra obtained 3 minutes and 5 hours after mixing. There was no further change in the spectrum.

Table 5.8: 0.21 M aniline and 0.10 M $CH_2(OH)(SO_3Na)$: peak assignments

time after mixing	δ / ppm	integral ratio	multiplicity	J / Hz	assignment
3 minutes	4.24	1	s	-	$CH_2(OH)(SO_3Na)$
	4.67	-	-	-	D_2O, -NH_2
	6.69	3	d	8	Ar-H2
	6.72		t	8	Ar-H4
	7.09	2	t	8	Ar-H3
5 hours	4.28	1	s	-	-$NHCH_2SO_3^-$
	4.67	-	-	-	D_2O, -NH_2
	6.70	3	d	8	Ar-H2
	6.74		t	8	Ar-H4'
	6.75		t	8	Ar-H4
	6.77		d	8	Ar-H2'
	7.11	2	t	8	Ar-H3
	7.14		t	8	Ar-H3'

After 3 minutes there is no evidence of product formation. However after 36 minutes there are peaks present due to the 1 : 1 adduct $C_6H_5NHCH_2SO_3^-$ and the reaction is complete within 5 hours. After this time there is complete conversion of $CH_2(OH)(SO_3Na)$ to the product.

5.2.1.2 Uv / visible kinetic studies

5.2.1.2.1 Absorbance against wavelength spectra and absorbance against time plots

Absorbance against wavelength spectra were obtained for the reaction of 2.0×10^{-3} to 0.10 M aqueous $CH_2(OH)(SO_3Na)$ with 1.0×10^{-4} M aniline at 25 °C in aqueous solution. The spectrum of 1.0×10^{-4} M aniline alone was obtained for comparison. The spectra with aqueous $CH_2(OH)(SO_3Na)$ added show a shift to higher wavelength with a corresponding increase in absorbance as compared to the spectrum of 1.0×10^{-4} M aniline alone. The higher the concentration of aqueous $CH_2(OH)(SO_3Na)$, the greater the change in spectrum observed. All reactions are complete within 85 minutes.

Figure 5.6 shows the change over time in the spectrum for the reaction with 0.10 M $CH_2(OH)(SO_3Na)$ as compared to that of aniline alone. Table 5.9 shows the peak positions and extinction coefficients (ε) for the two spectra.

Figure 5.6: Change over time in the absorbance against wavelength spectrum for the reaction of 1.0×10^{-4} M aniline with 0.10 M $CH_2(OH)(SO_3Na)$, 25 °C, aqueous solution

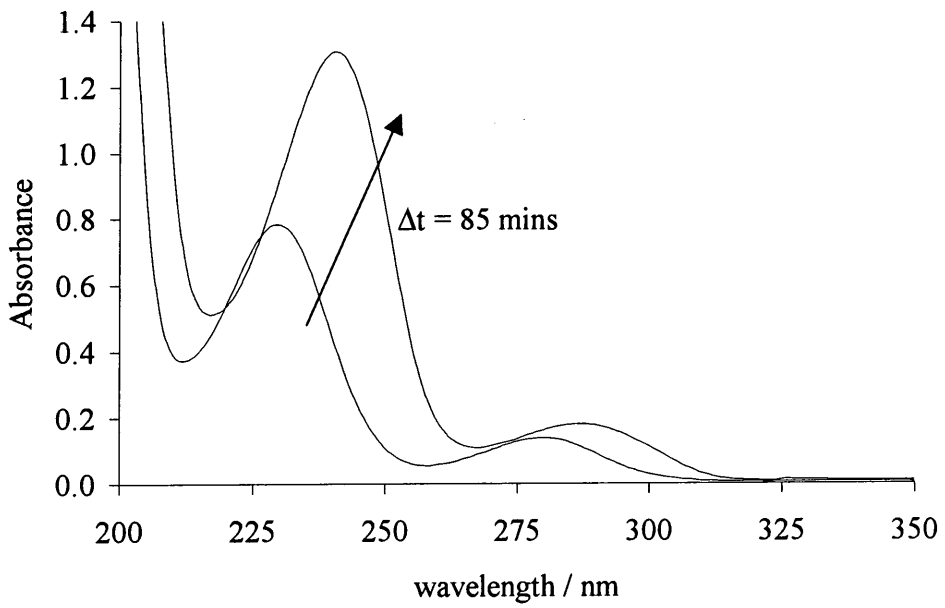

Table 5.9: Spectral appearance in aqueous solution of 1.0×10^{-4} M aniline and the final spectrum in the presence of 0.10 M $CH_2(OH)(SO_3Na)$

$[CH_2(OH)(SO_3Na)]$ / M	λ_{max} / nm ($\varepsilon^{\dagger}$/ mol^{-1} dm^3 cm^{-1})
none	230 (7800); 280 (1400)
0.10	241 (13100); 287 (1800)

† based on the assumption that all the aniline reacts to give 1.0×10^{-4} M product

Plots of absorbance against time were obtained for the reaction of 1.0×10^{-4} M or 5.1×10^{-5} M aniline with 2.0×10^{-3} to 0.10 M aqueous $CH_2(OH)(SO_3Na)$ at 25 °C. Formation of the product at 245 nm was followed. The solutions were either unbuffered or buffered at pH 6.0 to 8.2: the pH values of the unbuffered solutions were found to be

around pH 6.6. Plots were first order (Figure 5.7): the k_{obs} / s^{-1} values obtained are shown in Table 5.10.

Figure 5.7: Absorbance against time plots for the reaction of 1.0×10^{-4} M aniline with 2.0×10^{-3} to 0.10 M aqueous $CH_2(OH)(SO_3Na)$ at 25 °C in unbuffered aqueous solution

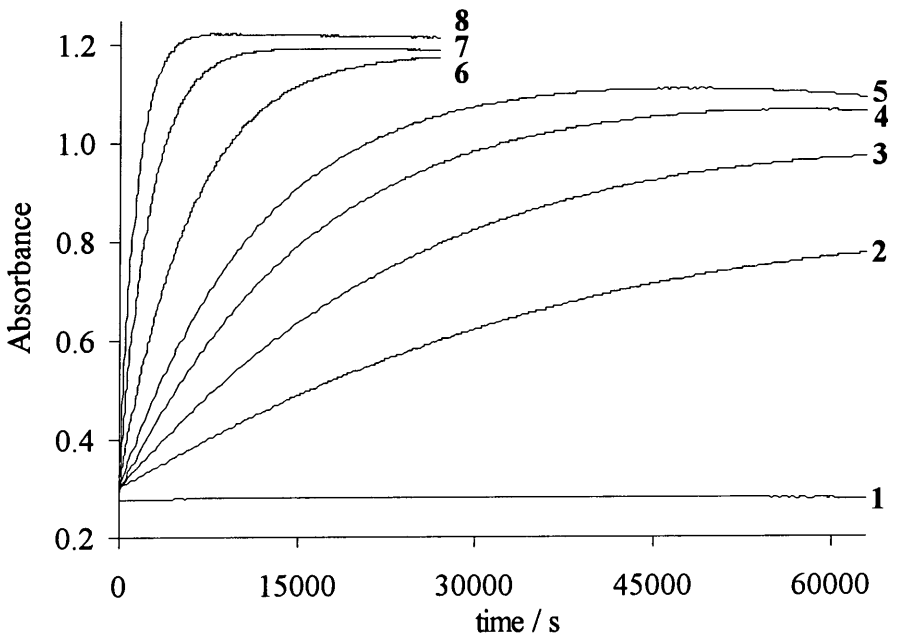

1 = aniline alone; **2** = 2.0×10^{-3} M $CH_2(OH)(SO_3Na)$; **3** = 4.0×10^{-3} M; **4** = 7.0×10^{-3} M; **5** = 0.010 M; **6** = 0.020 M; **7** = 0.050 M; **8** = 0.10 M

From Table 5.10 it can be seen that pH has little effect on the rate constant: the pK_a of aniline[2] is 4.60 therefore at all the pH values used aniline will be present predominantly as the reactive free amine form. Altering the aniline concentration from 1.0×10^{-4} to 5.1×10^{-5} M also has little effect on the value of the rate constant obtained.

Table 5.10: k_{obs} / s^{-1} values for the reaction of aniline with aqueous $CH_2(OH)(SO_3Na)$ at 25 °C in aqueous solution

[aniline] / M	[$CH_2(OH)(SO_3Na)$] / M	pH†	k_{obs} / s^{-1}
1.0×10^{-4}	2.0×10^{-3}	-	$2.45 \times 10^{-5} \pm 1 \times 10^{-7}$
1.0×10^{-4}	4.0×10^{-3}	-	$4.40 \times 10^{-5} \pm 1 \times 10^{-7}$
1.0×10^{-4}	7.0×10^{-3}	-	$6.44 \times 10^{-5} \pm 1 \times 10^{-7}$
1.0×10^{-4}	7.0×10^{-3}	6.0	$6.68 \times 10^{-5} \pm 1 \times 10^{-7}$
1.0×10^{-4}	7.0×10^{-3}	7.1	$6.94 \times 10^{-5} \pm 1 \times 10^{-7}$
1.0×10^{-4}	7.0×10^{-3}	8.2	$6.19 \times 10^{-5} \pm 1 \times 10^{-7}$
1.0×10^{-4}	0.010	-	$8.89 \times 10^{-5} \pm 1 \times 10^{-7}$
1.0×10^{-4}	0.020	-	$1.66 \times 10^{-4} \pm 1 \times 10^{-7}$
1.0×10^{-4}	0.020	6.0	$1.88 \times 10^{-4} \pm 1 \times 10^{-7}$
1.0×10^{-4}	0.020	7.1	$1.90 \times 10^{-4} \pm 3 \times 10^{-7}$
1.0×10^{-4}	0.020	8.2	$1.70 \times 10^{-4} \pm 3 \times 10^{-7}$
1.0×10^{-4}	0.050	-	$3.99 \times 10^{-4} \pm 3 \times 10^{-7}$
1.0×10^{-4}	0.10	-	$7.93 \times 10^{-4} \pm 1 \times 10^{-6}$
5.1×10^{-5}	0.10	-	$8.29 \times 10^{-4} \pm 8 \times 10^{-7}$

† where no pH is quoted the solution was unbuffered and pH ~ 6.6

The rate constant k_{obs} / s^{-1} refers to the overall rate constant for the formation of $C_6H_5NHCH_2SO_3^-$, shown in Scheme 5.1.

Scheme 5.1: $C_6H_5NH_2 + CH_2(OH)(SO_3^-) \underset{k_b}{\overset{k_f}{\rightleftharpoons}} C_6H_5NHCH_2SO_3^- + H_2O$

Plotting k_{obs} / s^{-1} against [$CH_2(OH)(SO_3Na)$] / M for the reaction with 1.0×10^{-4} M aniline in unbuffered aqueous solution gives a linear plot and allows the determination (Appendix 1) of the forward and back rate constants, k_f / $dm^3\ mol^{-1}\ s^{-1}$ and k_b / s^{-1}, equal to the gradient and intercept respectively (Figure 5.8).

Figure 5.8: k_{obs} / s^{-1} against $[CH_2(OH)(SO_3Na)]$ / M for the reaction with 1.0×10^{-4} M aniline in unbuffered aqueous solution, 25 °C

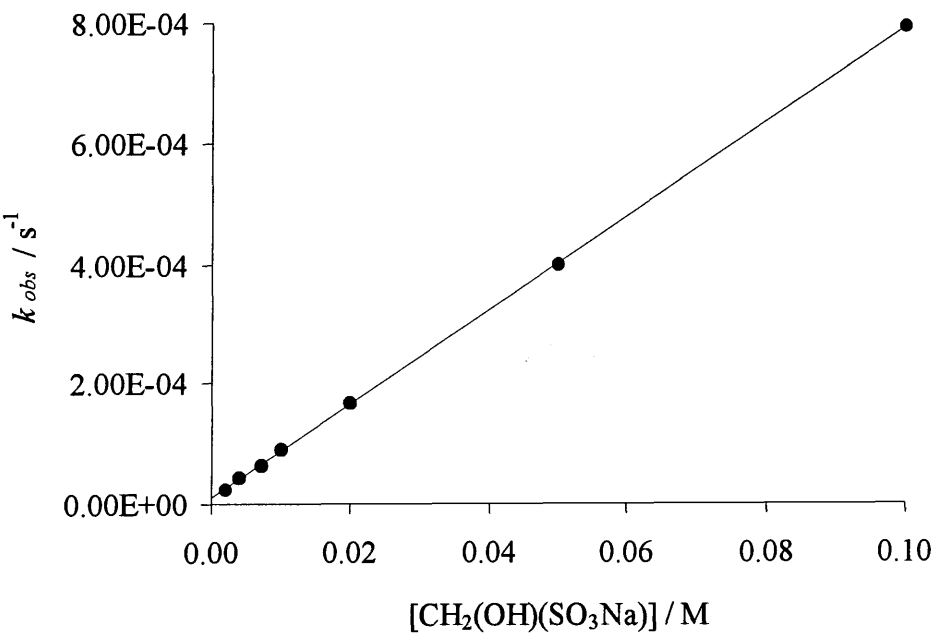

Linear regression yields values of k_f / dm^3 mol^{-1} s^{-1} and k_b / s^{-1} equal to $7.82 \times 10^{-3} \pm 2 \times 10^{-5}$ and $1.01 \times 10^{-5} \pm 8 \times 10^{-7}$ respectively: a correlation coefficient of 0.999 is obtained. These values give an equilibrium constant, K, equal to k_f / k_b, of 780 ± 60 dm^3 mol^{-1}. From Figure 5.7 it is clear that the reaction is an equilibrium as the final absorbance obtained increases with increasing $CH_2(OH)(SO_3Na)$ concentration.

5.2.1.2.2 Reaction in the presence of added sulfite ions

The effect of the presence of added sulfite ions in the system was investigated. Plots of absorbance against time were obtained for the reaction of 1.0×10^{-4} M aniline with 0.10 M aqueous $CH_2(OH)(SO_3Na)$ in the presence of 3.0×10^{-3} or 7.0×10^{-3} M aqueous sodium sulfite solution at 25 °C. The solutions were unbuffered or buffered at pH 6.1 to 8.1: the unbuffered solutions were found to have a pH of 8.0.

Formation of the product $C_6H_5NHCH_2SO_3^-$ was followed at 245 nm. Sulfite ions absorb in this region: spectra of 0.01, 0.05 and 0.10 M aqueous sodium sulfite solution were obtained and showed high absorbance around 250 nm and to shorter wavelength. For example, the extinction coefficient of sulfite ions at 245 nm was found to be

50 dm^3 mol^{-1} cm^{-1}. Therefore the appropriate concentration of sulfite ions was added to the reference in order to subtract the absorbance due to the presence of sulfite from the absorbance against time plots.

Where $[sulfite]_{stoich}$ is quoted this refers to the total concentration of aqueous sodium sulfite added externally to the system and does not include the concentration of sulfite ions present in solution due to dissociation of $CH_2(OH)(SO_3Na)$.

Plots were first order: the k_{obs} / s^{-1} values obtained are shown in Table 5.11.

Table 5.11: k_{obs} / s^{-1} values for the reaction of 1.0×10^{-4} M aniline with 0.10 M aqueous $CH_2(OH)(SO_3Na)$ with added sulfite ions at 25 °C in aqueous solution

pH†	$[sulfite]_{stoich}$ / M	k_{obs} / s^{-1}
-	none	$7.93 \times 10^{-4} \pm 1 \times 10^{-6}$
6.1	3.0×10^{-3}	$4.05 \times 10^{-4} \pm 4 \times 10^{-7}$
7.0	3.0×10^{-3}	$3.22 \times 10^{-4} \pm 2 \times 10^{-6}$
-	3.0×10^{-3}	$2.51 \times 10^{-4} \pm 2 \times 10^{-6}$
8.1	3.0×10^{-3}	$2.16 \times 10^{-4} \pm 2 \times 10^{-7}$
-	7.0×10^{-3}	$1.11 \times 10^{-4} \pm 6 \times 10^{-7}$

† where no pH is quoted the solution was unbuffered and pH ~ 6.6 or 8.0 if in the presence of sulfite ions

The results show that the value of the rate constant is considerably lower in the presence of added sulfite ions. If free formaldehyde, HCHO, is the reactive species in the reaction of $CH_2(OH)(SO_3Na)$ with amines then the reaction must proceed initially via dissociation of $CH_2(OH)(SO_3Na)$ to give HCHO (Chapter 4). If this is the case, in the presence of additional sulfite ions the rate of formation of the product $C_6H_5NHCH_2SO_3^-$ may be expected to decrease as more free formaldehyde will react with the sulfite ions to give the unreactive $CH_2(OH)(SO_3Na)$. Hence less free formaldehyde will be present to react with the aniline. The experimental results obtained here support this theory.

The rate constant decreases as the pH increases from 6.1 to 8.1. The pK_a value for the bisulfite / sulfite equilibrium[4] is 7.2. Formaldehyde reacts more rapidly with sulfite ions than with bisulfite ions (Chapter 4) therefore at pH values above 7.2, where sulfite is the dominant species, the unreactive $CH_2(OH)(SO_3Na)$ will form more readily. Hence less free formaldehyde will be present as the pH increases and the rate of formation of the product $C_6H_5NHCH_2SO_3^-$ will be slower.

5.2.2 Reaction of $CH_2(OH)(SO_3Na)$ with 4-methylaniline

5.2.2.1 ^1H NMR studies

The reaction of $CH_2(OH)(SO_3Na)$ with 4-methylaniline in 95 % D_2O / 5 % methyl-d_3 alcohol-d, CD_3OD, by volume was followed using ^1H NMR spectroscopy. 4-methylaniline is not readily soluble in aqueous solution at the concentrations required therefore a mixed solvent system was used.

For comparison, the spectrum of 0.22 M 4-methylaniline (**5.2**) in 95 % D_2O / 5 % CD_3OD was obtained (Figure 5.9, Table 5.12).

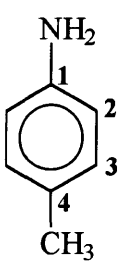

5.2

Table 5.12: ^1H NMR spectrum of 4-methylaniline in 95 % D_2O / 5% CD_3OD: peak assignments

δ / ppm	integral ratio	multiplicity	J / Hz	assignment
2.10	3	s	-	**-CH_3**
4.67	-	-	-	D_2O, **-NH_2**
6.64	2	d	8.0	Ar-**H2**
6.95	2	d	8.0	Ar-**H3**

Figure 5.9: ^{1}H NMR spectrum of 4-methylaniline in 95 % D_2O / 5 % CD_3OD

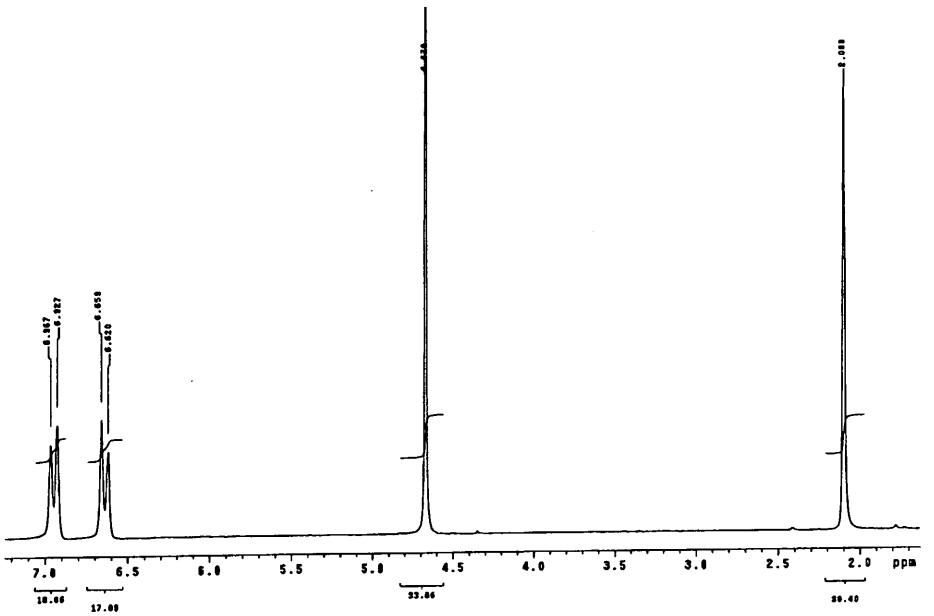

The spectrum of 0.20 M 4-methylaniline and 0.20 M $CH_2(OH)(SO_3Na)$ was obtained, then with each reagent in excess: 0.20 M 4-methylaniline with 0.40 M $CH_2(OH)(SO_3Na)$ and 0.21 M 4-methylaniline with 0.11 M $CH_2(OH)(SO_3Na)$. A spectrum was recorded immediately (3 to 5 minutes) after addition of the $CH_2(OH)(SO_3Na)$ then again after approximately 30 minutes and 1 hour and continued until there was no further change in the spectrum.

There are two possible products that may form in the reaction. Firstly, a 1 : 1 4-methylaniline : $CH_2(OH)(SO_3Na)$ adduct 4-$CH_3C_6H_4NHCH_2SO_3^-$, **5.6**, can form. In the presence of excess $CH_2(OH)(SO_3Na)$, a second molecule may react to give a 1 : 2 4-methylaniline : $CH_2(OH)(SO_3Na)$ adduct 4-$CH_3C_6H_4N(CH_2SO_3^-)_2$, **5.7**.

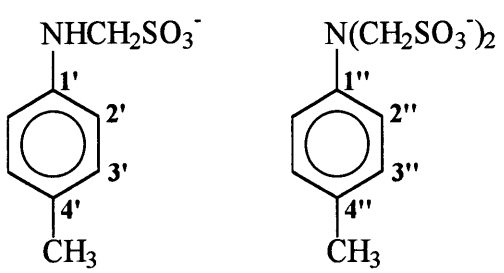

5.6 **5.7**

5.2.2.1.1 Equimolar 4-methylaniline and $CH_2(OH)(SO_3Na)$

The results obtained for the reaction of equimolar 0.20 M 4-methylaniline and $CH_2(OH)(SO_3Na)$ are shown in Figures 5.10 and 5.11 which show the spectra obtained 3 minutes and 1 hour after mixing. There was no further change in the spectrum over time. Tables 5.13 and 5.14 summarise the information obtained from the two spectra.

Figure 5.10: 0.20 M 4-methylaniline and 0.20 M $CH_2(OH)(SO_3Na)$: 3 min after mixing

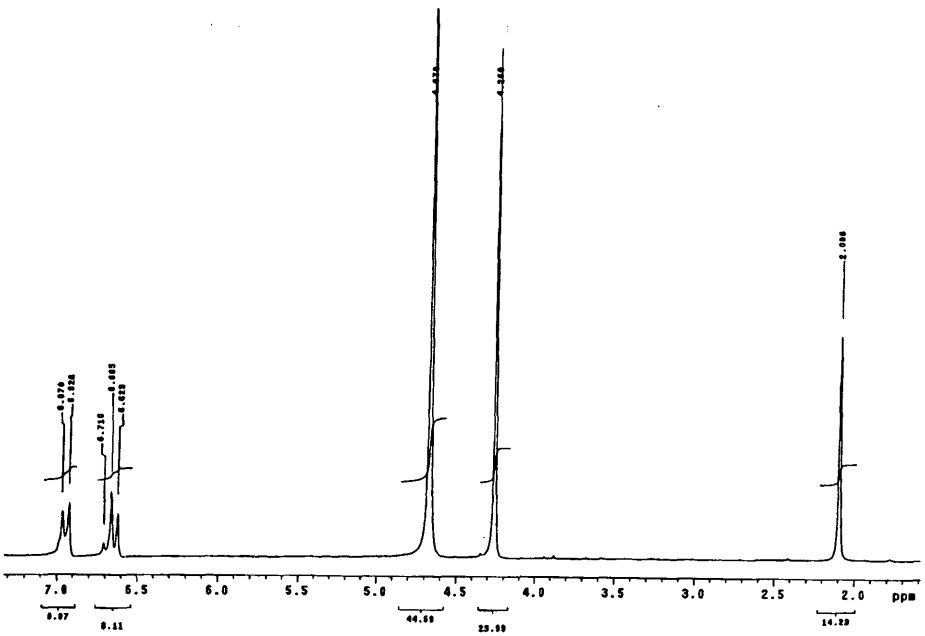

Table 5.13: Peak assignments: 3 minutes after mixing

time after mixing	δ / ppm	integral ratio	multiplicity	J / Hz	assignment
3 minutes	2.10	3	s	-	$-CH_3$
	4.26	5	s	-	$CH_2(OH)(SO_3Na)$
	4.67	-	-	-	D_2O, $-NH_2$
	6.64	2	d	8.0	Ar-**H2**
	6.69		d	-	Ar-**H2'**
	6.95	2	d	8.0	Ar-**H3**

Figure 5.11: 0.20 M 4-methylaniline and 0.20 M $CH_2(OH)(SO_3Na)$: 1 hr after mixing

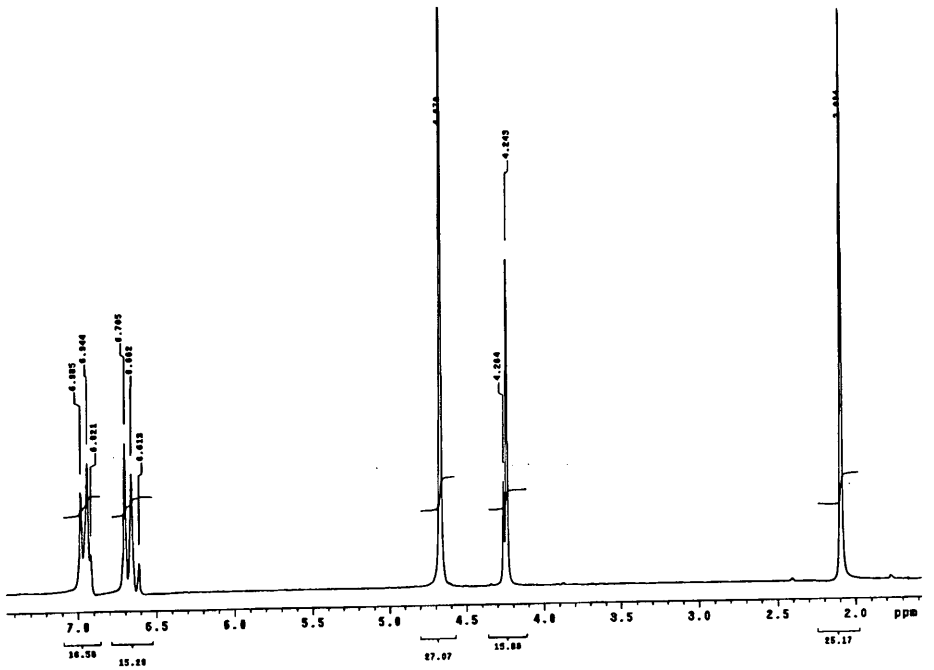

Table 5.14: Peak assignments: 1 hour after mixing

time after mixing	δ / ppm	integral ratio	multiplicity	J / Hz	assignment
1 hour	2.10	3	s	-	$-CH_3$
	4.24	2	s	-	$-NHCH_2SO_3^-$
	4.26		s	-	$CH_2(OH)(SO_3Na)$
	4.67	-	-	-	D_2O, NH_2
	6.64	2	d	-	Ar-**H2**
	6.68		d	8.0	Ar-**H2'**
	6.93	2	d	-	Ar-**H3**
	6.96		d	8.0	Ar-**H3'**

The spectra show the formation of the 1 : 1 adduct $4\text{-}CH_3C_6H_4NHCH_2SO_3^-$ over time. After 3 minutes the spectrum shows a small change in the aromatic region. Within 39 minutes there is considerable product formation, with the appearance of peaks at δ 4.24 ppm and new peaks in the aromatic region. The reaction is complete within 1 hour. The peaks due to $CH_2(OH)(SO_3Na)$ and 4-methylaniline decrease in intensity over time. However complete conversion to the product is not obtained as there is still some evidence of small amounts of both starting materials in the final spectrum.

There is no evidence of formation of the 1 : 2 adduct 4-$CH_3C_6H_4N(CH_2SO_3^-)_2$. As with aniline, the presence of the -$CH_2SO_3^-$ electron withdrawing group on 4-methylaniline will make the nitrogen less nucleophilic than that in the parent compound therefore reducing the tendency to add a second $CH_2(OH)(SO_3Na)$ molecule. Hence no 1 : 2 adduct is observed.

5.2.2.1.2 $CH_2(OH)(SO_3Na)$ in excess

The spectra obtained for the reaction of 0.20 M 4-methylaniline and 0.40 M $CH_2(OH)(SO_3Na)$ also show the formation of the 1 : 1 adduct 4-$CH_3C_6H_4NHCH_2SO_3^-$. Again there is no evidence of formation of the 1 : 2 adduct 4-$CH_3C_6H_4N(CH_2SO_3^-)_2$ even though $CH_2(OH)(SO_3Na)$ is present in excess. Table 5.15 summarises the spectra obtained 5 and 38 minutes after mixing. There was no further change in the spectrum over time.

Table 5.15: 0.20 M 4-methylaniline and 0.40 M $CH_2(OH)(SO_3Na)$: peak assignments

time after mixing	δ / ppm	integral ratio	multiplicity	J / Hz	assignment
5 minutes	2.11	3	s	-	-CH_3
	4.28	9	s	-	$CH_2(OH)(SO_3Na)$
	4.67	-	-	-	D_2O, -NH_2
	6.66	2	d	8.0	Ar-**H2**
	6.70		d	8.0	Ar-**H2'**
	6.96	2	d	8.0	Ar-**H3**
	6.98		d	8.0	Ar-**H3'**
38 minutes	2.12	3	s	-	-CH_3
	4.27	4	s	-	-$NHCH_2SO_3^-$
	4.29		s	-	$CH_2(OH)(SO_3Na)$
	4.67	-	-	-	D_2O, -NH_2
	6.71	2	d	8.0	Ar-**H2'**
	6.99	2	d	8.0	Ar-**H3'**

After only 5 minutes there is evidence of product formation in the form of new peaks in the aromatic region. After 38 minutes the reaction is complete. After this time all the 4-methylaniline has reacted and the peaks due to the $-CH_2-$ groups in $CH_2(OH)(SO_3Na)$ and the 1 : 1 adduct $4\text{-}CH_3C_6H_4NHCH_2SO_3^-$ are approximately equal in intensity. This corresponds to one equivalent of $CH_2(OH)(SO_3Na)$ reacting with the 4-methylaniline and one equivalent remaining in solution. The peaks in the aromatic region are also very clean which implies only one product is formed, namely the 1 : 1 adduct $4\text{-}CH_3C_6H_4NHCH_2SO_3^-$.

5.2.2.1.3 4-Methylaniline in excess

The spectra obtained for the reaction of 0.21 M 4-methylaniline and 0.11 M $CH_2(OH)(SO_3Na)$ show the formation of the 1 : 1 adduct $4\text{-}CH_3C_6H_4NHCH_2SO_3^-$. Table 5.16 summarises the spectra obtained 3 minutes and 1 hour after mixing. There was no further change in the spectrum over time.

Table 5.16: 0.21 M 4-methylaniline and 0.11 M $CH_2(OH)(SO_3Na)$: peak assignments

time after mixing	δ / ppm	integral ratio	multiplicity	J / Hz	assignment
3 minutes	2.12	3	s	-	$-CH_3$
	4.29	2	s	-	$CH_2(OH)(SO_3Na)$
	4.67	-	-	-	D_2O, $-NH_2$
	6.67	2	d	8.0	Ar-**H2**
	6.71		d	8.0	Ar-**H2'**
	6.98	2	d	8.0	Ar-**H3**
1 hour	2.14	3	s	-	$-CH_3$
	4.29	2	s	-	$-NHCH_2SO_3^-$
	4.67	-	-	-	D_2O, $-NH_2$
	6.68	2	d	8.0	Ar-**H2**
	6.73		d	8.0	Ar-**H2'**
	6.98	2	d	8.0	Ar-**H3**
	7.01		d	8.0	Ar-**H3'**

After 3 minutes there is very little change in the spectrum, with only a small change in the aromatic region indicating reaction. However after 38 minutes there are significant peaks present due to the 1 : 1 adduct $4\text{-}CH_3C_6H_4NHCH_2SO_3^-$ and the reaction is complete within 1 hour. After this time there is complete conversion of $CH_2(OH)(SO_3Na)$ to the product.

5.2.2.2 Uv / visible kinetic studies

5.2.2.2.1 Absorbance against wavelength spectra and absorbance against time plots

Absorbance against wavelength spectra were obtained for the reaction of 0.10 M aqueous $CH_2(OH)(SO_3Na)$ with 1.0×10^{-4} M 4-methylaniline at 25 °C in aqueous solution. The spectrum shows a shift to higher wavelength over time with a corresponding increase in absorbance as compared to the spectrum of 1.0×10^{-4} M 4-methylaniline alone. The reaction is complete within 25 minutes.

Figure 5.12 shows the change over time in the spectrum with 0.10 M $CH_2(OH)(SO_3Na)$ as compared to that of 4-methylaniline alone. Table 5.17 shows the peak positions and extinction coefficients (ε) for the two spectra.

Figure 5.12: Absorbance against wavelength spectrum for 1.0×10^{-4} M 4-methylaniline with 0.10 M $CH_2(OH)(SO_3Na)$, 25 °C, aqueous solution

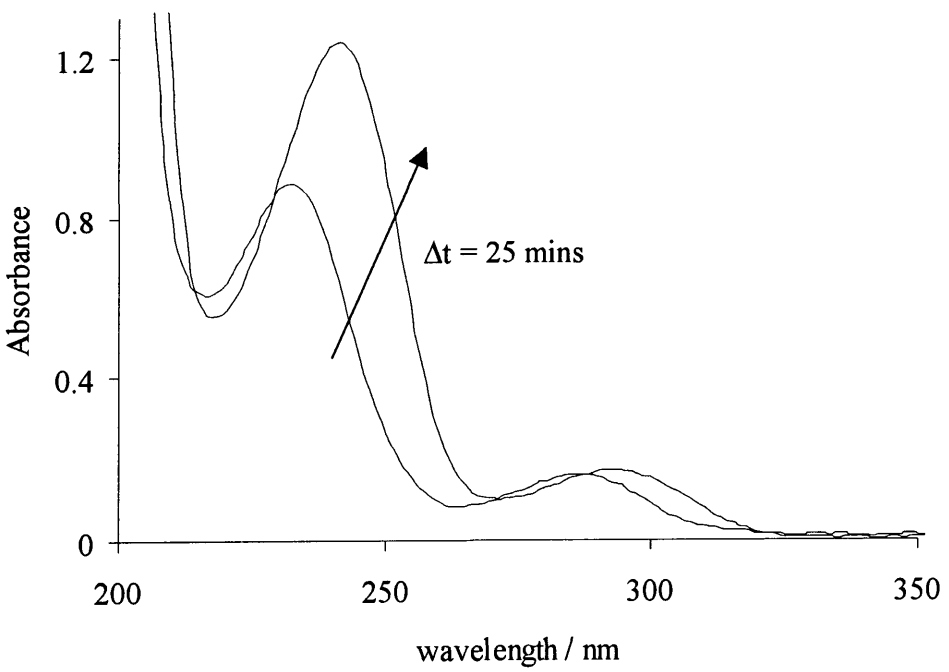

Table 5.17: Spectral appearance in aqueous solution of 1.0×10^{-4} M 4-methylaniline and the final spectrum in the presence of 0.10 M $CH_2(OH)(SO_3Na)$

$[CH_2(OH)(SO_3Na)]$ / M	λ_{max} / nm ($\varepsilon^{\dagger}$/ mol^{-1} dm^3 cm^{-1})
none	232 (8900); 287 (1600)
0.10	241 (12400); 291 (1700)

† based on the assumption that all the 4-methylaniline reacts to give 1.0×10^{-4} M product

Plots of absorbance against time were obtained for the reaction of 1.0×10^{-4} M 4-methylaniline with 2.0×10^{-3} to 0.10 M aqueous $CH_2(OH)(SO_3Na)$ at 25 °C at pH 5.8 and 7.9. Formation of the product at 240 nm was followed. Plots were first order: the k_{obs} / s^{-1} values obtained are shown in Table 5.18.

Table 5.18: k_{obs} / s^{-1} values for the reaction of 1.0×10^{-4} 4-methylaniline with aqueous $CH_2(OH)(SO_3Na)$ at 25 °C, pH 5.8 and 7.9

$[CH_2(OH)(SO_3Na)]$ / M	pH	k_{obs} / s^{-1}
2.0×10^{-3}	5.8	$2.12 \times 10^{-4} \pm 5 \times 10^{-7}$
4.0×10^{-3}	5.8	$3.22 \times 10^{-4} \pm 8 \times 10^{-7}$
8.0×10^{-3}	5.8	$5.15 \times 10^{-4} \pm 1 \times 10^{-6}$
0.01	5.8	$6.13 \times 10^{-4} \pm 2 \times 10^{-6}$
0.10	5.8	$5.04 \times 10^{-3} \pm 2 \times 10^{-5}$
0.10	7.9	$4.00 \times 10^{-3} \pm 1 \times 10^{-5}$

Altering the pH does not greatly affect the rate constant obtained. Plotting k_{obs} / s^{-1} against $[CH_2(OH)(SO_3Na)]$ / M for the reaction at pH 5.8 gives a linear plot and allows the determination of the forward and back rate constants, k_f / dm^3 mol^{-1} s^{-1} and k_b / s^{-1}, equal to the gradient and intercept respectively. Linear regression yields values of k_f / dm^3 mol^{-1} s^{-1} and k_b / s^{-1} equal to $4.92 \times 10^{-2} \pm 6 \times 10^{-5}$ and $1.20 \times 10^{-4} \pm 3 \times 10^{-6}$ respectively: a correlation coefficient of 0.999 is obtained. These values give an equilibrium constant, K, equal to k_f/ k_b, of 410 ± 10 dm^3 mol^{-1}.

5.2.2.2.2 Reaction in the presence of added sulfite ions

The effect of the presence of added sulfite ions in the system was investigated. Plots of absorbance against time were obtained for the reaction of 1.0×10^{-4} M aniline with 0.10 M aqueous $CH_2(OH)(SO_3Na)$ in the presence of 1.0×10^{-3} to 0.010 M aqueous sodium sulfite solution at 25 °C at pH 5.8 and 8.9.

Formation of the product $4\text{-}CH_3C_6H_4NHCH_2SO_3^-$ at 240 nm was followed. Sulfite ions absorb in this region therefore the appropriate concentration of sulfite ions was added to the reference in order to subtract the absorbance due to the presence of sulfite from the absorbance against time plots. Where $[\text{sulfite}]_{\text{stoich}}$ is quoted this refers to the total concentration of aqueous sodium sulfite added externally to the system and does not include the concentration of sulfite ions present in solution due to the dissociation of $CH_2(OH)(SO_3Na)$. Plots were first order (Figure 5.13): the k_{obs} / s^{-1} values obtained are shown in Table 5.19.

Figure 5.13: Absorbance against time plots for the reaction of 1.0×10^{-4} M 4-methylaniline with 0.10 M $CH_2(OH)(SO_3Na)$ with added sulfite ions at 25 °C, pH 5.8

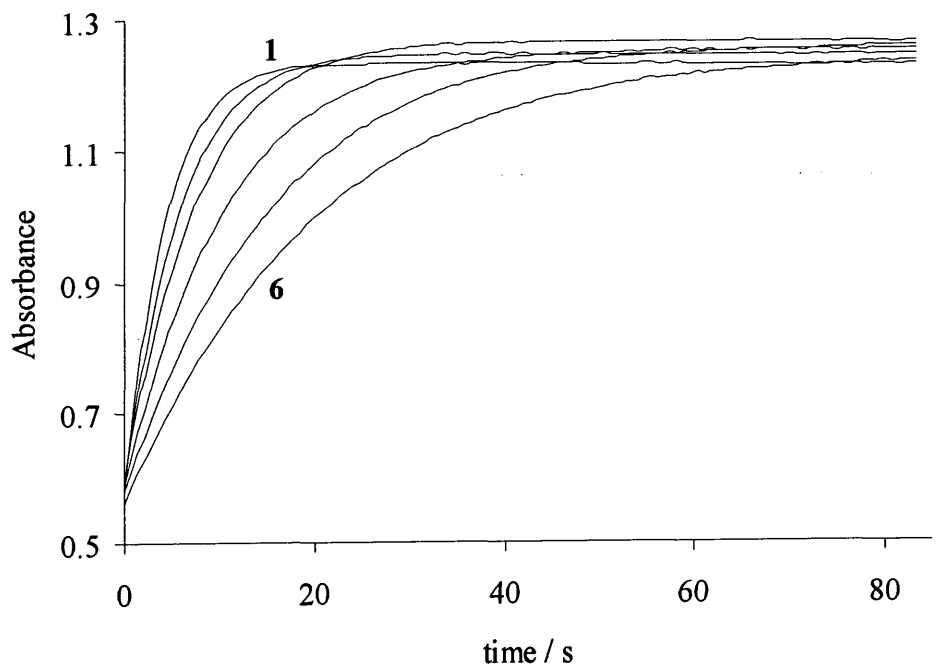

1 = no sulfite; **2** = 1.0×10^{-3} M sulfite ions; **3** = 2.2×10^{-3} M;
4 = 4.0×10^{-3} M; **5** = 7.0×10^{-3} M; **6** = 0.010 M

Table 5.19: k_{obs} / s^{-1} values for the reaction of 1.0×10^{-4} M 4-methylaniline with 0.10 M aqueous $CH_2(OH)(SO_3Na)$ with added sulfite ions at 25 °C, pH 5.8 and 7.9

pH	$[sulfite]_{stoich}$ / M	k_{obs} / s^{-1}	$k_{obs}.[sulfite]_{stoich}$ / s^{-1} M
5.8	0	$4.58 \times 10^{-3} \pm 6 \times 10^{-5}$	-
	1.0×10^{-3}	$3.07 \times 10^{-3} \pm 8 \times 10^{-6}$	3.1×10^{-6}
	2.2×10^{-3}	$2.27 \times 10^{-3} \pm 7 \times 10^{-6}$	5.0×10^{-6}
	4.0×10^{-3}	$1.75 \times 10^{-3} \pm 6 \times 10^{-6}$	7.0×10^{-6}
	7.0×10^{-3}	$1.18 \times 10^{-3} \pm 3 \times 10^{-6}$	8.3×10^{-6}
	0.010	$9.33 \times 10^{-4} \pm 3 \times 10^{-6}$	9.3×10^{-6}
7.9	0	$3.68 \times 10^{-3} \pm 1 \times 10^{-5}$	-
	1.0×10^{-3}	$1.95 \times 10^{-3} \pm 4 \times 10^{-5}$	2.0×10^{-6}
	2.0×10^{-3}	$1.62 \times 10^{-3} \pm 9 \times 10^{-6}$	3.2×10^{-6}
	4.4×10^{-3}	$8.23 \times 10^{-4} \pm 3 \times 10^{-6}$	3.6×10^{-6}
	7.0×10^{-3}	$6.36 \times 10^{-4} \pm 2 \times 10^{-6}$	4.5×10^{-6}
	0.010	$2.92 \times 10^{-4} \pm 2 \times 10^{-6}$	2.9×10^{-6}

The rate of reaction is considerably slower in the presence of added sulfite ions. Multiplying k_{obs} / s^{-1} by $[sulfite]_{stoich}$ / M at pH 7.9 gives an approximately constant value which implies an inverse dependence of k_{obs} / s^{-1} on the sulfite ion concentration. However this relationship is not strictly obtained at pH 5.8.

The results in Table 5.19 indicate a dependence of k_{obs} / s^{-1} on pH. This was investigated by studying the reaction of 1.0×10^{-4} M 4-methylaniline and 0.10 M aqueous $CH_2(OH)(SO_3Na)$ with 0.01 M added sulfite ions at 25 °C in the pH range 5.1 to 8.9. Plots were first order: the k_{obs} / s^{-1} values obtained are shown in Table 5.20.

Table 5.20: k_{obs} / s^{-1} values for the reaction of 1.0×10^{-4} M 4-methylaniline and 0.10 M aqueous $CH_2(OH)(SO_3Na)$ with 0.01 M added sulfite ions, 25 °C, pH 5.1 to 8.9

pH	k_{obs} / s^{-1}	adjusted† k_{obs} / s^{-1}
5.1	$1.19 \times 10^{-3} \pm 5 \times 10^{-6}$	$2.33 \times 10^{-3} \pm 1 \times 10^{-5}$
5.9	$1.47 \times 10^{-3} \pm 1 \times 10^{-5}$	$1.69 \times 10^{-3} \pm 1 \times 10^{-5}$
7.0	$1.39 \times 10^{-3} \pm 1 \times 10^{-5}$	$1.39 \times 10^{-3} \pm 1 \times 10^{-5}$
8.1	$1.07 \times 10^{-3} \pm 7 \times 10^{-6}$	$1.07 \times 10^{-3} \pm 7 \times 10^{-6}$
8.9	$8.16 \times 10^{-4} \pm 1 \times 10^{-6}$	$8.16 \times 10^{-4} \pm 1 \times 10^{-6}$

† corrected to allow for the reduction in free amine concentration due to protonation

The pK_a of 4-methylaniline is 5.08 therefore at pH 5.1 and 5.9 there will be less than the stoichiometric amount of 4-methylaniline present as the reactive unprotonated free form of the base. This can be corrected for by multiplying the k_{obs} / s^{-1} value obtained by the stoichiometric 4-methylaniline concentration, 1.0×10^{-4} M, and dividing by the actual concentration of free reactive 4-methylaniline, equal to 5.1×10^{-5} M and 8.7×10^{-5} M for pH 5.1 and 5.9 respectively. Plotting $\log(k_{obs} / s^{-1})$ against pH using these corrected values gives a linear plot with a correlation coefficient of 0.986 (Figure 5.14).

Figure 5.14: Plot of $\log(k_{obs} / s^{-1})$ against pH for the reaction of 1.0×10^{-4} M 4-methylaniline with 0.10 M $CH_2(OH)(SO_3Na)$ with 0.01 M added sulfite ions, 25 °C

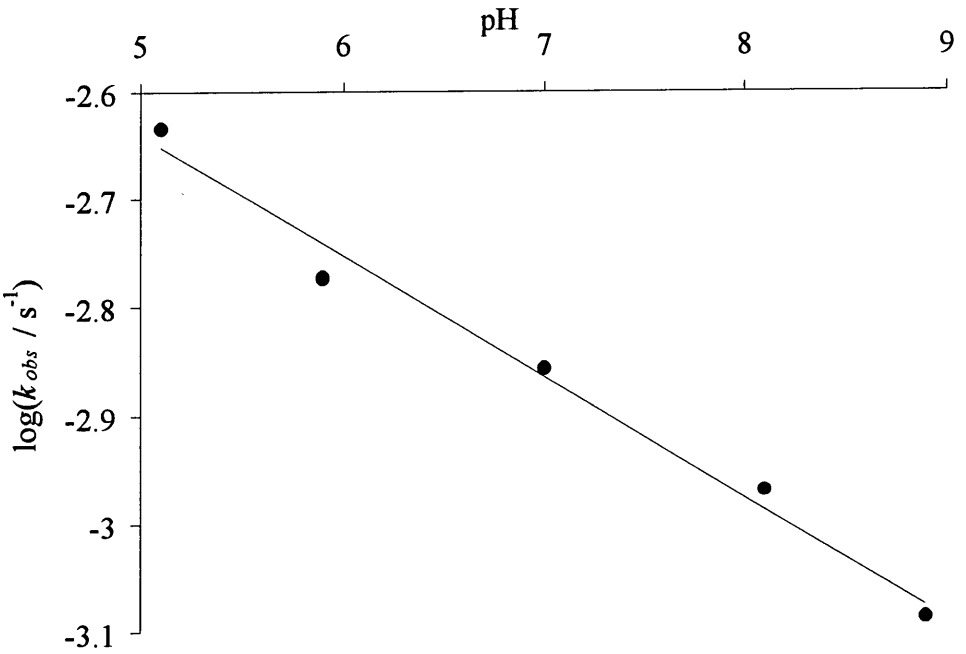

To investigate whether the reaction is subject to specific or general acid / base catalysis, the reaction of 1.0×10^{-4} M 4-methylaniline with 0.10 M aqueous $CH_2(OH)(SO_3Na)$ in the presence of 0.10 M added sulfite ions was studied at pH 5.9. Potassium dihydrogen phosphate / sodium hydroxide buffers were used: the buffer concentration was altered whilst retaining a constant buffer ratio. Plots were first order: the k_{obs} / s^{-1} values obtained are shown in Table 5.21.

Table 5.21: k_{obs} / s^{-1} values for the reaction of 1.0×10^{-4} M 4-methylaniline, 0.10 M $CH_2(OH)(SO_3Na)$, 0.01 M added sulfite ions, pH 5.9, altered buffer concentrations

buffer concentration / M		k_{obs} / s^{-1}
$[KH_2PO_4]_{stoich}$	$[NaOH]_{stoich}$	
0.07	0.008	$1.13 \times 10^{-3} \pm 2 \times 10^{-6}$
0.10	0.011	$1.15 \times 10^{-3} \pm 5 \times 10^{-6}$
0.13	0.015	$1.64 \times 10^{-3} \pm 1 \times 10^{-5}$
0.17	0.019	$1.43 \times 10^{-3} \pm 2 \times 10^{-6}$
0.20	0.022	$1.45 \times 10^{-3} \pm 1 \times 10^{-6}$

The rate constant obtained shows no clear dependence on the buffer concentration, which indicates the reaction is subject to specific rather than general catalysis.

5.2.3 Reaction of $CH_2(OH)(SO_3Na)$ with 4-dimethylaminoaniline

5.2.3.1 Uv / visible kinetic studies

5.2.3.1.1 Absorbance against wavelength spectra and absorbance against time plots

Absorbance against wavelength spectra were obtained for the reaction of 2.0×10^{-3} to 0.10 M aqueous $CH_2(OH)(SO_3Na)$ with 1.0×10^{-4} M 4-dimethylaminoaniline at 25 °C in aqueous solution. The spectrum of 1.0×10^{-4} M 4-dimethylaminoaniline alone was obtained for comparison. The spectra with aqueous $CH_2(OH)(SO_3Na)$ added show a shift to higher wavelength with a corresponding increase in absorbance as compared to the spectrum of 1.0×10^{-4} M 4-dimethylaminoaniline alone. All reactions are complete within 10 minutes.

Figure 5.15 shows the change over time in the spectrum for the reaction with 0.10 M $CH_2(OH)(SO_3Na)$ as compared to that of 4-dimethylaminoaniline alone. Table 5.22 shows the peak positions and extinction coefficients (ε) for the two spectra. 4-Dimethylaminoaniline is not readily soluble in water therefore the ε values calculated may be lower than the true values if the actual concentration of 4-dimethylaminoaniline is lower than expected due to poor solubility.

Table 5.22: Spectral appearance of 1.0×10^{-4} M 4-dimethylaminoaniline and the final spectrum in the presence of 0.10 M $CH_2(OH)(SO_3Na)$ in aqueous solution

$[CH_2(OH)(SO_3Na)]$ / M	λ_{max} / nm ($\varepsilon^{\dagger}$/ mol^{-1} dm^3 cm^{-1})
none	245 (10700); 299 (1700)
0.10	251 (13800); 297 (1800)

† based on the assumption that all the 4-dimethylaminoaniline reacts to give 1.0×10^{-4} M product

Figure 5.15: Change over time in the absorbance against wavelength spectrum for the reaction of 1.0×10^{-4} M 4-dimethylaminoaniline with 0.10 M $CH_2(OH)(SO_3Na)$, 25 °C

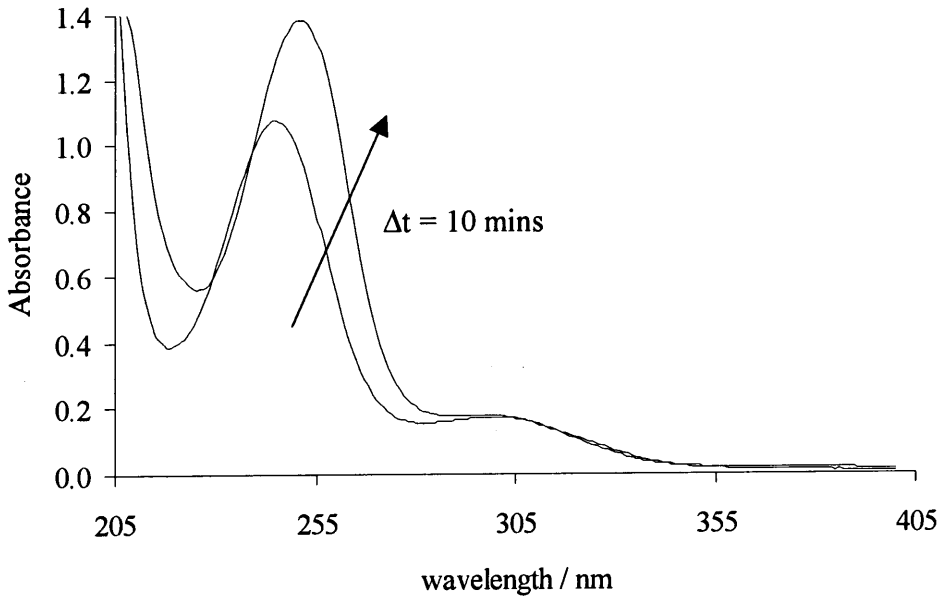

Plots of absorbance against time were obtained for the reaction of 1.0×10^{-4} M 4-dimethylaminoaniline with 2.0×10^{-3} to 0.10 M aqueous $CH_2(OH)(SO_3Na)$ at 25 °C. 4-Dimethylaminoaniline is not readily soluble in aqueous solution therefore a stock solution in acetonitrile or dioxan was prepared, giving a final solvent composition of 98 % water / 2 % acetonitrile or dioxan by volume. Formation of the product at 251 or 260 nm was followed. Plots were first order: the k_{obs} / s^{-1} values obtained are shown in Table 5.23.

Table 5.23: k_{obs} / s^{-1} values for the reaction of 4-dimethylaminoaniline with aqueous $CH_2(OH)(SO_3Na)$ at 25 °C in 98 % water / 2 % acetonitrile or dioxan

$[CH_2(OH)(SO_3Na)]$ / M	k_{obs} / s^{-1}		A_∞
	2 % acetonitrile	2 % dioxan	
2.0×10^{-3}	$5.36 \times 10^{-4} \pm 5 \times 10^{-6}$	$5.57 \times 10^{-4} \pm 3 \times 10^{-7}$	1.21
7.0×10^{-3}	$1.14 \times 10^{-3} \pm 6 \times 10^{-6}$	$1.15 \times 10^{-3} \pm 1 \times 10^{-6}$	1.31
0.021	$2.39 \times 10^{-3} \pm 9 \times 10^{-7}$	$2.15 \times 10^{-3} \pm 5 \times 10^{-6}$	1.37
0.052	$4.00 \times 10^{-3} \pm 3 \times 10^{-7}$	$3.58 \times 10^{-3} \pm 9 \times 10^{-6}$	1.38
0.103	$6.29 \times 10^{-3} \pm 2 \times 10^{-7}$	$5.54 \times 10^{-3} \pm 1 \times 10^{-5}$	1.39

There is little difference in the rate constants obtained in the two solvent systems, indicating that the 2 % organic component has little effect on the kinetics. The absorbance values at reaction completion, A_∞, show that the reaction goes largely to the product. Hence the forward rate term, k_f, dominates.

The values show a general increase with increasing concentration of $CH_2(OH)(SO_3Na)$ but the increase is not linear. This may be due to the fact that in these solutions neither the pH nor the concentration of sulfite ions in solution were controlled. Since the pK_a value of 4-dimethylaminoaniline is 6.59, values of rate constants in these solutions are likely to be dependent on the pH of the solution.

5.2.3.1.2 Reaction in the presence of added sulfite ions

The effect of the presence of added sulfite ions in the system was investigated. Plots of absorbance against time were obtained for the reaction of 1.0×10^{-4} M 4-dimethylaminoaniline with 0.10 M aqueous $CH_2(OH)(SO_3Na)$ in the presence of 2.0×10^{-3} to 0.010 M aqueous sodium sulfite solution at 25 °C at pH 5.9 and 8.0 in a 98 % water / 2 % acetonitrile by volume solvent.

Formation of the product $4\text{-}N(CH_3)_2C_6H_4NHCH_2SO_3^-$ at 260 nm was followed. Sulfite ions absorb in this region: spectra of 0.01, 0.05 and 0.10 M aqueous sodium sulfite solution were obtained and showed high absorbance around 250 nm and to shorter wavelength. For example, the extinction coefficient of sulfite ions at 245 nm was found to be 50 $dm^3\ mol^{-1}\ cm^{-1}$. Therefore the appropriate concentration of sulfite ions was added to the reference in order to subtract the absorbance due to the presence of sulfite from the absorbance against time plots.

Where $[sulfite]_{stoich}$ is quoted this refers to the total concentration of aqueous sodium sulfite added externally to the system and does not include the concentration of sulfite ions present in solution due to dissociation of $CH_2(OH)(SO_3Na)$.

Plots were first order: the k_{obs} / s^{-1} values obtained are shown in Table 5.24.

Table 5.24: k_{obs} / s^{-1} values for the reaction of 1.0×10^{-4} M 4-dimethylaminoaniline with 0.10 M aqueous $CH_2(OH)(SO_3Na)$ in the presence of added sulfite ions in 98 % water / 2 % acetonitrile, 25 °C, pH 5.9 and 8.0

pH	$[sulfite]_{stoich}$ / M	k_{obs} / s^{-1}	$k_{obs}.[sulfite]_{stoich}$ / s^{-1} M
5.9	0	$3.53 \times 10^{-3} \pm 1.3 \times 10^{-5}$	-
	2.0×10^{-3}	$1.29 \times 10^{-3} \pm 4 \times 10^{-6}$	2.6×10^{-6}
	4.0×10^{-3}	$6.45 \times 10^{-4} \pm 8 \times 10^{-7}$	2.6×10^{-6}
	7.0×10^{-3}	$4.44 \times 10^{-4} \pm 8 \times 10^{-7}$	3.1×10^{-6}
	0.010	$2.80 \times 10^{-4} \pm 6 \times 10^{-7}$	2.8×10^{-6}
8.0	0	$7.47 \times 10^{-3} \pm 1.7 \times 10^{-4}$	-
	2.0×10^{-3}	$2.07 \times 10^{-3} \pm 1.3 \times 10^{-5}$	4.1×10^{-6}
	4.0×10^{-3}	$1.18 \times 10^{-3} \pm 6 \times 10^{-6}$	4.7×10^{-6}
	7.0×10^{-3}	$7.55 \times 10^{-4} \pm 1 \times 10^{-6}$	5.3×10^{-6}
	0.010	$5.13 \times 10^{-4} \pm 5 \times 10^{-7}$	5.1×10^{-6}

The rate of reaction is considerably slower in the presence of added sulfite ions. Multiplying k_{obs} / s^{-1} by $[sulfite]_{stoich}$ / M gives an approximately constant value at each pH which implies an inverse dependence of k_{obs} / s^{-1} on the sulfite ion concentration.

The rate constant increases as the pH increases from 5.9 to 8.0. The pK_a of 4-dimethylaminoaniline is 6.59 therefore as the pH increases more of the reactive unprotonated free base form will be present so the rate of formation of the product will increase.

5.2.4 Decomposition of $C_6H_5NHCH_2SO_3^-$

5.2.4.1 Reaction of aniline with aqueous iodine solution

An absorbance against wavelength spectrum was obtained for a solution of 1.0×10^{-4} M aniline with 4×10^{-4} M aqueous iodine solution added. The solution immediately decolourised and there was no evidence in the spectrum of peaks of high absorbance due to aqueous iodine solution. Therefore the reaction of aniline with aqueous iodine solution is rapid.

Plots of absorbance against time were obtained for the reaction of 1.1×10^{-3} to 0.030 M aniline with 4×10^{-4} M aqueous iodine solution at pH 5.0, 25 °C, using stopped flow spectrophotometry. First order plots were obtained and fitted using a single exponential equation (Figure 5.16). As aqueous iodine solution has an extinction coefficient of 13400 ± 300 mol^{-1} dm^3 cm^{-1} at 350 nm, the initial absorbances were above the limit of the instrument. Therefore when the plots were fitted, the initial data with an absorbance above 2 absorbance units was not included. The results are shown in Table 5.25.

Figure 5.16: Absorbance against time plot at 350 nm with single exponential fit superimposed for the reaction of 0.010 M aniline with 4×10^{-4} M aqueous iodine solution at pH 5.0, 25 °C

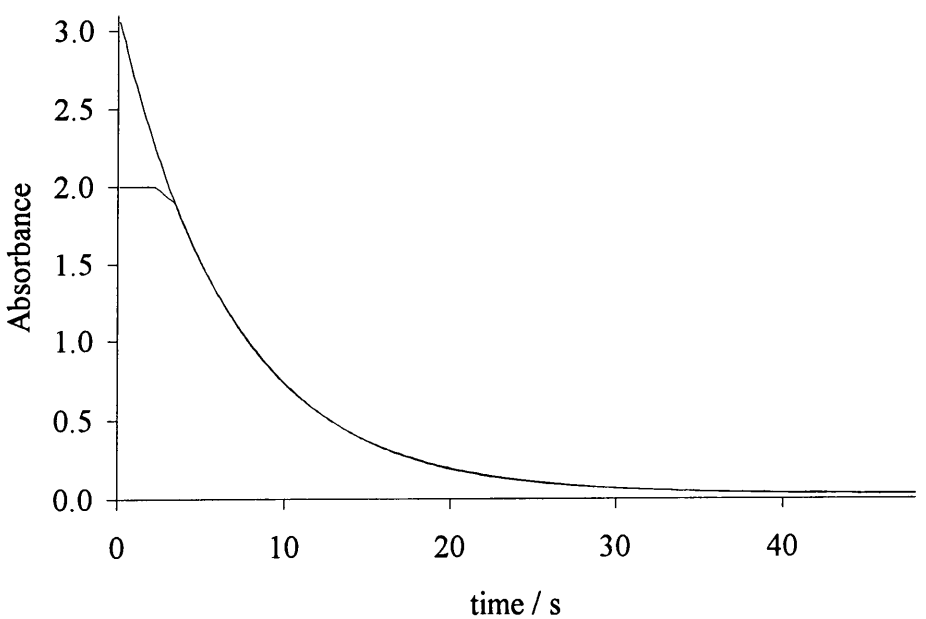

Table 5.25: k_{obs} / s^{-1} values for the reaction of aniline with 4×10^{-4} M aqueous iodine solution, pH 5.0, 25 °C

$[C_6H_5NH_2]$ / M	k_{obs} / s^{-1}
1.1×10^{-3}	$0.031 \pm 3 \times 10^{-4}$
5.5×10^{-3}	$0.081 \pm 1 \times 10^{-3}$
0.010	$0.148 \pm 3 \times 10^{-3}$
0.020	$0.322 \pm 4 \times 10^{-3}$
0.030	$0.562 \pm 9 \times 10^{-3}$

Scheme 5.2 shows the reaction of aniline with aqueous iodine solution. This may be expressed in terms of the rate equation given in Equation 5.1, where $[I_2]_\tau$ is the sum of $[I_2]$ plus $[I_3^-]$ and k_2 is the second order rate constant.

Scheme 5.2:

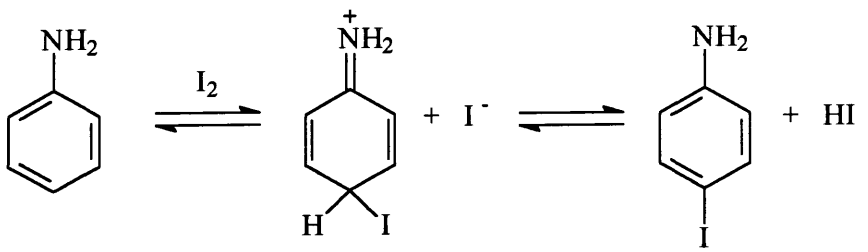

$$-\frac{d[I_2]_\tau}{dt} = k_2[C_6H_5NH_2][I_2]_\tau \qquad \textbf{(5.1)}$$

Since aniline is in large excess, its concentration will remain essentially constant during the reaction. This leads to Equations 5.2 and 5.3, where k_{obs} is the observed first order rate constant.

$$-\frac{d[I_2]_\tau}{dt} = k_{obs}[I_2]_\tau \qquad \textbf{(5.2)}$$

$$k_{obs} = k_2[C_6H_5NH_2] \qquad \textbf{(5.3)}$$

Allowance must be made for the protonation of aniline which has a pK_a value[2] of 4.60: it is expected that only the unprotonated aniline will react. The acid dissociation constant, K_a, is given in Equation 5.4.

$$K_a = \frac{[C_6H_5NH_2][H^+]}{[C_6H_5NH_3^+]} \qquad (5.4)$$

The stoichiometric concentration of aniline is equal to the sum of the concentrations of free base and protonated aniline (Equation 5.5).

$$[\text{aniline}]_{\text{stoich}} = [C_6H_5NH_2] + [C_6H_5NH_3^+] \qquad (5.5)$$

Therefore the concentration of free aniline is given by Equation 5.6.

$$[C_6H_5NH_2] = [\text{aniline}]_{\text{stoich}} \cdot \frac{K_a}{K_a + [H^+]} \qquad (5.6)$$

Re-writing Equation 5.3 in terms of $[\text{aniline}]_{\text{stoich}}$ and rearranging for k_2 gives:

$$k_2 = \frac{k_{obs}}{[\text{aniline}]_{\text{stoich}}} \cdot \frac{K_a + [H^+]}{K_a} \qquad (5.7)$$

Therefore values of the second order rate constant, k_2 / $dm^3\ mol^{-1}\ s^{-1}$, for the reaction of aniline with aqueous iodine solution can be calculated. Table 5.26 shows the values calculated using the results in Table 5.25.

Table 5.26: k_2 / $dm^3\ mol^{-1}\ s^{-1}$ values for the reaction of aniline with aqueous iodine solution, 25 °C

$[C_6H_5NH_2]$ / M	k_2 / $dm^3\ mol^{-1}\ s^{-1}$
1.1×10^{-3}	39 ± 1
5.5×10^{-3}	21 ± 1
0.010	21 ± 1
0.020	23 ± 1
0.030	26 ± 1

These values give an average second order rate constant, k_2, for the reaction of aniline with aqueous iodine solution of 26 ± 8 dm^3 mol^{-1} s^{-1}.

This reaction involves electrophilic substitution by the iodine on aniline. The first step is electrophilic attack by the iodine and the second step involves deprotonation of the intermediate. It is likely that, as is usual with electrophilic aromatic substitution, the first step will be rate limiting.[5] Hence k_2 refers to this step. This reaction is peripheral to the work described and therefore was not investigated further.

5.2.4.2 Reaction of $C_6H_5NHCH_2SO_3^-$ with aqueous iodine solution

One of the steps in the formation of the 1 : 1 adduct $C_6H_5NHCH_2SO_3^-$ is likely to be addition of sulfite to the iminium ion, $C_6H_5\overset{+}{N}H{=}CH_2$. The kinetics of the reverse process was examined by initially forming $C_6H_5NHCH_2SO_3^-$ and following its decomposition by reacting liberated bisulfite / sulfite ions with aqueous iodine solution. The reaction of bisulfite / sulfite ions with aqueous iodine solution has been studied here (Chapter 4, Section 4.2.1): the results indicate that the decolourisation of iodine by aqueous sodium sulfite solution is a very rapid reaction.

If the reaction of $C_6H_5NHCH_2SO_3^-$ with aqueous iodine solution is written in terms of Scheme 5.3, where S(IV) is the sum contribution from both sulfite and bisulfite ions and $[I_2]_\tau$ is the sum of $[I_2]$ plus $[I_3^-]$, then the rate expression for the reaction can be derived as shown below (Equations 5.8 and 5.9).

Scheme 5.3: $C_6H_5NHCH_2SO_3^- \underset{k_f}{\overset{k_b}{\rightleftharpoons}} C_6H_5\overset{+}{N}H{=}CH_2 + S(IV) \xrightarrow[k]{\text{iodine}_{(aq)}}$ products

Assuming S(IV) is a steady state intermediate:

$$[S(IV)] = \frac{k_b[C_6H_5NHCH_2SO_3^-]}{k_f[C_6H_5\overset{+}{N}H{=}CH_2] + k[I_2]_\tau} \qquad \textbf{(5.8)}$$

$$-\frac{d[I_2]_\tau}{dt} = \frac{kk_b[C_6H_5NHCH_2SO_3^-][I_2]_\tau}{k_f[C_6H_5\overset{+}{N}H{=}CH_2] + k[I_2]_\tau} \qquad \textbf{(5.9)}$$

The equilibrium concentration of $C_6H_5N^+H{=}CH_2$ is likely to be very low since it can rapidly deprotonate or hydrate to form *N*-(hydroxymethyl)aniline, $C_6H_5NHCH_2OH$. Therefore it is expected that the dominant term in the denominator of Equation 5.9 will be $k[I_2]_\tau$. For comparison, Le Hénaff[1] obtained a k_f value of 6.8×10^{-5} s^{-1} for the analogous reaction with ammonia at 20 °C. Hence the rate equation reduces to Equation 5.10.

$$-\frac{d[I_2]_\tau}{dt} = k_b[C_6H_5NHCH_2SO_3^-] \qquad \textbf{(5.10)}$$

Therefore the reaction should be zero order with respect to total aqueous iodine solution concentration.

Plots of absorbance against time at 350 nm were obtained for the reaction of 5.0×10^{-3} to 0.024 M $C_6H_5NHCH_2SO_3^-$ with 4×10^{-4} M aqueous iodine solution at 25 °C in the pH range 4.1 to 5.2. A stock solution of $C_6H_5NHCH_2SO_3^-$ was prepared by reacting 0.21 M aniline with 0.20 M $CH_2(OH)(SO_3Na)$ and allowing the solution to stand for 19 to 20 hours prior to use.

Although zero order kinetics were expected, first order decomposition was actually observed (Figure 5.17). The plots were fitted using a single exponential equation to obtain k_{obs} / s^{-1} values (Table 5.27). As aqueous iodine solution has an extinction coefficient of 13400 ± 300 mol^{-1} dm^3 cm^{-1} at 350 nm, the initial absorbances were above the limit of the instrument. Therefore when the plots were fitted, the initial data with an absorbance above 2 absorbance units was not included.

Figure 5.17: Absorbance against time plot at 350 nm with single exponential fit superimposed for the reaction of 0.010 M $C_6H_5NHCH_2SO_3^-$ with 4×10^{-4} M aqueous iodine solution at pH 5.0, 25 °C

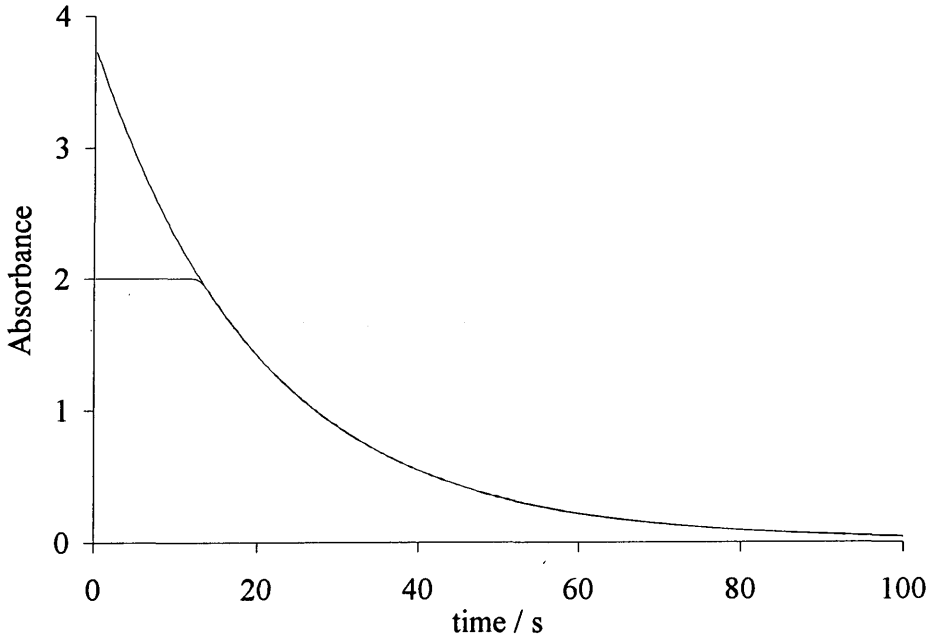

Table 5.27: k_{obs} / s^{-1} values for the reaction of $C_6H_5NHCH_2SO_3^-$ with 4×10^{-4} M aqueous iodine solution at 25 °C, pH 4.1 to 5.2

pH	$[C_6H_5NHCH_2SO_3^-]$ / M	k_{obs} / s^{-1}
4.1	0.020	$0.064 \pm 2 \times 10^{-3}$
4.3	0.020	$0.075 \pm 7 \times 10^{-4}$
4.6	0.020	$0.088 \pm 2 \times 10^{-3}$
5.0	5.0×10^{-3}	$0.024 \pm 9 \times 10^{-4}$
5.0	0.010	$0.049 \pm 7 \times 10^{-4}$
5.0	0.020	$0.106 \pm 1 \times 10^{-3}$
5.0	0.024	$0.130 \pm 9 \times 10^{-4}$
5.2	0.020	$0.145 \pm 1 \times 10^{-3}$

k_{obs} / s^{-1} increases linearly with increasing concentration and increases as the pH increases. However, as first order rather than zero order kinetics are obtained it is apparent that the reaction being followed is not that of aqueous iodine solution with

bisulfite / sulfite ions liberated from the decomposition of $C_6H_5NHCH_2SO_3^-$ if the rate expression given in Equation 5.10 is correct.

An alternative is that the results obtained are primarily due to the reaction of aqueous iodine solution with unreacted aniline present in solution. This was shown here to be a fast reaction and therefore any aniline present will compete with the sulfite / bisulfite in the reaction with aqueous iodine solution. This would account for the first order plots obtained rather than the zero order plots expected. It would also explain the dependence on pH: the pK_a of aniline is 4.60 therefore as the pH increases from pH 4.1 to 5.2 more of the reactive unprotonated aniline will be present. To investigate this theory, the reaction of iodine with $C_6H_5NHCH_2SO_3^-$ was studied where $C_6H_5NHCH_2SO_3^-$ was prepared initially with aniline in great excess: 0.21 M aniline and 0.08 M $CH_2(OH)(SO_3Na)$ was used. In this situation, when the stock $C_6H_5NHCH_2SO_3^-$ solution is diluted, residual aniline will be present. If it is assumed that the $CH_2(OH)(SO_3Na)$ reacts quantitatively, as is found in ^1H NMR spectroscopy, then the concentration of residual aniline present can be calculated.

Plots of absorbance against time at 350 nm were obtained for the reaction of 2.0×10^{-3} to 0.011 M $C_6H_5NHCH_2SO_3^-$ in the presence of 3.3×10^{-3} to 0.018 M residual aniline at 25 °C, pH 5.1. First order plots were obtained and fitted using a single exponential equation to obtain k_{obs} / s^{-1} values (Table 5.28).

Table 5.28: k_{obs} / s^{-1} values for the reaction of $C_6H_5NHCH_2SO_3^-$ and 4×10^{-4} M aqueous iodine solution in the presence of residual aniline, 25 °C, pH 5.1

$[C_6H_5NHCH_2SO_3^-]$ / M	[residual $C_6H_5NH_2$] / M	k_{obs} / s^{-1}
2.0×10^{-3}	3.3×10^{-3}	$0.028 \pm 3 \times 10^{-4}$
4.0×10^{-3}	6.5×10^{-3}	$0.063 \pm 1 \times 10^{-3}$
8.0×10^{-3}	0.013	$0.154 \pm 2 \times 10^{-3}$
0.011	0.018	$0.259 \pm 5 \times 10^{-3}$

These rate constants agree reasonably with the results obtained for the reaction of aniline with aqueous iodine solution (Table 5.25) which leads to the conclusion that this is in fact the reaction observed, at least primarily, rather than the reaction of aqueous iodine solution with bisulfite / sulfite ions liberated from the decomposition of $C_6H_5NHCH_2SO_3^-$. Therefore it is not possible to follow the decomposition of $C_6H_5NHCH_2SO_3^-$ using this method.

5.3 CONCLUSION

5.3.1 Summary

The reaction of aniline and 4-methylaniline with $CH_2(OH)(SO_3Na)$ was investigated using ^1H NMR spectroscopy. In both cases there was evidence of 1 : 1 adduct formation, producing $C_6H_5NHCH_2SO_3^-$ and $4\text{-}CH_3C_6H_4NHCH_2SO_3^-$ respectively. Formation of the product is favourable: there is complete conversion of the minor reaction component to the product. The chemical shifts of the product species in D_2O, or 95 % D_2O / 5 % CD_3OD in the case of 4-methylaniline, are outlined in Scheme 5.4 along with those of the parent compounds. The exchangeable $-NH_2$ protons will be included under the D_2O solvent peak at δ 4.67 ppm.

Scheme 5.4:

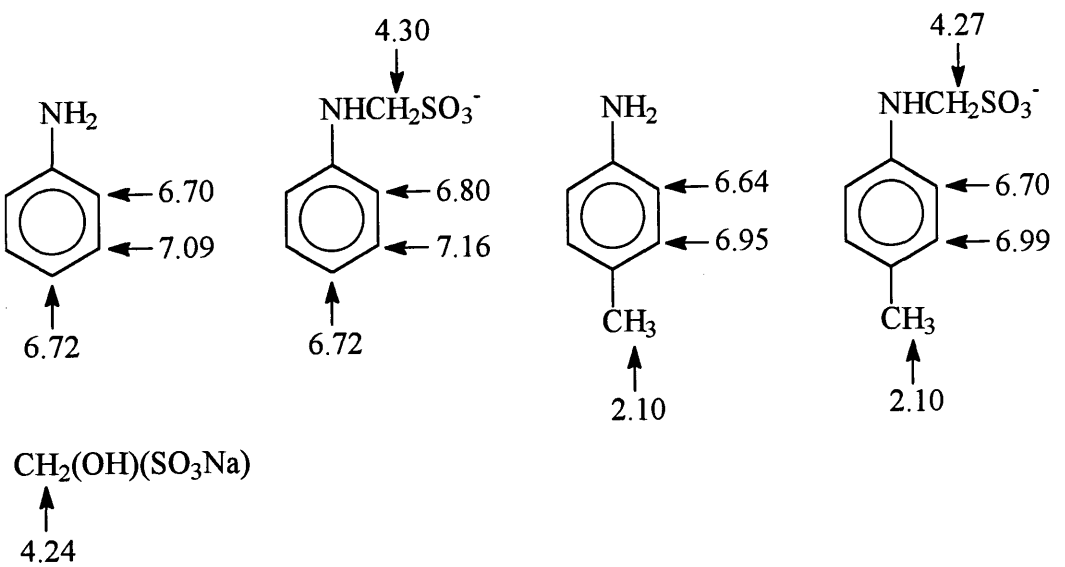

When $CH_2(OH)(SO_3Na)$ was present in excess, peaks due to the $-CH_2-$ groups in $CH_2(OH)(SO_3Na)$ and the product were approximately equal in intensity which corresponds to one equivalent of $CH_2(OH)(SO_3Na)$ reacting with the amine and one equivalent staying in solution. There was no evidence of 1 : 2 adduct formation, $RN(CH_2SO_3^-)_2$, for either amine. The presence of the electron withdrawing group $-CH_2SO_3^-$ will make the nitrogen less nucleophilic than in the parent compound so reducing the tendency for reaction with a second $CH_2(OH)(SO_3Na)$ molecule.

Le Hénaff [1] observed the 1 : 2 adduct $NH(CH_2SO_3^-)_2$ as well as the 1 : 1 adduct $NH_2CH_2SO_3^-$ in the reaction with ammonia and also suggests that formation of $N(CH_2SO_3^-)_3$ may be possible.

From ^1H NMR measurements it can be seen that formation of the product of reaction with 4-methylaniline is faster than that with aniline. The 4-CH_3 group is electron donating so the nitrogen in 4-methylaniline will be a better nucleophile than that in aniline. Hence the forward reaction will be faster with 4-methylaniline.

The reaction of aniline, 4-methylaniline and 4-dimethylaminoaniline with $CH_2(OH)(SO_3Na)$ was investigated using uv / vis spectroscopy. The rate and equilibrium constants determined in this study are summarised in Table 5.29. The equilibrium constant, K, is equal to k_f / k_b.

Table 5.29: Rate and equilibrium constants obtained at 25 °C

amine	k_f / dm^3 mol^{-1} s^{-1}	k_b / s^{-1}	K / dm^3 mol^{-1}
aniline	$7.8 \times 10^{-3} \pm 2 \times 10^{-5}$	$1.0 \times 10^{-5} \pm 8 \times 10^{-7}$	780 ± 60
4-methylaniline	$4.9 \times 10^{-2} \pm 6 \times 10^{-5}$	$1.2 \times 10^{-4} \pm 3 \times 10^{-6}$	410 ± 10

From uv / vis spectroscopy it can be seen that formation of the product of reaction with 4-dimethylaminoaniline is faster than that with 4-methylaniline, which is faster than that with aniline. The reaction of amine with formaldehyde involves nucleophilic attack of the amine on the carbonyl group. Therefore the relative reactivities of the amines can be rationalised according to their pK_a values which are 6.59, 5.08 and 4.60 for 4-dimethylaminoaniline, 4-methylaniline, and aniline respectively.

Le Hénaff[1] quotes values for the equilibrium constants, K and K' (Equations 5.11 and 5.12), for the formation of the 1 : 1 and 1 : 2 adducts from ammonia at 20 °C equal to 735 and 385 dm^3 mol^{-1} respectively.

$$K = \frac{[NH_2CH_2SO_3^-]}{[NH_3][CH_2(OH)(SO_3^-)]} \qquad (5.11)$$

$$K' = \frac{[NH(CH_2SO_3^-)_2]}{[NH_2CH_2SO_3^-][CH_2(OH)(SO_3^-)]} \qquad (5.12)$$

The value obtained here for the formation of the 1 : 1 aniline adduct is similar to that for the equilibrium constant, K, obtained by Le Hénaff for the analogous reaction with ammonia. The value obtained for 4-methylaniline is lower as the back reaction is more favourable for this amine.

The reaction in the presence of added sulfite ions was investigated: the rate of reaction was considerably slower in the presence of added sulfite ions and in most cases the observed rate constant showed an inverse dependence on sulfite ion concentration. Le Hénaff[1] states that the analogous reaction with ammonia is also greatly retarded by the presence of free sulfite.

The reaction of hydroxymethanesulfonate, $CH_2(OH)(SO_3Na)$, with amines proceeds initially via dissociation of the hydroxymethanesulfonate to give free formaldehyde, the reactive species, and either sulfite or bisulfite ions depending on the pH of the system (Chapter 4). Free formaldehyde then reacts with the amine via nucleophilic attack of the nitrogen lone pair of electrons on the carbonyl carbon in formaldehyde to produce an *N*-(hydroxymethyl)amine (Chapter 2). This reaction will be in competition with the reaction of free formaldehyde with sulfite / bisulfite ions to regenerate the hydroxymethanesulfonate. Therefore in the presence of added sulfite ions, the rate of formation of the product, $RNHCH_2SO_3^-$, will decrease as more free formaldehyde will react with sulfite ions to give unreactive $CH_2(OH)(SO_3Na)$ and less free formaldehyde will be present to react with the amine. The *N*-(hydroxymethyl)amine formed dehydrates in acid conditions or loses hydroxyl ion to give an iminium ion which then reacts with sulfite ions to give the product, $RNHCH_2SO_3^-$.

The kinetics of the reaction of aniline with aqueous iodine solution was investigated. A value of 26 ± 8 $dm^3\ mol^{-1}\ s^{-1}$ was obtained for the second order rate constant for the reaction of aniline with aqueous iodine solution at 25 °C at pH 5.0 using a 0.12 M

sodium acetate / 0.05 M acetic acid buffer. Berliner[3] has previously studied the kinetics and found the reaction to be subject to base catalysis. The studies here therefore cannot be directly compared to the work by Berliner as different buffers and experimental conditions were used: Berliner worked in the pH range 5.6 to 7.6 using phosphate buffers.

Attempts to follow the decomposition of the product $C_6H_5NHCH_2SO_3^-$ to the iminium ion $C_6H_5N^+H{=}CH_2$ by adding aqueous iodine solution to react with liberated sulfite / bisulfite ions were unsuccessful. The competing reaction of residual aniline with aqueous iodine solution was found to more favourable and only this process was observed.

5.3.2 Mechanism

Scheme 5.5 shows the likely mechanism for the reaction of $CH_2(OH)(SO_3Na)$ with anilines.

Scheme 5.5:

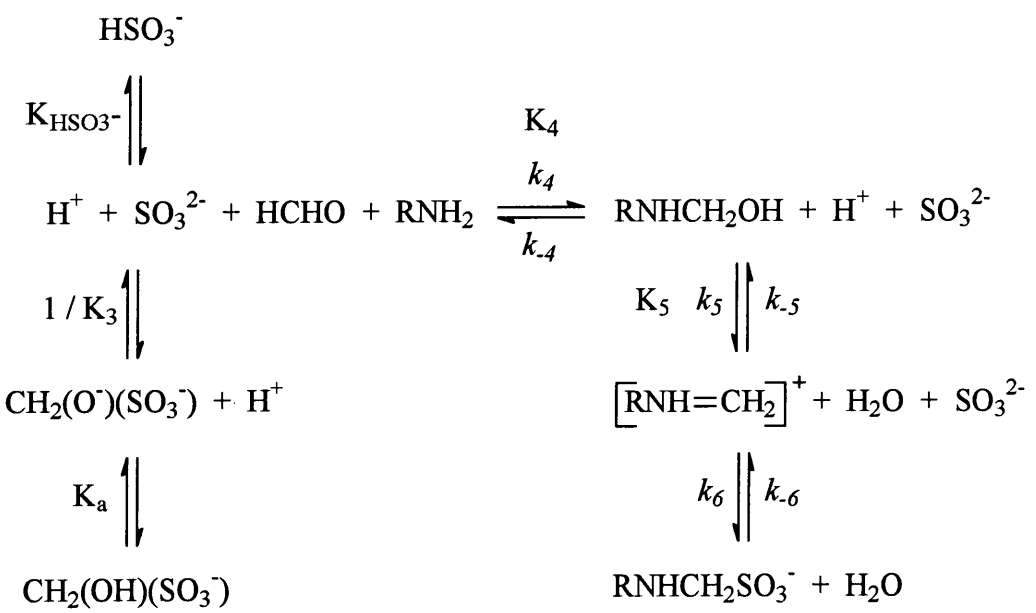

This involves dissociation of $CH_2(OH)(SO_3Na)$ to produce formaldehyde which reacts with the amine to give an *N*-(hydroxymethyl)amine. This is followed by acid catalysed formation of the iminium ion which reacts rapidly with sulfite to give the product. Most

of the kinetic measurements have been made with sufficiently high concentrations of $CH_2(OH)(SO_3Na)$ to ensure that the reaction goes largely to completion. Hence the forward rate term will dominate the observed kinetics. The rate constants obtained show an inverse dependence on added sulfite concentration. They also show a very weak dependence on pH: the results in Table 5.20 show that a change of four pH units causes a less than three-fold change in the value of the rate constant.

The results in Chapter 4 show that under the conditions used here the decomposition of $CH_2(OH)(SO_3Na)$ to give free formaldehyde, HCHO, will be a rapid equilibrium. The rate constant for reaction of HCHO with sulfite ions is around[6] 1×10^7 mol^{-1} dm^3 s^{-1}. The rate constant for formaldehyde hydration is approximately[7] 10 s^{-1} and the rate constant for reaction with aniline is 1.5×10^4 dm^3 mol^{-1} s^{-1} (Chapter 2). Therefore using an aniline concentration of 10^{-4} mol dm^{-3}, the reaction of HCHO with water or with amine will not compete with the reaction with sulfite when $[SO_3^{2-}] \geq 10^{-5}$ dm^3 mol^{-1}. Therefore HCHO is effectively a steady state intermediate in equilibrium with $CH_2(OH)(SO_3^-)$.

It is expected that the reaction of the iminium ion $[RNH{=}CH_2]^+$ with SO_3^{2-} is rapid, probably diffusion controlled, as iminium ions are generally unstable. The iminium ion has the potential of also reacting with aqueous amine or water present in the system (Chapter 1, Section 1.3.4) but these reactions will not be competing here as the reaction with sulfite is so rapid. For comparison, Eldin and Jencks[8] have studied the reaction of iminium ions with RS^- as the nucleophile and state the reaction is diffusion controlled with a rate constant of 10^9 dm^3 mol^{-1} s^{-1}.

Therefore the rate determining step in Scheme 5.5 is likely to be either the reaction of HCHO with RNH_2 (Case 1) or dehydration of the *N*-(hydroxymethyl)amine $RNHCH_2OH$ to give the iminium ion (Case 2). Both of these cases will be considered in turn.

Case 1: The reaction of HCHO with RNH_2 is rate limiting

In this case, the assumption is that k_4 is rate limiting. Therefore the overall rate equation is given by Equation 5.13.

$$\text{rate} = k_4[\text{HCHO}][\text{RNH}_2] \tag{5.13}$$

The concentration of free HCHO can be expressed in terms of $CH_2(OH)(SO_3Na)$ concentration (Equations 5.14 to 5.16).

$$K_a = \frac{[CH_2(O^-)(SO_3^-)][H^+]}{[CH_2(OH)(SO_3^-)]} \tag{5.14}$$

$$K_3 = \frac{[CH_2(O^-)(SO_3^-)]}{[HCHO][SO_3^{2-}]} \tag{5.15}$$

$$\therefore [HCHO] = \frac{K_a[CH_2(OH)(SO_3^-)]}{K_3[H^+][SO_3^{2-}]} \tag{5.16}$$

Sulfite is a better nucleophile than bisulfite and it is likely that reaction will occur predominantly with sulfite. The concentration of free SO_3^{2-} ions can be determined from the stoichiometric concentration of sulfite added (Equations 5.17 to 5.20).

$$K_{HSO3^-} = \frac{[SO_3^{2-}][H^+]}{[HSO_3^-]} \tag{5.17}$$

$$[\text{sulfite}]_{\text{stoich}} = [HSO_3^-] + [SO_3^{2-}] \tag{5.18}$$

$$[\text{sulfite}]_{\text{stoich}} = \frac{[SO_3^{2-}][H^+]}{K_{HSO3^-}} + [SO_3^{2-}] \tag{5.19}$$

$$\therefore [SO_3^{2-}] = \frac{K_{HSO3^-}[\text{sulfite}]_{\text{stoich}}}{[H^+] + K_{HSO3^-}} \tag{5.20}$$

Substituting Equation 5.20 into Equation 5.16 gives the following equations:

$$[HCHO] = \frac{K_a[CH_2(OH)(SO_3^-)]}{K_3[\text{sulfite}]_{\text{stoich}}} \cdot \frac{K_{HSO3^-} + [H^+]}{K_{HSO3^-}[H^+]} \tag{5.21}$$

$$\therefore \text{ rate} = \frac{k_4 K_a[CH_2(OH)(SO_3^-)]}{K_3[\text{sulfite}]_{stoich}} \cdot \frac{K_{HSO3^-} + [H^+]}{K_{HSO3^-}[H^+]} \cdot [RNH_2] \quad \textbf{(5.22)}$$

Under the experimental conditions employed here, $[CH_2(OH)(SO_3^-)] >> [RNH_2]$, so the reaction is pseudo first order and k_{obs}, the observed first order rate constant, is given by Equation 5.23.

$$k_{obs} = \frac{k_4 K_a[CH_2(OH)(SO_3^-)]}{K_3[\text{sulfite}]_{stoich}} \cdot \frac{K_{HSO3^-} + [H^+]}{K_{HSO3^-}[H^+]} \quad \textbf{(5.23)}$$

Equation 5.23 predicts that in solutions where pH < pK_{HSO3^-} the value of k_{obs} should be independent of acidity. Here the equilibrium to produce free formaldehyde is dissociation of $CH_2(OH)(SO_3^-)$ to give bisulfite ions (Scheme 5.6).

Scheme 5.6: $CH_2(OH)(SO_3^-) \rightleftharpoons HCHO + HSO_3^-$

In solutions where pH > pK_{HSO3^-} there should be an inverse dependence of k_{obs} on proton concentration since here the relevant equilibrium is that shown in Scheme 5.7.

Scheme 5.7: $CH_2(OH)(SO_3^-) \rightleftharpoons HCHO + H^+ + SO_3^{2-}$

Values of $k_{obs}[\text{sulfite}]_{stoich}$ / mol dm^{-3} s^{-1} were obtained experimentally. Theoretical values can be calculated by applying Equation 5.23 and using Sørensen and Andersen's[6a] values of $K_a = 2.0 \times 10^{-12}$ mol dm^{-3} and $K_3 = 2.2 \times 10^5$ mol^{-1} dm^3, along with a K_{HSO3^-} value[4] of 6.3×10^{-8} mol dm^{-3} and $[CH_2(OH)(SO_3Na)] = 0.10$ mol dm^{-3} under the experimental conditions used. Values of k_4 are reported in Chapter 2: a value of 1.5×10^5 dm^3 mol^{-1} s^{-1} was obtained for aniline and 2.4×10^5 dm^3 mol^{-1} s^{-1} for 4-methylaniline and 4-dimethylaminoaniline.

Table 5.30 summarises the experimental and calculated values obtained for $k_{obs}[\text{sulfite}]_{stoich}$ / mol dm^{-3} s^{-1} for the three amines studied.

Table 5.30: Experimental and calculated k_{obs}[sulfite]$_{stoich}$ / mol dm^{-3} s^{-1} values

amine	pH	k_{obs}[sulfite]$_{stoich}$ / mol dm^{-3} s^{-1}	
		experimental†	calculated
aniline	6	1.2×10^{-6}	2.3×10^{-6}
	7	1.0×10^{-6}	3.5×10^{-6}
	8	6.5×10^{-7}	1.9×10^{-5}
4-methylaniline	6	6.5×10^{-6}	3.6×10^{-6}
	7	1.4×10^{-5}	5.6×10^{-6}
	8	3.2×10^{-6}	2.1×10^{-5}
4-dimethylaminoaniline	6	2.8×10^{-6}	3.6×10^{-6}
	8	4.8×10^{-6}	2.5×10^{-5}

† average value quoted for experiments performed with more than one [sulfite]$_{stoich}$ / M

The values in Table 5.30 show reasonable agreement between the calculated and experimental values at pH 6 and 7. However there is significant deviation at pH 8: the calculated values are considerably greater than the experimental values, indicating the possibility of a change in rate determining step at higher pH from the reaction of HCHO with RNH_2 to dehydration of the *N*-(hydroxymethyl)amine to the iminium ion.

Case 2: Dehydration of the *N*-(hydroxymethyl)amine to the iminium ion is rate limiting

In this case, the assumption is that k_5 is rate limiting. Therefore the overall rate equation is given by Equation 5.24.

$$\text{rate} = k_5[RNHCH_2OH][H^+] \qquad \textbf{(5.24)}$$

The concentration of $RNHCH_2OH$ is related to the concentrations of free HCHO and amine by the equilibrium constant K_4 (Equation 5.25).

$$K_4 = \frac{[RNHCH_2OH]}{[HCHO][RNH_2]} \qquad \textbf{(5.25)}$$

Substituting this into Equation 5.21 gives:

$$\text{rate} = k_5K_4[\text{HCHO}][\text{RNH}_2][\text{H}^+] \qquad \textbf{(5.26)}$$

Substituting Equation 5.24 into Equation 5.26 gives:

$$\text{rate} = \frac{k_5K_4K_a[\text{CH}_2(\text{OH})(\text{SO}_3^-)]}{K_3[\text{sulfite}]_{\text{stoich}}} \cdot \frac{K_{\text{HSO3-}} + [\text{H}^+]}{K_{\text{HSO3-}}} \cdot [\text{RNH}_2] \qquad \textbf{(5.27)}$$

Under the experimental conditions employed here, $[\text{CH}_2(\text{OH})(\text{SO}_3^-)] >> [\text{RNH}_2]$, so the reaction is pseudo first order and k_{obs}, the observed first order rate constant, is given by Equation 5.28.

$$k_{obs} = \frac{k_5K_4K_a[\text{CH}_2(\text{OH})(\text{SO}_3^-)]}{K_3[\text{sulfite}]_{\text{stoich}}} \cdot \frac{K_{\text{HSO3-}} + [\text{H}^+]}{K_{\text{HSO3-}}} \qquad \textbf{(5.28)}$$

K_4 values were determined in Chapter 2: approximately 6×10^4 dm^3 mol^{-1} is obtained for all three amines studied here. Using this value and Sørensen and Andersen's[6a] values of $K_a = 2.0 \times 10^{-12}$ mol dm^{-3} and $K_3 = 2.2 \times 10^5$ mol^{-1} dm^3, along with a $K_{\text{HSO3-}}$ value[4] of 6.3×10^{-8} mol dm^{-3} and $[\text{CH}_2(\text{OH})(\text{SO}_3\text{Na})] = 0.10$ mol dm^{-3}, an average value of k_5 equal to 3.0×10^7 dm^3 mol^{-1} s^{-1} can be calculated using the experimental $k_{obs}[\text{sulfite}]_{\text{stoich}}$ / mol dm^{-3} s^{-1} values in Table 5.30. The value obtained for k_5 is not unreasonable given that Kallen[9] reports a value of 1.4×10^8 dm^3 mol^{-1} s^{-1} for the acid catalysed reaction of the *N*-(hydroxymethyl)amine formed from cysteine and formaldehyde.

To summarise, at low and neutral pH the rate determining step is likely to be the reaction of HCHO with RNH_2. At higher pH the rate determining step becomes dehydration of the *N*-(hydroxymethyl)amine to the iminium ion: this is an acid catalysed reaction and therefore at high pH can become rate limiting. At pH values where pH > $\text{pK}_{\text{HSO3-}}$, the steps preceding k_5 show an inverse dependence on proton concentration. Therefore when k_5, the acid catalysed step, becomes rate determining the experimentally observed rate constant, k_{obs}, is predicted to remain independent of acidity.

5.4 EXPERIMENTAL

5.4.1 ^{1}H NMR experiments

The reactions of aniline and of 4-methylaniline with $CH_2(OH)(SO_3Na)$ were followed using ^{1}H NMR spectroscopy. Initially the spectrum of 0.20 to 0.23 M amine alone was obtained, then the spectrum in the presence of equimolar $CH_2(OH)(SO_3Na)$ (0.2 M each), then with each reagent in excess (0.2 M amine with 0.4 or 0.1 M $CH_2(OH)(SO_3Na)$). The solutions were made immediately prior to use. The amine was placed in the NMR tube: neat aniline was used, however 4-methylaniline is a solid which is not readily soluble in aqueous solution therefore a stock solution in methyl-d_3 alcohol-d, CD_3OD, was prepared. 1 cm^3 D_2O was then added to the NMR tube followed by the $CH_2(OH)(SO_3Na)$ which was added at the NMR machine side. The ^{1}H NMR spectrum of 0.20 M $CH_2(OH)(SO_3Na)$ in D_2O was also obtained for comparison.

Spectra were recorded immediately (3 to 5 minutes) after mixing, then 30 minutes, 1 hour and 2 or 5 hours after mixing and continued until there was no further change in the spectrum. The time of mixing refers to the time at which $CH_2(OH)(SO_3Na)$ was added to the NMR tube. The time of each spectrum was taken as the time when the spectrometer started to acquire the spectrum.

4-Methylaniline is not readily soluble in aqueous solution at the concentrations required. Therefore the solubility in different solvents was tested. 4-Methylaniline was found to dissolve in acetonitrile but when water was added the solution was not miscible. 4-Methylaniline was also found to dissolve readily in methanol. Therefore a stock solution in CD_3OD was prepared. A 5 % CD_3OD / 95 % water by volume solvent was used for the ^{1}H NMR: a high D_2O content was used so that the spectra could be compared with those of aniline in D_2O and with the uv / vis spectra carried out in aqueous solution. The ^{1}H NMR spectrum of CHD_2OD is characterised by a quintet at δ 3.35 ppm. However it was not visible in any spectra as it was present in too small a proportion.

When D_2O was added to the stock solution of 4-methylaniline in CD_3OD, oil globules formed and the solution froze easily. However when heated under the tap the solution

became homogeneous with no oil globules. The solution was also heated under the tap if the solution froze between recording spectra.

^{1}H NMR spectra were recorded using a 200 MHz Varian Mercury - 200 spectrometer. The δ 4.67 ppm singlet due to residual protons in the deuterated solvent, D_2O, was used for locking purposes and as the reference peak for all spectra. Chemical shifts are quoted to 2 decimal places. Coupling constants are given where the multiplicity is greater than a singlet and are quoted to the nearest whole number.

It was not possible to follow the reaction of 4-dimethylaminoaniline using ^{1}H NMR spectroscopy in a solvent composed mainly of D_2O: 4-dimethylaminoaniline is not soluble in aqueous solution. Although soluble in acetonitrile, when a stock solution was prepared in d_3-acetonitrile, CD_3CN, and a 5 % CD_3CN / 95 % water by volume solvent used for the NMR, the peaks were broad and very low in intensity. 4-Dimethylaminoaniline was also found to be fairly soluble in methanol but when a stock solution was made in CD_3OD and a 5 % CD_3OD / 95 % water by volume solvent used in NMR, again the peaks were broad and very low in intensity.

5.4.2 Uv / vis experiments

Absorbance against wavelength spectra were obtained for the reaction of 1.0×10^{-4} M aniline, 4-methylaniline and 4-dimethylaminoaniline with 2.0×10^{-3} to 0.10 M $CH_2(OH)(SO_3Na)$. 4-Methylaniline is soluble in aqueous solution at the concentrations used: lower concentrations were used than for the ^{1}H NMR experiments where a 5 % CD_3OD / 95 % D_2O by volume solvent system was required. 4-Dimethylaminoaniline is not readily soluble in water therefore the ε values calculated may be lower than the true values if the actual concentration of 4-dimethylaminoaniline is lower than expected due to poor solubility.

Spectra were obtained using a UV-2101 PC Shimadzu Corporation or Perkin – Elmer Lambda 2 uv / vis spectrometer at 25 °C with 1 cm stoppered quartz cuvettes, taking scans every 5 or 10 minutes for up to 3 or 4 hours using a scan speed of 480 nm min^{-1}. The cuvettes were left in the spectrometer for at least 10 minutes prior to use to allow

the temperature to equilibrate to 25 °C. Addition of the amine solution was used to initiate the reaction. Extinction coefficients are quoted to 2 or 3 significant figures and were calculated using only one spectrum in most cases.

Plots of absorbance against time were obtained for the reaction of 5.0×10^{-5} or 1.0×10^{-4} M amine with 2.0×10^{-3} to 0.10 M aqueous $CH_2(OH)(SO_3Na)$ at 25 °C. The effect of the presence of added sulfite ions in the system was investigated: the reaction of 1.0×10^{-4} M amine with 0.10 M aqueous $CH_2(OH)(SO_3Na)$ solution in the presence of 1.0×10^{-3} to 0.010 M aqueous sodium sulfite solution was studied at 25 °C.

Plots were recorded using a Perkin – Elmer Lambda 2 or 12 uv / vis spectrometer at 25 °C with 1 cm stoppered quartz cuvettes. The time interval ranged from 30 seconds to 3½ minutes and the overall reaction time from 1½ to 17½ hours depending on the pH and concentrations used. The cuvettes were left in the spectrometer for at least 10 minutes prior to use to allow the temperature to equilibrate at 25 °C. Addition of the amine solution was used to initiate the reaction. The formation of the product was followed at 245 nm when using aniline, 240 nm for 4-methylaniline and 251 or 260 nm for 4-dimethylaminoaniline. 4-Dimethylaminoaniline is not readily soluble in aqueous solution therefore a stock solution in acetonitrile or dioxan was prepared, giving a final solvent composition of 2 % acetonitrile or dioxan / 98 % water by volume. The reaction in 2 % acetonitrile was performed twice: excellent agreement in the results was obtained.

Figure 5.8 includes results from three experiments carried out under identical conditions. As a control, the reaction with 0.10 M $CH_2(OH)(SO_3Na)$ was performed in all three experiments and the reaction with 2.0×10^{-3} M in two experiments. Excellent agreement was obtained: the rate constants for these two concentrations are quoted as an average.

The spectrum of $CH_2(OH)(SO_3Na)$ does not show any significant absorbance in the uv / vis spectrum. However sulfite ions do absorb in this region: spectra of 0.01, 0.05 and 0.10 M aqueous sodium sulfite solution were obtained and showed high absorbance around 250 nm and to shorter wavelength. For example, the extinction coefficient of sulfite ions at 245 nm was found to be 50 $dm^3\ mol^{-1}\ cm^{-1}$. Therefore the appropriate

concentration of sulfite ions was added to the reference in order to subtract the absorbance due to the presence of sulfite from the absorbance against time plots. Where $[sulfite]_{stoich}$ is quoted this refers to the total concentration of aqueous sodium sulfite added externally to the system and does not include the concentration of sulfite ions present in solution due to dissociation of $CH_2(OH)(SO_3Na)$.

First order kinetics were observed and plots were fitted using the PECSS program installed on the Perkin – Elmer Lambda 2 spectrometer or by plotting $\ln(A_\infty - A)$ against time / s using Microsoft Excel and performing linear regression. Correlation coefficients of 0.981 to 0.999 were obtained. Rate constants are quoted to 2 decimal places.

The buffers employed and the corresponding stoichiometric buffer concentrations in the final solutions are shown in Table 5.31. Where buffers were used, the appropriate volume of buffer was also present in the reference cuvette.

Table 5.31: Buffer concentrations, in aqueous solution

amine	pH	component A	$[A]_{stoich}$ / M	component B	$[B]_{stoich}$ / M
aniline	6	KH_2PO_4	0.033	NaOH	4.0×10^{-3}
4-CH_3		KH_2PO_4	0.20	NaOH	0.022
4-$N(CH_3)_2$		KH_2PO_4	0.20	NaOH	0.022
all amines	7	KH_2PO_4	0.033	NaOH	0.020
aniline	8	KH_2PO_4	0.033	NaOH	0.031
4-CH_3		KH_2PO_4	0.20	NaOH	0.19
4-$N(CH_3)_2$		KH_2PO_4	0.20	NaOH	0.19

The pH values of all solutions were determined using a Jenway 3020 pH meter calibrated using pH 7 and pH 10 (for alkaline solutions) or pH 4 (for acidic solutions) buffers. pH values are quoted to one decimal place.

5.4.3 Decomposition of $C_6H_5NHCH_2SO_3^-$

The reaction of 1.1×10^{-3} to 0.030 M aniline with 4×10^{-4} M aqueous iodine solution at pH 5.0 was investigated. The reaction of 5.0×10^{-3} to 0.024 M $C_6H_5NHCH_2SO_3^-$ with 4×10^{-4} M aqueous iodine solution in the pH range 4.1 to 5.2 was investigated. The reaction in the presence of residual iodine was also studied.

Plots of absorbance against time were obtained at 350 nm using an Applied Photophysics DX.17MV BioSequential Stopped – flow ASVD Spectrometer with a 1 cm path length at 24.8 – 25.1 °C. Five or ten averages were obtained, each the average of three runs of 50 to 200 seconds depending on the pH and the concentration of $C_6H_5NHCH_2SO_3^-$ or aniline used. The appropriate aqueous $C_6H_5NHCH_2SO_3^-$ or aniline solution was placed in one syringe and the aqueous iodine solution with the appropriate buffer solution in the other.

In the reaction of $C_6H_5NHCH_2SO_3^-$, it was the intention to follow the zero order disappearance of the aqueous iodine solution but first order disappearance was actually observed. The averages were fitted using the single exponential equation on the !SX.17MV program installed on the spectrometer. All plots showed good first order fits. Rate constants are quoted to three decimal places. As aqueous iodine solution has an extinction coefficient of 13400 ± 300 mol^{-1} dm^3 cm^{-1} at 350 nm, the initial absorbances at the concentrations used were above the limit of the instrument, therefore when the plots were fitted the initial data was not included. Data with an absorbance above 2 absorbance units was not included: fitting was started from the first 1 to 25 seconds of the plot, depending on the pH and the concentration of $C_6H_5NHCH_2SO_3^-$ or aniline used.

The $C_6H_5NHCH_2SO_3^-$ solutions were prepared by mixing 0.21 M aniline and 0.20 M $CH_2(OH)(SO_3Na)$, or 0.08 M $CH_2(OH)(SO_3Na)$ for the experiment in the presence of residual aniline, in water and allowing the solution to stand for 19 to 20 hours prior to use. The solution was then diluted to the appropriate concentration. $C_6H_5NHCH_2SO_3^-$ concentrations are quoted given the assumption that all the $CH_2(OH)(SO_3Na)$ reacted to form the product. The solution was left for a long period of time to ensure reaction completion.

Acetic acid / sodium acetate buffers were used to control the pH. The pK_a value corresponding to the acetate / acetic acid equilibrium[10] is 4.75. Using Equation 5.29, the acetic acid and sodium acetate concentrations required could be calculated for a particular pH using a constant acetic acid stock concentration of 0.15 M for pH values below 5 and a constant sodium acetate stock concentration of 0.36 M at pH 5 and above.

$$pH = pK_a + \log\left(\frac{[salt]}{[acid]}\right) \qquad (5.29)$$

The stoichiometric buffer concentrations present in the final reaction mixtures at each pH are shown in Table 5.32.

Table 5.32: Buffer concentrations, in aqueous solution

pH	$[CH_3COOH]_{stoich}$ / M	$[CH_3COONa]_{stoich}$ / M
4.1	0.54	0.12
4.3	0.27	0.12
4.6	0.13	0.12
5.0	0.05	0.12
5.1	0.025	0.06
5.2	0.05	0.18

A spectrum of aqueous iodine solution in buffer was obtained: no change in the spectrum was observed at the concentrations used.

The pH values of all solutions were determined using a Jenway 3020 pH meter calibrated using pH 7 and pH 4 buffers. pH values are quoted to one decimal place.

5.5 REFERENCES

1. P. Le Hénaff, *Compt. Rend. Acad. Sci.*, 1963, **256**, 3090

2. D. D. Perrin, 'Dissociation constants of organic bases in aqueous solution', Butterworths, London, 1965 and 1972 Supplement

3. E. Berliner, *J. Am. Chem. Soc.*, 1950, **72**, 4003

4. (a) E. Hayon, A. Treinin and J. Wilf, *J. Am. Chem. Soc.*, 1972, **94**, 47; (b) H. V. Tartar and H. H. Garretson, *J. Am. Chem. Soc.*, 1941, **63**, 808

5. J. March, 'Advanced Organic Chemistry', Wiley - Interscience, New York, 1992, 4th Ed., pp. 501

6. (a) P. E. Sørensen and V. S. Andersen, *Acta Chem. Scand.*, 1970, **24**, 1301; (b) S. D. Boyce and M. R. Hoffmann, *J. Phys. Chem.*, 1984, **88**, 4740

7. R. P. Bell and P. G. Evans, *Proc. Roy. Soc. London*, 1966, **291A**, 297

8. (a) S. Eldin and W. P. Jencks, *J. Am. Chem. Soc.*, 1995, **117**, 4851; (b) S. Eldin, J. A. Digits, S.-T. Huang and W. P. Jencks, *ibid.*, 6631

9. R. G. Kallen, *J. Am. Chem. Soc.*, 1971, **93**, 6236

10. 'CRC Handbook of Chemistry and Physics', CRC Press, Florida, 1982, 63rd Ed., D171

CHAPTER 6

Reaction of hydroxymethanesulfonate, $CH_2(OH)(SO_3Na)$, with benzylamine and benzylamine derivatives

CHAPTER 6: Reaction of hydroxymethanesulfonate, $CH_2(OH)(SO_3Na)$, with benzylamine and benzylamine derivatives

6.1 INTRODUCTION

There have been no studies reported in the literature on the reaction of hydroxymethanesulfonate, $CH_2(OH)(SO_3Na)$, with benzylamine and benzylamine derivatives. The reaction of $CH_2(OH)(SO_3Na)$ with benzylamine and four benzylamine derivatives was therefore investigated here using ^1H NMR and uv / vis spectroscopy to gain a better understanding of the reaction kinetics and mechanism. The effect of the presence of added sulfite ions in the system was also investigated.

The amines studied are shown in Table 6.1. This range of benzylamines was chosen to enable investigation of the effects of pK_a, the presence of electron donating and withdrawing groups and the effect of substitution on the amino nitrogen.

Table 6.1: Amines† studied in the reaction with $CH_2(OH)(SO_3Na)$

amine		pK_a	amine		pK_a
benzylamine	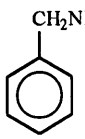 **6.1**	9.33	4-nitrobenzylamine	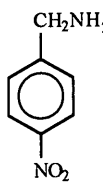 **6.4**	8.50
4-methoxybenzylamine	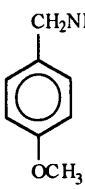 **6.2**	9.51	*N*-methylbenzylamine§	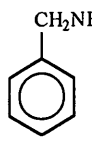 **6.5**	9.59
4-methylbenzylamine	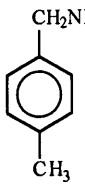 **6.3**	9.54			

† pK_a values correspond to dissociation of the protonated amines, 25 °C, reference 1

§ also known as *N*-benzylmethylamine

The reaction has been studied in the pH range 5 to 10 using uv / vis spectroscopy. The benzylamines used have pK_a values in the range 8.50 to 9.59 so will be extensively protonated under these conditions. Since the reaction is likely to involve the free amine, protonation will substantially reduce the observed reactivity.

The acid dissociation constant of a benzylamine with the general formula $RC_6H_4CH_2NHR'$ is defined by Scheme 6.1 and Equation 6.1.

Scheme 6.1:

$$RC_6H_4CH_2\overset{+}{N}H_2R' \underset{}{\overset{K_{a(amine)}}{\rightleftharpoons}} RC_6H_4CH_2NHR' + H^+$$

$$K_{a(amine)} = \frac{[RC_6H_4CH_2NHR'][H^+]}{[RC_6H_4CH_2\overset{+}{N}H_2R']} \qquad \textbf{(6.1)}$$

The stoichiometric concentration of benzylamine is equal to the sum of the concentrations of the unprotonated and protonated forms (Equation 6.2).

$$[RC_6H_4CH_2NHR']_{stoich} = [RC_6H_4CH_2NHR'] + [RC_6H_4CH_2\overset{+}{N}H_2R'] \qquad \textbf{(6.2)}$$

Substituting Equation 6.1 into Equation 6.2 and rearranging gives:

$$[RC_6H_4CH_2NHR'] = [RC_6H_4CH_2NHR']_{stoich} \cdot \frac{K_{a(amine)}}{K_{a(amine)} + [H^+]} \qquad \textbf{(6.3)}$$

The uv / vis spectroscopy studies described here show the formation of $RC_6H_4CH_2NHCH_2SO_3^-$ products from benzylamines and $CH_2(OH)(SO_3Na)$. The observed rate constant, k_{obs} / s^{-1}, refers to the overall rate constant for the formation of $RC_6H_4CH_2NHCH_2SO_3^-$, shown in Scheme 6.2.

Scheme 6.2:

$$RC_6H_4CH_2NHR' + CH_2(OH)(SO_3^-) \underset{k_b}{\overset{k_f}{\rightleftharpoons}} RC_6H_4CH_2NHCH_2SO_3^- + H_2O$$

The equilibrium constant, K, for this process is equal to:

$$K = \frac{k_f}{k_b} = \frac{[RC_6H_4CH_2NHCH_2SO_3^-]}{[RC_6H_4CH_2NHR'][CH_2(OH)(SO_3^-)]} \quad \textbf{(6.4)}$$

If measurements are made in terms of the stoichiometric amine concentration as opposed to reactive free amine then the values obtained for the apparent equilibrium constant, $K_{(app)}$, and forward rate constant, $k_{f(app)}$, will be lower than the true values as indicated by Equations 6.3 to 6.5.

$$K_{(app)} = \frac{k_{f(app)}}{k_b} = \frac{[RC_6H_4CH_2NHCH_2SO_3^-]}{[RC_6H_4CH_2NHR']_{stoich}[CH_2(OH)(SO_3^-)]} \quad \textbf{(6.5)}$$

$$K = K_{(app)} \cdot \frac{K_{a(amine)} + [H^+]}{K_{a(amine)}} \quad \textbf{(6.6)}$$

$$k_f = k_{f(app)} \cdot \frac{K_{a(amine)} + [H^+]}{K_{a(amine)}} \quad \textbf{(6.7)}$$

The pK_a values for nitrogen protonation of the product, $RC_6H_4CH_2NHCH_2SO_3^-$, are lower than 6 (Chapter 7, Section 7.2.2.5). Therefore these species will not be affected by protonation of the nitrogen in the pH range studied.

6.2 RESULTS AND DISCUSSION

6.2.1 Reaction of $CH_2(OH)(SO_3Na)$ with benzylamine

6.2.1.1 ^1H NMR studies

Initially the spectra of the starting materials, benzylamine and $CH_2(OH)(SO_3Na)$, were obtained for comparison. The ^1H NMR of 0.20 M $CH_2(OH)(SO_3Na)$ in D_2O is described in Chapter 5, Section 5.2.1.1, Figure 5.1 and Table 5.2. Figure 6.1 and Table 6.2 describe the ^1H NMR spectrum of 0.20 M benzylamine (**6.1**) in D_2O.

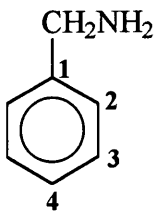

6.1

Figure 6.1: ^1H NMR spectrum of benzylamine in D_2O

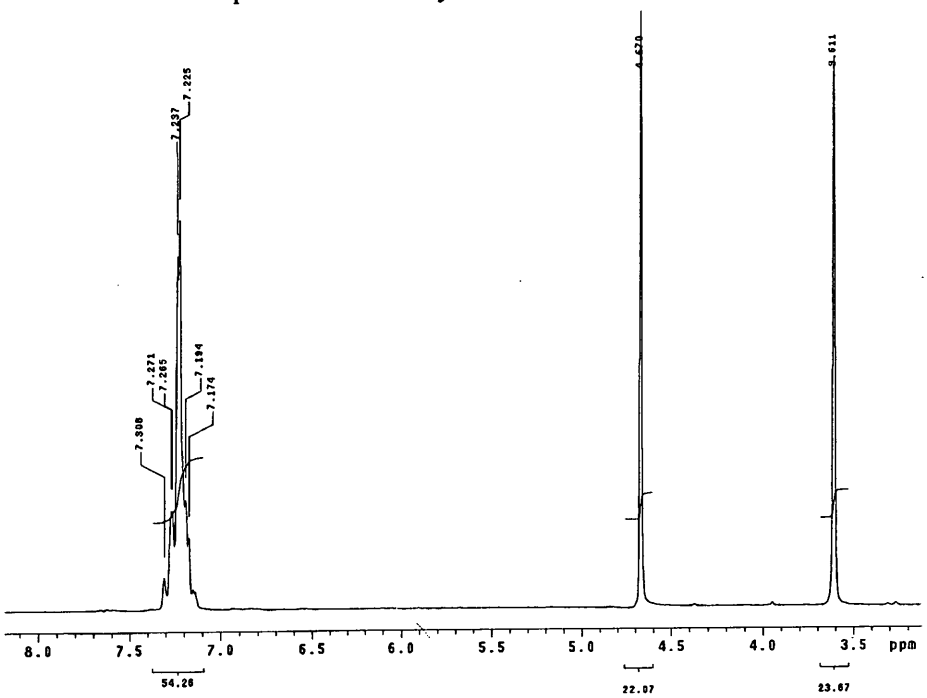

Table 6.2: ^1H NMR spectrum of benzylamine in D_2O: peak assignments

δ / ppm	integral ratio	multiplicity	J / Hz	assignment
3.61	2	s	-	$-CH_2NH_2$
4.67	-	-	-	D_2O
7.23	5	m	-	Ar-H2, H3, H4

The spectrum of 0.20 M benzylamine and 0.20 M $CH_2(OH)(SO_3Na)$ was obtained, then with each reagent in excess: 0.20 M benzylamine with 0.40 M $CH_2(OH)(SO_3Na)$ and 0.21 M benzylamine with 0.10 M $CH_2(OH)(SO_3Na)$. A spectrum was recorded immediately (2 to 5 minutes) after addition of the $CH_2(OH)(SO_3Na)$, then again after approximately 15 minutes, 30 minutes, 1 hour and 5 hours, and continued until there was no further change in the spectrum.

There are two possible products that may form in the reaction. Firstly, a 1 : 1 benzylamine : $CH_2(OH)(SO_3Na)$ adduct $C_6H_5CH_2NHCH_2SO_3^-$, **6.6**, can form. In the presence of excess $CH_2(OH)(SO_3Na)$, a second molecule may react to give a 1 : 2 benzylamine : $CH_2(OH)(SO_3Na)$ adduct, $C_6H_5CH_2N(CH_2SO_3^-)_2$, **6.7**.

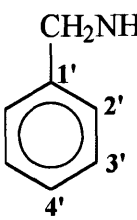

6.6

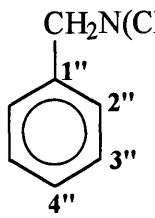

6.7

6.2.1.1.1 Equimolar benzylamine and $CH_2(OH)(SO_3Na)$

The results obtained for the reaction of equimolar 0.20 M benzylamine and $CH_2(OH)(SO_3Na)$ are shown in Figures 6.2 and 6.3 which show the spectra obtained 5 minutes and 32 minutes after mixing respectively. There was no further change in the spectrum over time. Tables 6.3 and 6.4 summarise the information obtained from the two spectra.

Table 6.3: Peak assignments: 5 minutes after mixing

time after mixing	δ / ppm	integral ratio	multiplicity	J / Hz	assignment
5 minutes	3.70	2	s	-	$-CH_2NHCH_2SO_3^-$
	3.90	2	s	-	$-NHCH_2SO_3^-$
	4.67	-	-	-	D_2O, $-NH_2$
	7.30	5	m	-	Ar-**H2'**, **H3'**, **H4'**

Figure 6.2: 0.20 M benzylamine and 0.20 M $CH_2(OH)(SO_3Na)$: 5 minutes after mixing

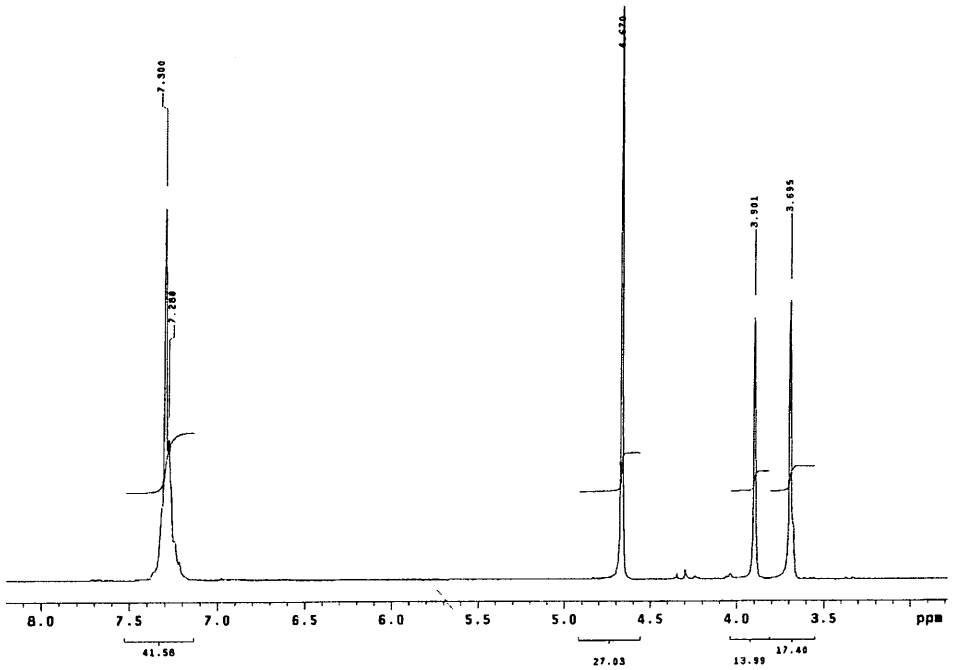

Figure 6.3: 0.20 M benzylamine and 0.20 M $CH_2(OH)(SO_3Na)$: 32 mins after mixing

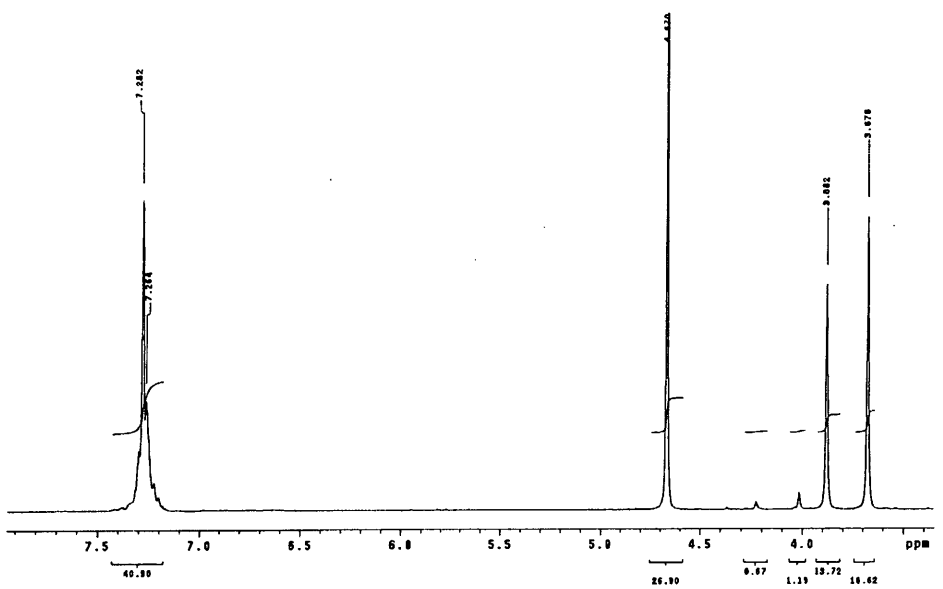

Table 6.4: Peak assignments: 32 minutes after mixing

time after mixing	δ / ppm	integral ratio	multiplicity	J / Hz	assignment
32 minutes	3.68	2	s	-	$-CH_2NHCH_2SO_3^-$
	3.88	2	s	-	$-NHCH_2SO_3^-$
	4.02	-	s	-	$-N(CH_2SO_3^-)_2$
	4.23	-	s	-	$-CH_2N(CH_2SO_3^-)_2$
	4.67	-	-	-	D_2O, $-NH_2$
	7.28	5	m	-	Ar-**H2'**, **H3'**, **H4'**

Peaks due to the reactants have disappeared within 5 minutes: new peaks in the spectrum at δ 3.7 and 3.9 ppm indicate complete conversion of the reactants to the 1 : 1 adduct $C_6H_5CH_2NHCH_2SO_3^-$. There is a visible change in the peaks in the aromatic region: peaks due to the 1 : 1 adduct $C_6H_5CH_2NHCH_2SO_3^-$ appear at a higher frequency than those due to the parent compound, benzylamine. After 32 minutes the spectrum shows the presence of a small amount of the 1 : 2 adduct $C_6H_5CH_2N(CH_2SO_3^-)_2$ with small peaks at δ 4.02 and 4.23 ppm with a 2 : 1 intensity ratio. The major product of the reaction is still the 1 : 1 adduct $C_6H_5CH_2NHCH_2SO_3^-$.

6.2.1.1.2 $CH_2(OH)(SO_3Na)$ in excess

The spectra obtained for the reaction of 0.20 M benzylamine and 0.40 M $CH_2(OH)(SO_3Na)$ also show formation of the 1 : 1 adduct and, over time, the 1 : 2 adduct. Table 6.5 summarises the spectra obtained 3 minutes and 5 hours after mixing. There was no further change in the spectrum over time.

Table 6.5: 0.20 M benzylamine and 0.40 M $CH_2(OH)(SO_3Na)$: peak assignments

time after mixing	δ / ppm	integral ratio	multiplicity	J / Hz	assignment
3 minutes	3.69	1	s	-	$-CH_2NHCH_2SO_3^-$
	3.90	1	s	-	$-NHCH_2SO_3^-$
	4.30	1	s	-	$CH_2(OH)(SO_3Na)$
	4.67	-	-	-	D_2O, $-NH_2$
	7.30	3	m	-	Ar-**H2'**, **H3'**, **H4'**
5 hours	3.70	2	s	-	$-CH_2NHCH_2SO_3^-$
	3.90	2	s	-	$-NHCH_2SO_3^-$
	4.03	5	s	-	$-N(CH_2SO_3^-)_2$
	4.24	9	s	-	$-CH_2N(CH_2SO_3^-)_2$
	4.29		s	-	$CH_2(OH)(SO_3Na)$
	4.67	-	-	-	D_2O, $-NH_2$
	7.30	11	m	-	Ar-**H2'**, **H3'**, **H4'**
	7.40		m	-	Ar-**H2''**,**H3''**,**H4''**

After 3 minutes there is complete conversion of the benzylamine to the 1 : 1 adduct $C_6H_5CH_2NHCH_2SO_3^-$. After 13 minutes there is also evidence of formation of the 1 : 2 adduct $C_6H_5CH_2N(CH_2SO_3^-)_2$. Over time the peaks due to the 1 : 1 adduct decrease in intensity and those due to the 1 : 2 adduct increase. This implies conversion of the 1 : 1 adduct to the 1 : 2 adduct over time due to further reaction with $CH_2(OH)(SO_3Na)$, present in excess. After 5 hours the reaction is complete: virtually all of the $CH_2(OH)(SO_3Na)$ has reacted after this time and the 1 : 1 and 1 : 2 adducts are present in approximately equal amounts.

6.2.1.1.3 Benzylamine in excess

The spectra obtained for the reaction of 0.20 M benzylamine and 0.10 M $CH_2(OH)(SO_3Na)$ show formation of the 1 : 1 adduct $C_6H_5CH_2NHCH_2SO_3^-$. Table 6.6 summarises the spectra obtained 2 minutes and 14 minutes after mixing. There was no further change in the spectrum.

Table 6.6: 0.20 M benzylamine and 0.10 M $CH_2(OH)(SO_3Na)$: peak assignments

time after mixing	δ / ppm	integral ratio	multiplicity	J / Hz	assignment
2 minutes	3.65	3	s	-	$-CH_2NH_2$
	3.66		s	-	$-CH_2NHCH_2SO_3^-$
	3.87	1	s	-	$-NHCH_2SO_3^-$
	4.67	-	-	-	D_2O, $-NH_2$
	7.25	7	m	-	Ar-**H2**, **H3**, **H4**
	7.28		m	-	Ar-**H2'**, **H3'**, **H4'**
14 minutes	3.63	5	s	-	$-CH_2NH_2$
	3.66		s	-	$-CH_2NHCH_2SO_3^-$
	3.87	2	s	-	$-NHCH_2SO_3^-$
	4.67	-	-	-	D_2O, $-NH_2$
	7.25	12	m	-	Ar-**H2**, **H3**, **H4**
	7.27		m	-	Ar-**H2'**, **H3'**, **H4'**

After 2 minutes there is evidence of formation of the 1 : 1 adduct $C_6H_5CH_2NHCH_2SO_3^-$ and the reaction is complete within 14 minutes. After this time there is complete conversion of $CH_2(OH)(SO_3Na)$ to the product.

6.2.1.2 Uv / visible kinetic studies

6.2.1.2.1 Absorbance against wavelength spectra and absorbance against time plots

Absorbance against wavelength spectra were obtained for the reaction of 2.0×10^{-3} to 0.10 M aqueous $CH_2(OH)(SO_3Na)$ with 2.0×10^{-3} M benzylamine at 25 °C in aqueous solution. The spectrum of 2.0×10^{-3} M benzylamine alone was obtained for comparison. The spectra with aqueous $CH_2(OH)(SO_3Na)$ added show a shift to lower wavelength and an increase in absorbance as compared to the spectrum of 2.0×10^{-3} M benzylamine alone. The higher the concentration of aqueous $CH_2(OH)(SO_3Na)$, the greater the change in spectrum observed. All reactions are complete within 1½ hours.

Figure 6.4 shows the change over time in the spectrum for the reaction with 0.10 M $CH_2(OH)(SO_3Na)$ as compared to that of benzylamine alone. Table 6.7 shows the peak positions and extinction coefficients (ε) for the two spectra.

Figure 6.4: Change over time in the absorbance against wavelength spectrum for 2.0×10^{-3} M benzylamine with 0.10 M $CH_2(OH)(SO_3Na)$, 25 °C, aqueous solution

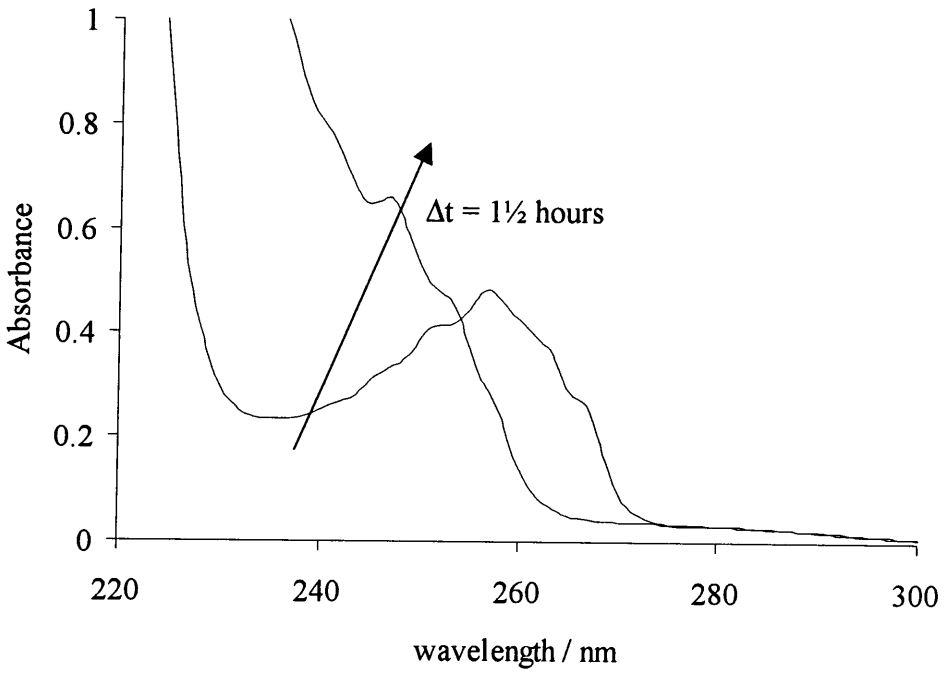

Table 6.7: Spectral appearance in aqueous solution of 2.0×10^{-3} M benzylamine and the final spectrum in the presence of 0.10 M $CH_2(OH)(SO_3Na)$

$[CH_2(OH)(SO_3Na)]$ / M	λ_{max} / nm ($\varepsilon^{\dagger}$/ mol^{-1} dm^3 cm^{-1})
none	257 (240)
0.10	247 (330)

† based on the assumption that all the benzylamine reacts to give 2.0×10^{-3} M product

Plots of absorbance against time were obtained for the reaction of 2.0×10^{-3} M benzylamine with 0.010 to 0.10 M aqueous $CH_2(OH)(SO_3Na)$ at 25 °C using conventional uv / vis spectrometry. Formation of the product at 240 nm was followed. The solutions were unbuffered or buffered at pH 6.0 to 8.0: the unbuffered solutions

were found to be pH 7.9. Plots were first order (Figure 6.5): the k_{obs} / s^{-1} values obtained are shown in Table 6.8.

Figure 6.5: Absorbance against time plots for 2.0×10^{-3} M benzylamine with 0.010 to 0.10 M aqueous $CH_2(OH)(SO_3Na)$ at 25 °C in unbuffered aqueous solution

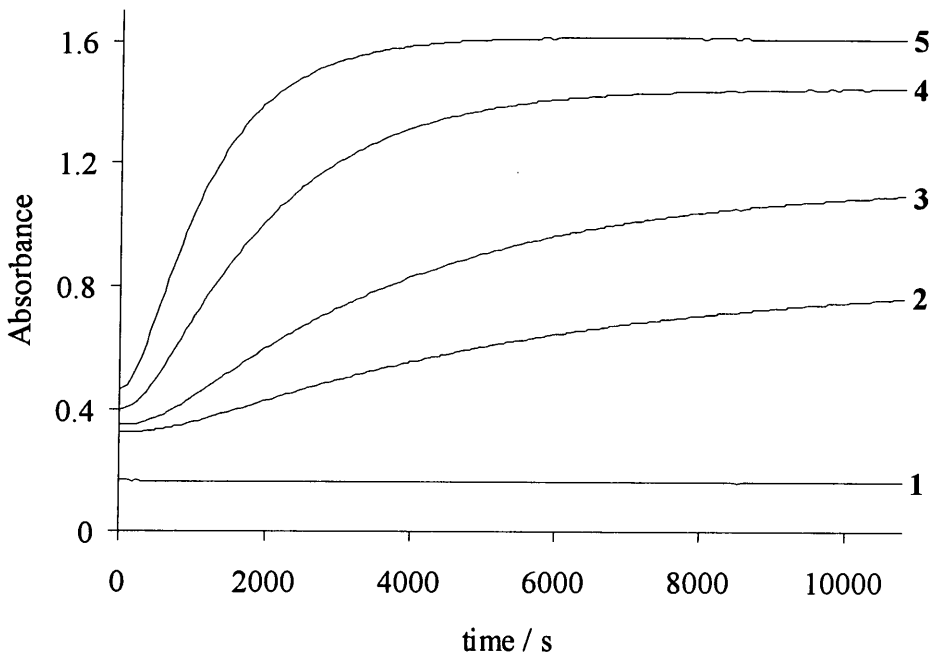

1 = benzylamine alone; **2** = 0.010 M $CH_2(OH)(SO_3Na)$; **3** = 0.020 M; **4** = 0.050 M; **5** = 0.10 M

Table 6.8: k_{obs} / s^{-1} values for the reaction of 2.0×10^{-3} M benzylamine with aqueous $CH_2(OH)(SO_3Na)$ at 25 °C in aqueous solution

$[CH_2(OH)(SO_3Na)]$ / M	pH†	k_{obs} / s^{-1}
0.010	-	$1.70 \times 10^{-4} \pm 2 \times 10^{-7}$
0.020	-	$2.70 \times 10^{-4} \pm 3 \times 10^{-7}$
0.050	6.0	$1.34 \times 10^{-4} \pm 1 \times 10^{-6}$
0.050	7.0	$4.33 \times 10^{-4} \pm 6 \times 10^{-6}$
0.050	-	$5.30 \times 10^{-4} \pm 1 \times 10^{-6}$
0.050	8.0	$1.03 \times 10^{-3} \pm 2 \times 10^{-5}$
0.10	-	$9.11 \times 10^{-4} \pm 4 \times 10^{-6}$

† where no pH is quoted the solution was unbuffered and pH ~ 7.9

The k_{obs} / s^{-1} value obtained increases as the pH increases from pH 6.0 to 8.0. This can be explained in terms of the concentration of unprotonated benzylamine present: the pK_a of benzylamine[1] is 9.33 therefore as the pH value increases, more of the reactive free amine form will be present.

The rate constant k_{obs} / s^{-1} refers to the overall rate constant for the formation of $C_6H_5CH_2NHCH_2SO_3^-$, shown in Scheme 6.2. Plotting k_{obs} / s^{-1} against $[CH_2(OH)(SO_3Na)]$ / M for the reaction in unbuffered aqueous solution gives a linear plot and allows the determination of the forward and back rate constants, $k_{f(app)}$ / dm^3 mol^{-1} s^{-1} and k_b / s^{-1}, equal to the gradient and intercept respectively (Figure 6.6).

Figure 6.6: k_{obs} / s^{-1} against $[CH_2(OH)(SO_3Na)]$ / M for the reaction with 2.0×10^{-3} M benzylamine in unbuffered aqueous solution, 25 °C

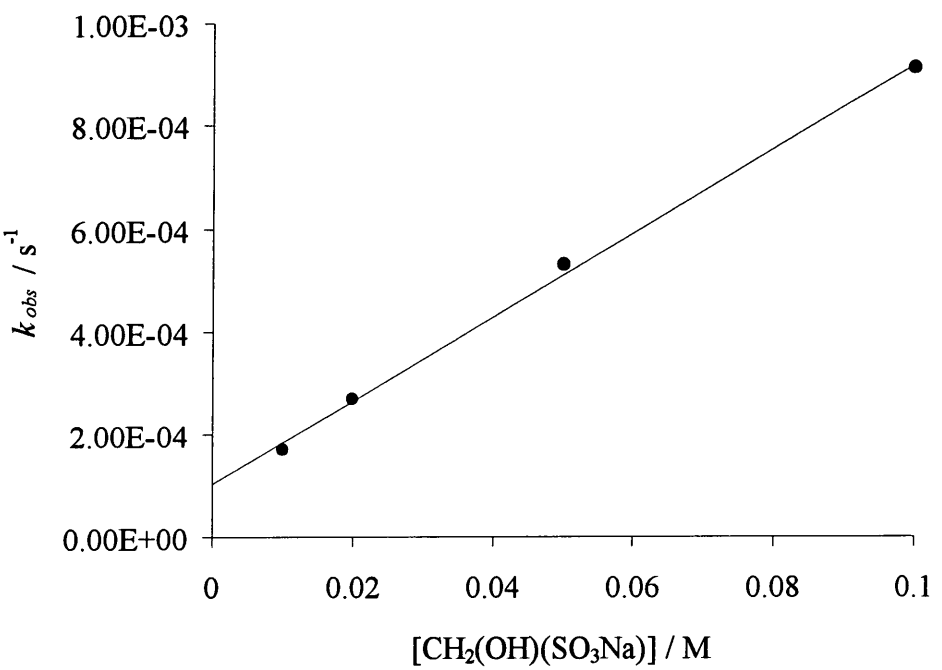

Linear regression yields values of $k_{f(app)}$ and k_b of $8.17 \times 10^{-3} \pm 2.6 \times 10^{-4}$ dm^3 mol^{-1} s^{-1} and $1.02 \times 10^{-4} \pm 1.5 \times 10^{-5}$ s^{-1} respectively: a correlation coefficient of 0.998 is obtained. These values give an equilibrium constant, $K_{(app)}$, equal to $k_{f(app)}$ / k_b, of 80 ± 10 dm^3 mol^{-1}. From Figure 6.5 it is clear that the reaction is an equilibrium as the final absorbance obtained increases with increasing $CH_2(OH)(SO_3Na)$ concentration. The true value of K will be larger than $K_{(app)}$ as shown in Equation 6.6.

6.2.1.2.2 Absorbance against time plots: initial fast reaction

In Figure 6.5 there is an initial plateau in the absorbance before the first order formation, which implies there is an initial faster reaction occurring. To investigate this, absorbance against time plots were obtained for the reaction of 5.5×10^{-4} to 2.0×10^{-3} M benzylamine with 3.0×10^{-3} to 0.010 M $CH_2(OH)(SO_3Na)$ using stopped flow spectrophotometry (Table 6.9).

Table 6.9: k_{obs} / s^{-1} values for the reaction of benzylamine with aqueous $CH_2(OH)(SO_3Na)$ at 25 °C in aqueous solution: initial reaction

$[C_6H_5CH_2NH_2]$ / M	$[CH_2(OH)(SO_3Na)]$ / M	k_{obs} / s^{-1}
5.5×10^{-4}	0.010	0.256 ± 0.008
1.0×10^{-3}	3.0×10^{-3}	0.321 ± 0.018
1.0×10^{-3}	5.0×10^{-3}	0.286 ± 0.012
1.0×10^{-3}	0.010	0.263 ± 0.006
1.0×10^{-3}	0.030	0.248 ± 0.009
1.0×10^{-3}	0.050	0.243 ± 0.009
2.0×10^{-3}	0.010	0.287 ± 0.006

Altering the benzylamine concentration from 5.5×10^{-4} to 2.0×10^{-3} M has little effect on the rate constant obtained. When the benzylamine concentration is kept constant and the $CH_2(OH)(SO_3Na)$ concentration varied, the observed rate constant shows a slight inverse dependence on $CH_2(OH)(SO_3Na)$ concentration. Plotting k_{obs} / s^{-1} against 1 / ($[CH_2(OH)(SO_3Na)]$ / M) gives a linear plot (Figure 6.7).

Figure 6.7: k_{obs} / s^{-1} against 1 / ([$CH_2(OH)(SO_3Na)$] / M) for the reaction with 1.0×10^{-3} benzylamine, 25 °C, aqueous solution

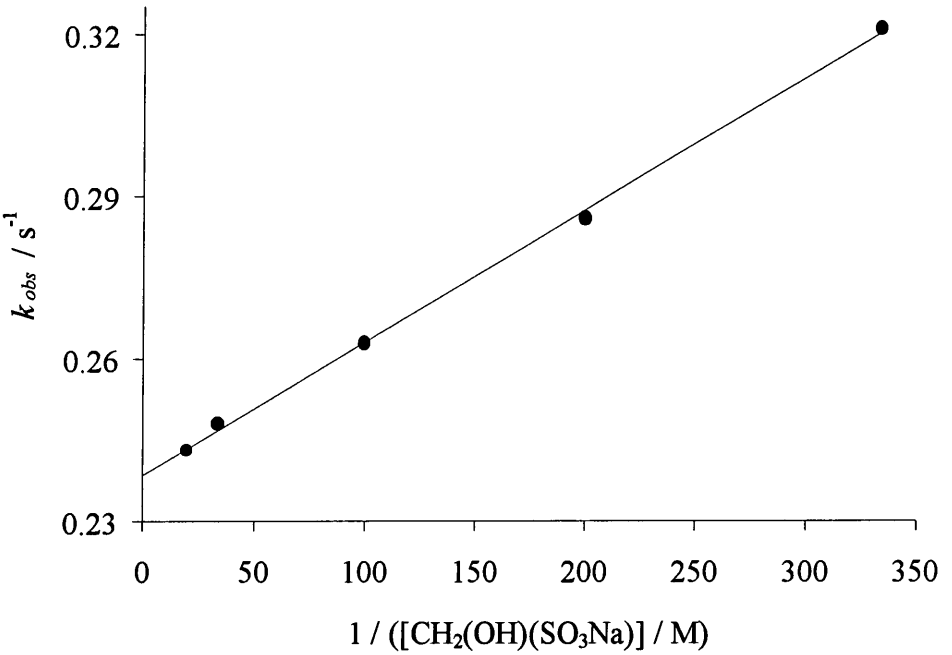

Linear regression yields values for the gradient and intercept of $2.45 \times 10^{-4} \pm 5 \times 10^{-6}$ mol dm^{-3} s^{-1} and $0.239 \pm 9 \times 10^{-4}$ s^{-1} respectively : a correlation coefficient of 0.999 is obtained.

It is not clear what this initial faster reaction corresponds to. It could be interpreted as being due to the formation of the 1 : 1 benzylamine : $CH_2(OH)(SO_3Na)$ adduct $C_6H_5CH_2NHCH_2SO_3^-$ and the slower reaction to the formation of the 1 : 2 benzylamine : $CH_2(OH)(SO_3Na)$ adduct $C_6H_5CH_2N(CH_2SO_3^-)_2$ observed in the ^1H NMR. However the observed inverse dependence on $CH_2(OH)(SO_3Na)$ concentration would not be expected if it corresponded to the formation of an adduct: therefore this explanation can be discounted. It is therefore formation of the 1 : 1 adduct that is the main reaction being followed using conventional spectrometry.

6.2.2 Reaction of $CH_2(OH)(SO_3Na)$ with 4-methoxybenzylamine

6.2.2.1 ^{1}H NMR studies

The reaction of $CH_2(OH)(SO_3Na)$ with 4-methoxybenzylamine in D_2O was followed using ^{1}H NMR. For comparison, the spectrum of 0.21 M 4-methoxybenzylamine (**6.2**) in D_2O was obtained (Figure 6.8, Table 6.10).

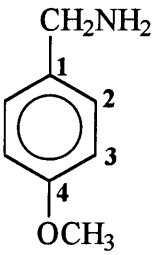

6.2

Figure 6.8: ^{1}H NMR spectrum of 4-methoxybenzylamine in D_2O

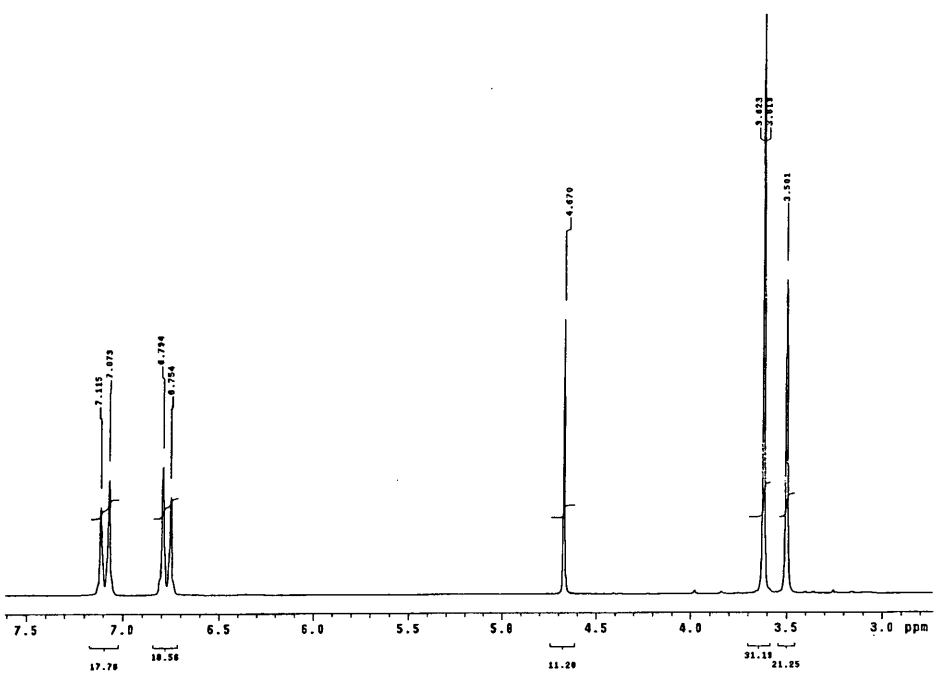

Table 6.10: ^{1}H NMR spectrum of 4-methoxybenzylamine in D_2O: peak assignments

δ / ppm	integral ratio	multiplicity	J / Hz	assignment
3.50	2	s	-	-CH_2NH_2
3.62	3	s	-	-OCH_3
4.67	-	-	-	D_2O, -NH_2
6.77	2	d	8	Ar-**H3**
7.09	2	d	8	Ar-**H2**

The spectrum of 0.19 M 4-methoxybenzylamine and 0.20 M $CH_2(OH)(SO_3Na)$ was obtained, then with each reagent in excess: 0.19 M 4-methoxybenzylamine with 0.40 M $CH_2(OH)(SO_3Na)$ and 0.21 M 4-methoxybenzylamine with 0.10 M $CH_2(OH)(SO_3Na)$. A spectrum was recorded immediately (3 to 6 minutes) after addition of the $CH_2(OH)(SO_3Na)$ then again after approximately 30 minutes, 1 hour and 2 or 3 hours and continued until there was no further change in the spectrum.

There are two possible products that may form in the reaction. Firstly, a 1 : 1 4-methoxybenzylamine : $CH_2(OH)(SO_3Na)$ adduct 4-$CH_3OC_6H_4CH_2NHCH_2SO_3^-$, **6.8**, can form. In the presence of excess $CH_2(OH)(SO_3Na)$, a second molecule may react to produce 4-$CH_3OC_6H_4CH_2N(CH_2SO_3^-)_2$, **6.9**, the 1 : 2 4-methoxybenzylamine : $CH_2(OH)(SO_3Na)$ adduct.

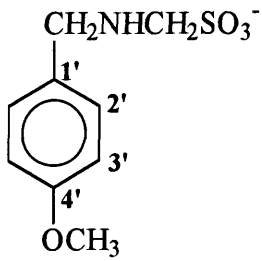

6.8

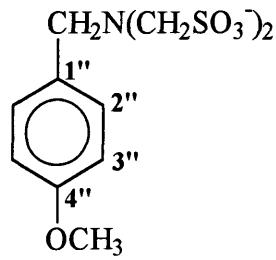

6.9

6.2.2.1.1 Equimolar 4-methoxybenzylamine and $CH_2(OH)(SO_3Na)$

The results obtained for the reaction of equimolar 0.19 M 4-methoxybenzylamine and 0.20 M $CH_2(OH)(SO_3Na)$ are shown in Figures 6.9 and 6.10 which show the spectra obtained 6 minutes and 36 minutes after mixing. There was no further change in the spectrum over time. Tables 6.11 and 6.12 summarise the information obtained from the two spectra.

Figure 6.9: 0.19 M 4-methoxybenzylamine and 0.20 M $CH_2(OH)(SO_3Na)$: 6 minutes after mixing

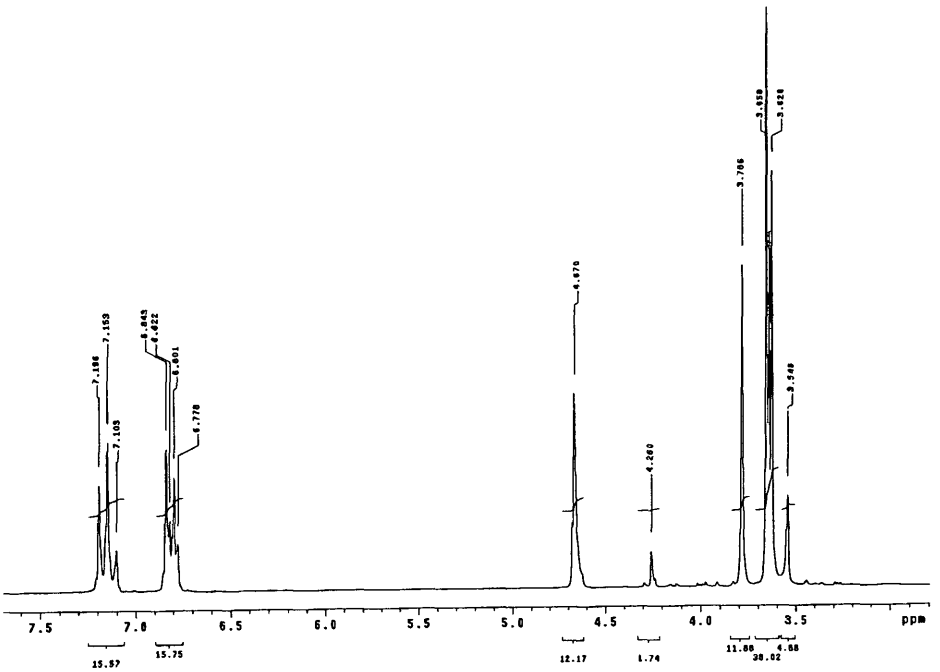

Table 6.11: Peak assignments: 6 minutes after mixing

time after mixing	δ / ppm	integral ratio	multiplicity	J / Hz	assignment
6 minutes	3.55	3	s	-	$-CH_2NH_2$
	3.63	22	s	-	$-OCH_3$
	3.66		s	-	$-CH_2NHCH_2SO_3^-$
	3.79	7	s	-	$-NHCH_2SO_3^-$
	4.26	1	s	-	$CH_2(OH)(SO_3Na)$
	4.67	-	-	-	D_2O, $-NH_2$
	6.80	9	d	8	Ar-**H3**
	6.82		d	8	Ar-**H3'**
	7.10	9	d	8	Ar-**H2**
	7.17		d	8	Ar-**H2'**

Figure 6.10: 0.19 M 4-methoxybenzylamine and 0.20 M $CH_2(OH)(SO_3Na)$: 36 minutes after mixing

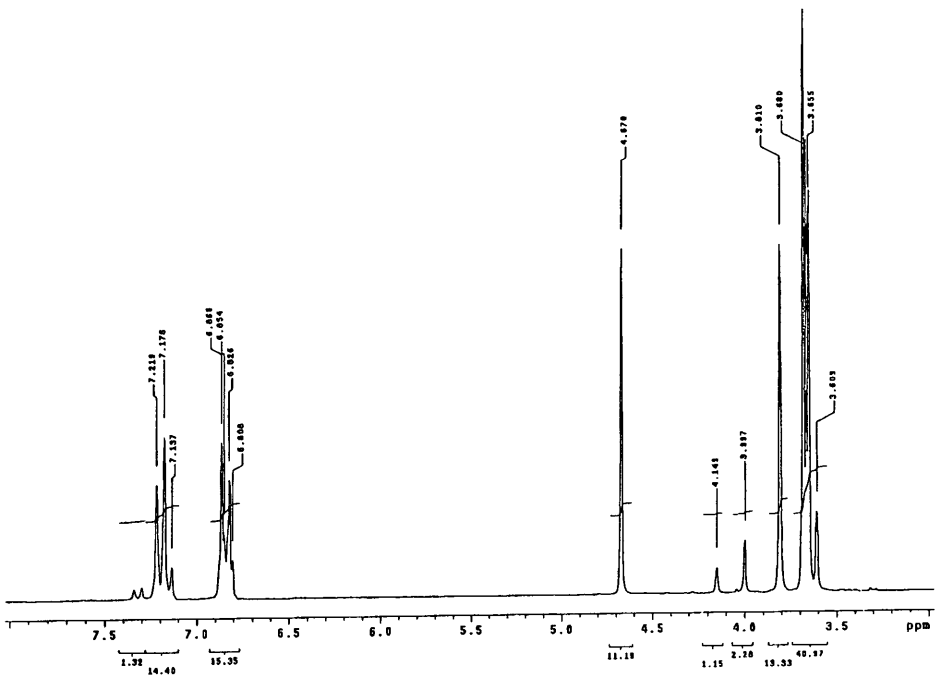

Table 6.12: Peak assignments: 36 minutes after mixing

time after mixing	δ / ppm	integral ratio	multiplicity	J / Hz	assignment
36 minutes	3.61	36	s	-	-CH_2NH_2
	3.66		s	-	-OCH_3
	3.68		s	-	-$CH_2NHCH_2SO_3^-$
	3.81	12	s	-	-$NHCH_2SO_3^-$
	4.00	2	s	-	-$N(CH_2SO_3^-)_2$
	4.15	1	s	-	-$CH_2N(CH_2SO_3^-)_2$
	4.67	-	-	-	D_2O, -NH_2
	6.83	13	d	8	Ar-**H3**
	6.85		d	8	Ar-**H3'**
	7.15	13	d	8	Ar-**H2**
	7.20		d	8	Ar-**H2'**
	7.32	1	d	8	Ar-**H2''**

The spectra show the formation of both the 1 : 1 adduct 4-$CH_3OC_6H_4CH_2NHCH_2SO_3^-$ and the 1 : 2 adduct 4-$CH_3OC_6H_4CH_2N(CH_2SO_3^-)_2$ over time. After only 6 minutes there is considerable 1 : 1 adduct 4-$CH_3OC_6H_4CH_2NHCH_2SO_3^-$ formation with the appearance of peaks at δ 3.66 and δ 3.79 ppm. There is also a change in the aromatic region, with the product peaks resonating at a slightly higher frequency than the corresponding peaks in the parent compound, 4-methoxybenzylamine. After 36 minutes new peaks due to the 1 : 2 adduct 4-$CH_3OC_6H_4CH_2N(CH_2SO_3^-)_2$ at δ 4.00 and δ 4.15 ppm are present and small peaks in the aromatic region at slightly higher frequency than the 1 : 1 adduct. There is no further change in the spectrum after 36 minutes.

The peaks due to $CH_2(OH)(SO_3Na)$ and 4-methoxybenzylamine decrease in intensity over time. Although all the $CH_2(OH)(SO_3Na)$ reacts, there is still some evidence of a small amount of amine in the final spectrum. The major product of reaction is the 1 : 1 adduct 4-$CH_3OC_6H_4CH_2NHCH_2SO_3^-$, which forms immediately, with a smaller proportion of the 1 : 2 adduct 4-$CH_3OC_6H_4CH_2N(CH_2SO_3^-)_2$ forming over time.

6.2.2.1.2 $CH_2(OH)(SO_3Na)$ in excess

The spectra obtained for the reaction of 0.20 M 4-methoxybenzylamine and 0.40 M $CH_2(OH)(SO_3Na)$ also show the formation of 4-$CH_3OC_6H_4CH_2NHCH_2SO_3^-$, the 1 : 1 adduct and, over time, the 1 : 2 adduct 4-$CH_3OC_6H_4CH_2N(CH_2SO_3^-)_2$. Table 6.13 summarises the spectra obtained 3 minutes and 1 hour after mixing. There was no further change in the spectrum over time.

After only 3 minutes all the 4-methoxybenzylamine reacts to give the 1 : 1 adduct 4-$CH_3OC_6H_4CH_2NHCH_2SO_3^-$. Within 30 minutes there is also substantial 1 : 2 adduct, 4-$CH_3OC_6H_4CH_2N(CH_2SO_3^-)_2$, formation. The reaction is complete within 1 hour, when the amount of 1 : 2 adduct is almost equal to the amount of 1 : 1 adduct present.

Table 6.13: 0.20 M 4-methoxybenzylamine and 0.40 M $CH_2(OH)(SO_3Na)$: peak assignments

time after mixing	δ / ppm	integral ratio	multiplicity	J / Hz	assignment
3 minutes	3.65	11	s	-	-OC**H**$_3$
	3.67		s	-	-C**H**$_2$NHCH$_2$SO$_3^-$
	3.80	4	s	-	-NHC**H**$_2$SO$_3^-$
	4.28	3	s	-	C**H**$_2$(OH)(SO$_3$Na)
	4.67	-	-	-	D$_2$O, -N**H**$_2$
	6.84	4	d	8	Ar-**H3'**
	7.19	4	d	8	Ar-**H2'**
1 hour	3.67	21	s	-	-OC**H**$_3$
	3.69		s	-	-C**H**$_2$NHCH$_2$SO$_3^-$
	3.82	6	s	-	-NHC**H**$_2$SO$_3^-$
	4.01	9	s	-	-N(C**H**$_2$SO$_3^-$)$_2$
	4.16	4	s	-	-C**H**$_2$N(CH$_2$SO$_3^-$)$_2$
	4.29	1	s	-	C**H**$_2$(OH)(SO$_3$Na)
	4.67	-	-	-	D$_2$O, -N**H**$_2$
	6.84	10	d	8	Ar-**H3'**
	6.85		d	8	Ar-**H3''**
	7.21	5	d	8	Ar-**H2'**
	7.33	5	d	8	Ar-**H2''**

6.2.2.1.3 4-Methoxybenzylamine in excess

The spectra obtained for the reaction of 0.20 M 4-methoxybenzylamine and 0.10 M $CH_2(OH)(SO_3Na)$ show the formation of the 1 : 1 adduct 4-$CH_3OC_6H_4CH_2NHCH_2SO_3^-$ only. Table 6.14 summarises the spectra obtained 3 minutes and 36 minutes after mixing. There was no further change in the spectrum over time.

After 3 minutes virtually all the $CH_2(OH)(SO_3Na)$ has reacted and after 36 minutes the reaction is complete. There is complete conversion of $CH_2(OH)(SO_3Na)$ to the 1 : 1 adduct 4-$CH_3OC_6H_4CH_2NHCH_2SO_3^-$.

Table 6.14: 0.20 M 4-methoxybenzylamine and 0.10 M $CH_2(OH)(SO_3Na)$: peak assignments

time after mixing	δ / ppm	integral ratio	multiplicity	J / Hz	assignment
3 minutes	3.53	4	s	-	$-CH_2NH_2$
	3.62	10	s	-	$-OCH_3$
	3.65		s	-	$-CH_2NHCH_2SO_3^-$
	3.78	2	s	-	$-NHCH_2SO_3^-$
	4.67	-	-	-	D_2O, $-NH_2$
	6.80	5	d	8	Ar-**H3**
	6.82		d	8	Ar-**H3'**
	7.12	5	d	8	Ar-**H2**
	7.16		d	8	Ar-**H2'**
36 minutes	3.53	3	s	-	$-CH_2NH_2$
	3.62	9	s	-	$-OCH_3$
	3.65		s	-	$-CH_2NHCH_2SO_3^-$
	3.77	2	s	-	$-NHCH_2SO_3^-$
	4.67	-	-	-	D_2O, $-NH_2$
	6.79	4	d	8	Ar-**H3**
	6.81		d	8	Ar-**H3'**
	7.11	4	d	8	Ar-**H2**
	7.16		d	8	Ar-**H2'**

6.2.2.2 Uv / visible kinetic studies

6.2.2.2.1 Absorbance against wavelength spectra and absorbance against time plots

Absorbance against wavelength spectra were obtained for the reaction of 0.10 M aqueous $CH_2(OH)(SO_3Na)$ with 1.0×10^{-3} M 4-methoxybenzylamine at 25 °C in aqueous solution. The spectrum shows an increase in absorbance around 240 nm and a decrease at 270 nm as compared to the spectrum of 1.0×10^{-3} M 4-methoxybenzylamine alone. The reaction is complete within 40 minutes.

Figure 6.11 shows the change over time in the spectrum with 0.10 M $CH_2(OH)(SO_3Na)$ as compared to that of 4-methoxybenzylamine alone. Table 6.15 shows the peak positions and extinction coefficients (ε) for the two spectra.

Figure 6.11: Change over time in absorbance against wavelength spectrum for 0.10 M $CH_2(OH)(SO_3Na)$, 1.0×10^{-3} M 4-methoxybenzylamine at 25 °C in aqueous solution

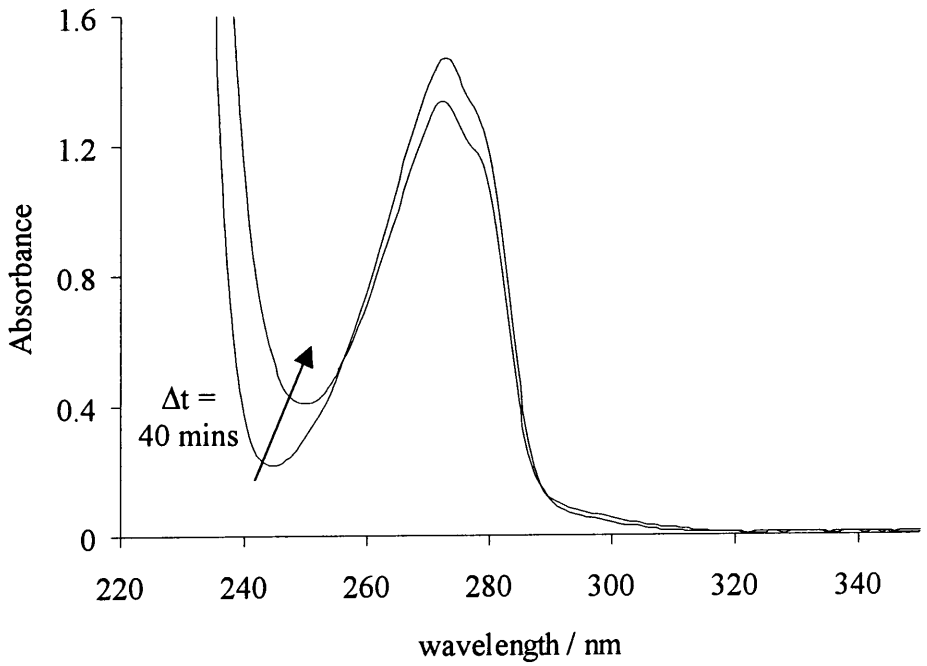

Table 6.15: Spectral appearance in aqueous solution of 1.0×10^{-3} M 4-methoxybenzylamine and the final spectrum with 0.10 M $CH_2(OH)(SO_3Na)$

$[CH_2(OH)(SO_3Na)]$ / M	λ_{max} / nm ($\varepsilon^{\dagger}$/ mol^{-1} dm^3 cm^{-1})
none	272 (1500)
0.10	272 (1300)

† based on the assumption that all the 4-methoxybenzylamine reacts to give 1.0×10^{-3} M product

Plots of absorbance against time were obtained for the reaction of 1.0×10^{-3} M 4-methoxybenzylamine with 0.010 to 0.10 M aqueous $CH_2(OH)(SO_3Na)$ at 25 °C at pH 7.0 to 10.1. Formation of the product at 240 nm was followed. Plots were first order: the k_{obs} / s^{-1} values obtained are shown in Table 6.16. There was no faster reaction detected here.

Table 6.16: k_{obs} / s^{-1} obtained at different pH with 1.0×10^{-3} M 4-methoxybenzylamine and varied $CH_2(OH)(SO_3Na)$ concentration

$[CH_2(OH)(SO_3Na)]$ / M	k_{obs} / s^{-1}			
	pH 7.0	pH 8.1	pH 8.9	pH 10.1
0.010	$1.73 \times 10^{-4} \pm 5 \times 10^{-7}$	$2.78 \times 10^{-4} \pm 7 \times 10^{-7}$	$3.77 \times 10^{-4} \pm 1 \times 10^{-6}$	$3.52 \times 10^{-4} \pm 7 \times 10^{-7}$
0.020	$1.85 \times 10^{-4} \pm 5 \times 10^{-7}$	$3.99 \times 10^{-4} \pm 1 \times 10^{-6}$	$5.49 \times 10^{-4} \pm 2 \times 10^{-6}$	$5.00 \times 10^{-4} \pm 2 \times 10^{-6}$
0.050	$2.17 \times 10^{-4} \pm 5 \times 10^{-7}$	$7.83 \times 10^{-4} \pm 4 \times 10^{-6}$	$1.06 \times 10^{-3} \pm 6 \times 10^{-6}$	$9.93 \times 10^{-4} \pm 7 \times 10^{-6}$
0.10	$2.73 \times 10^{-4} \pm 9 \times 10^{-7}$	$1.42 \times 10^{-3} \pm 1 \times 10^{-5}$	$1.88 \times 10^{-3} \pm 2 \times 10^{-5}$	$1.83 \times 10^{-3} \pm 3 \times 10^{-5}$

Plotting k_{obs} / s^{-1} against [$CH_2(OH)(SO_3Na)$] / M using the data in Table 6.16 at a constant pH gives a linear plot and allows the determination of the forward and back rate constants, $k_{f(app)}$ / dm^3 mol^{-1} s^{-1} and k_b / s^{-1}, equal to the gradient and intercept respectively. Linear regression yielded correlation coefficients of 0.999. An equilibrium constant, $K_{(app)}$ / dm^3 mol^{-1}, equal to $k_{f(app)}$ / k_b, can be calculated for each pH (Table 6.17).

Table 6.17: $k_{f(app)}$ / dm^3 mol^{-1} s^{-1}, k_b / s^{-1} and $K_{(app)}$ / dm^3 mol^{-1} values for the reaction of 4-methoxybenzylamine with aqueous $CH_2(OH)(SO_3Na)$, 25 °C, pH 7.0 to 10.1

pH	$k_{f(app)}$ / dm^3 mol^{-1} s^{-1}	k_b / s^{-1}	$K_{(app)}$ / dm^3 mol^{-1}
7.0	$1.11 \times 10^{-3} \pm 9 \times 10^{-6}$	$1.62 \times 10^{-4} \pm 5 \times 10^{-7}$	6.8 ± 0.1
8.1	$1.27 \times 10^{-2} \pm 4 \times 10^{-5}$	$1.48 \times 10^{-4} \pm 3 \times 10^{-6}$	86 ± 2
8.9	$1.67 \times 10^{-2} \pm 1 \times 10^{-4}$	$2.15 \times 10^{-4} \pm 7 \times 10^{-6}$	77 ± 3
10.1	$1.65 \times 10^{-2} \pm 2 \times 10^{-4}$	$1.77 \times 10^{-4} \pm 9 \times 10^{-6}$	93 ± 5

The change in value of the equilibrium constant with pH for 4-methoxybenzylamine is merely a pK_a effect. The pK_a of 4-methoxybenzylamine[1] is 9.51 therefore at pH 7 the amine will be mainly in the unreactive protonated form.

The reaction of 1.0×10^{-3} M 4-methoxybenzylamine with a constant aqueous $CH_2(OH)(SO_3Na)$ concentration of 0.10 M was also followed at pH 5.1 to 10.1. The k_{obs} / s^{-1} values obtained are shown in Table 6.18. Figure 6.12 shows a plot of $\log(k_{obs} / s^{-1})$ against pH.

Table 6.18: k_{obs} / s^{-1} for the reaction of 1.0×10^{-3} M 4-methoxybenzylamine and 0.10 M $CH_2(OH)(SO_3Na)$, 25 °C, pH 5.1 to 10.1

pH	k_{obs} / s^{-1}
5.1	$2.79 \times 10^{-5} \pm 4 \times 10^{-8}$
5.9	$5.28 \times 10^{-5} \pm 1 \times 10^{-7}$
7.0	$2.73 \times 10^{-4} \pm 9 \times 10^{-7}$
8.1	$1.42 \times 10^{-3} \pm 1 \times 10^{-5}$
8.9	$1.88 \times 10^{-3} \pm 2 \times 10^{-5}$
10.1	$1.83 \times 10^{-3} \pm 3 \times 10^{-5}$

Figure 6.12: $\log(k_{obs} / s^{-1})$ against pH for the reaction of 0.10 M $CH_2(OH)(SO_3Na)$ with 1.0×10^{-3} M 4-methoxybenzylamine

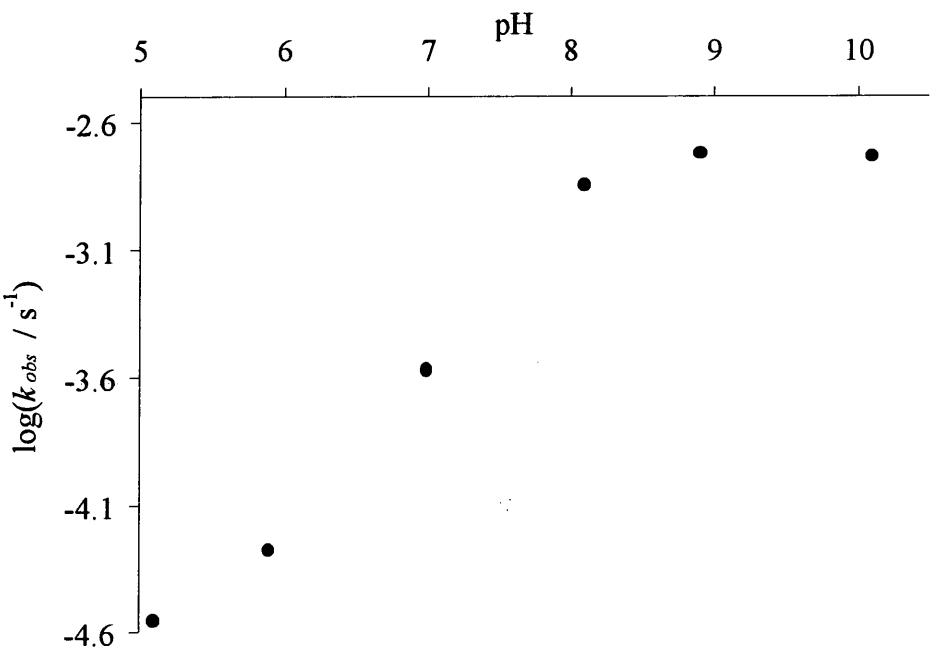

The value of $\log(k_{obs} / s^{-1})$ increases as the pH increases from pH 5 to 8 but reaches a maximum at around pH 9. This can be explained in terms of the concentration of unprotonated 4-methoxybenzylamine present: as the pH value increases from pH 5 to 9 more of the reactive free amine form will be present. Above pH 9 the amine will be predominantly in the reactive free form.

6.2.2.2.2 Ionic strength

In all experiments it has been assumed that effects due to ionic strength (I) are relatively small. To investigate this, the reaction of 1.0×10^{-3} M 4-methoxybenzylamine with an aqueous $CH_2(OH)(SO_3Na)$ concentration of 0.010 or 0.020 M at pH 8.2 was studied under conditions where the ionic strength was either not controlled or kept constant at 1.0 M using potassium chloride. The k_{obs} / s^{-1} values obtained are shown in Table 6.19.

Table 6.19: k_{obs} / s^{-1} values for the reaction of 1.0×10^{-4} M 4-methoxybenzylamine with aqueous $CH_2(OH)(SO_3Na)$, 25 °C, pH 8.2, with and without a constant I of 1.0 M

$[CH_2(OH)(SO_3Na)]$ / M	$I^{\dagger}$ / M	k_{obs} / s^{-1}
0.010	-	$2.60 \times 10^{-4} \pm 6 \times 10^{-7}$
0.010	1.0	$2.72 \times 10^{-4} \pm 5 \times 10^{-7}$
0.020	-	$4.55 \times 10^{-4} \pm 1 \times 10^{-6}$
0.020	1.0	$4.91 \times 10^{-4} \pm 2 \times 10^{-6}$

† where no I is quoted the ionic strength was not kept constant

Altering the ionic strength has little effect on the rate constant obtained. Therefore it can be assumed that ionic strength effects are relatively small.

6.2.2.2.3 Reaction in the presence of added sulfite ions

The effect of the presence of added sulfite ions in the system was investigated. Plots of absorbance against time were obtained for the reaction of 1.0×10^{-3} M 4-methoxybenzylamine with 0.10 M aqueous $CH_2(OH)(SO_3Na)$ in the presence of 2.0×10^{-3} to 0.010 M aqueous sodium sulfite solution at 25 °C, pH 8.1. Formation of the product $4\text{-}CH_3OC_6H_4CH_2NHCH_2SO_3^-$ at 240 nm was followed. Sulfite ions absorb in this region: spectra of 0.01, 0.05 and 0.10 M aqueous sodium sulfite solution were obtained and showed high absorbance around 250 nm and to shorter wavelength. For example, the extinction coefficient of sulfite ions at 245 nm was found to be 50 $dm^3\ mol^{-1}\ cm^{-1}$. Therefore the appropriate concentration of sulfite ions was added to

the reference in order to subtract the absorbance due to the presence of sulfite from the absorbance against time plots. Where $[sulfite]_{stoich}$ is quoted this refers to the total concentration of aqueous sodium sulfite added externally to the system and does not include the concentration of sulfite ions present in solution due to dissociation of $CH_2(OH)(SO_3Na)$. Plots were first order (Figure 6.13): the k_{obs} / s^{-1} values obtained are shown in Table 6.20.

Figure 6.13: Absorbance against time plots for the reaction of 1.0×10^{-3} M 4-methoxybenzylamine and 0.10 M $CH_2(OH)(SO_3Na)$, sulfite ions added, 25 °C, pH 8.1

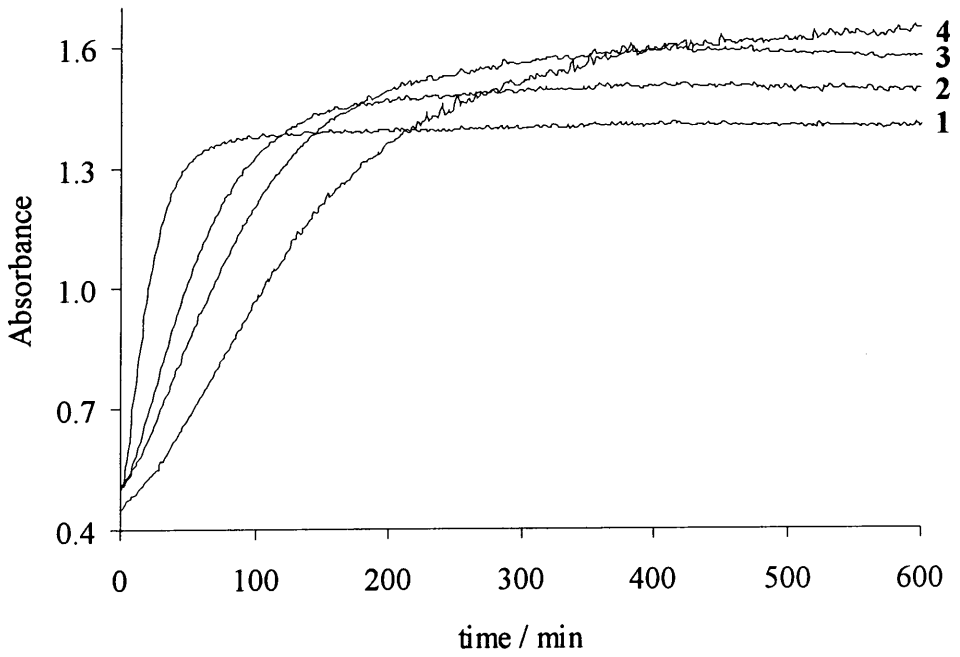

1 = no sulfite; **2** = 2.0×10^{-3} M sulfite ions; **3** = 4.0×10^{-3} M; **4** = 7.0×10^{-3} M

Table 6.20: k_{obs} / s^{-1} values for the reaction of 1.0×10^{-4} M 4-methoxybenzylamine with 0.10 M aqueous $CH_2(OH)(SO_3Na)$ with added sulfite ions at 25 °C, pH 8.1

$[sulfite]_{stoich}$ / M	k_{obs} / s^{-1}	$k_{obs}.[sulfite]_{stoich}$ / s^{-1} M
0	$8.09 \times 10^{-4} \pm 8 \times 10^{-6}$	-
2.0×10^{-3}	$3.17 \times 10^{-4} \pm 1 \times 10^{-6}$	6.3×10^{-7}
4.0×10^{-3}	$1.94 \times 10^{-4} \pm 1 \times 10^{-6}$	7.8×10^{-7}
7.0×10^{-3}	$1.27 \times 10^{-4} \pm 7 \times 10^{-7}$	8.9×10^{-7}
0.010	$7.50 \times 10^{-5} \pm 6 \times 10^{-7}$	7.5×10^{-7}

The rate constant of reaction is considerably slower in the presence of added sulfite ions. Multiplying k_{obs} / s^{-1} by $[sulfite]_{stoich}$ / M gives similar values which implies an inverse dependence of k_{obs} / s^{-1} on the sulfite ion concentration.

If free formaldehyde, HCHO, is the reactive species in the reaction of $CH_2(OH)(SO_3Na)$ with amines then the reaction must proceed initially via dissociation of $CH_2(OH)(SO_3Na)$ to give HCHO (Chapter 4). If this is the case, in the presence of additional sulfite ions the rate of formation of the product $4\text{-}CH_3OC_6H_4CH_2NHCH_2SO_3^-$ may be expected to decrease as more free formaldehyde will react with the sulfite ions to give the unreactive $CH_2(OH)(SO_3Na)$. Hence less free formaldehyde will be present to react with the 4-methoxybenzylamine. The experimental results obtained here support this theory.

6.2.3 Reaction of $CH_2(OH)(SO_3Na)$ with 4-methylbenzylamine

6.2.3.1 ^1H NMR studies

The reaction of $CH_2(OH)(SO_3Na)$ with 4-methylbenzylamine in a 97 % D_2O / 3 % methyl-d_3 alcohol-d, CD_3OD, by volume solvent was followed using ^1H NMR spectroscopy. 4-Methylbenzylamine is not readily soluble in aqueous solution at the concentrations required therefore a mixed solvent system was used. Lower concentrations of reactants had to be used for this amine to be soluble in a solvent system with this proportion of water. For comparison, the spectrum of 0.016 M 4-methylbenzylamine (**6.3**) in 97 % D_2O / 3 % CD_3OD by volume was obtained (Figure 6.14, Table 6.21).

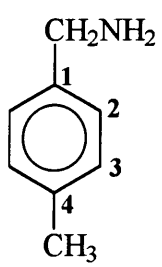

6.3

Figure 6.14: ^{1}H NMR spectrum of 4-methylbenzylamine in 97 % D_2O / 3 % CD_3OD

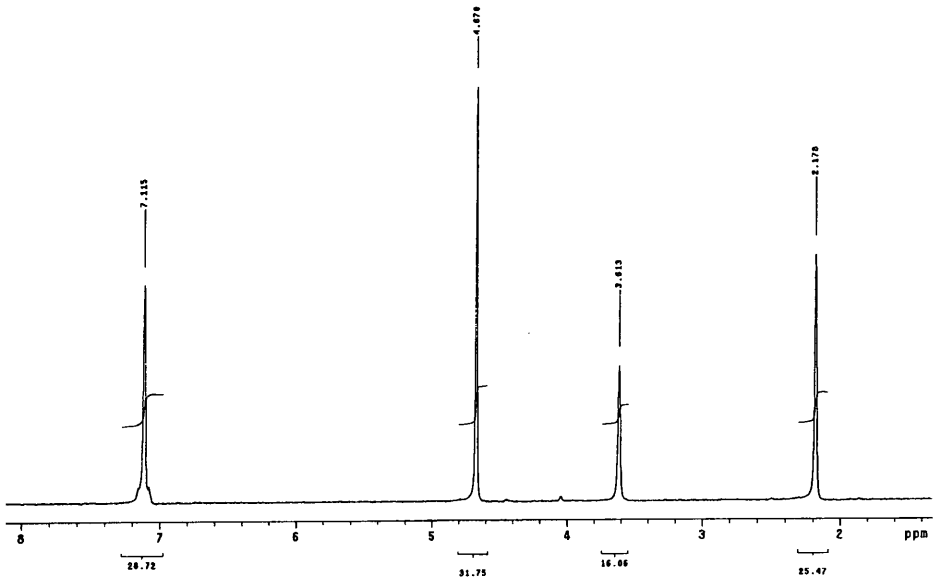

Table 6.21: ^{1}H NMR spectrum of 4-methylbenzylamine in 97 % D_2O / 3 % CD_3OD: peak assignments

δ / ppm	integral ratio	multiplicity	J / Hz	assignment
2.18	3	s	-	-$\mathbf{CH_3}$
3.61	2	s	-	-$\mathbf{CH_2}$$\mathbf{NH_2}$
4.67	-	-	-	D_2O, -$\mathbf{NH_2}$
7.12	4	m	-	Ar-**H2**, Ar-**H3**

The spectrum of 0.0150 M 4-methylbenzylamine and 0.0152 M $CH_2(OH)(SO_3Na)$ was obtained, then with each reagent in excess: 0.0152 M 4-methylbenzylamine with 0.030 M $CH_2(OH)(SO_3Na)$ and 0.0154 M 4-methylbenzylamine with 7.9×10^{-3} M $CH_2(OH)(SO_3Na)$. A spectrum was recorded immediately (3 to 4 minutes) after addition of the $CH_2(OH)(SO_3Na)$ then again after approximately 30 minutes, 1 hour and 2 hours and continued until there was no further change in the spectrum.

There are two possible products that may form in the reaction. Firstly, a 1 : 1 4-methylbenzylamine : $CH_2(OH)(SO_3Na)$ adduct 4-$CH_3C_6H_4CH_2NHCH_2SO_3^-$, **6.10**, can form. In the presence of excess $CH_2(OH)(SO_3Na)$, a second molecule may react to produce 4-$CH_3C_6H_4CH_2N(CH_2SO_3^-)_2$, **6.11**, the 1 : 2 4-methylbenzylamine : $CH_2(OH)(SO_3Na)$ adduct.

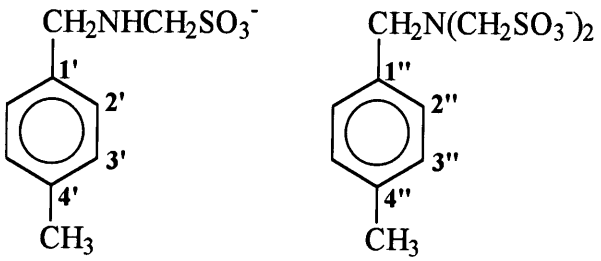

6.10 **6.11**

6.2.3.1.1 Equimolar 4-methylbenzylamine and $CH_2(OH)(SO_3Na)$

The results obtained for the reaction of equimolar 0.0152 M 4-methylbenzylamine and 0.0150 M $CH_2(OH)(SO_3Na)$ are shown in Figures 6.15 and 6.16 which show the spectra obtained 3 minutes and 38 minutes after mixing. There was no further change in the spectrum over time. Tables 6.22 and 6.23 summarise the information obtained from the two spectra.

Figure 6.15: 0.0152 M 4-methylbenzylamine and 0.0150 M $CH_2(OH)(SO_3Na)$: 3 minutes after mixing

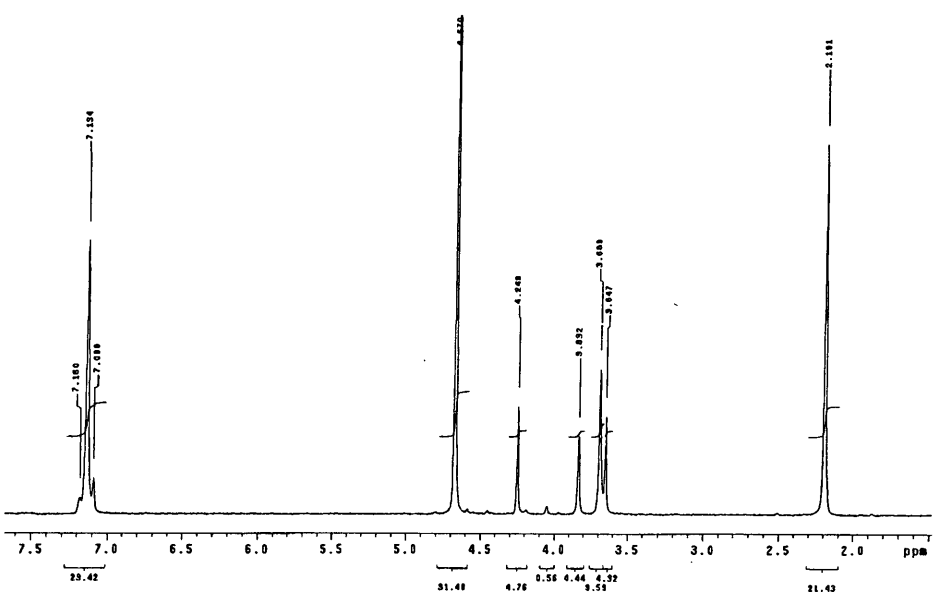

Table 6.22: Peak assignments: 3 minutes after mixing

time after mixing	δ / ppm	integral ratio	multiplicity	J / Hz	assignment
3 minutes	2.19	9	s	-	-C**H**$_3$
	3.65	2	s	-	-C**H**$_2$NHCH$_2$SO$_3^-$
	3.69	4	s	-	-C**H**$_2$NH$_2$
	3.83	2	s	-	-NHC**H**$_2$SO$_3^-$
	4.25	2	s	-	C**H**$_2$(OH)(SO$_3$Na)
	4.67	-	-	-	D$_2$O, -N**H**$_2$
	7.11	10	d	9	Ar-**H2**, Ar-**H3**
	7.16		d	9	Ar-**H2'**, Ar-**H3'**

Table 6.23: Peak assignments: 38 minutes after mixing

time after mixing	δ / ppm	integral ratio	multiplicity	J / Hz	assignment
38 minutes	2.19	10	s	-	-C**H**$_3$
	3.64	5	s	-	-C**H**$_2$NHCH$_2$SO$_3^-$
	3.71	2	s	-	-C**H**$_2$NH$_2$
	3.83	5	s	-	-NHC**H**$_2$SO$_3^-$
	4.24	-	s	-	C**H**$_2$(OH)(SO$_3$Na)
	4.67	-	-	-	D$_2$O, -N**H**$_2$
	7.11	12	d	9	Ar-**H2**, Ar-**H3**
	7.16		d	9	Ar-**H2'**, Ar-**H3'**

Figure 6.16: 0.0152 M 4-methylbenzylamine and 0.0150 M $CH_2(OH)(SO_3Na)$: 38 minutes after mixing

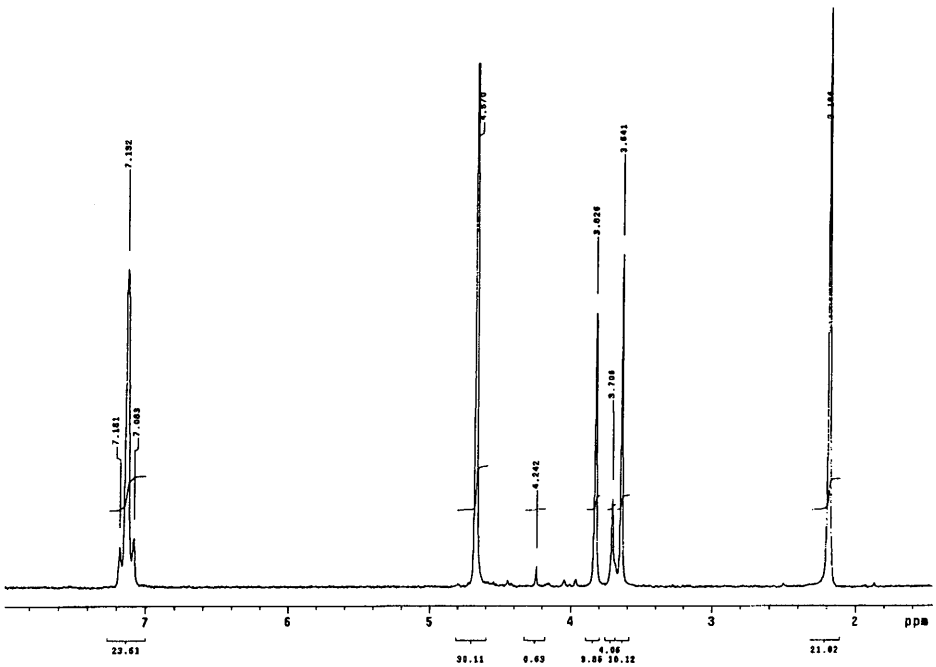

Within 3 minutes there is evidence of formation of the 1 : 1 adduct $4\text{-}CH_3C_6H_4CH_2NHCH_2SO_3^-$, with peaks at δ 3.65 and δ 3.83 ppm. These peaks increase in intensity over time. The reaction is complete within 38 minutes. The peak at δ 3.69 ppm is assigned to $\text{-}\mathbf{CH_2}NH_2$ in the parent compound, benzylamine. This is at a slightly higher resonance than expected but decreases in intensity over time as anticipated. After 38 minutes there is still evidence of unreacted amine in the aromatic region. Virtually all the $CH_2(OH)(SO_3Na)$ has reacted. There is no evidence of 1 : 2 adduct formation, $4\text{-}CH_3C_6H_4CH_2N(CH_2SO_3^-)_2$.

6.2.3.1.2 $CH_2(OH)(SO_3Na)$ in excess

The spectra obtained for the reaction of 0.0152 M 4-methylbenzylamine and 0.030 M $CH_2(OH)(SO_3Na)$ show the formation of the 1 : 1 adduct $4\text{-}CH_3C_6H_4CH_2NHCH_2SO_3^-$ and, over time, the 1 : 2 adduct, $4\text{-}CH_3C_6H_4CH_2N(CH_2SO_3^-)_2$. Table 6.24 summarises the spectra obtained 4 minutes and 1 hour after mixing. There was no further change in the spectrum over time.

Table 6.24: 0.0152 M 4-methylbenzylamine and 0.030 M $CH_2(OH)(SO_3Na)$: peak assignments

time after mixing	δ / ppm	integral ratio	multiplicity	J / Hz	assignment
4 minutes	2.20	3	s	-	-**C**$\mathbf{H_3}$
	3.65	1	s	-	-**C**$\mathbf{H_2}$NHC$\mathbf{H_2}$$SO_3^-$
	3.73	1	s	-	-**C**$\mathbf{H_2}$$NH_2$
	3.84	1	s	-	-NHC$\mathbf{H_2}$$SO_3^-$
	4.25	2	s	-	**C**$\mathbf{H_2}$(OH)(SO_3Na)
	4.67	-	-	-	D_2O, -N$\mathbf{H_2}$
	7.12	4	d	9	Ar-**H2**, Ar-**H3**
	7.17		d	9	Ar-**H2'**, Ar-**H3'**
1 hour	2.20	14	s	-	-**C**$\mathbf{H_3}$
	3.65	8	s	-	-**C**$\mathbf{H_2}$NHC$\mathbf{H_2}$$SO_3^-$
	3.84	8			-NHC$\mathbf{H_2}$$SO_3^-$
	3.91	1			-
	3.97	2			-N(C$\mathbf{H_2}$$SO_3^-$)$_2$
	4.16	1			-C$\mathbf{H_2}$N(C$H_2SO_3^-$)$_2$
	4.25	4			**C**$\mathbf{H_2}$(OH)(SO_3Na)
	4.67	-	-	-	D_2O, -N$\mathbf{H_2}$
	7.11	15			Ar-**H2**, Ar-**H3**
	7.16				Ar-**H2'**, Ar-**H3'**
	7.27	1			Ar-**H2''**, Ar-**H3''**

After 4 minutes there is substantial 1 : 1 adduct 4-$CH_3C_6H_4CH_2NHCH_2SO_3^-$ formation: benzylamine and the adduct are present in an approximately 1 : 1 ratio at this time. Within 36 minutes there is evidence of 1 : 2 adduct 4-$CH_3C_6H_4CH_2N(CH_2SO_3^-)_2$ formation with new peaks at δ 3.97 and δ 4.16 ppm in a 1 : 2 ratio. These peaks increase in intensity over time. New peaks in the aromatic region due to the 1 : 2 adduct also appear over time. The main product is the 1 : 1 adduct 4-$CH_3C_6H_4CH_2NHCH_2SO_3^-$.

The peak at δ 3.73 ppm is assigned to -C$\mathbf{H_2}$$NH_2$ in the parent compound, benzylamine. This is at a higher resonance than expected but decreases in intensity over time as

anticipated. After one hour this peak has disappeared completely. After 36 minutes a peak at δ 3.87 ppm is visible. After one hour this peak appears at δ 3.91 ppm. This peak has a relatively small intensity and could be due to an impurity in the sample.

6.2.3.1.3 4-Methylbenzylamine in excess

The spectra obtained for the reaction of 0.0154 M 4-methylbenzylamine and 7.9×10^{-3} M $CH_2(OH)(SO_3Na)$ show the formation of the 1 : 1 adduct $4\text{-}CH_3C_6H_4CH_2NHCH_2SO_3^-$. Table 6.25 summarises the spectra obtained 3 minutes and 30 minutes after mixing. There was no further change in the spectrum over time.

Table 6.25: 0.0154 M 4-methylbenzylamine and 7.9×10^{-3}M $CH_2(OH)(SO_3Na)$: peak assignments

time after mixing	δ / ppm	integral ratio	multiplicity	J / Hz	assignment
3 minutes	2.19	19	s	-	$-CH_3$
	3.65	12	s	-	$-CH_2NH_2$ and $-CH_2NHCH_2SO_3^-$
	3.83	3	s	-	$-NHCH_2SO_3^-$
	4.25	1	s	-	$CH_2(OH)(SO_3Na)$
	4.67	-	-	-	D_2O, $-NH_2$
	7.13	19	m	-	Ar-**H2**, **H3** and Ar-**H2'**, **H3'**
30 minutes	2.19	4	s	-	$-CH_3$
	3.65	3	s	-	$-CH_2NH_2$ and $-CH_2NHCH_2SO_3^-$
	3.84	1	s	-	$-NHCH_2SO_3^-$
	4.67	-	-	-	D_2O, $-NH_2$
	7.13	4	m	-	Ar-**H2**, **H3** and Ar-**H2'**, Ar-**H3'**

After 3 minutes there is evidence of 1 : 1 adduct 4-$CH_3C_6H_4CH_2NHCH_2SO_3^-$ formation. The reaction is complete within 30 minutes, After this time there is complete conversion of $CH_2(OH)(SO_3Na)$ to the product.

6.2.3.2 Uv / visible kinetic studies

4-Methylbenzylamine is not readily soluble in aqueous solution but is readily soluble in methanol, therefore a stock solution in methanol was prepared. Absorbance against wavelength spectra were obtained for the reaction of 0.10 M aqueous $CH_2(OH)(SO_3Na)$ with 1.0×10^{-3} M 4-methylbenzylamine at 25 °C in a 98 % water / 2 % methanol by volume solvent. The spectrum of 1.0×10^{-3} M 4-methylbenzylamine alone in a 98 % water / 2 % methanol by volume solvent was obtained for comparison. The spectrum with aqueous $CH_2(OH)(SO_3Na)$ added shows an increase in absorbance around 240 nm and a decrease in absorbance around 260 nm as compared to the spectrum of 1.0×10^{-3} M 4-methylbenzylamine alone. The reaction is complete within 1½ hours.

Figure 6.17 shows the change over time in the spectrum for the reaction with 0.10 M $CH_2(OH)(SO_3Na)$ as compared to that of 4-methylbenzylamine alone. Table 6.26 shows the peak positions and extinction coefficients (ε) for the two spectra.

Table 6.26: Spectral appearance in a 98 % water / 2 % methanol by volume solvent of 1.0×10^{-3} M 4-methylbenzylamine and with 0.10 M $CH_2(OH)(SO_3Na)$

$[CH_2(OH)(SO_3Na)]$ / M	λ_{max} / nm ($\varepsilon^{\dagger}$/ mol^{-1} dm^3 cm^{-1})
none	263 (430); 271 (330)
0.10	263 (370); 271 (260)

† based on the assumption that all the 4-methylbenzylamine reacts to give 1.0×10^{-3} M product

Figure 6.17: Change over time in the absorbance against wavelength spectrum for 1.0×10^{-3} M 4-methylbenzylamine, 0.10 M $CH_2(OH)(SO_3Na)$, 25 °C, in a 98 % 2.0 water / 2 % methanol by volume solvent

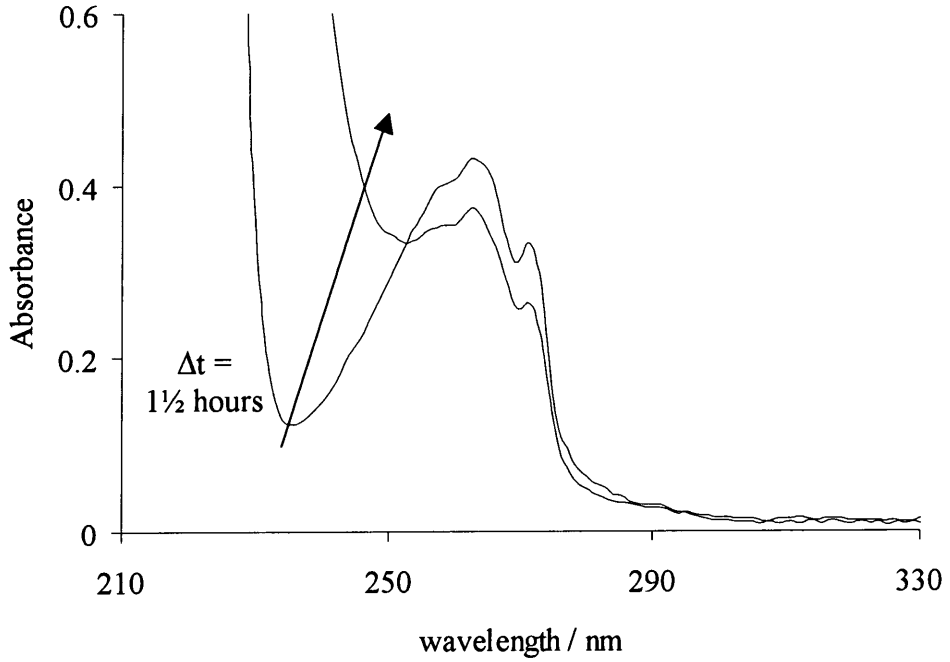

Plots of absorbance against time were obtained using conventional uv / vis spectrometry for the reaction of 1.0×10^{-3} M 4-methylbenzylamine with 0.010 to 0.10 M aqueous $CH_2(OH)(SO_3Na)$ at 25 °C in a 98 % water / 2 % methanol by volume solvent. Formation of the product at 240 nm was followed. The solutions were buffered at pH 7.0. Plots were first order: the k_{obs} / s^{-1} values obtained are shown in Table 6.27. There was no initial faster reaction detected.

Table 6.27: k_{obs} / s^{-1} values for the reaction of 4-methylbenzylamine with aqueous $CH_2(OH)(SO_3Na)$ at 25 °C in a 98 % water / 2 % methanol by volume solvent, pH 7.0

$[CH_2(OH)(SO_3Na)]$ / M	k_{obs} / s^{-1}
0.01	$9.02 \times 10^{-5} \pm 6.0 \times 10^{-6}$
0.02	$1.14 \times 10^{-4} \pm 2 \times 10^{-6}$
0.05	$3.52 \times 10^{-4} \pm 5 \times 10^{-6}$
0.08	$4.88 \times 10^{-4} \pm 6 \times 10^{-6}$
0.10	$5.45 \times 10^{-4} \pm 6 \times 10^{-6}$

Plotting k_{obs} / s^{-1} against [$CH_2(OH)(SO_3Na)$] / M gives a linear plot and allows the determination of the forward and back rate constants, $k_{f(app)}$ / dm^3 mol^{-1} s^{-1} and k_b / s^{-1}, equal to the gradient and intercept respectively.

Linear regression yields values of $k_{f(app)}$ and k_b of $5.39 \times 10^{-3} \pm 5.0 \times 10^{-4}$ dm^3 mol^{-1} s^{-1} and $3.75 \times 10^{-5} \pm 3.10 \times 10^{-5}$ s^{-1} respectively: a correlation coefficient of 0.975 is obtained. These values give an equilibrium constant, $K_{(app)}$, equal to $k_{f(app)} / k_b$, of 140 ± 120 dm^3 mol^{-1}.

6.2.4 Reaction of $CH_2(OH)(SO_3Na)$ with 4-nitrobenzylamine

6.2.4.1 ^1H NMR studies

4-Nitrobenzylamine is purchased as the hydrochloride. When the solid was used in this form to follow the reaction of $CH_2(OH)(SO_3Na)$ with 4-nitrobenzylamine in D_2O, no peaks due to a 1 : 1 or 1 : 2 adduct were observed. The protonated form of the amine will be less nucleophilic and hence the reaction will be retarded if not completely suppressed. Therefore the experiment was repeated with sodium hydroxide (NaOH) solution in D_2O added to neutralise the amine prior to reaction with $CH_2(OH)(SO_3Na)$. The maximum NaOH solution concentration that could be added to the 0.2 M amine solution without the solution becoming cloudy was 0.134 M, consequently the amine will not be completely neutralised. The cloudiness is likely to be due to precipitation of free amine which will be less soluble than its salt. $CH_2(OH)(SO_3Na)$ was found to react with NaOH, therefore the amine needs to be in slight excess in any case, to prevent $CH_2(OH)(SO_3Na)$ reacting with excess NaOH.

The spectrum of 0.20 M 4-nitrobenzylamine hydrochloride in D_2O was obtained initially (Figure 6.18, Table 6.28): this spectrum will be mainly due to protonated 4-nitrobenzylamine, $4\text{-}NO_2C_6H_4CH_2NH_3^+$. The spectrum of 0.19 M 4-nitrobenzylamine hydrochloride with 0.134 M NaOH solution in D_2O was also obtained (Figure 6.19, Table 6.29). This spectrum will be mainly due to unprotonated 4-nitrobenzylamine, $4\text{-}NO_2C_6H_4CH_2NH_2$, **6.4**, with a small amount of the protonated form present.

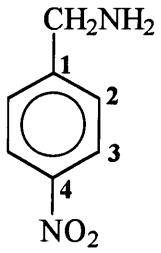

6.4

Figure 6.18: ^{1}H NMR spectrum of 4-nitrobenzylamine hydrochloride in D_2O

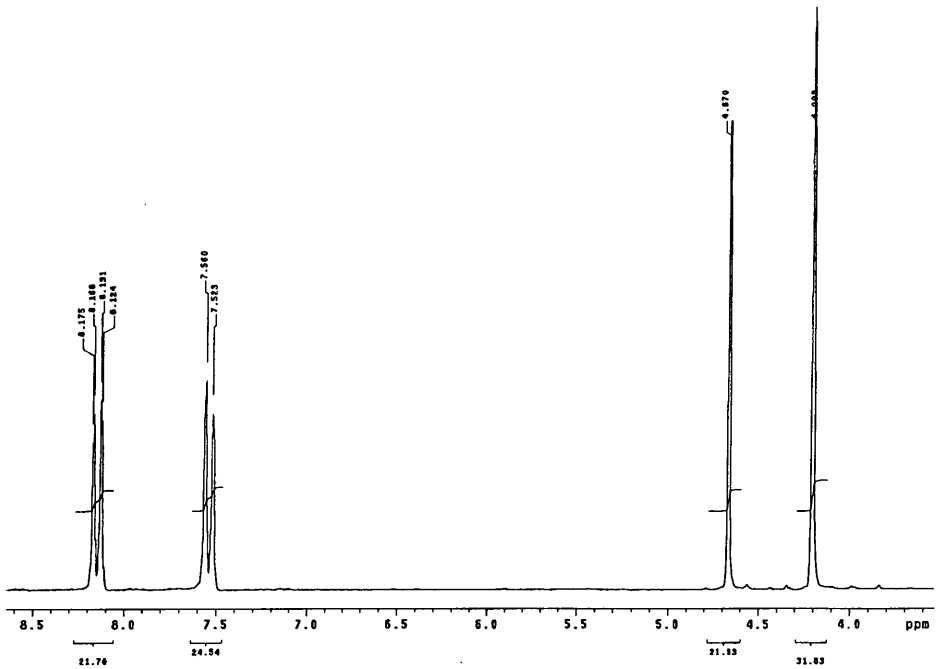

Table 6.28: ^{1}H NMR spectrum of 4-nitrobenzylamine hydrochloride in D_2O: peak assignments

δ / ppm	integral ratio	multiplicity	J / Hz	assignment
4.20	2	s	-	$-CH_2N^+H_3$
4.67	-	-	-	D_2O, $-NH_2$
7.54	2	d	7.5	Ar-**H2**
8.15	2	d	7.5	Ar-**H3**

Figure 6.19: ^{1}H NMR spectrum of 0.19 M 4-nitrobenzylamine hydrochloride with 0.134 M NaOH in D_2O

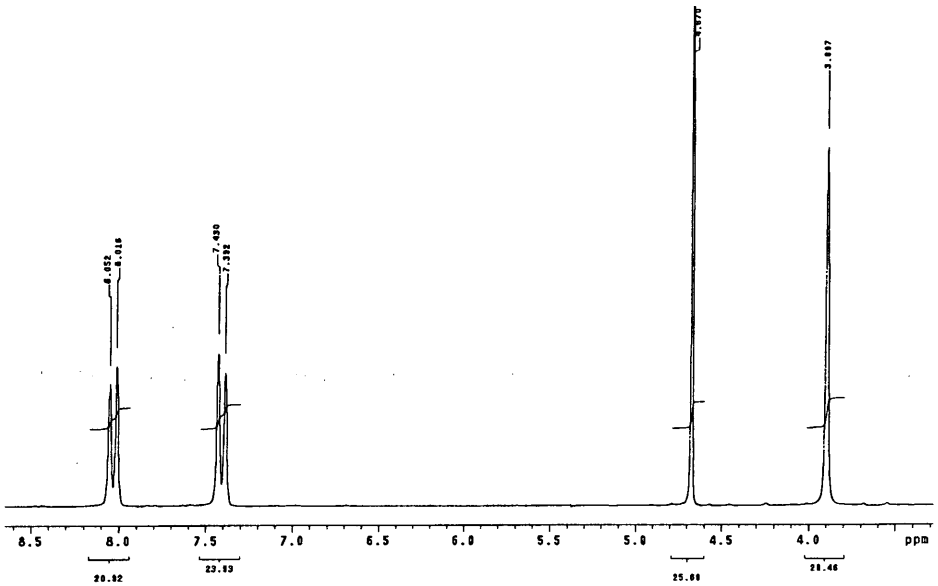

Table 6.29: ^{1}H NMR of 0.19 M 4-nitrobenzylamine hydrochloride with 0.134 M NaOH in D_2O: peak assignments

δ / ppm	integral ratio	multiplicity	J / Hz	assignment
3.90	2	s	-	-$\mathbf{CH_2}$$NH_2$
4.67	-	-	-	D_2O, -$\mathbf{NH_2}$
7.41	2	d	7.5	Ar-**H2**
8.03	2	d	7.5	Ar-**H3**

The spectrum of 4-nitrobenzylamine shows a shift upfield to lower δ / ppm when neutralised.

The spectrum of 0.18 M 4-nitrobenzylamine hydrochloride, neutralised with 0.13 M NaOH, and 0.18 M $CH_2(OH)(SO_3Na)$ was obtained, then with each reagent in excess: 0.18 M 4-nitrobenzylamine hydrochloride with 0.35 M $CH_2(OH)(SO_3Na)$ and 0.19 M 4-nitrobenzylamine hydrochloride with 0.09 M $CH_2(OH)(SO_3Na)$, each in the presence of 0.13 M NaOH. A spectrum was recorded immediately (3 to 4 minutes) after addition of the $CH_2(OH)(SO_3Na)$ then again after approximately 30 minutes and 1 hour. After this time the solutions became cloudy and it was not possible to obtain further spectra.

There are two possible products that may form in the reaction. Firstly, a 1 : 1 4-nitrobenzylamine : $CH_2(OH)(SO_3Na)$ adduct $4\text{-}NO_2C_6H_4CH_2NHCH_2SO_3^-$, **6.12**, can form. In the presence of excess $CH_2(OH)(SO_3Na)$, a second molecule may react to give a 1 : 2 4-nitrobenzylamine : $CH_2(OH)(SO_3Na)$ adduct, $4\text{-}NO_2C_6H_4CH_2N(CH_2SO_3^-)_2$, **6.13**.

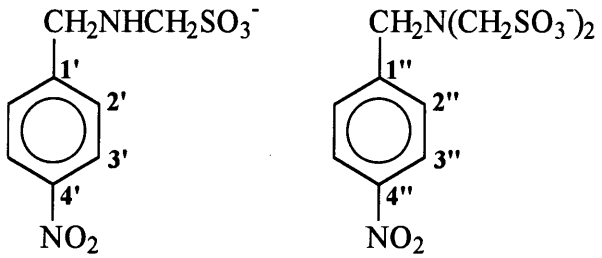

6.12 **6.13**

6.2.4.1.1 Equimolar 4-nitrobenzylamine and $CH_2(OH)(SO_3Na)$

The results obtained for the reaction of equimolar 0.18 M 4-nitrobenzylamine hydrochloride with 0.13 M NaOH and 0.18 M $CH_2(OH)(SO_3Na)$ are shown in Figures 6.20, 6.21 and 6.22 which show the spectra obtained 3 minutes, 31 minutes and 1 hour after mixing respectively. Tables 6.30, 6.31 and 6.32 summarise the information obtained from the three spectra.

Figure 6.20: 0.18 M 4-nitrobenzylamine hydrochloride with 0.13 M NaOH and 0.18 M $CH_2(OH)(SO_3Na)$: 3 minutes after mixing

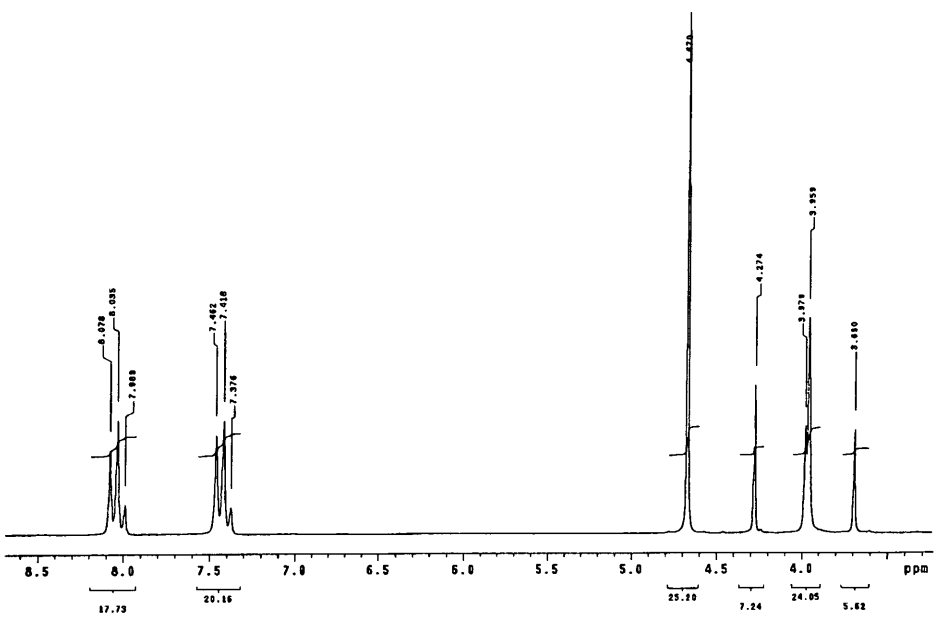

Table 6.30: Peak assignments: 3 minutes after mixing

time after mixing	δ / ppm	integral ratio	multiplicity	J / Hz	assignment
3 minutes	3.69	1	s	-	-C**H**$_2$NHCH$_2$SO$_3^-$
	3.96	4	s	-	-C**H**$_2$NH$_2$
	3.98		s	-	-NHC**H**$_2$SO$_3^-$
	4.27	1	s	-	C**H**$_2$(OH)(SO$_3$Na)
	4.67	-	-	-	D$_2$O, -N**H**$_2$
	7.40	4	d	9	Ar-**H2**
	7.44		d	9	Ar-**H2'**
	8.01	3	d	9	Ar-**H3**
	8.06		d	9	Ar-**H3'**

Table 6.31: Peak assignments: 31 minutes after mixing

time after mixing	δ / ppm	integral ratio	multiplicity	J / Hz	assignment
31 minutes	3.70	7	s	-	-C**H**$_2$NHCH$_2$SO$_3^-$
	3.99	7	s	-	-NHC**H**$_2$SO$_3^-$
	4.19	3	s	-	-C**H**$_2$N$^+$H$_3$
	4.28	1	s	-	C**H**$_2$(OH)(SO$_3$Na)
	4.67	-	-	-	D$_2$O, -N**H**$_2$
	7.41	7	d	9	Ar-**H2'**
	7.52		d	9	Ar-**H2**
	8.03	7	d	9	Ar-**H3'**
	8.11		d	9	Ar-**H3**

Figure 6.21: 0.18 M 4-nitrobenzylamine hydrochloride with 0.13 M NaOH and 0.18 M $CH_2(OH)(SO_3Na)$: 31 minutes after mixing

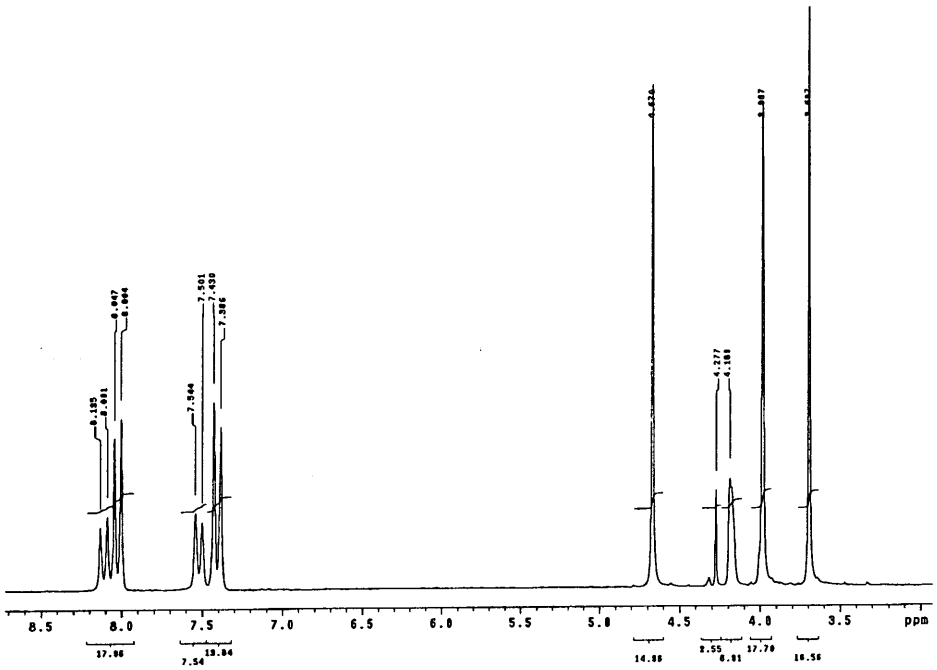

Figure 6.22: 0.18 M 4-nitrobenzylamine hydrochloride with 0.13 M NaOH and 0.18 M $CH_2(OH)(SO_3Na)$: 1 hour after mixing

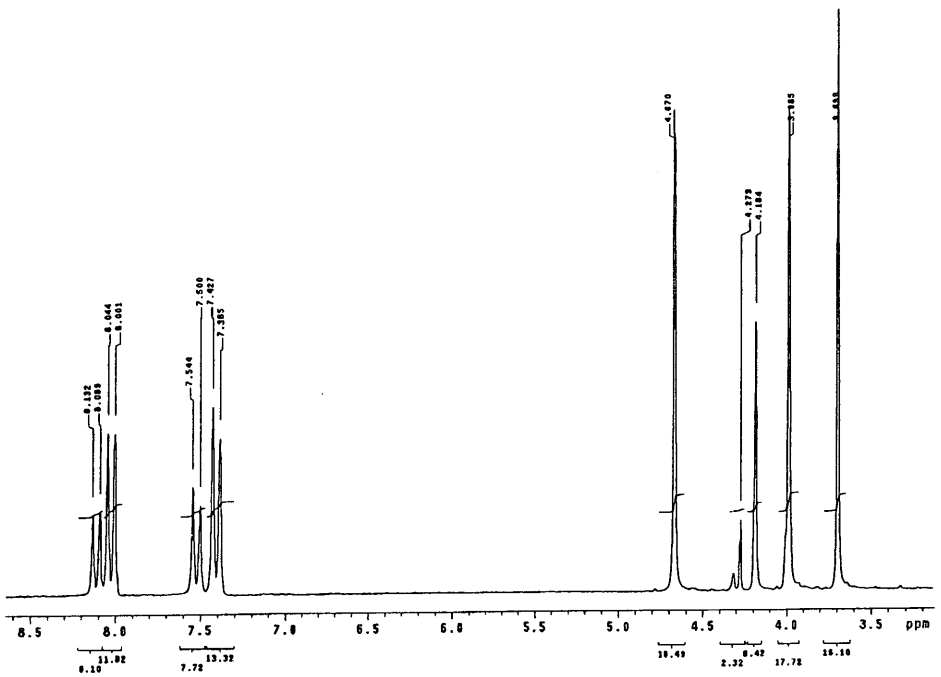

Table 6.32: Peak assignments: 1 hour after mixing

time after mixing	δ / ppm	integral ratio	multiplicity	J / Hz	assignment
1 hour	3.69	7	s	-	$-CH_2NHCH_2SO_3^-$
	3.99	7	s	-	$-NHCH_2SO_3^-$
	4.18	4	s	-	$-CH_2N^+H_3$
	4.27	1	s	-	$CH_2(OH)(SO_3Na)$
	4.67	-	-	-	D_2O, $-NH_2$
	7.41	5	d	9	Ar-**H2'**
	7.52	3	d	9	Ar-**H2**
	8.02	5	d	9	Ar-**H3'**
	8.11	3	d	9	Ar-**H3**

After 3 minutes there is evidence of formation of a small amount of 1 : 1 adduct $4\text{-}NO_2C_6H_4CH_2NHCH_2SO_3^-$ in addition to peaks due to $CH_2(OH)(SO_3Na)$ and unprotonated 4-nitrobenzylamine. After 31 minutes there is substantial 1 : 1 adduct formation and no unprotonated 4-nitrobenzylamine remaining. However there is evidence of protonated 4-nitrobenzylamine due to the appearance of a peak corresponding to $-CH_2N^+H_3$ at δ 4.19 ppm and peaks in the aromatic region at δ 7.52 and δ 8.11 ppm. The reaction is complete within 1 hour. After this time the reaction mixture consists of 1 : 1 adduct and protonated 4-nitrobenzylamine in an approximately 2 : 1 ratio.

There is no evidence of formation of a 1 : 2 adduct. The presence of the $4\text{-}NO_2$ electron withdrawing group on benzylamine will reduce the nucleophilicity of the nitrogen therefore reducing the tendency to add a second $CH_2(OH)(SO_3Na)$ molecule.

6.2.4.1.2 $CH_2(OH)(SO_3Na)$ in excess

The spectra obtained for the reaction of 0.18 M 4-nitrobenzylamine hydrochloride with 0.13 M NaOH and 0.35 M $CH_2(OH)(SO_3Na)$ show formation of the 1 : 1 adduct $4\text{-}NO_2C_6H_4CH_2NHCH_2SO_3^-$ and the presence of protonated 4-nitrobenzylamine.

Table 6.33 summarises the spectra obtained 3 minutes and 33 minutes after mixing. There was no further change in the spectrum over time.

Table 6.33: 0.18 M 4-nitrobenzylamine hydrochloride with 0.13 M NaOH and 0.35 M $CH_2(OH)(SO_3Na)$: peak assignments

time after mixing	δ / ppm	integral ratio	multiplicity	J / Hz	assignment
3 minutes	3.70	1	s	-	$-CH_2NHCH_2SO_3^-$
	3.99	1	s	-	$-NHCH_2SO_3^-$
	4.08	2	s	-	$-CH_2N^+H_3$
	4.29	2	s	-	$CH_2(OH)(SO_3Na)$
	4.67	-	-	-	D_2O, $-NH_2$
	7.41	2	d	9	Ar-**H2'**
	7.49		d	9	Ar-**H2**
	8.03	2	d	9	Ar-**H3'**
	8.10		d	9	Ar-**H3**
33 minutes	3.72	2	s	-	$-CH_2NHCH_2SO_3^-$
	4.01	2	s	-	$-NHCH_2SO_3^-$
	4.22	2	s	-	$-CH_2N^+H_3$
	4.29	2	s	-	$CH_2(OH)(SO_3Na)$
	4.67	-	-	-	D_2O, $-NH_2$
	7.43	1	d	9	Ar-**H2'**
	7.55	1	d	9	Ar-**H2**
	8.04	1	d	9	Ar-**H3'**
	8.14	1	d	9	Ar-**H3**

Within 3 minutes there is 1 : 1 adduct $4\text{-}NO_2C_6H_4CH_2NHCH_2SO_3^-$ formation. There is also evidence of protonated 4-nitrobenzylamine in the spectrum. The peak due to $-CH_2N^+H_3$ is relatively broad and is at a slightly lower frequency than expected. This is probably an averaged peak due to both protonated and unreacted unprotonated 4-nitrobenzylamine.

The reaction is complete within 33 minutes. After this time there is no unprotonated 4-nitrobenzylamine remaining and the 1 : 1 adduct and protonated 4-nitrobenzylamine are present in approximately equal proportions.

6.2.4.1.3 4-Nitrobenzylamine in excess

The spectra obtained for the reaction of 0.19 M 4-nitrobenzylamine hydrochloride with 0.13 M NaOH and 0.09 M $CH_2(OH)(SO_3Na)$ show formation of the 1 : 1 adduct $C_6H_5CH_2NHCH_2SO_3^-$ and the presence of protonated 4-nitrobenzylamine. Table 6.34 summarises the spectra obtained 4 minutes and 33 minutes after mixing.

Table 6.34: 0.19 M 4-nitrobenzylamine hydrochloride with 0.13 M NaOH and 0.09 M $CH_2(OH)(SO_3Na)$: peak assignments

time after mixing	δ / ppm	integral ratio	multiplicity	J / Hz	assignment
4 minutes	3.68	1	s	-	-CH_2NHCH$_2SO_3^-$
	3.97	6	s	-	-NHC$H_2SO_3^-$
	4.01		s	-	-CH_2NH_2 and -$CH_2N^+H_3$
	4.27	1	s	-	$CH_2(OH)(SO_3Na)$
	4.67	-	-	-	D_2O, -NH_2
	7.39	4	d	9	Ar-**H2'**
	7.46		d	9	Ar-**H2**
	8.00	4	d	9	Ar-**H3'**
	8.07		d	9	Ar-**H3**
33 minutes	3.68	1	s	-	-CH_2NHCH$_2SO_3^-$
	3.97	1	s	-	-NHC$H_2SO_3^-$
	4.06	2	s	-	-CH_2NH_2 and -$CH_2N^+H_3$
	4.67	-	-	-	D_2O, -NH_2
	7.39	2	d	9	Ar-**H2'**
	7.47		d	9	Ar-**H2**
	8.00	2	d	9	Ar-**H3'**
	8.08		d	9	Ar-**H3**

Within 4 minutes there is 1 : 1 adduct $4\text{-}NO_2C_6H_4CH_2NHCH_2SO_3^-$ formation. The peaks increase in intensity over time and the reaction is complete within 33 minutes. After this time, all the $CH_2(OH)(SO_3Na)$ has reacted. There is also evidence of unreacted unprotonated 4-nitrobenzylamine and protonated 4-nitrobenzylamine in the spectrum. This mixture gives averaged peaks at frequencies intermediate between the unprotonated and protonated 4-nitrobenzylamine spectra.

6.2.4.2 Uv / visible kinetic studies

Absorbance against wavelength spectra were obtained for the reaction of 0.10 M aqueous $CH_2(OH)(SO_3Na)$ with 2.0×10^{-4} M 4-nitrobenzylamine hydrochloride at 25 °C in aqueous solution. The spectrum shows a shift to higher wavelength over time as compared to the spectrum of 2.0×10^{-4} M 4-nitrobenzylamine hydrochloride alone. The reaction is complete within 2 hours.

Figure 6.23 shows the change over time in the spectrum with 0.10 M $CH_2(OH)(SO_3Na)$ as compared to that of 4-nitrobenzylamine hydrochloride alone. Table 6.35 summarises the peak positions and extinction coefficients (ε) for the two spectra.

Figure 6.22: Change over time in absorbance against wavelength spectrum for 0.10 M $CH_2(OH)(SO_3Na)$, 2.0×10^{-4} M 4-nitrobenzylamine hydrochloride at 25 °C in aqueous solution

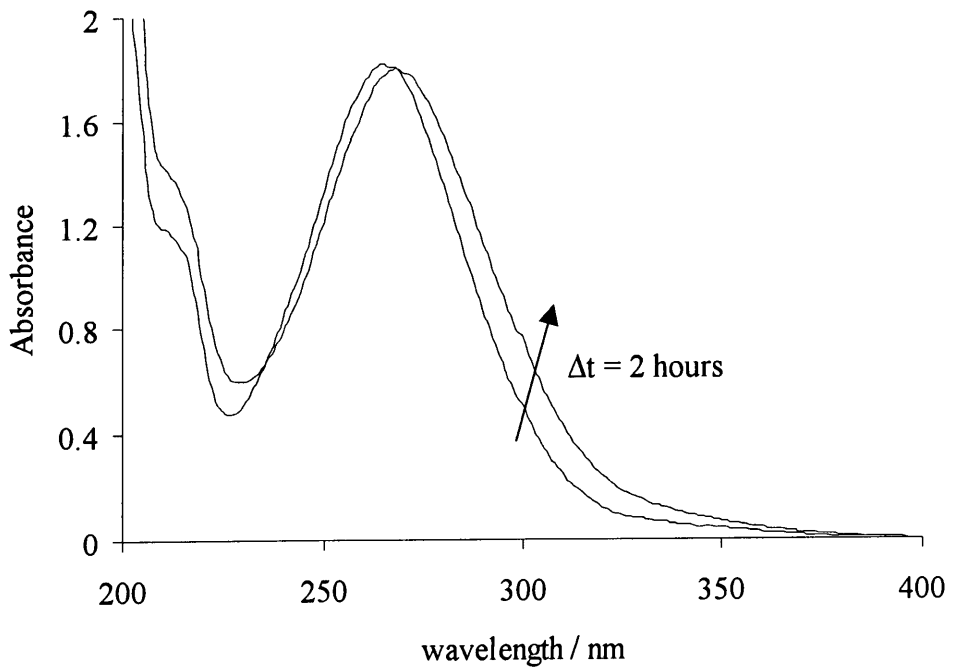

Table 6.35: Spectral appearance in aqueous solution of 2.0×10^{-4} M 4-nitrobenzylamine hydrochloride and with 0.10 M $CH_2(OH)(SO_3Na)$

$[CH_2(OH)(SO_3Na)]$ / M	λ_{max} / nm ($\varepsilon^{\dagger}$/ mol^{-1} dm^3 cm^{-1})
none	265 (9100)
0.10	268 (9000)

† based on the assumption that all the 4-nitrobenzylamine hydrochloride reacts to give 2×10^{-4} M product

Plots of absorbance against time were obtained for the reaction of 2.0×10^{-4} M 4-nitrobenzylamine hydrochloride with 0.010 to 0.10 M aqueous $CH_2(OH)(SO_3Na)$ at 25 °C, pH 7.0. As $CH_2(OH)(SO_3Na)$ is added in great excess, prior neutralisation of the 4-nitrobenzylamine hydrochloride was deemed unnecessary. Formation of the product at 315 nm was followed (Figure 6.24).

Figure 6.24: Plots of absorbance against time for the reaction of 2.0×10^{-4} M 4-nitrobenzylamine hydrochloride with aqueous $CH_2(OH)(SO_3Na)$ at 25 °C, pH 7.0

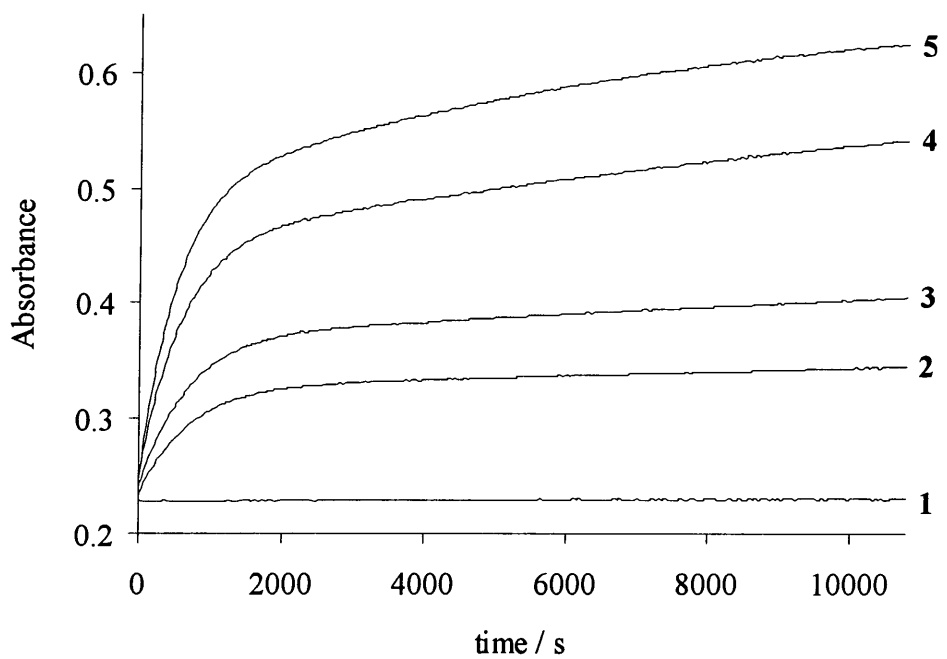

1 = no $CH_2(OH)(SO_3Na)$; **2** = 0.01 M $CH_2(OH)(SO_3Na)$; **3** = 0.02 M; **4** = 0.05 M; **5** = 0.10 M

The plots indicate that there are two processes occurring: two first order reactions. The two processes are relatively well separated therefore each was fitted separately. The k_{obs} / s^{-1} values obtained are shown in Table 6.36.

Table 6.36: k_{obs} / s^{-1} values for the reaction of 4×10^{-3} M 4-nitrobenzylamine hydrochloride with aqueous $CH_2(OH)(SO_3Na)$ at 25 °C, pH 7.0

$[CH_2(OH)(SO_3Na)]$ / M	first reaction†		second reaction§	
	k_{obs} / s^{-1}	A_∞	k_{obs} / s^{-1}	A_∞
0.010	$1.45 \times 10^{-3} \pm 5 \times 10^{-6}$	0.33	$8.24 \times 10^{-5} \pm 5 \times 10^{-7}$	0.36
0.020	$1.38 \times 10^{-3} \pm 3 \times 10^{-5}$	0.38	$1.29 \times 10^{-4} \pm 9 \times 10^{-7}$	0.42
0.050	$1.65 \times 10^{-3} \pm 6 \times 10^{-5}$	0.47	$1.48 \times 10^{-4} \pm 9 \times 10^{-7}$	0.57
0.10	$1.54 \times 10^{-3} \pm 5 \times 10^{-5}$	0.54	$1.86 \times 10^{-4} \pm 9 \times 10^{-7}$	0.65

† fitted using data from 0 to 1224 - 1512 s

§ fitted using data from 3600 to 10800 s

The value of the second rate constant increases with increasing $CH_2(OH)(SO_3Na)$ concentration, whereas the rate constant for the initial reaction shows no real dependence on concentration. Plotting k_{obs} / s^{-1} against $[CH_2(OH)(SO_3Na)]$ / M for the second reaction gives a linear plot with a gradient and intercept equal to $9.92 \times 10^{-4} \pm 2.75 \times 10^{-4}$ dm^3 mol^{-1} and $9.17 \times 10^{-5} \pm 1.57 \times 10^{-5}$ s^{-1} respectively. Linear regression gives a correlation coefficient of 0.866. These values give an equilibrium constant, $K_{(app)}$, equal to 11 ± 4 dm^3 mol^{-1}.

The observation of two rate processes in this system is difficult to rationalise. The ^1H NMR spectra do not show evidence of formation of an adduct with 1 : 2 stoichiometry, so the likely product is the 1 : 1 adduct. It is possible that the initial reaction corresponds to formation of an intermediate, such as the *N*-(hydroxymethyl)amine, and the second reaction relates to formation of the adduct. However no intermediate is observed in the ^1H NMR spectra. It is possible that there is variation in the sulfite concentration over time and it is this that causes the apparent change in absorbance against time plot.

6.2.5 Reaction of $CH_2(OH)(SO_3Na)$ with *N*-methylbenzylamine

6.2.5.1 ^{1}H NMR studies

N-Methylbenzylamine is not readily soluble in aqueous solution at the concentrations required therefore a mixed solvent system was used. The reaction of $CH_2(OH)(SO_3Na)$ with *N*-methylbenzylamine in a 97 % D_2O / 3 % methyl-d_3 alcohol-d, CD_3OD, by volume solvent was followed using ^{1}H NMR spectroscopy. Lower concentrations of reactants had to be used for this amine to be soluble in a solvent system with this proportion of water. Initially, the spectrum of 0.016 M *N*-methylbenzylamine (**6.5**) in 97 % D_2O / 3 % CD_3OD by volume was obtained for comparison (Figure 6.25, Table 6.37).

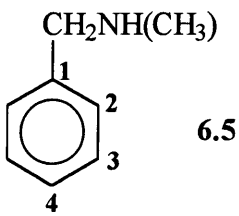

6.5

Figure 6.25: ^{1}H NMR spectrum of *N*-methylbenzylamine in 97 % D_2O / 3 % CD_3OD

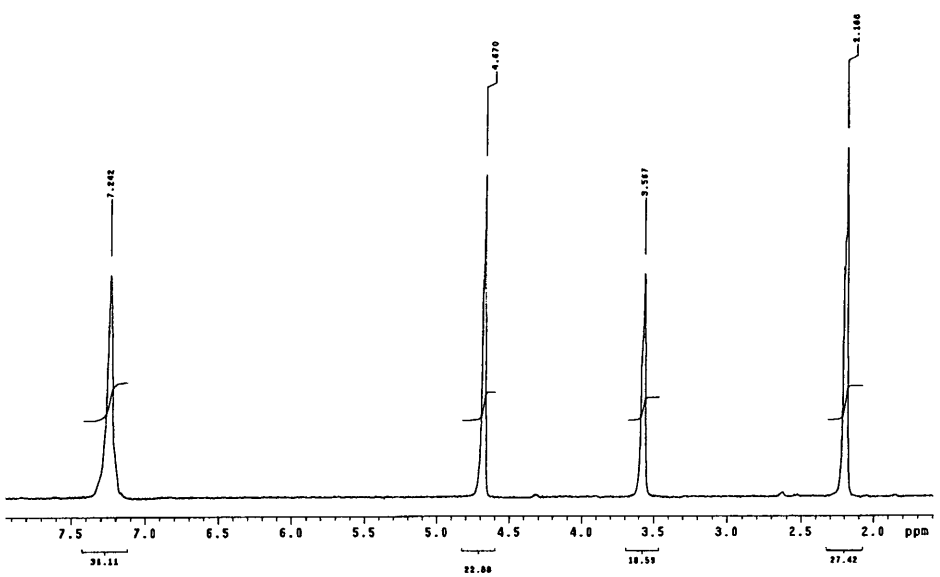

Table 6.37: ^{1}H NMR spectrum of *N*-methylbenzylamine in 97 % D_2O / 3 % CD_3OD: peak assignments

δ / ppm	integral ratio	multiplicity	J / Hz	assignment
2.19	3	s	-	-NH(CH_3)
3.57	2	s	-	-CH_2NH(CH_3)
4.67	-	-	-	D_2O, -NH_2
7.24	5	m	-	Ar-**H2**, **H3**, and **H4**

The spectrum of 0.0150 M *N*-methylbenzylamine and 0.0150 M $CH_2(OH)(SO_3Na)$ was obtained, then with each reagent in excess: the spectra of 0.0150 M *N*-methylbenzylamine and 0.030 M $CH_2(OH)(SO_3Na)$ and the spectra of 0.0152 M *N*-methylbenzylamine and 7.9×10^{-3} M $CH_2(OH)(SO_3Na)$ were acquired. All reactions were followed over time: a spectrum was recorded immediately (3 minutes) after addition of the $CH_2(OH)(SO_3Na)$ then again after approximately 30 minutes, 1 hour and 2 hours and continued until there was no further change in the spectrum.

There is only one product that can form in the reaction, a 1 : 1 *N*-methylbenzylamine : $CH_2(OH)(SO_3Na)$ adduct $C_6H_5CH_2N(CH_3)(CH_2SO_3^-)$, **6.14**. A 1 : 2 adduct is not possible as the amine is secondary rather than primary.

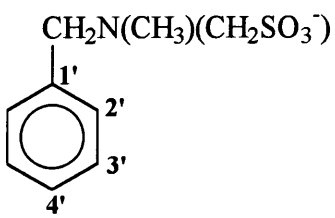

6.14

6.2.5.1.1 Equimolar *N*-methylbenzylamine and $CH_2(OH)(SO_3Na)$

The results obtained for the reaction of equimolar 0.015 M *N*-methylbenzylamine and 0.015 M $CH_2(OH)(SO_3Na)$ are shown in Figure 6.26 which shows the spectrum obtained 3 minutes after mixing. There was no further change in the spectrum over time. Table 6.38 summarises the information obtained from the spectrum.

Figure 6.26: 0.015 M *N*-methylbenzylamine and 0.015 M $CH_2(OH)(SO_3Na)$: 3 minutes after mixing

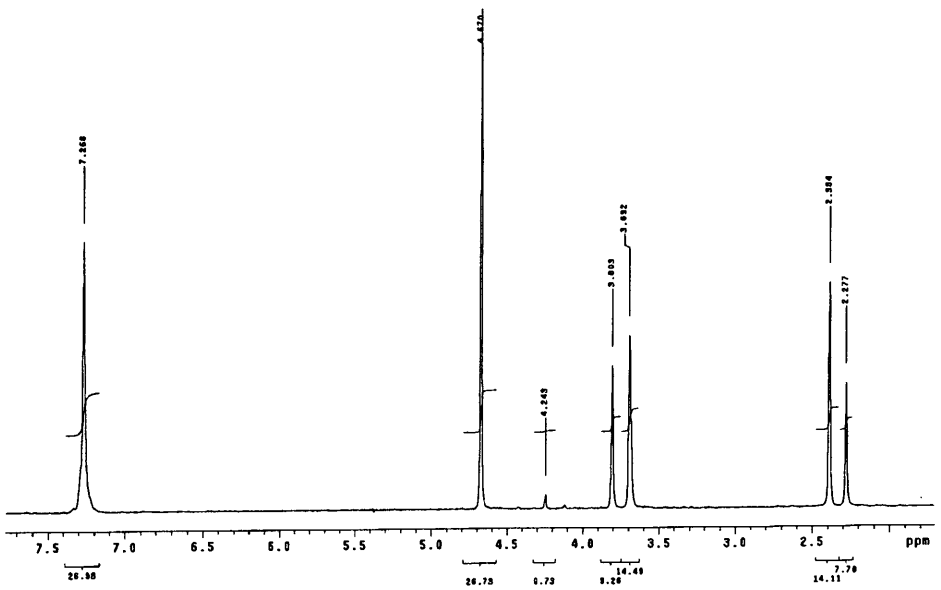

Table 6.38: Peak assignments: 3 minutes after mixing

time after mixing	δ/ppm	integral ratio	multiplicity	J/Hz	assignment
3 minutes	2.28	3	s	-	-NH(**CH$_3$**)
	2.38	6	s	-	-N(**CH$_3$**)($CH_2SO_3^-$)
	3.69	6	s	-	-**CH$_2$**NH(CH_3)
	3.69		s	-	.**CH$_2$**N(CH_3)($CH_2SO_3^-$)
	3.80	4	s	-	-N(CH_3)(**CH$_2$**SO_3^-)
	4.24	-	s	-	**CH$_2$**(OH)(SO_3Na)
	4.67	-	-	-	D_2O, -**NH$_2$**
	7.27	15	m	-	Ar-**H2**, **H3**, **H4** and Ar-**H2'**, **H3'**, **H4'**

The reaction is complete within 3 minutes. After this time there is evidence of formation of the 1 : 1 adduct $C_6H_5CH_2N(CH_3)(CH_2SO_3^-)$. There is still a small amount of unreacted *N*-methylbenzylamine and $CH_2(OH)(SO_3Na)$ remaining.

6.2.5.1.2 $CH_2(OH)(SO_3Na)$ in excess

The spectra obtained for the reaction of 0.015 M *N*-methylbenzylamine and 0.030 M $CH_2(OH)(SO_3Na)$ show the formation of the 1 : 1 adduct $C_6H_5CH_2N(CH_3)(CH_2SO_3^-)$. Table 6.39 summarises the spectrum obtained 3 minutes after mixing. There was no further change in the spectrum over time.

Table 6.39: 0.015 M *N*-methylbenzylamine and 0.03 M $CH_2(OH)(SO_3Na)$: peak assignments

time after mixing	δ/ppm	integral ratio	multiplicity	J/Hz	assignment
3 minutes	2.39	3	s	-	-N(**CH₃**)($CH_2SO_3^-$)
	3.70	2	s	-	.**CH₂**N(CH_3)($CH_2SO_3^-$)
	3.81	2	s	-	-N(CH_3)(**CH₂**SO_3^-)
	4.25	1	s	-	**CH₂**(OH)(SO_3Na)
	4.67	-	-	-	D_2O, -N**H₂**
	7.27	5	m	-	Ar-**H2'**, **H3'**, **H4'**

After 3 minutes there is substantial 1 : 1 adduct $C_6H_5CH_2N(CH_3)(CH_2SO_3^-)$ formation. There is complete conversion of the *N*-methylbenzylamine to the adduct after this time.

6.2.5.1.3 *N*-Methylbenzylamine in excess

The spectra obtained for the reaction of 0.0152 M *N*-methylbenzylamine and 7.9×10^{-3} M $CH_2(OH)(SO_3Na)$ show the formation of the 1 : 1 adduct $C_6H_5CH_2N(CH_3)(CH_2SO_3^-)$. Table 6.40 summarises the spectrum obtained 3 minutes after mixing. There was no further change in the spectrum over time.

After 3 minutes there is evidence of 1 : 1 adduct $C_6H_5CH_2N(CH_3)(CH_2SO_3^-)$ formation. After this time there is complete conversion of $CH_2(OH)(SO_3Na)$ to the product.

Table 6.40: 0.0152 M *N*-methylbenzylamine and 7.9×10^{-3}M $CH_2(OH)(SO_3Na)$: peak assignments

time after mixing	δ/ppm	integral ratio	multiplicity	J/Hz	assignment
3 minutes	2.22	6	s	-	-NH($\mathbf{CH_3}$)
	2.39	3	s	-	-N($\mathbf{CH_3}$)($CH_2SO_3^-$)
	3.61	4	s	-	-$\mathbf{CH_2}$NH(CH_3)
	3.70	2	s	-	.$\mathbf{CH_2}$N(CH_3)($CH_2SO_3^-$)
	3.81	2	s	-	-N(CH_3)($\mathbf{CH_2}SO_3^-$)
	4.67	-	-	-	D_2O, -$\mathbf{NH_2}$
	7.26	10	s	-	Ar-**H2**, **H3**, **H4**
	7.27		s	-	Ar-**H2'**, **H3'**, **H4'**

6.2.5.2 Uv / visible kinetic studies

6.2.5.2.1 Absorbance against wavelength spectra and absorbance against time plots

N-Methylbenzylamine is not readily soluble in aqueous solution but is readily soluble in methanol, therefore a stock solution in methanol was prepared. Absorbance against wavelength spectra were obtained for the reaction of 0.10 M aqueous $CH_2(OH)(SO_3Na)$ with 1.0×10^{-3} M *N*-methylbenzylamine at 25 °C in 98 % water / 2 % methanol by volume solvent. The spectrum of 1.0×10^{-3} M *N*-methylbenzylamine alone in a 98 % water / 2 % methanol by volume solvent was obtained for comparison. The spectrum shows an increase in absorbance around 230 nm and a decrease in absorbance around 260 nm as compared to the spectrum of 1.0×10^{-3} M *N*-methylbenzylamine alone. The reaction is complete within 15 minutes.

Figure 6.27 shows the change over time in the spectrum with 0.10 M $CH_2(OH)(SO_3Na)$ as compared to that of *N*-methylbenzylamine alone. Table 6.41 shows the peak positions and extinction coefficients (ε) for the two spectra.

Figure 6.27: Change over time in absorbance against wavelength spectrum for 0.10 M $CH_2(OH)(SO_3Na)$, 1.0×10^{-3} M *N*-methylbenzylamine, 25 °C, in a 98 % water / 2 % methanol by volume solvent

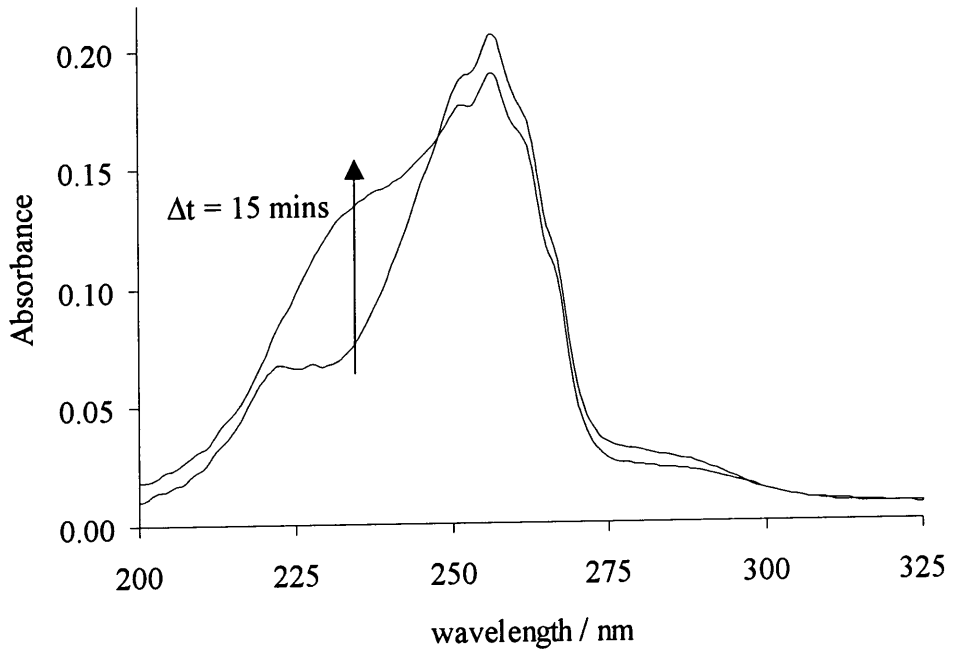

Table 6.41: Spectral appearance in a 98 % water / 2 % methanol by volume solvent of 1.0×10^{-3} M *N*-methylbenzylamine and with 0.10 M $CH_2(OH)(SO_3Na)$

$[CH_2(OH)(SO_3Na)]$ / M	λ_{max} / nm ($\varepsilon^{\dagger}$/ mol^{-1} dm^3 cm^{-1})
none	256 (200)
0.10	256 (190)

† based on the assumption that all the *N*-methylbenzylamine reacts to give 1.0×10^{-3} M product

Plots of absorbance against time were obtained for the reaction of 2.0×10^{-3} M *N*-methylbenzylamine with 0.030 to 0.10 M aqueous $CH_2(OH)(SO_3Na)$ at 25 °C, pH 7.0 in a 98 % water / 2 % methanol by volume solvent. Formation of the product at 230 nm was followed (Figure 6.28).

Figure 6.28: Plots of absorbance against time for the reaction of 2.0×10^{-3} M *N*-methylbenzylamine with aqueous $CH_2(OH)(SO_3Na)$ at 25 °C, pH 7.0

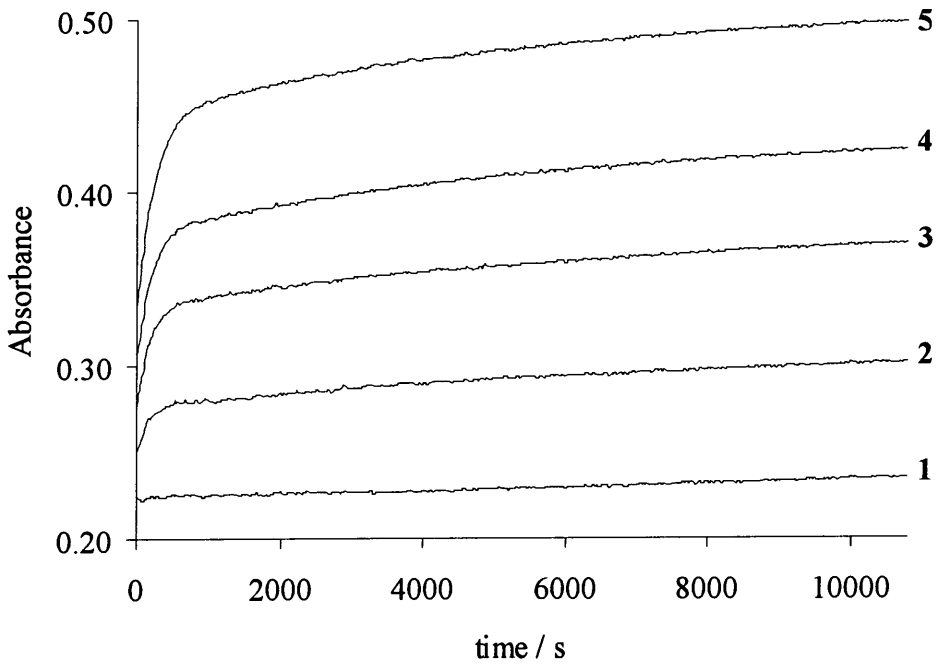

1 = no $CH_2(OH)(SO_3Na)$; **2** = 0.03 M $CH_2(OH)(SO_3Na)$; **3** = 0.05 M; **4** = 0.08 M; **5** = 0.10 M

The plots indicate that there are two processes occurring: two first order reactions. The two processes are relatively well separated therefore each was fitted separately. The k_{obs} / s^{-1} values obtained are shown in Table 6.42.

Table 6.42: k_{obs} / s^{-1} values for the reaction of *N*-methylbenzylamine with aqueous $CH_2(OH)(SO_3Na)$ at 25 °C, pH 7.0

$[CH_2(OH)(SO_3Na)]$ / M	first reaction†		second reaction§	
	k_{obs} / s^{-1}	A_∞	k_{obs} / s^{-1}	A_∞
0.030	$5.11 \times 10^{-3} \pm 1.1 \times 10^{-4}$	0.28	$7.41 \times 10^{-5} \pm 4 \times 10^{-7}$	0.32
0.050	$4.53 \times 10^{-3} \pm 5 \times 10^{-5}$	0.34	$9.06 \times 10^{-5} \pm 3 \times 10^{-7}$	0.39
0.080	$3.56 \times 10^{-3} \pm 4 \times 10^{-5}$	0.39	$1.21 \times 10^{-5} \pm 4 \times 10^{-7}$	0.44
0.10	$3.26 \times 10^{-3} \pm 3 \times 10^{-5}$	0.43	$1.55 \times 10^{-4} \pm 4 \times 10^{-7}$	0.51

† fitted using data from 0 to 500 s

§ fitted using data from 2300 - 2500 to 10800 s

The second rate constant increases with increasing $CH_2(OH)(SO_3Na)$ concentration, however the rate constant for the initial reaction shows a slight decrease.

Plotting k_{obs} / s^{-1} against [$CH_2(OH)(SO_3Na)$] / M for the second reaction gives a linear plot with a gradient and intercept equal to $1.19 \times 10^{-3} \pm 8 \times 10^{-5}$ dm^3 mol^{-1} and $3.59 \times 10^{-5} \pm 5.3 \times 10^{-6}$ s^{-1} respectively. Linear regression yields a correlation coefficient of 0.991. These values give an equilibrium constant, $K_{(app)}$, equal to 33 ± 3 dm^3 mol^{-1}. As with reaction with 4-nitrobenzylamine, the observation of two rate processes is difficult to rationalise. However the kinetics were simplified in the presence of added sulfite ions, where a single rate process was observed.

6.2.5.2.2 Reaction in the presence of added sulfite ions

The effect of the presence of added sulfite ions in the system was investigated. Plots of absorbance against time were obtained for the reaction of 2.0×10^{-3} M *N*-methylbenzylamine with 0.10 M aqueous $CH_2(OH)(SO_3Na)$ in the presence of 2.0×10^{-3} to 0.010 M aqueous sodium sulfite solution at 25 °C, pH 8.1, in a 98 % water / 2 % methanol by volume solvent. Formation of the product $C_6H_5CH_2NH(CH_3)CH_2SO_3^-$ at 230 nm was followed. Sulfite ions absorb in this region: spectra of 0.01, 0.05 and 0.10 M aqueous sodium sulfite solution were obtained and showed high absorbance around 250 nm and to shorter wavelength. For example, the extinction coefficient of sulfite ions at 245 nm was found to be 50 dm^3 mol^{-1} cm^{-1}. Therefore the appropriate concentration of sulfite ions was added to the reference in order to subtract the absorbance due to the presence of sulfite from the absorbance against time plots.

Where $[sulfite]_{stoich}$ is quoted this refers to the total concentration of aqueous sodium sulfite added externally to the system and does not include the concentration of sulfite ions present in solution due to dissociation of $CH_2(OH)(SO_3Na)$.

Plots were first order: the k_{obs} / s^{-1} values obtained are shown in Table 6.43.

Table 6.43: k_{obs} / s^{-1} values for the reaction of 2.0×10^{-3} M *N*-methylbenzylamine with 0.10 M aqueous $CH_2(OH)(SO_3Na)$ with added sulfite ions at 25 °C, pH 7.0

$[sulfite]_{stoich}$ / M	k_{obs} / s^{-1}	$k_{obs}.[sulfite]_{stoich}$ / s^{-1} M
0	$3.94 \times 10^{-3} \pm 1 \times 10^{-4}$	-
2.0×10^{-3}	$1.26 \times 10^{-4} \pm 2 \times 10^{-7}$	2.5×10^{-7}
4.0×10^{-3}	$7.26 \times 10^{-5} \pm 3 \times 10^{-7}$	2.9×10^{-7}
7.0×10^{-3}	$3.65 \times 10^{-5} \pm 4 \times 10^{-8}$	2.6×10^{-7}
0.010	$2.39 \times 10^{-5} \pm 6 \times 10^{-8}$	2.4×10^{-7}

The rate of reaction is considerably slower in the presence of added sulfite ions. Multiplying k_{obs} / s^{-1} by $[sulfite]_{stoich}$ / M gives an approximately constant value which implies an inverse dependence of k_{obs} / s^{-1} on the sulfite ion concentration. If free formaldehyde, HCHO, is the reactive species in the reaction of $CH_2(OH)(SO_3Na)$ with amines then the reaction must proceed initially via dissociation of $CH_2(OH)(SO_3Na)$ to give HCHO (Chapter 4). If this is the case, in the presence of additional sulfite ions the rate of formation of the product $C_6H_5CH_2NH(CH_3)CH_2SO_3^-$ may be expected to decrease as more free formaldehyde will react with the sulfite ions to give the unreactive $CH_2(OH)(SO_3Na)$. Hence less free formaldehyde will be present to react with the *N*-methylbenzylamine. The experimental results obtained here support this theory. $CH_2(OH)(SO_3Na)$ was used in great excess therefore the forward rate term will dominate the rate expression.

6.3 CONCLUSION

6.3.1 Summary

The reaction of benzylamine and four benzylamine derivatives with $CH_2(OH)(SO_3Na)$ was investigated using ^1H NMR spectroscopy. There was evidence of both 1 : 1 and 1 : 2 adduct formation for the reaction with benzylamine, 4-methoxybenzylamine, and 4-methylbenzylamine. However only the 1 : 1 adduct was observed for the reaction with 4-nitrobenzylamine. The presence of the 4-NO_2 electron withdrawing group lowers the nucleophilicity of the benzylamine nitrogen therefore the tendency to add a second $CH_2(OH)(SO_3Na)$ molecule is reduced.

Only the 1 : 1 adduct was observed in the reaction with *N*-methylbenzylamine as the 1 : 2 adduct cannot form. The formation of the 1 : 1 adduct with *N*-methylbenzylamine is much faster than with the other benzylamines. This is due to the presence of the electron donating methyl group adjacent to the nitrogen which greatly increases the nucleophilicity of the benzylamine nitrogen.

The chemical shifts of the product species in D_2O, or 97 % D_2O / 3 % CD_3OD in the case of 4-methyl- and *N*-methyl- benzylamine, are outlined in Scheme 6.3 along with those of the parent compounds. The exchangeable -NH_2 protons will be included under the D_2O solvent peak at δ 4.67 ppm.

Scheme 6.3:

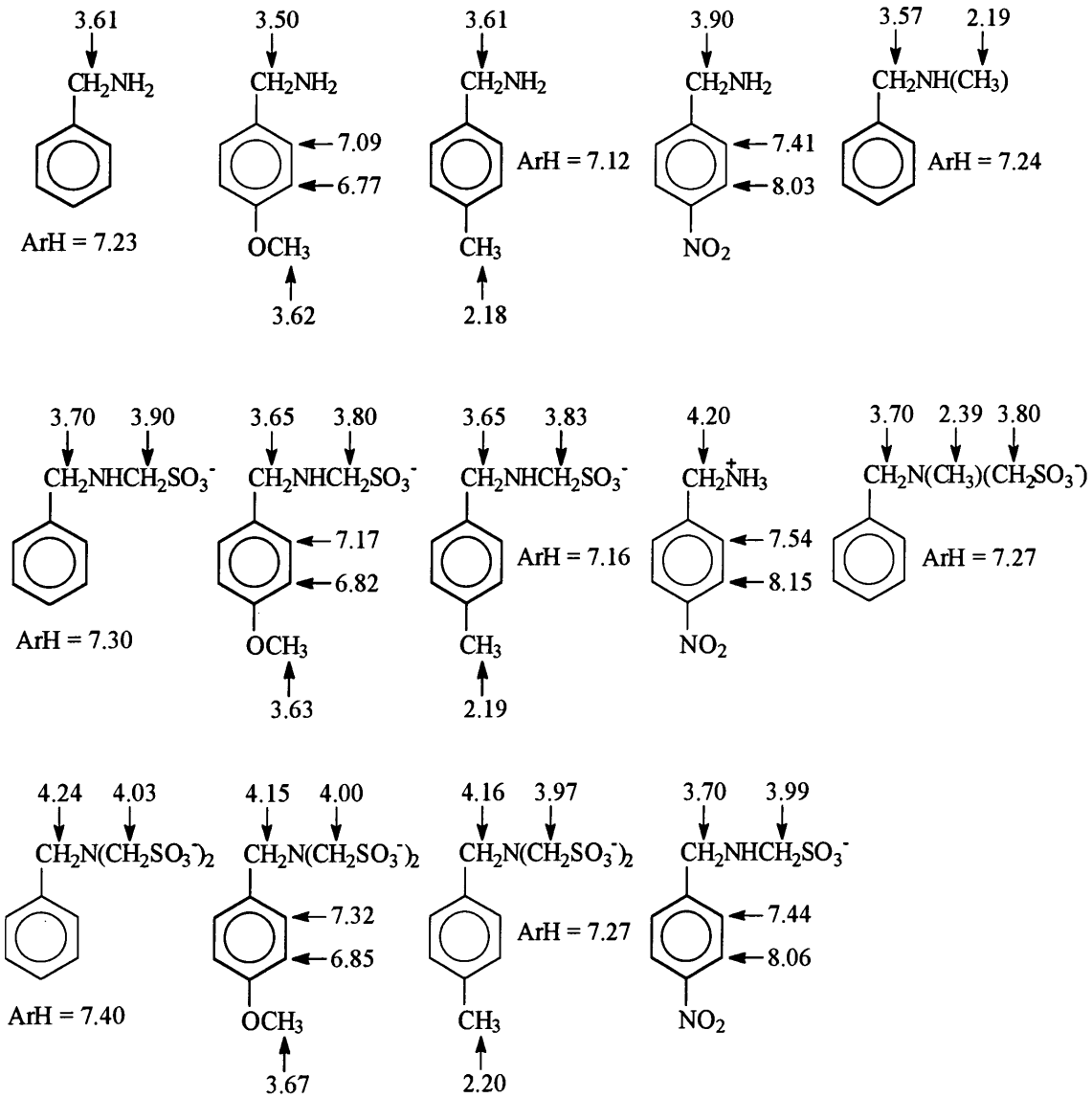

The reaction of benzylamine and the four benzylamine derivatives with $CH_2(OH)(SO_3Na)$ was investigated using uv / vis spectroscopy. Altering the ionic strength had little effect on the rate constants obtained. The rate and equilibrium constants for formation of the 1 : 1 adducts determined in this study are summarised in Table 6.44 where the equilibrium constant, $K_{(app)}$, is equal to $k_{f(app)} / k_b$.

Table 6.44: Rate and equilibrium constants† obtained at 25 °C using the amines 4-$RC_6H_4CH_2NHR'$

R	R'	pH	$k_{f(app)}$ / $dm^3\ mol^{-1}\ s^{-1}$	k_b / s^{-1}	$K_{(app)}$ / $dm^3\ mol^{-1}$
H	H	unbuffered	$8.2 \times 10^{-3} \pm 3 \times 10^{-4}$	$1.0 \times 10^{-4} \pm 2 \times 10^{-5}$	80 ± 10
$-OCH_3$	H	7.0	$1.1 \times 10^{-3} \pm 9 \times 10^{-6}$	$1.6 \times 10^{-4} \pm 5 \times 10^{-7}$	6.8 ± 0.1
		8.1	$1.3 \times 10^{-2} \pm 4 \times 10^{-5}$	$1.5 \times 10^{-4} \pm 3 \times 10^{-6}$	86 ± 2
		8.9	$1.7 \times 10^{-2} \pm 1 \times 10^{-4}$	$2.2 \times 10^{-4} \pm 7 \times 10^{-6}$	77 ± 3
		10.1	$1.7 \times 10^{-2} \pm 2 \times 10^{-4}$	$1.8 \times 10^{-4} \pm 9 \times 10^{-6}$	93 ± 5
$-CH_3$	H	7.0	$5.4 \times 10^{-3} \pm 5 \times 10^{-4}$	$3.8 \times 10^{-5} \pm 3 \times 10^{-5}$	140 ± 120
$-NO_2$	H	7.0	$9.9 \times 10^{-4} \pm 3 \times 10^{-4}$	$9.2 \times 10^{-5} \pm 2 \times 10^{-5}$	11 ± 4
H	$-CH_3$	7.0	$1.2 \times 10^{-3} \pm 8 \times 10^{-5}$	$3.6 \times 10^{-5} \pm 5 \times 10^{-6}$	33 ± 3

† values for the second reaction observed for R = $-NO_2$, R' = H and R = H, R' = $-CH_3$

The values of $k_{f(app)}$ and $K_{(app)}$ will be dependent on pH as shown in Equations 6.6 and 6.7. The increase in value of $K_{(app)}$ with increasing pH observed for reaction with 4-methoxybenzylamine is due to the increase in proportion of free unprotonated base as the pH increases. The pK_a of 4-methoxybenzylamine is 9.51 therefore the levelling off of the $K_{(app)}$ value with pH may have been expected to occur at higher pH values than is observed experimentally.

For the reaction with benzylamine, an initial fast reaction was observed that was investigated using stopped flow spectrophotometry. It is not clear what this initial faster reaction corresponds to. Two first order processes were observed for the reaction of 4-nitro- and *N*-methyl- benzylamine with $CH_2(OH)(SO_3Na)$. This cannot be due to formation of a 1 : 1 adduct followed by subsequent formation of a 1 : 2 adduct as a 1 : 2 adduct is not observed with either of these compounds. The initial reaction does not show any real dependence on $CH_2(OH)(SO_3Na)$. This initial reaction could be the formation of an intermediate such as the *N*-(hydroxymethyl)amine or the iminium ion or an artefact induced by variation in sulfite concentration over time. In hindsight it would

have been advisable to make all kinetic measurements and equilibrium studies in solutions where both the pH and the concentration of free sulfite were controlled.

The reaction in the presence of added sulfite ions was investigated for two of the benzylamine derivatives: the rate of reaction was considerably slower in the presence of added sulfite ions and the observed rate constant showed an inverse dependence on sulfite ion concentration.

The reaction of hydroxymethanesulfonate, $CH_2(OH)(SO_3Na)$, with amines proceeds initially via dissociation of the hydroxymethanesulfonate to give free formaldehyde, the reactive species, and either sulfite or bisulfite ions depending on the pH of the system (Chapter 4). Free formaldehyde then reacts with the amine via nucleophilic attack of the nitrogen lone pair of electrons on the carbonyl carbon in formaldehyde to produce an *N*-(hydroxymethyl)amine (Chapter 2). This reaction will be in competition with the reaction of free formaldehyde with sulfite / bisulfite ions to regenerate hydroxymethanesulfonate. Therefore in the presence of added sulfite ions, the rate of formation of the product, $RCH_2NR'CH_2SO_3^-$, will decrease as more free formaldehyde will react with sulfite ions to give unreactive $CH_2(OH)(SO_3Na)$ and less free formaldehyde will be present to react with the amine. The *N*-(hydroxymethyl)amine formed dehydrates in acid conditions or loses hydroxyl ion to give an iminium ion which then reacts with sulfite ions to give the product, $RCH_2NR'CH_2SO_3^-$.

6.3.2 Mechanism

The likely mechanism is shown in Scheme 6.4. The experiments were generally performed at pH values lower than the pK_a values of the amines. Therefore the amine will be present mainly in the unreactive protonated form. The equilibrium between the protonated amine and the reactive unprotonated amine must therefore be included in the mechanism.

Scheme 6.4:

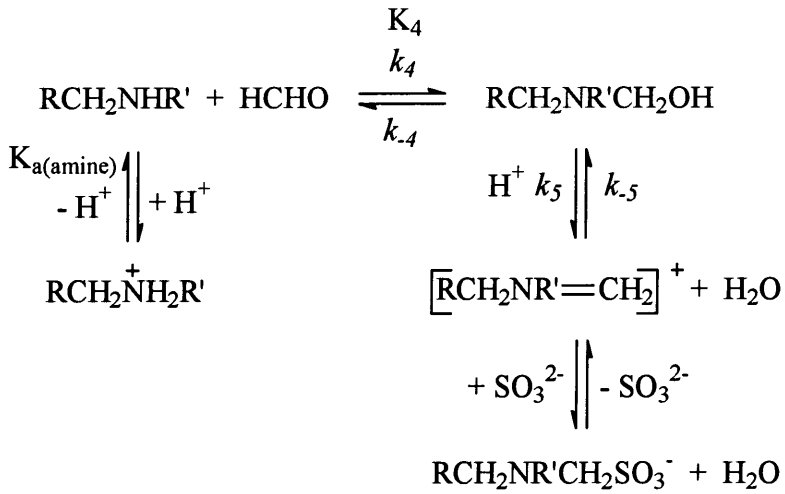

It is probable that the mechanism of the reaction will be the same when the amine is an aniline or benzylamine. The results obtained for anilines show that there is a change in rate determining step with pH: at low and neutral pH the rate determining step is likely to be the reaction of HCHO with RNH_2 whereas at higher pH the rate determining step becomes dehydration of the *N*-(hydroxymethyl)amine to the iminium ion. These findings are discussed in detail in Chapter 5.

At low and neutral pH, k_4 is rate limiting and, for anilines, k_{obs}, the observed first order rate constant, is given by Equation 6.8.

$$k_{obs} = \frac{k_4 K_a[CH_2(OH)(SO_3^-)]}{K_3[\text{sulfite}]_{stoich}} \cdot \frac{K_{HSO3^-} + [H^+]}{K_{HSO3^-}[H^+]} \qquad \textbf{(6.8)}$$

The pK_a values of anilines are much lower than those of benzylamines. When benzylamines are used the pK_a of the amine must be incorporated into the rate equation. Equation 6.2 relates the concentration of free amine to the stoichiometric concentration. At low and neutral pH when k_4 is rate limiting, k_{obs}, the observed first order rate constant, is given by Equation 6.9.

$$k_{obs} = \frac{k_4 K_a[CH_2(OH)(SO_3^-)]}{K_3[\text{sulfite}]_{stoich}} \cdot \frac{K_{HSO3^-} + [H^+]}{K_{HSO3^-}[H^+]} \cdot \frac{K_{a(amine)}}{K_{a(amine)} + [H^+]} \qquad \textbf{(6.9)}$$

Values of k_{obs}[sulfite]$_{stoich}$ / mol dm^{-3} s^{-1} were obtained experimentally. Table 6.45 summarises the values obtained for the two amines studied.

Table 6.45: Experimental k_{obs}[sulfite]$_{stoich}$ / mol dm^{-3} s^{-1} values†

amine	pH	k_{obs}[sulfite]$_{stoich}$ / mol dm^{-3} s^{-1}
4-methoxybenzylamine	8	7.6×10^{-7}
N-methylbenzylamine	7	2.6×10^{-7}

† average value quoted as experiments performed with more than one [sulfite]$_{stoich}$ / M

Values of k_4 can be determined by applying Equation 6.9 and using the experimental values of k_{obs}[sulfite]$_{stoich}$ / mol dm^{-3} s^{-1} along with Sørensen and Andersen's[2] values of $K_a = 2.0 \times 10^{-12}$ mol dm^{-3} and $K_3 = 2.2 \times 10^5$ mol^{-1} dm^3, and a K_{HSO3^-} value[3] of 6.3×10^{-8} mol dm^{-3}. Under the experimental conditions used, [CH_2(OH)(SO_3Na)] is equal to 0.10 mol dm^{-3}. The pK_a values of 4-methoxybenzylamine and *N*-methylbenzylamine are 9.51 and 9.59 respectively.

The calculated k_4 values for 4-methoxybenzylamine and *N*-methylbenzylamine are 2.3×10^5 and 4.3×10^6 dm^3 mol^{-1} s^{-1} respectively. In Chapter 2, k_4 values of 8.0×10^3 to 2.4×10^5 dm^3 mol^{-1} s^{-1} were obtained for anilines.

Values of k_4 for the reaction of benzylamines and benzylamine derivatives have not been reported in the literature. However, a correlation is expected between k_4 values, measuring the nucleophilicities of the amines, and their basicities, as measured by pK_a values. Atherton[4] has calculated a Brønsted β value, relating nucleophilicity and basicity, of around 0.26 for this reaction. Therefore a value for k_4 of around 10^7 dm^3 mol^{-1} s^{-1} might be expected for reaction of an amine whose conjugate acid has a pK_a value of around 9.

The value of k_4 obtained here for *N*-methylbenzylamine is in approximate agreement with the expected value of 10^7 dm^3 mol^{-1} s^{-1}. However the value obtained for 4-methoxybenzylamine is lower, 2.3×10^5 dm^3 mol^{-1} s^{-1}. This suggests that a step other

than nucleophilic attack of the amine on HCHO is rate limiting. It is therefore necessary to consider the possibility that, as is the case for aniline, dehydration of the *N*-(hydroxymethyl)benzylamine can become the rate determining step and k_5 is rate limiting.

The rate expression derived for anilines for the observed first order rate constant, k_{obs}, applying the assumption that k_5 is rate limiting is given in Equation 6.10.

$$k_{obs} = \frac{k_5 K_4 K_a [CH_2(OH)(SO_3^-)]}{K_3 [\text{sulfite}]_{\text{stoich}}} \cdot \frac{K_{HSO3^-} + [H^+]}{K_{HSO3^-}} \qquad \textbf{(6.10)}$$

As before, the pK_a of the amine must be built into this equation for benzylamines. Therefore k_{obs} at high pH is given by Equation 6.11 when the amine is a benzylamine.

$$k_{obs} = \frac{k_5 K_4 K_a [CH_2(OH)(SO_3^-)]}{K_3 [\text{sulfite}]_{\text{stoich}}} \cdot \frac{K_{HSO3^-} + [H^+]}{K_{HSO3^-}} \cdot \frac{K_{a(\text{amine})}}{K_{a(\text{amine})} + [H^+]} \qquad \textbf{(6.11)}$$

Abrams and Kallen[5] report that the value of K_4, the equilibrium constant for *N*-(hydroxymethyl)amine formation, is not strongly dependent on the nature of the amine and is approximately 4×10^4 dm^3 mol^{-1} in terms of free HCHO. Using this value together with the values of $k_{obs}[\text{sulfite}]_{\text{stoich}}$ in Table 6.45 and the other known equilibrium constants, a value of k_5 equal to 8×10^8 dm^3 mol^{-1} s^{-1} can be calculated. This value is not unreasonable given that values greater than 10^8 dm^3 mol^{-1} s^{-1} have previously been reported for the proton catalysed dehydration of *N*-(hydroxymethyl)amines formed from diprotic amines.[6]

To summarise, the rate limiting step for the overall reaction is likely to change from formation of the *N*-(hydroxymethyl)amine to *N*-(hydroxymethyl)amine dehydration as the pH increases from 6 to 8.

6.4 EXPERIMENTAL

6.4.1 ^{1}H NMR experiments

The reactions of benzylamine and four benzylamine derivatives with $CH_2(OH)(SO_3Na)$ were followed using ^{1}H NMR spectroscopy. Initially the spectrum of 0.015 to 0.2 M amine alone was obtained, then the spectrum in the presence of equimolar $CH_2(OH)(SO_3Na)$ (0.2 M or 0.015 M each), then with each reagent in excess (0.2 M amine with 0.4 or 0.1 M $CH_2(OH)(SO_3Na)$ or 0.015 M amine with 0.030 or 7.9×10^{-3} M $CH_2(OH)(SO_3Na)$). The concentrations used were determined by the solubility of the amine. The solutions were made immediately prior to use. The amine was placed in the NMR tube: neat amine was used or, if using a solid, a solution in D_2O was prepared. 4-Methyl- and *N*-methyl- benzylamine are not readily soluble in aqueous solution therefore a stock solution in methyl-d_3 alcohol-d, CD_3OD, was prepared. 1 cm^3 D_2O was then added to the NMR tube followed by the $CH_2(OH)(SO_3Na)$ which was added at the NMR machine side. A final solvent system of 3 % CD_3OD / 97 % water by volume was used for the 4-methyl- and *N*-methyl- benzylamines. The ^{1}H NMR spectrum of CHD_2OD is characterised by a quintet at δ 3.35 ppm. However it was not visible in any spectra as it was present in too small a proportion.

4-Nitrobenzylamine is purchased as the hydrochloride. Therefore the solution was neutralised prior to addition of $CH_2(OH)(SO_3Na)$ by adding an NaOH in D_2O solution. The maximum NaOH solution concentration that could be added to a 0.2 M amine solution without the solution becoming cloudy was 0.134 M. $CH_2(OH)(SO_3Na)$ reacts with NaOH therefore the amine must necessarily be in slight excess to prevent this reaction from occurring.

Spectra were recorded immediately (2 to 5 minutes) after mixing, then 30 minutes, 1 hour and 5 hours after mixing and continued until there was no further change in the spectrum. A spectrum after 15 minutes was also obtained for the reaction with benzylamine. The time of mixing refers to the time at which $CH_2(OH)(SO_3Na)$ was added to the NMR tube. The time of each spectrum was taken as the time when the spectrometer started to acquire the spectrum.

^{1}H NMR spectra were recorded using a 200 MHz Varian Mercury - 200 spectrometer. The δ 4.67 ppm singlet due to residual protons in the deuterated solvent, D_2O, was used for locking purposes and as the reference peak for all spectra. Chemical shifts are quoted to 2 decimal places. Coupling constants are given where the multiplicity is greater than a singlet and are quoted to the nearest whole number.

6.4.2 Uv / vis experiments

Absorbance against wavelength spectra were obtained for the reaction of the amine (2.0×10^{-4} to 2.0×10^{-3} M) with 2.0×10^{-3} to 0.10 M $CH_2(OH)(SO_3Na)$. Mixed solvent systems of 2 % methanol / 98 % water by volume were used for 4-methyl and *N*-methyl- benzylamine as these amines are not soluble in aqueous solution.

Spectra were obtained using a UV-2101 PC Shimadzu Corporation or Perkin – Elmer Lambda 2 uv / vis spectrometer at 25 °C with 1 cm stoppered quartz cuvettes, taking scans every 5 or 15 minutes for up to 3 or 7½ hours using a scan speed of 480 nm min^{-1}. The cuvettes were left in the spectrometer for at least 10 minutes prior to use to allow the temperature to equilibrate to 25 °C. Addition of the amine solution was used to initiate the reaction. Extinction coefficients are quoted to 2 or 3 significant figures and were calculated using only one spectrum in most cases.

Plots of absorbance against time were obtained for the reaction of the amine (2.0×10^{-4} to 2.0×10^{-3} M) with 0.01 to 0.10 M aqueous $CH_2(OH)(SO_3Na)$ at 25 °C. The effect of the presence of added sulfite ions in the system was investigated for two amines: the reaction of 1.0×10^{-4} or 2.0×10^{-3} M amine with 0.10 M aqueous $CH_2(OH)(SO_3Na)$ solution in the presence of 2.0×10^{-3} to 0.010 M aqueous sodium sulfite solution was studied at 25 °C at pH 7 or 8.

Plots were recorded using a Perkin – Elmer Lambda 2 or 12 uv / vis spectrometer at 25 °C with 1 cm stoppered quartz cuvettes. The data interval ranged from 20 seconds to 17½ minutes and the overall reaction time from 3 to 16 hours depending on the pH and concentrations used. The cuvettes were left in the spectrometer for at least 10 minutes prior to use to allow the temperature to equilibrate at 25 °C. Addition of the amine solution was used to initiate the reaction. Formation of the product was followed at

240 nm when using benzylamine, 4-methoxybenzylamine and 4-methylbenzylamine, 315 nm for 4-nitrobenzylamine and 230 nm for *N*-methylbenzylamine. Mixed solvent systems of 2 % methanol / 98 % water by volume were used for reactions with 4-methyl and *N*-methyl- benzylamine.

The spectrum of $CH_2(OH)(SO_3Na)$ does not show any significant absorbance in the uv / vis spectrum. However sulfite ions do absorb in this region: spectra of 0.01, 0.05 and 0.10 M aqueous sodium sulfite solution were obtained and showed high absorbance around 250 nm and to shorter wavelength. For example, the extinction coefficient of sulfite ions at 245 nm was found to be 50 dm^3 mol^{-1} cm^{-1}. Therefore the appropriate concentration of sulfite ions was added to the reference in order to subtract the absorbance due to the presence of sulfite from the absorbance against time plots. Where $[sulfite]_{stoich}$ is quoted this refers to the total concentration of aqueous sodium sulfite added externally to the system and does not include the concentration of sulfite ions present in solution due to dissociation of $CH_2(OH)(SO_3Na)$.

For experiments where the ionic strength was kept constant, potassium chloride was used to maintain an ionic strength of 1.0 M.

First order plots were fitted using the PECSS program installed on the Perkin – Elmer Lambda 2 spectrometer or by plotting $\ln(A_\infty - A)$ against time / s using Microsoft Excel and performing linear regression. Rate constants are quoted to 2 decimal places. Linear regression on Microsoft Excel was used to calculate $k_{f(app)}$ and k_b values, equal to the gradient and intercept respectively. Values are quoted to three significant figures. The equilibrium constant, $K_{(app)}$, is quoted to two significant figures. The percentage error in $K_{(app)}$ was calculated using Equation 6.12. The percentage error was then converted to an absolute value of $K_{(app)}$.

$$\%\text{ error in } K_{(app)} = \sqrt{[(\%\text{ error in } k_{f(app)})^2 + (\%\text{ error in } k_b)^2]} \qquad \textbf{(6.12)}$$

The buffers employed and the corresponding stoichiometric buffer concentrations in the final solutions are shown in Table 6.46. Where buffers were used, the appropriate volume of buffer was also present in the reference cuvette.

Table 6.46: Buffer concentrations, in aqueous solution

pH	component A	$[A]_{stoich}$ / M	component B	$[B]_{stoich}$ / M
6	KH_2PO_4	0.19	NaOH	0.011
7	KH_2PO_4	0.19	NaOH	0.022
8	KH_2PO_4	0.19	NaOH	0.18
9	$Na_2B_4O_7.10\ H_2O$	0.016	HCl	6.0×10^{-3}
10	$Na_2B_4O_7.10\ H_2O$	0.032	NaOH	0.046

The pH values of all solutions were determined using a Jenway 3020 pH meter calibrated using pH 7 and pH 10 (for alkaline solutions) or pH 4 (for acidic solutions) buffers. pH values are quoted to one decimal place.

Plots of absorbance against time were obtained at 240 nm for the reaction of 5.5×10^{-4} to 3.0×10^{-3} M benzylamine with 3.0×10^{-3} to 0.10 M aqueous $CH_2(OH)(SO_3Na)$ at 25 °C using stopped flow spectrophotometry to study the initial faster reaction. Plots were recorded using an Applied Photophysics DX.17MV BioSequential Stopped – flow ASVD Spectrometer at 25.1 – 25.2 °C with a cell of 1 cm path length. Ten averages were obtained, each the average of three runs of 50 seconds. The appropriate aqueous benzylamine solution was placed in one syringe and the aqueous $CH_2(OH)(SO_3Na)$ solution in the other. The averages were fitted to obtain first order rate constants, k_{obs} / s^{-1}, using the single exponential fit function on the !SX.17MV program installed on the spectrometer. Values of k_{obs} / s^{-1} are quoted to three decimal places.

6.5 REFERENCES

1. D. D. Perrin, 'Dissociation Constants of Organic Bases in Aqueous Solution', Butterworths, London, 1965 and 1972 Supplement

2. P. E. Sørensen and V. S. Andersen, *Acta Chem. Scand.*, 1970, **24**, 1301

3. (a) E. Hayon, A. Treinin and J. Wilf, *J. Am. Chem. Soc.*, 1972, **94**, 47; (b) H. V. Tartar and H. H. Garretson, *J. Am. Chem. Soc.*, 1941, **63**, 808

4. J. H. Atherton, unpublished work

5. W. R. Abrams and R. G. Kallen, *J. Am. Chem. Soc.*, 1976, **98**, 7777

6. R. G. Kallen, *J. Am. Chem. Soc.*, 1971, **93**, 6236

CHAPTER 7

Decomposition of $RCH_2NR'CH_2SO_3^-$ adducts

CHAPTER 7: Decomposition of $RCH_2NR'CH_2SO_3^-$ adducts

7.1 INTRODUCTION

Formation of the 1 : 1 and 1 : 2 adducts $RCH_2NR'CH_2SO_3^-$ and $RCH_2N(CH_2SO_3^-)_2$ from benzylamines and $CH_2(OH)(SO_3Na)$ has been studied (Chapter 6). Here the decomposition of the major products, the 1 : 1 adducts, was studied by pre-forming the adducts using equimolar concentrations of the reagents and following the decomposition in buffered solution. The effect of the presence of added aqueous formaldehyde solution and added sulfite ions in the system was also investigated.

In addition to studying the overall decomposition, the first step in the decomposition involving the release of sulfite to form the iminium ion, $[RCH_2NR'=CH_2]^+$, was investigated by reacting liberated sulfite ions with added aqueous iodine solution.

The 1 : 1 benzylamines : $CH_2(OH)(SO_3Na)$ adducts **7.1** to **7.4** were studied.

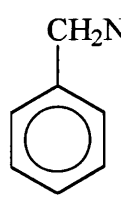

7.1

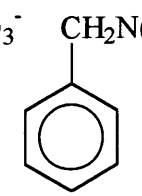

7.2

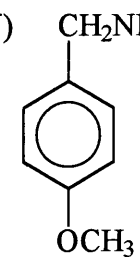

7.3

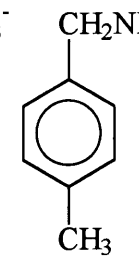

7.4

7.2 RESULTS AND DISCUSSION

7.2.1 Decomposition of $RCH_2NR'CH_2SO_3^-$ to the starting materials

Decomposition of the 1 : 1 benzylamine : $CH_2(OH)(SO_3Na)$ adducts $RCH_2NR'CH_2SO_3^-$ was studied at a range of pH values. The effect of the presence of added aqueous formaldehyde solution and added sulfite ions in the system was also investigated. The reactions were followed using uv / vis spectroscopy. This method gives no indication of the identity of the species being observed therefore the results are not easy to interpret.

7.2.1.1 Benzylamine adduct: $C_6H_5CH_2NHCH_2SO_3^-$

7.2.1.1.1 Absorbance against wavelength spectra and absorbance against time plots

A stock solution of 0.073 M benzylamine and 0.070 M $CH_2(OH)(SO_3Na)$ in water was left to react for 5 minutes to ensure formation of the adduct $C_6H_5CH_2NHCH_2SO_3^-$. The solution was then diluted and absorbance against wavelength spectra obtained for the decomposition of 2.0×10^{-3} M $C_6H_5CH_2NHCH_2SO_3^-$ at pH 6.0 and 7.0. Figure 7.1 shows the change over time in the spectrum of the adduct at pH 7.0.

Figure 7.1: Change over time in the absorbance against wavelength spectrum for 2.0×10^{-3} M $C_6H_5CH_2NHCH_2SO_3^-$ at 25 °C, pH 7.0

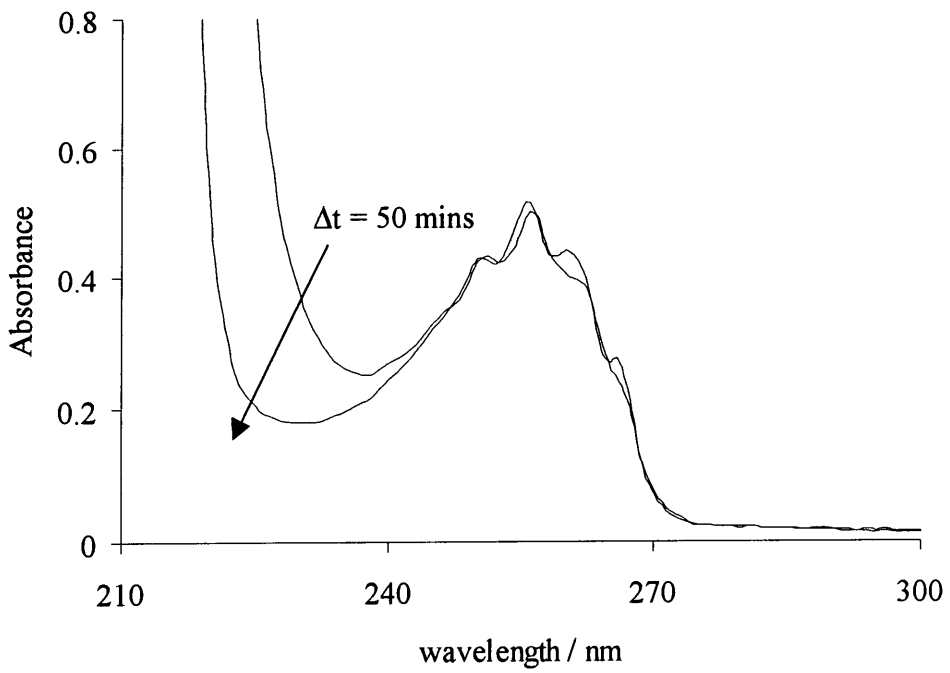

The spectrum decreases in absorbance over time around 230 nm: the reaction is complete within 50 minutes. The spectrum at pH 6 shows a similar but slower change: the reaction is complete within 4 hours. The final spectrum is similar to that of benzylamine: the adduct appears to decompose back to the starting materials.

Absorbance against time plots at 230 nm were obtained for a solution of 2.0×10^{-3} M $C_6H_5CH_2NHCH_2SO_3^-$ at pH 5.1 to 8.8 (Figure 7.2).

Figure 7.2: Absorbance against time plots for 2.0×10^{-3} M $C_6H_5CH_2NHCH_2SO_3^-$ at 25 °C, pH 5.1 to 8.8

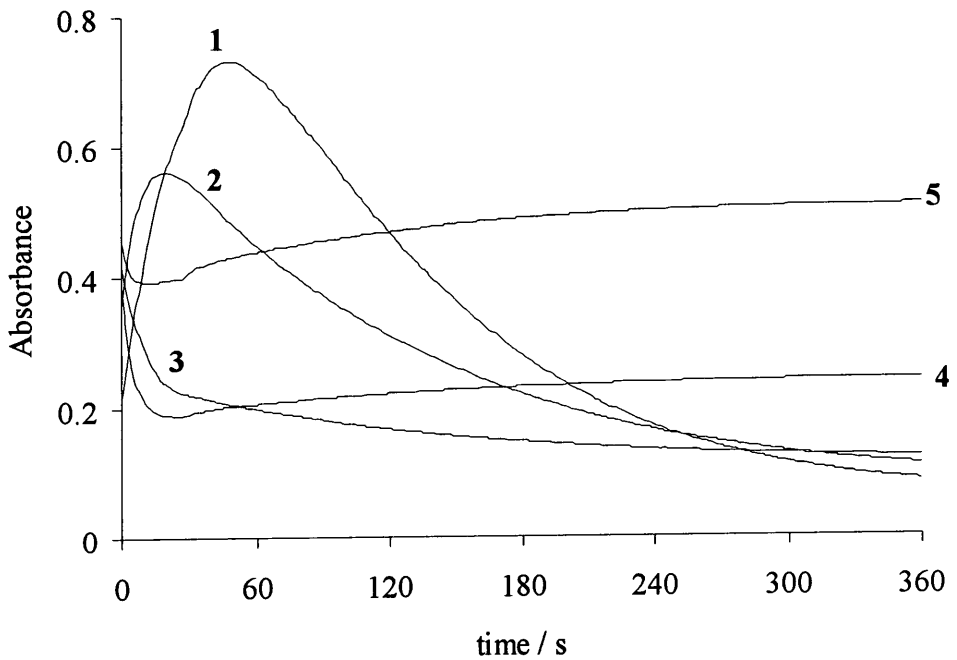

1 = pH 5.1; **2** = pH 6.0; **3** = pH 7.0; **4** = pH 8.1; **5** = pH 8.8

At pH 5.1 and 6.0 there is an initial increase in absorbance followed by a first order decomposition. This increase is probably due to pK_a effects. The pK_a of the benzylamine adduct is 5.4 (Section 7.2.2.1.3) therefore at pH 5 and 6 the adduct will be present in a large proportion as the protonated form, $C_6H_5CH_2N^+HCH_2SO_3^-$. The first step in the decomposition of the adduct is likely to occur predominantly through the unprotonated amine as it involves expulsion of sulfite to give a cationic iminium ion.

At pH 7.0 there appears to be two decomposition processes occurring. At pH 8.1 and 8.8 there is an initial decomposition followed by an increase in absorbance. The

decomposition of the adduct consists of a number of steps (Scheme 7.1) therefore the kinetics of decomposition are complex.

Scheme 7.1:

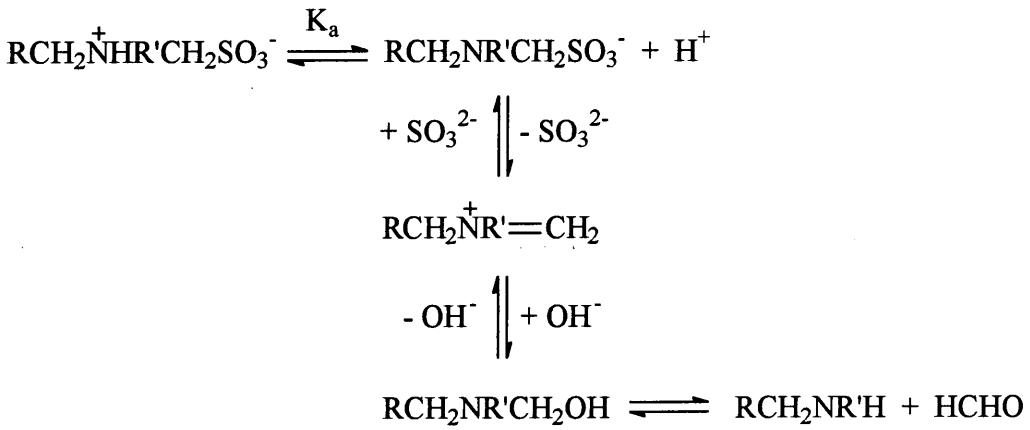

A probable intermediate in the decomposition pathway is the *N*-(hydroxymethyl)amine $RCH_2NR'CH_2OH$. The presence of a $-CH_2OH$ group lowers the pK_a value with respect to the protonated amine $RCH_2N^+R'H_2$ by 2 to 3 pH units.[1] Hence the pK_a for the *N*-(hydroxymethyl)amine formed from benzylamine will be approximately 7. Figure 7.2 shows that the intermediate is prominent at pH 5.1 and 6.0. At these values the *N*-(hydroxymethyl)amine will be present in its protonated form, $RCH_2N^+HR'CH_2OH$. The positive charge on the nitrogen will be expected to reduce the rate of expulsion of formaldehyde, hence increasing the lifetime of the intermediate.

7.2.1.1.2 Decomposition in the presence of added sulfite ions

The effect of the presence of added sulfite ions on the decomposition of the adduct $C_6H_5CH_2NHCH_2SO_3^-$ was investigated. Plots of absorbance against time were obtained for solutions of 2.0×10^{-3} M $C_6H_5CH_2NHCH_2SO_3^-$ in the presence of 6.0×10^{-4} to 2.0×10^{-3} M aqueous sodium sulfite solution at 25 °C, pH 6.0 and 7.0 (Figures 7.3 and 7.4). Decomposition of the adduct $C_6H_5CH_2NHCH_2SO_3^-$ was followed at 230 nm. Sulfite ions absorb in this region: spectra of 0.01, 0.05 and 0.10 M aqueous sodium sulfite solution show high absorbance around 250 nm and to shorter wavelength. For example, the extinction coefficient of sulfite ions at 245 nm was found to be 50 $dm^3\ mol^{-1}\ cm^{-1}$. Therefore the appropriate concentration of sulfite ions was added to

the reference in order to subtract the absorbance due to the presence of sulfite from the absorbance against time plots.

Where $[sulfite]_{stoich}$ is quoted this refers to the total concentration of aqueous sodium sulfite added externally to the system and does not include the concentration of sulfite ions present in solution due to dissociation of $C_6H_5CH_2NHCH_2SO_3^-$.

Figure 7.3: Absorbance against time plots for 2.0×10^{-3} M $C_6H_5CH_2NHCH_2SO_3^-$ with 6.0×10^{-4} to 2.0×10^{-3} M added aqueous sodium sulfite solution, 25 °C, pH 6.0

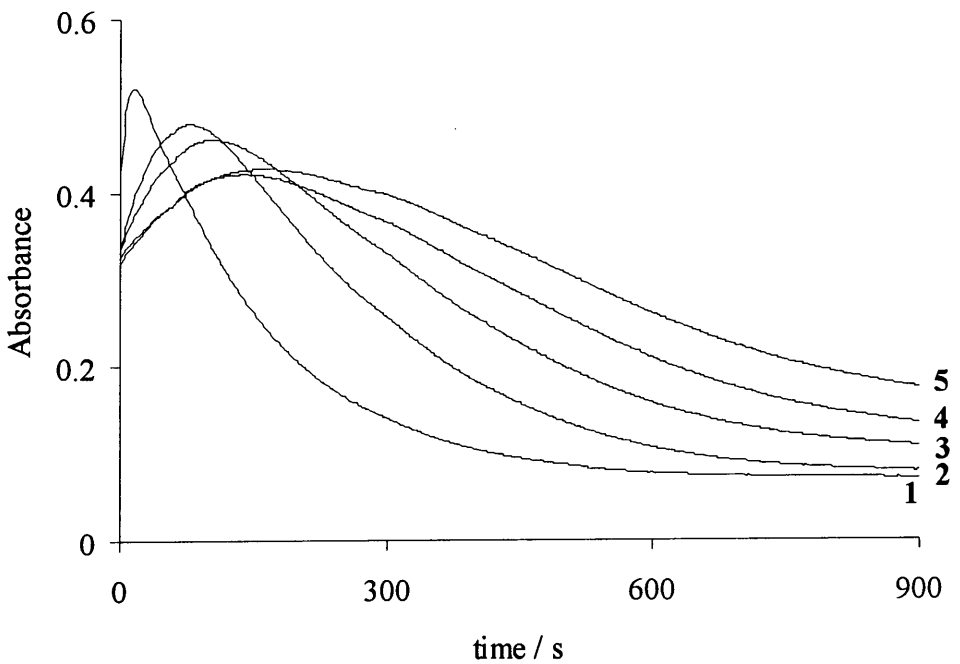

1 = no sulfite; **2** = 6.0×10^{-4} M $[sulfite]_{stoich}$; **3** = 1.0×10^{-3} M; **4** = 1.6×10^{-3} M; **5** = 2.0×10^{-3} M

Figure 7.4: Absorbance against time plots for 2.0×10^{-3} M $C_6H_5CH_2NHCH_2SO_3^-$ with 6.0×10^{-4} to 2.0×10^{-3} M added aqueous sodium sulfite solution, 25 °C, pH 7.0

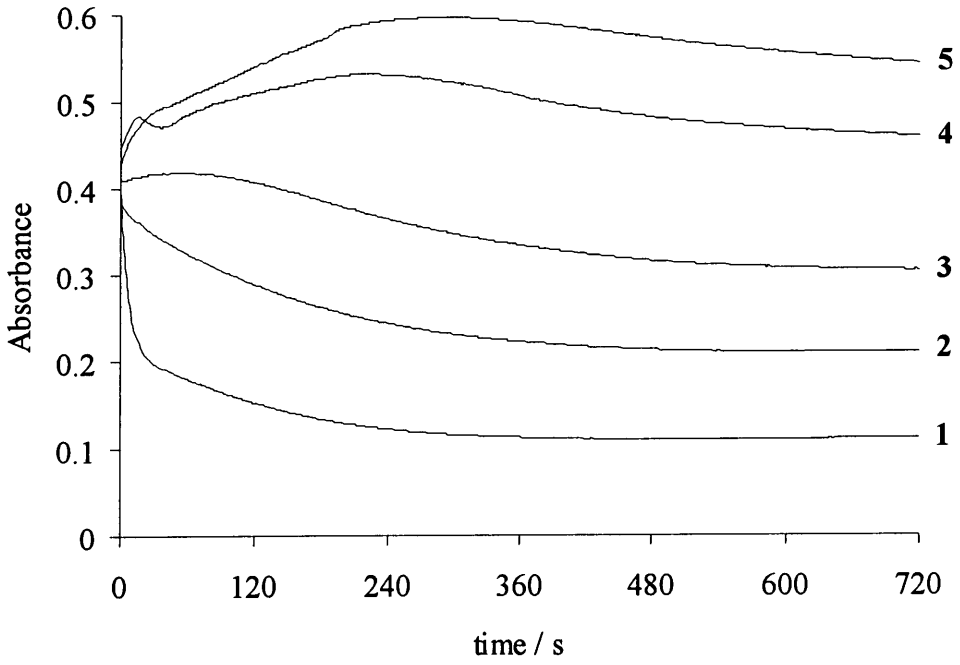

1 = no sulfite; **2** = 6.0×10^{-4} M $[sulfite]_{stoich}$; **3** = 1.0×10^{-3} M; **4** = 1.6×10^{-3} M; **5** = 2.0×10^{-3} M

Addition of sulfite ions decreases the rate of decomposition. In fact at pH 7.0 the addition of the highest concentrations of sulfite ions appears to generate the adduct prior to decomposition, characterised be an initial increase in absorbance. From Scheme 7.1 it may be expected that the addition of sulfite ions would decrease the rate of decomposition of the adduct: the presence of additional sulfite ions will push the equilibrium between the adduct and the iminium ion towards the adduct.

7.2.1.2 *N*-Methylbenzylamine adduct: $C_6H_5CH_2N(CH_3)(CH_2SO_3^-)$

7.2.1.2.1 Absorbance against wavelength spectra and absorbance against time plots

A solution of 0.022 M *N*-methylbenzylamine and 0.020 M $CH_2(OH)(SO_3Na)$ was left to react for 3 minutes to ensure formation of the $C_6H_5CH_2N(CH_3)(CH_2SO_3^-)$ adduct. *N*-Methylbenzylamine is not soluble in water therefore a stock solution in methanol was

prepared. After dilution, a final solvent composition of < 1 % methanol / > 99 % water by volume obtained.

Absorbance against wavelength spectra were obtained for the decomposition of 1.0×10^{-3} M $C_6H_5CH_2N(CH_3)(CH_2SO_3^-)$ at pH 6.0 to 8.8. Figure 7.5 shows the change over time in the spectrum of the adduct at pH7.0.

Figure 7.5: Change over time in the absorbance against wavelength spectrum for 1.0×10^{-3} M $C_6H_5CH_2N(CH_3)(CH_2SO_3^-)$ at 25 °C, pH 7.0

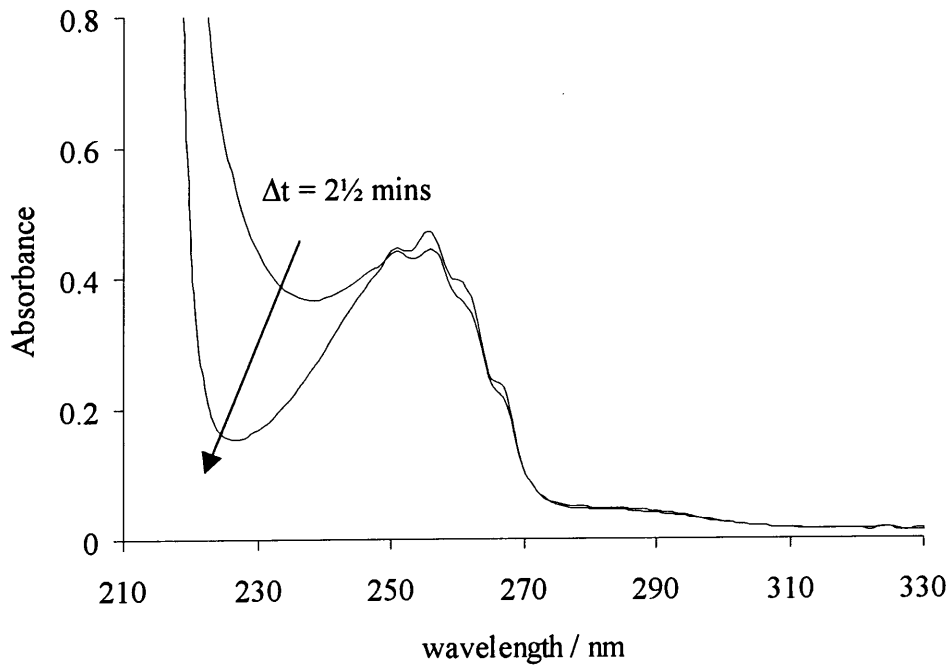

The spectrum decreases in absorbance over time around 230 nm. The reaction is complete within 2½ minutes. The rate of decomposition is faster than that for the benzylamine adduct: the analogous reaction with the benzylamine adduct took 50 minutes to reach completion. The spectra at pH 6.0, 8.2 and 8.8 show a similar change: the reaction is complete within 12 minutes, 1½ minutes and 30 seconds respectively. The final spectrum is similar to that of *N*-methylbenzylamine: the adduct appears to decompose back to the starting materials.

Absorbance against time plots at 230 nm were obtained for a solution of 1.0×10^{-3} M $C_6H_5CH_2N(CH_3)(CH_2SO_3^-)$ at pH 5.0 to 8.8 (Figure 7.6).

Figure 7.6: Absorbance against time plots for 1.0×10^{-3} M $C_6H_5CH_2N(CH_3)(CH_2SO_3^-)$ at 25 °C, pH 5.0 to 8.2

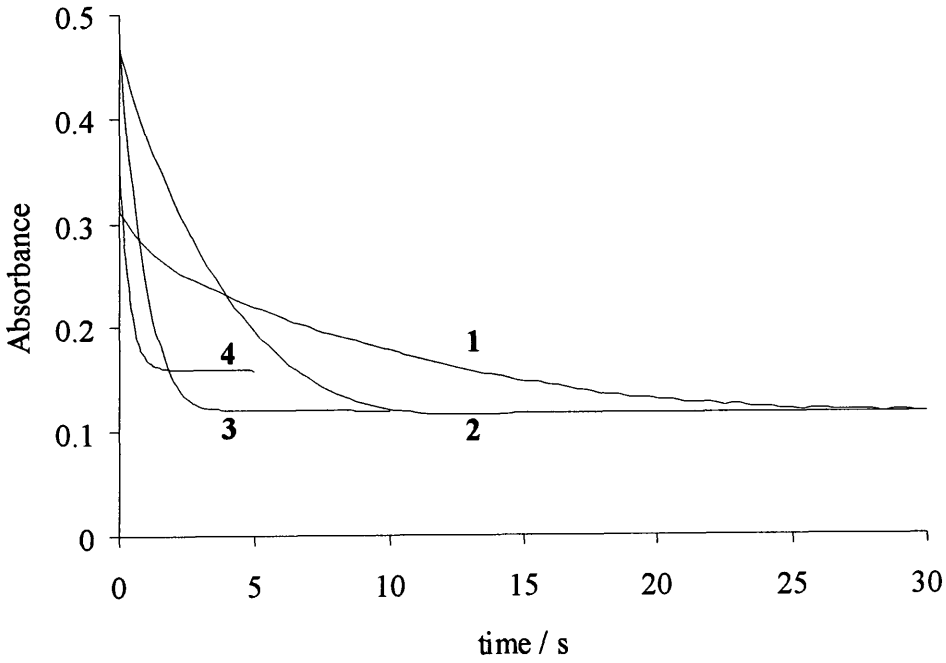

1 = pH 5.0; **2** = pH 6.0; **3** = pH 7.0; **4** = pH 8.2

The plots are first order: the k_{obs} / s^{-1} values obtained are shown in Table 7.1. Figure 7.7 shows a plot of $\log(k_{obs} / s^{-1})$ against pH.

Table 7.1: k_{obs} / s^{-1} values for the decomposition of 1.0×10^{-3} M $C_6H_5CH_2N(CH_3)(CH_2SO_3^-)$ at 25 °C, pH 5.0 to 8.2

pH	k_{obs} / s^{-1}
5.0	$1.90 \times 10^{-3} \pm 2 \times 10^{-5}$
6.0	$4.92 \times 10^{-3} \pm 6 \times 10^{-5}$
7.0	$1.68 \times 10^{-2} \pm 2 \times 10^{-4}$
8.2	$5.33 \times 10^{-2} \pm 6 \times 10^{-4}$

Figure 7.7: Log(k_{obs} / s^{-1}) against pH for decomposition of $C_6H_5CH_2N(CH_3)(CH_2SO_3^-)$

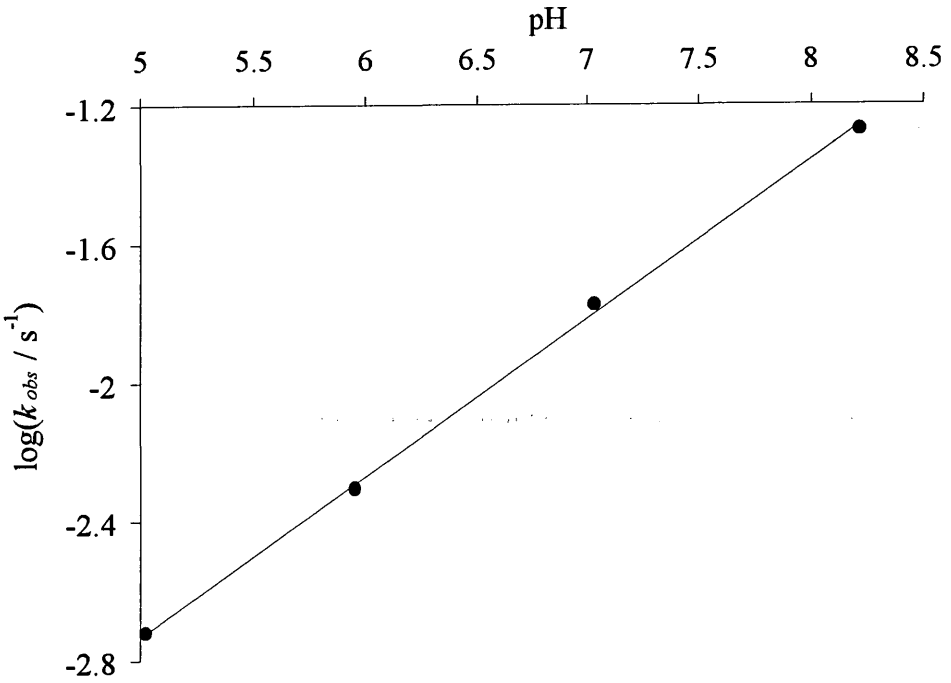

The log(k_{obs} / s^{-1}) values increase linearly with increasing pH. The pK_a of the *N*-methylbenzylamine adduct $C_6H_5CH_2N(CH_3)(CH_2SO_3^-)$ is 4.9 (Section 7.2.2.4.2). Therefore this change with pH is not due to the ionisation state of the adduct. However it is possible that it reflects the extent of protonation of the *N*-(hydroxymethyl)amine intermediate, $C_6H_5CH_2N(CH_3)(CH_2OH)$, which can become progressively protonated with increasing acidity.

7.2.1.2.2 Decomposition in the presence of added aqueous formaldehyde solution

The effect of the presence of added aqueous formaldehyde solution, $HCHO_{(aq)}$, on the decomposition of the adduct $C_6H_5CH_2N(CH_3)(CH_2SO_3^-)$ was investigated.

Absorbance against time plots at 230 nm were obtained using stopped flow spectrophotometry for a solution of 1.0×10^{-3} M $C_6H_5CH_2N(CH_3)(CH_2SO_3^-)$ in the presence of 0.010 to 0.10 M added aqueous formaldehyde solution at pH 6.0 and 7.0 (Figure 7.8). First order plots were obtained: the k_{obs} / s^{-1} values are shown in Table 7.2.

Figure 7.8: Absorbance against time plot for 1.0×10^{-3} M $C_6H_5CH_2N(CH_3)(CH_2SO_3^-)$ with 0.10 M added aqueous formaldehyde solution, 25 °C, pH 6.0 with single exponential fit superimposed

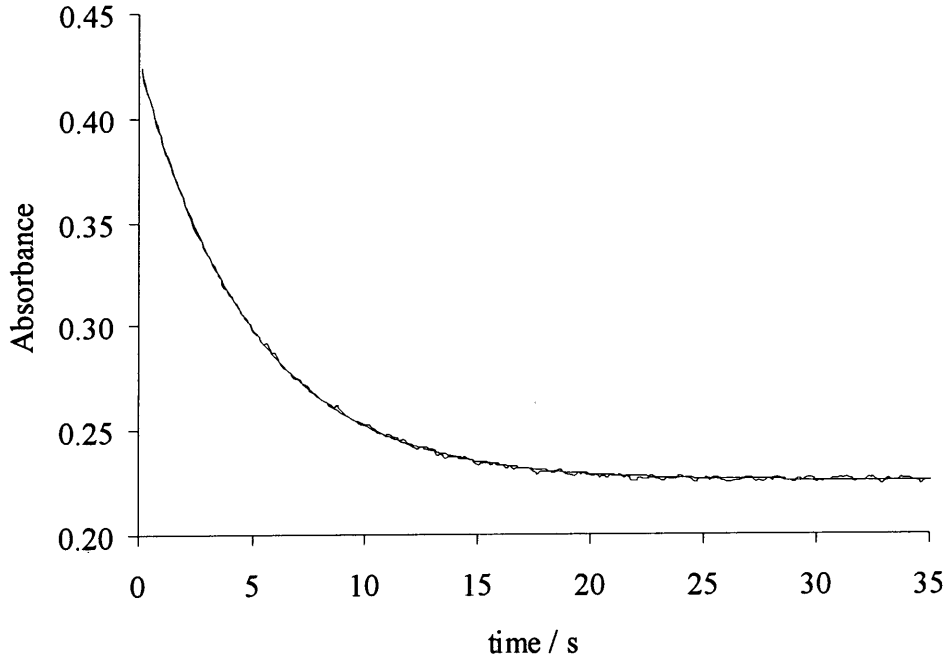

Table 7.2: k_{obs} / s^{-1} values for the decomposition of 1.0×10^{-3} M $C_6H_5CH_2N(CH_3)(CH_2SO_3^-)$ with added aqueous formaldehyde solution, 25 °C

$[HCHO_{(aq)}]$ / M	k_{obs} / s^{-1}	
	pH 6.0	pH 7.0
0	$4.92 \times 10^{-3} \pm 6 \times 10^{-5}$	$0.017 \pm 2 \times 10^{-4}$
0.010	$0.095 \pm 1 \times 10^{-3}$	$0.199 \pm 9 \times 10^{-4}$
0.020	$0.126 \pm 1 \times 10^{-3}$	$0.234 \pm 2 \times 10^{-3}$
0.050	$0.166 \pm 2 \times 10^{-3}$	$0.258 \pm 3 \times 10^{-3}$
0.080	$0.183 \pm 1 \times 10^{-3}$	$0.268 \pm 3 \times 10^{-3}$
0.10	$0.192 \pm 9 \times 10^{-3}$	$0.274 \pm 2 \times 10^{-3}$

The addition of $HCHO_{(aq)}$ increases the rate of decomposition: the higher the concentration of $HCHO_{(aq)}$ added the greater the increase. From Scheme 7.1 it may be expected that the addition of $HCHO_{(aq)}$ would increase the rate of decomposition of the

adduct: $HCHO_{(aq)}$ will react with sulfite ions released when the adduct decomposes to the iminium ion, $[C_6H_5CH_2N(CH_3)=CH_2]^+$, to form $CH_2(OH)(SO_3^-)$. The limiting value of around 0.3 s^{-1} obtained is close to the value of 0.58 s^{-1} obtained when the released sulfite is irreversibly removed by reaction with aqueous iodine solution (Section 7.2.2.4.2). This implies the aqueous formaldehyde here is acting in the same way as the iodine by removing the released sulfite.

7.2.1.2.3 Decomposition in the presence of added sulfite ions

The effect of the presence of added sulfite ions on the decomposition of the adduct $C_6H_5CH_2N(CH_3)(CH_2SO_3^-)$ was investigated. Plots of absorbance against time were obtained for solutions of 1.0×10^{-3} M $C_6H_5CH_2N(CH_3)(CH_2SO_3^-)$ in the presence of 6.0×10^{-4} to 2.0×10^{-3} M aqueous sodium sulfite solution at 25 °C, pH 6.0 (Figure 7.9) and 7.0. Decomposition of the adduct $C_6H_5CH_2N(CH_3)(CH_2SO_3^-)$ was followed at 230 nm. Sulfite ions absorb in this region: spectra of 0.01, 0.05 and 0.10 M aqueous sodium sulfite solution show high absorbance around 250 nm and to shorter wavelength. Therefore the appropriate concentration of sulfite ions was added to the reference in order to subtract the absorbance due to the presence of sulfite from the absorbance against time plots.

Where $[sulfite]_{stoich}$ is quoted this refers to the total concentration of aqueous sodium sulfite added externally to the system and does not include the concentration of sulfite ions present in solution due to dissociation of $C_6H_5CH_2N(CH_3)(CH_2SO_3^-)$.

Addition of sulfite ions decreases the rate of decomposition. The results obtained at pH 7.0 show a similar trend. From Scheme 7.1 it may be expected that the addition of sulfite ions would decrease the rate of decomposition of the adduct: the presence of additional sulfite ions will push the equilibrium between the adduct and the iminium ion towards the adduct.

Figure 7.9: Absorbance against time plots for 1.0×10^{-3} M $C_6H_5CH_2N(CH_3)CH_2SO_3^-$ with 6.0×10^{-4} to 2.0×10^{-3} M added aqueous sodium sulfite solution, 25 °C, pH 7.0

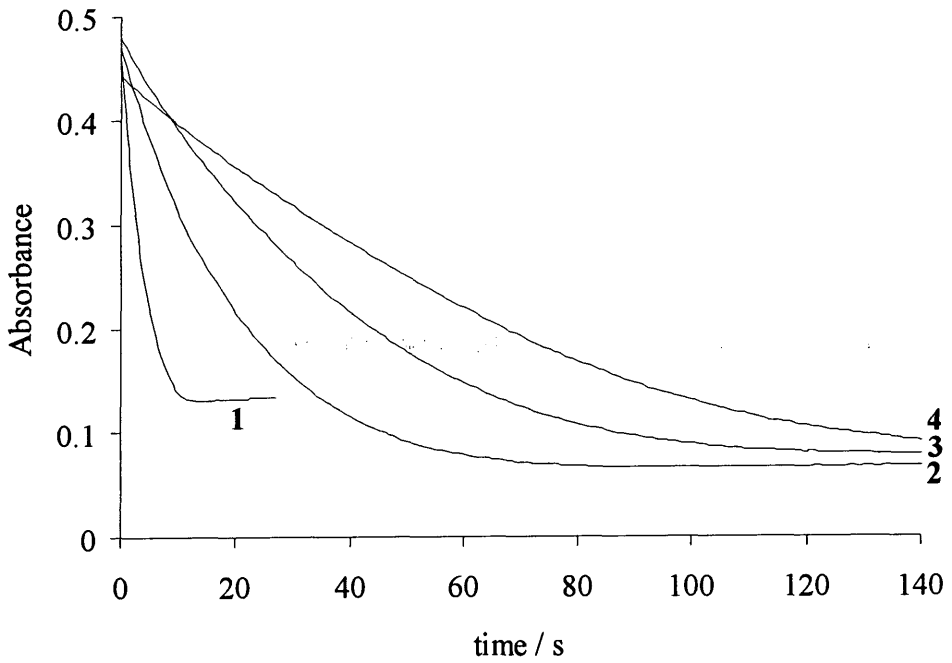

1 = no sulfite; **2** = 6.0×10^{-4} M $[sulfite]_{stoich}$; **3** = 1.0×10^{-3} M; **4** = 2.0×10^{-3} M

7.2.2 Decomposition of $RCH_2NR'CH_2SO_3^-$ to the iminium ion

The first step in the decomposition of 1 : 1 benzylamine : $CH_2(OH)(SO_3Na)$ adducts, $RCH_2NR'CH_2SO_3^-$, namely the release of sulfite to form the iminium ion, $[RCH_2NR'=CH_2]^+$, was investigated by reacting liberated sulfite ions with added aqueous iodine solution.

Initially the reaction of each amine with aqueous iodine solution was investigated: the absorbance against wavelength spectrum of each amine in the presence of 4×10^{-4} M aqueous iodine solution at pH 5.1 was followed over time. None of the amines used showed any reaction with aqueous iodine solution.

The 1 : 1 amine : $CH_2(OH)(SO_3Na)$ adduct was formed by reacting the amine with $CH_2(OH)(SO_3Na)$ in high concentration. The stock solution was prepared with the

amine present in slight excess as residual $CH_2(OH)(SO_3Na)$ may react with aqueous iodine solution (Chapter 4). This stock solution was left for a certain time, depending on the amine used, to ensure formation of the adduct. The stock solution was then diluted to a range of concentrations and the reaction with 4.0×10^{-4} M aqueous iodine solution investigated at pH 4.0 to 8.9. The disappearance of the aqueous iodine solution at 350 nm was followed.

The reaction of $RCH_2NR'CH_2SO_3^-$ with aqueous iodine solution may be written in terms of Scheme 7.2, where S(IV) is the sum contribution from both sulfite and bisulfite ions.

Scheme 7.2:

$$RCH_2\overset{+}{N}HR'CH_2SO_3^- \underset{}{\overset{K_a}{\rightleftharpoons}} RCH_2NR'CH_2SO_3^- + H^+$$

$$k_b \Big\downarrow \Big\uparrow k_f$$

$$RCH_2\overset{+}{N}R'{=}CH_2 + S(IV) \xrightarrow[k]{\text{iodine}_{(aq)}} \text{products}$$

Equation 7.1 shows the derived rate expression for the analogous reaction involving the aniline adduct (Chapter 5, Section 5.2.4.2) where $[I_2]_\tau$ is the sum of $[I_2]$ plus $[I_3^-]$.

$$-\frac{d[I_2]_\tau}{dt} = k_b[C_6H_5NHCH_2SO_3^-] \qquad (7.1)$$

Anilines have lower pK_a values than benzylamines therefore the pK_a values do not need to be incorporated: aniline adducts are expected to be present in the reactive unprotonated form at the pH values studied. The pK_a values of the benzylamines used are in the range 9.33 to 9.59 therefore in the pH range studied the adduct will probably be present in the protonated form, $RCH_2N^+HR'CH_2SO_3^-$. Decomposition of the adduct is likely to occur predominantly through the unprotonated adduct as it involves expulsion of sulfite to give a cationic iminium ion. Therefore the acid dissociation constant of the adduct must be included in the rate expression.

The stoichiometric concentration of the adduct, $[RCH_2NR'CH_2SO_3^-]_{stoich}$, is equal to the sum of the concentrations of the reactive form, $RCH_2NR'CH_2SO_3^-$, and the protonated form, $RCH_2N^+HR'CH_2SO_3^-$. These concentrations are related by the acid dissociation constant K_a (Equations 7.2 and 7.3).

$$[RCH_2NR'CH_2SO_3^-]_{stoich} = [RCH_2NR'CH_2SO_3^-] + [RCH_2\overset{+}{N}HR'CH_2SO_3^-] \quad (7.2)$$

$$K_a = \frac{[RCH_2NR'CH_2SO_3^-][H^+]}{[RCH_2\overset{+}{N}HR'CH_2SO_3^-]} \quad (7.3)$$

$$\text{Therefore } [RCH_2NR'CH_2SO_3^-] = \frac{K_a}{K_a + [H^+]} \cdot [RCH_2NR'CH_2SO_3^-]_{stoich} \quad (7.4)$$

The rate expression is therefore given by Equation 7.5.

$$-\frac{d[I_2]_\tau}{dt} = \frac{k_b K_a}{K_a + [H^+]} \cdot [RCH_2NR'CH_2SO_3^-]_{stoich} \quad (7.5)$$

$$\text{Therefore } k_{obs} = \frac{k_b K_a}{K_a + [H^+]} \cdot [RCH_2NR'CH_2SO_3^-]_{stoich} \quad (7.6)$$

The two limiting cases are:

Case 1: at low pH, where $[H^+] >> K_a$

In this case, Equation 7.6 reduces to:

$$\frac{k_{obs}}{[RCH_2NR'CH_2SO_3^-]_{stoich}} = \frac{k_b K_a}{[H^+]} \quad (7.7)$$

$$\text{Therefore } \log\left(\frac{k_{obs}}{[RCH_2NR'CH_2SO_3^-]_{stoich}}\right) = \log(k_b K_a) + pH \quad (7.8)$$

Therefore a plot of log (k_{obs} / $[RCH_2NR'CH_2SO_3^-]_{stoich}$) against pH should give a linear plot with a gradient of unity.

Case 2: at high pH, where $K_a >> [H^+]$

Here Equation 7.6 reduces to:

$$\frac{k_{obs}}{[RCH_2NR'CH_2SO_3^-]_{stoich}} = k_b \qquad (7.9)$$

Therefore at high pH the rate constant will show no dependence on pH.

Equation 7.5 shows that the reaction should be zero order with respect to total aqueous iodine solution concentration. Zero order plots were obtained and k_{obs} / mol dm^{-3} s^{-1} was determined by dividing the gradient of the plot by 13400 mol^{-1} dm^3 cm^{-1}, the extinction coefficient of iodine at 350 nm.

7.2.2.1 Benzylamine adduct: $C_6H_5CH_2NHCH_2SO_3^-$

7.2.2.1.1 Rate constant for decomposition to the iminium ion

A stock solution of 0.073 M benzylamine and 0.070 M $CH_2(OH)(SO_3Na)$ in water was left to react for 5 minutes to ensure formation of the adduct $C_6H_5CH_2NHCH_2SO_3^-$.

The reaction of 2.5×10^{-3} to 0.010 M $C_6H_5CH_2NHCH_2SO_3^-$ with 4.0×10^{-4} M aqueous iodine solution at pH 5.1, 25 °C was followed using stopped flow spectrophotometry. Zero order kinetics were observed (Figure 7.10). The k_{obs} / mol dm^{-3} s^{-1} values are shown in Table 7.3.

Figure 7.10: Absorbance against time plot of 0.010 M $C_6H_5CH_2NHCH_2SO_3^-$ with 4.0×10^{-4} M aqueous iodine solution at pH 5.1, 25 °C with linear fit superimposed

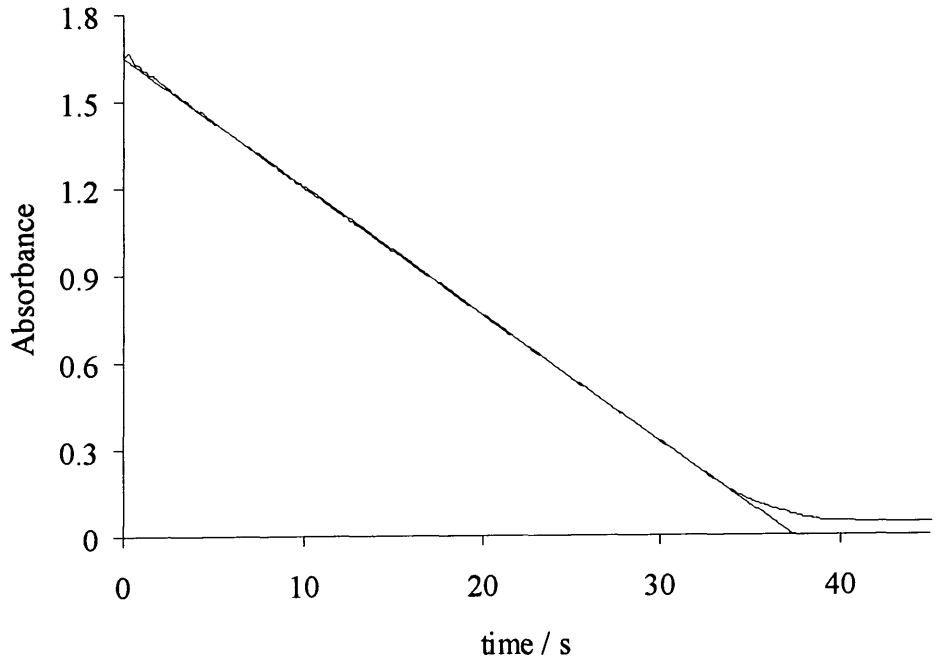

Table 7.3: k_{obs} / mol dm^{-3} s^{-1} values with varied $C_6H_5CH_2NHCH_2SO_3^-$ concentration at pH 5.1, 25 °C

$[C_6H_5CH_2NH_2CH_2SO_3^-]$ / M	k_{obs} / mol dm^{-3} s^{-1}
2.5×10^{-3}	$5.24 \times 10^{-6} \pm 1.3 \times 10^{-6}$
5.0×10^{-3}	$1.20 \times 10^{-5} \pm 6 \times 10^{-7}$
7.6×10^{-3}	$2.11 \times 10^{-5} \pm 5 \times 10^{-7}$
0.010	$3.10 \times 10^{-5} \pm 8 \times 10^{-7}$

The k_{obs} / mol dm^{-3} s^{-1} value increases with increasing $C_6H_5CH_2NHCH_2SO_3^-$ concentration. The pK_a of the adduct must be determined before the corresponding k_b values can be calculated.

7.2.2.1.2 Effect of varying the $C_6H_5CH_2NHCH_2SO_3^-$ stock solution composition

To determine whether the composition of the initial stock solution of $C_6H_5CH_2NHCH_2SO_3^-$ is important, the experiment was repeated at pH 5.1 with $C_6H_5CH_2NHCH_2SO_3^-$ prepared with each of the reagents in excess. First the adduct was formed with benzylamine in excess (0.070 M benzylamine with 0.050 M $CH_2(OH)(SO_3Na)$) then with $CH_2(OH)(SO_3Na)$ in excess (0.050 M benzylamine with 0.070 M $CH_2(OH)(SO_3Na)$). In both cases the solution was left to react for 5 minutes.

The k_{obs} / mol dm^{-3} s^{-1} values obtained are shown in Table 7.4.

Table 7.4: k_{obs} / mol dm^{-3} s^{-1} values at pH 5.1, 25 °C where the $C_6H_5CH_2NHCH_2SO_3^-$ stock solution was prepared with one reagent in excess

Reagent in excess	$[C_6H_5CH_2NHCH_2SO_3^-]_{stoich}$ / M	k_{obs} / mol dm^{-3} s^{-1}
benzylamine	2.5×10^{-3}	$5.78 \times 10^{-6} \pm 1.3 \times 10^{-7}$
	5.0×10^{-3}	$1.43 \times 10^{-5} \pm 3 \times 10^{-7}$
	7.6×10^{-3}	$2.47 \times 10^{-5} \pm 6 \times 10^{-7}$
	0.010	$3.83 \times 10^{-5} \pm 9 \times 10^{-7}$
$CH_2(OH)(SO_3Na)$	2.5×10^{-3}	$5.87 \times 10^{-6} \pm 1.3 \times 10^{-7}$
	5.0×10^{-3}	$1.38 \times 10^{-5} \pm 3 \times 10^{-7}$
	7.6×10^{-3}	$2.35 \times 10^{-5} \pm 6 \times 10^{-7}$
	0.010	$3.51 \times 10^{-5} \pm 1.0 \times 10^{-6}$

Corresponding rate constants agree well and are similar to those obtained when the stock $C_6H_5CH_2NHCH_2SO_3^-$ solution was prepared using approximately equimolar benzylamine and $CH_2(OH)(SO_3Na)$ (Table 7.3). Equation 7.6 shows that a plot of k_{obs} / mol dm^{-3} s^{-1} against $[C_6H_5CH_2NHCH_2SO_3^-]_{stoich}$ / mol dm^{-3} should be a linear with a gradient equal to $(k_bK_a / K_a + [H^+]) / s^{-1}$. Linear plots were obtained: the $(k_bK_a / K_a + [H^+]) / s^{-1}$ values are shown in Table 7.5. Correlation coefficients between 0.987 and 0.992 were obtained using linear regression.

Table 7.5: $(k_b K_a / K_a + [H^+]) / s^{-1}$ values at pH 5.1 where the $C_6H_5CH_2NHCH_2SO_3^-$ stock solution was prepared with equimolar reagents or with one reagent in excess

Reagent in excess	$(k_b K_a / K_a + [H^+]) / s^{-1}$
equimolar	$3.4 \times 10^{-3} \pm 2 \times 10^{-4}$
benzylamine	$4.3 \times 10^{-3} \pm 4 \times 10^{-4}$
$CH_2(OH)(SO_3Na)$	$3.9 \times 10^{-3} \pm 3 \times 10^{-4}$

The values obtained are similar which implies that the method of preparation of the adduct $C_6H_5CH_2NHCH_2SO_3^-$ is not significant: the presence of residual benzylamine or $CH_2(OH)(SO_3Na)$ does not affect the rate constant obtained.

7.2.2.1.3 pH study

The effect of pH was investigated by studying the reaction of 5.0×10^{-3} M $C_6H_5CH_2NHCH_2SO_3^-$ with 4.0×10^{-4} M aqueous iodine solution at pH 4.0 to 8.7, 25 °C. The stock $C_6H_5CH_2NHCH_2SO_3^-$ solution was prepared using 0.073 M benzylamine and 0.070 M $CH_2(OH)(SO_3Na)$. The k_{obs} / mol dm^{-3} s^{-1} and corresponding $(k_{obs} / [C_6H_5CH_2NH_2CHSO_3^-]_{stoich})$ / s^{-1} values are shown in Table 7.6.

Table 7.6: k_{obs} / mol dm^{-3} s^{-1} and $(k_{obs}/[C_6H_5CH_2NHCH_2SO_3^-]_{stoich})$ / s^{-1} values at pH 4.0 to 8.7, 25 °C, where $[C_6H_5CH_2NHCH_2SO_3^-]_{stoich} = 5.0 \times 10^{-3}$ mol dm^{-3}

pH	k_{obs} / mol dm^{-3} s^{-1}	$(k_{obs}/[C_6H_5CH_2NHCH_2SO_3^-]_{stoich})$ / s^{-1}
4.0	$1.95 \times 10^{-6} \pm 5 \times 10^{-8}$	$3.9 \times 10^{-4} \pm 1 \times 10^{-5}$
4.4	$3.25 \times 10^{-6} \pm 8 \times 10^{-8}$	$6.5 \times 10^{-4} \pm 2 \times 10^{-5}$
4.7	$6.24 \times 10^{-6} \pm 1.4 \times 10^{-7}$	$1.2 \times 10^{-3} \pm 3 \times 10^{-5}$
5.1	$1.20 \times 10^{-5} \pm 6 \times 10^{-7}$	$2.4 \times 10^{-3} \pm 1 \times 10^{-4}$
5.3	$1.60 \times 10^{-5} \pm 6 \times 10^{-7}$	$3.2 \times 10^{-3} \pm 1 \times 10^{-4}$
5.9	$3.10 \times 10^{-5} \pm 8 \times 10^{-7}$	$6.2 \times 10^{-3} \pm 2 \times 10^{-4}$
7.0	$3.83 \times 10^{-5} \pm 9 \times 10^{-7}$	$7.7 \times 10^{-3} \pm 2 \times 10^{-4}$
8.2	$4.21 \times 10^{-5} \pm 1.0 \times 10^{-6}$	$8.4 \times 10^{-3} \pm 2 \times 10^{-4}$
8.7	$2.93 \times 10^{-5} \pm 1.2 \times 10^{-6}$	$5.9 \times 10^{-3} \pm 2 \times 10^{-4}$

At high pH, k_b is approximately equal to k_{obs} / $[C_6H_5CH_2NHCH_2SO_3^-]_{stoich}$ (Equation 7.9). Therefore the value of k_b can be approximated to the limiting value of k_{obs} / $[C_6H_5CH_2NHCH_2SO_3^-]_{stoich}$. The values in Table 7.6 imply a k_b value of approximately 8.0×10^{-3} s^{-1}.

Using this value of k_b and the k_{obs} / $[C_6H_5CH_2NHCH_2SO_3^-]_{stoich}$ values given in Table 7.4, a value of K_a can be determined at each pH using Equation 7.7. Table 7.7 shows the K_a and corresponding pK_a values calculated using this method. Values cannot be calculated for pH values above 6 as above this the k_{obs} / $[C_6H_5CH_2NHCH_2SO_3^-]_{stoich}$ values become constant.

Table 7.7: Calculated K_a and pK_a values at each pH

pH	K_a	pK_a
4.0	$4.8 \times 10^{-6} \pm 1 \times 10^{-7}$	5.3
4.4	$4.1 \times 10^{-6} \pm 1 \times 10^{-7}$	5.4
4.7	$4.3 \times 10^{-6} \pm 1 \times 10^{-7}$	5.4
5.1	$5.3 \times 10^{-6} \pm 3 \times 10^{-7}$	5.3
5.3	$3.7 \times 10^{-6} \pm 2 \times 10^{-7}$	5.4
5.9	$4.0 \times 10^{-6} \pm 2 \times 10^{-7}$	5.4

The average K_a is 4.0×10^{-6} corresponding to a pK_a of 5.4. Figure 7.11 shows a plot of $\log[(k_{obs} / [C_6H_5CH_2NHCH_2SO_3^-]_{stoich}) / s^{-1}]$ against pH for the experimental data with a calculated plot using a pK_a of 5.4 superimposed.

The calculated plot shows a good fit for the data. The pK_a of benzylamine is 9.33, therefore the presence of the $-CH_2SO_3^-$ group, an electron withdrawing group, reduces the pK_a by approximately four pH units.

Figure 7.11: Log[(k_{obs} / $[C_6H_5CH_2NHCH_2SO_3^-]_{stoich}$) / s^{-1}] against pH with a calculated plot using a pK_a of 5.4 superimposed

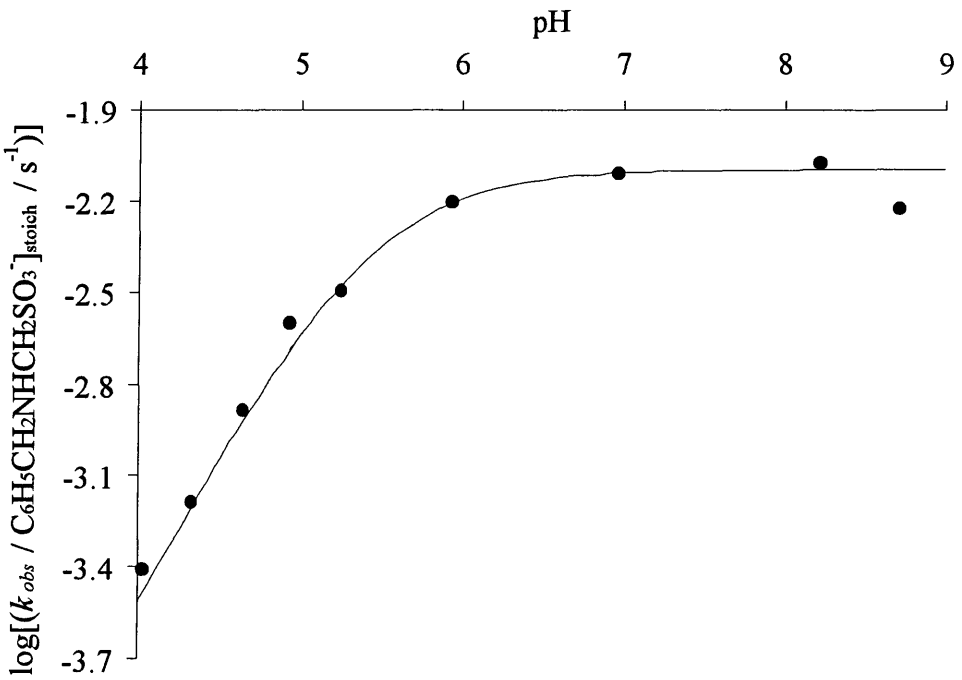

7.2.2.2 4-Methoxybenzylamine adduct: $4\text{-}CH_3OC_6H_4CH_2NHCH_2SO_3^-$

A stock solution of 0.052 M 4-methoxybenzylamine and 0.050 M $CH_2(OH)(SO_3Na)$ in water was left to react for 8 minutes to ensure formation of the adduct $4\text{-}CH_3OC_6H_4CH_2NHCH_2SO_3^-$.

7.2.2.2.1 Rate constant for decomposition to the iminium ion

The reaction of 2.5×10^{-3} to 0.010 M $4\text{-}CH_3OC_6H_4CH_2NHCH_2SO_3^-$ with 4.0×10^{-4} M aqueous iodine solution at pH 5.1, 25 °C was investigated. The k_{obs} / mol dm^{-3} s^{-1} values obtained are shown in Table 7.8.

Table 7.8: k_{obs} / mol dm^{-3} s^{-1} values with varied [4-$CH_3OC_6H_4CH_2NHCH_2SO_3^-$] / M at pH 5.1, 25 °C

[4-$CH_3OC_6H_4CH_2NHCH_2SO_3^-$] / M	k_{obs} / mol dm^{-3} s^{-1}
2.5×10^{-3}	$4.71 \times 10^{-6} \pm 1.2 \times 10^{-7}$
5.0×10^{-3}	$1.30 \times 10^{-5} \pm 3 \times 10^{-7}$
7.6×10^{-3}	$2.43 \times 10^{-5} \pm 6 \times 10^{-7}$
0.010	$3.88 \times 10^{-5} \pm 9 \times 10^{-7}$

The k_{obs} values obtained are similar to the corresponding values obtained for the decomposition of the benzylamine adduct.

7.2.2.2.2 pH study

The effect of pH was investigated by studying the reaction of 5.0×10^{-3} M 4-$CH_3OC_6H_4CH_2NH_2CH_2SO_3^-$ with 4.0×10^{-4} M aqueous iodine solution at pH 4.0 to 8.9, 25 °C. The k_{obs} / mol dm^{-3} s^{-1} and (k_{obs} / [4-$CH_3OC_6H_4CH_2NHCH_2SO_3^-$]$_{stoich}$) / s^{-1} values obtained are shown in Table 7.9.

Table 7.9: k_{obs} / mol dm^{-3} s^{-1} and (k_{obs}/[4-$CH_3OC_6H_4CH_2NHCH_2SO_3^-$]$_{stoich}$) / s^{-1} values at pH 4.0 to 8.9, 25 °C, [4-$CH_3OC_6H_4CH_2NHCH_2SO_3^-$]$_{stoich}$ = 5.0×10^{-3} mol dm^{-3}

pH	k_{obs} / mol dm^{-3} s^{-1}	(k_{obs}/[4-$CH_3OC_6H_4CH_2NHCH_2SO_3^-$]$_{stoich}$) / s^{-1}
4.0	$1.98 \times 10^{-6} \pm 5 \times 10^{-8}$	$4.0 \times 10^{-4} \pm 1 \times 10^{-5}$
4.4	$3.26 \times 10^{-6} \pm 8 \times 10^{-8}$	$6.5 \times 10^{-4} \pm 2 \times 10^{-5}$
4.7	$5.90 \times 10^{-6} \pm 1.5 \times 10^{-7}$	$1.2 \times 10^{-3} \pm 3 \times 10^{-5}$
5.1	$1.30 \times 10^{-5} \pm 4 \times 10^{-7}$	$2.6 \times 10^{-3} \pm 8 \times 10^{-5}$
5.3	$1.69 \times 10^{-5} \pm 4 \times 10^{-7}$	$3.4 \times 10^{-3} \pm 8 \times 10^{-5}$
6.1	$3.79 \times 10^{-5} \pm 1.0 \times 10^{-6}$	$7.6 \times 10^{-3} \pm 2 \times 10^{-4}$
7.1	$5.37 \times 10^{-5} \pm 1.3 \times 10^{-6}$	$1.1 \times 10^{-2} \pm 3 \times 10^{-4}$
8.3	$5.81 \times 10^{-5} \pm 1.4 \times 10^{-6}$	$1.2 \times 10^{-2} \pm 3 \times 10^{-4}$
8.9	$5.16 \times 10^{-5} \pm 1.4 \times 10^{-6}$	$1.0 \times 10^{-2} \pm 3 \times 10^{-4}$

The value of k_b can be approximated to the limiting value of k_{obs} / [4-$CH_3OC_6H_4CH_2NHCH_2SO_3^-$]$_{stoich}$. Therefore k_b is approximately 1.1×10^{-2} s^{-1}. Calculated K_a and corresponding pK_a values using this value of k_b are shown in Table 7.10. Values cannot be calculated for pH values above pH 6 as above this pH the k_{obs}/[4-$CH_3OC_6H_4CH_2NHCH_2SO_3^-$]$_{stoich}$ values become constant.

Table 7.10: Calculated K_a and pK_a values at each pH

pH	K_a	pK_a
4.0	$3.4 \times 10^{-6} \pm 9 \times 10^{-8}$	5.5
4.4	$2.8 \times 10^{-6} \pm 7 \times 10^{-8}$	5.6
4.7	$2.7 \times 10^{-6} \pm 7 \times 10^{-8}$	5.6
5.1	$2.5 \times 10^{-6} \pm 6 \times 10^{-8}$	5.6
5.3	$2.3 \times 10^{-6} \pm 5 \times 10^{-8}$	5.6
6.1	$1.9 \times 10^{-6} \pm 5 \times 10^{-8}$	5.7

The average K_a is 2.5×10^{-6} corresponding to a pK_a of 5.6. Figure 7.12 shows a plot of log[(k_{obs} / [4-$CH_3OC_6H_4CH_2NHCH_2SO_3^-$]$_{stoich}$) / s^{-1}] against pH for the experimental data with a calculated plot using a pK_a of 5.6 superimposed.

The calculated plot shows a good fit for the data. The pK_a of 4-methoxybenzylamine is 9.51, therefore the presence of the -$CH_2SO_3^-$ group, an electron withdrawing group, reduces the pK_a by approximately four pH units.

Figure 7.12: Log[(k_{obs}/[4-$CH_3OC_6H_4CH_2NH_2CH_2SO_3^-$]$_{stoich}$) / s^{-1}] against pH with a calculated plot using a pK_a of 5.6 superimposed

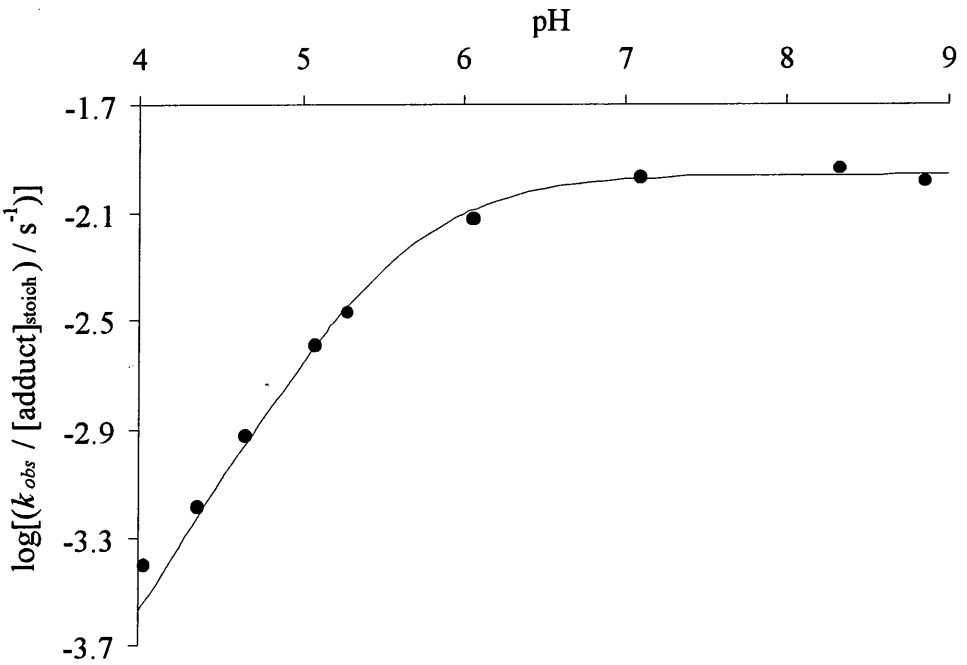

7.2.2.3 4-Methylbenzylamine adduct: 4-$CH_3C_6H_4CH_2NHCH_2SO_3^-$

4-Methylbenzylamine is not soluble in water. Therefore a stock solution in methanol was prepared. A final solvent composition of < 1 % methanol / > 99 % water by volume was used.

A stock solution of 0.022 M 4-methylbenzylamine and 0.020 M $CH_2(OH)(SO_3Na)$ was left to react for 2 minutes to ensure formation of the 4-$CH_3C_6H_4CH_2NHCH_2SO_3^-$ adduct. Lower concentrations of $CH_2(OH)(SO_3Na)$ and amine were used to prepare the stock solution of the adduct than for the previous amines due to the low solubility of 4-methylbenzylamine.

7.2.2.3.1 Rate constant for decomposition to the iminium ion

The reaction of 2.5×10^{-3} to 0.010 M 4-$CH_3C_6H_4CH_2NHCH_2SO_3^-$ with 4.0×10^{-4} M aqueous iodine solution at pH 5.1, 25 °C was investigated. The k_{obs} / mol dm^{-3} s^{-1} values obtained are shown in Table 7.11.

Table 7.11: k_{obs} / mol dm^{-3} s^{-1} values with varied [4-$CH_3C_6H_4CH_2NHCH_2SO_3^-$] / M at pH 5.1, 25 °C

[4-$CH_3C_6H_4CH_2N_2CH_2SO_3^-$] / M	k_{obs} / mol dm^{-3} s^{-1}
2.5×10^{-3}	$5.51 \times 10^{-6} \pm 3.2 \times 10^{-7}$
5.0×10^{-3}	$1.45 \times 10^{-5} \pm 4 \times 10^{-7}$
7.5×10^{-3}	$2.43 \times 10^{-5} \pm 6 \times 10^{-7}$
0.010	$3.63 \times 10^{-5} \pm 8 \times 10^{-7}$

The k_{obs} values obtained are similar to the corresponding values obtained for the decomposition of the benzylamine and 4-methoxybenzylamine adducts.

7.2.2.3.2 pH study

The effect of pH was investigated by studying the reaction of 5.0×10^{-3} M 4-$CH_3C_6H_4CH_2NHCH_2SO_3^-$ with 4.0×10^{-4} M aqueous iodine solution at pH 4.0 to 8.8, 25 °C. The k_{obs} / mol dm^{-3} s^{-1} and (k_{obs} / [4-$CH_3C_6H_4CH_2NHCH_2SO_3^-$]$_{stoich}$) / s^{-1} values obtained are shown in Table 7.12.

Table 7.12: k_{obs} / mol dm^{-3} s^{-1} and (k_{obs}/[4-$CH_3C_6H_4CH_2NHCH_2SO_3^-$]$_{stoich}$) / s^{-1} values at pH 4.0 to 8.8, 25 °C, [4-$CH_3C_6H_4CH_2NHCH_2SO_3^-$]$_{stoich}$ = 5.0×10^{-3} mol dm^{-3}

pH	k_{obs} / mol dm^{-3} s^{-1}	(k_{obs}/[4-$CH_3C_6H_4CH_2NHCH_2SO_3^-$]$_{stoich}$) / s^{-1}
4.0	$2.15 \times 10^{-6} \pm 5 \times 10^{-8}$	$4.3 \times 10^{-4} \pm 1 \times 10^{-5}$
4.4	$3.71 \times 10^{-6} \pm 1.1 \times 10^{-7}$	$7.4 \times 10^{-4} \pm 2 \times 10^{-5}$
4.7	$6.63 \times 10^{-6} \pm 1.6 \times 10^{-7}$	$1.3 \times 10^{-3} \pm 3 \times 10^{-5}$
5.1	$1.39 \times 10^{-5} \pm 4 \times 10^{-7}$	$2.8 \times 10^{-3} \pm 8 \times 10^{-5}$
5.3	$1.84 \times 10^{-5} \pm 5 \times 10^{-7}$	$3.7 \times 10^{-3} \pm 9 \times 10^{-5}$
6.1	$3.97 \times 10^{-5} \pm 9 \times 10^{-7}$	$7.9 \times 10^{-3} \pm 2 \times 10^{-4}$
7.1	$5.28 \times 10^{-5} \pm 1.3 \times 10^{-6}$	$1.1 \times 10^{-2} \pm 3 \times 10^{-4}$
8.3	$5.61 \times 10^{-5} \pm 1.3 \times 10^{-6}$	$1.1 \times 10^{-2} \pm 3 \times 10^{-4}$
8.8	$4.05 \times 10^{-5} \pm 1.1 \times 10^{-6}$	$8.1 \times 10^{-3} \pm 2 \times 10^{-4}$

The value of k_b can be approximated to the limiting value of k_{obs} / [4-$CH_3C_6H_4CH_2NHCH_2SO_3^-$]$_{stoich}$. Therefore k_b is approximately 1.1 × 10^{-2} s^{-1}. Calculated K_a and corresponding pK_a values using this value of k_b are shown in Table 7.13. Values cannot be calculated for pH values above pH 6 as above this pH the k_{obs}/[4-$CH_3C_6H_4CH_2NHCH_2SO_3^-$]$_{stoich}$ values become constant.

Table 7.13: Calculated K_a and pK_a values at each pH

pH	K_a	pK_a
4.0	$3.6 \times 10^{-6} \pm 8 \times 10^{-8}$	5.4
4.4	$3.3 \times 10^{-6} \pm 9 \times 10^{-8}$	5.5
4.7	$3.0 \times 10^{-6} \pm 7 \times 10^{-8}$	5.5
5.1	$2.8 \times 10^{-6} \pm 8 \times 10^{-8}$	5.6
5.3	$2.5 \times 10^{-6} \pm 7 \times 10^{-8}$	5.6
6.1	$2.2 \times 10^{-6} \pm 5 \times 10^{-8}$	5.7

The average K_a is 3.2 × 10^{-6} corresponding to a pK_a of 5.5. Figure 7.13 shows a plot of log[(k_{obs} / [4-$CH_3C_6H_4CH_2NHCH_2SO_3^-$]$_{stoich}$) / s^{-1}] against pH for the experimental data with a calculated plot using a pK_a of 5.5 superimposed.

The calculated plot shows a good fit for the data. The pK_a of 4-methylbenzylamine is 9.54, therefore the presence of the -$CH_2SO_3^-$ group, an electron withdrawing group, reduces the pK_a by approximately four pH units.

Figure 7.13: Log[(k_{obs}/[4-$CH_3C_6H_4CH_2NHCH_2SO_3^-$]$_{stoich}$) / s^{-1}] against pH with a calculated plot using a pK_a of 5.5 superimposed

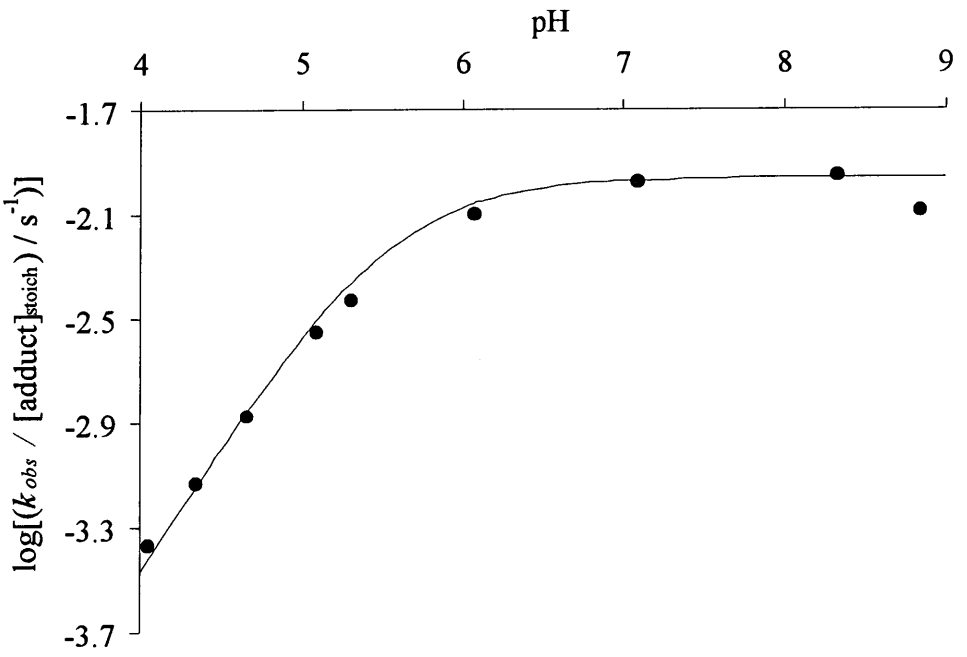

7.2.2.4 *N*-Methylbenzylamine adduct: $C_6H_5CH_2N(CH_3)(CH_2SO_3^-)$

N-Methylbenzylamine is not soluble in water. Therefore a stock solution in methanol was prepared. A final solvent composition of < 1 % methanol / > 99 % water by volume was used.

A stock solution of 0.022 M *N*-methylbenzylamine and 0.020 M $CH_2(OH)(SO_3Na)$ was left to react for 3 minutes to ensure formation of the $C_6H_5CH_2N(CH_3)(CH_2SO_3^-)$ adduct.

7.2.2.4.1 Rate constant for decomposition to the iminium ion

The reaction of 1.0×10^{-3} to 5.0×10^{-3} M $C_6H_5CH_2NH(CH_3)(CH_2SO_3^-)$ with 4.0×10^{-4} M aqueous iodine solution at pH 5.1, 25 °C was investigated. The k_{obs} / mol dm^{-3} s^{-1} values obtained are shown in Table 7.14.

Table 7.14: k_{obs} / mol dm^{-3} s^{-1} values with varied [$C_6H_5CH_2N(CH_3)(CH_2SO_3^-)$] / M at pH 5.1, 25 °C

[$C_6H_5CH_2N(CH_3)(CH_2SO_3^-)$] / M	k_{obs} / mol dm^{-3} s^{-1}
1.0×10^{-3}	$1.08 \times 10^{-4} \pm 3 \times 10^{-6}$
2.5×10^{-3}	$6.57 \times 10^{-4} \pm 1.7 \times 10^{-5}$
3.5×10^{-3}	$1.02 \times 10^{-3} \pm 7 \times 10^{-5}$
5.0×10^{-3}	$1.70 \times 10^{-3} \pm 5 \times 10^{-5}$

The k_{obs} values obtained are substantially larger than those obtained for the decomposition of the benzylamine, 4-methoxybenzylamine and 4-methylbenzylamine adducts.

7.2.2.4.2 pH study

The effect of pH was investigated by studying the reaction of 5.0×10^{-3} M $C_6H_5CH_2N(CH_3)(CH_2SO_3^-)$ with 4.0×10^{-4} M aqueous iodine solution at pH 4.0 to 8.9, 25 °C. The k_{obs} / mol dm^{-3} s^{-1} and (k_{obs} / [$C_6H_5CH_2N(CH_3)(CH_2SO_3^-)$]$_{stoich}$) / s^{-1} values obtained are shown in Table 7.15.

Table 7.15: k_{obs} / mol dm^{-3} s^{-1} and (k_{obs}/[$C_6H_5CH_2N(CH_3)(CH_2SO_3^-)$]$_{stoich}$) / s^{-1} values at pH 4.0 to 8.9, 25 °C, [$C_6H_5CH_2N(CH_3)(CH_2SO_3^-)$]$_{stoich}$ = 5.0×10^{-3} mol dm^{-3}

pH	k_{obs} / mol dm^{-3} s^{-1}	(k_{obs}/[$C_6H_5CH_2N(CH_3)(CH_2SO_3^-)$]$_{stoich}$) / s^{-1}
4.0	$4.10 \times 10^{-4} \pm 3.0 \times 10^{-5}$	$0.082 \pm 6 \times 10^{-3}$
4.4	$6.75 \times 10^{-4} \pm 3.3 \times 10^{-5}$	$0.135 \pm 7 \times 10^{-3}$
4.7	$8.28 \times 10^{-4} \pm 9.7 \times 10^{-5}$	0.166 ± 0.019
5.1	$1.70 \times 10^{-3} \pm 5 \times 10^{-5}$	0.340 ± 0.010
5.3	$2.08 \times 10^{-3} \pm 8 \times 10^{-5}$	0.416 ± 0.016
6.1	$2.78 \times 10^{-3} \pm 7 \times 10^{-5}$	0.556 ± 0.014
7.1	$2.99 \times 10^{-3} \pm 8 \times 10^{-5}$	0.598 ± 0.016
8.5	$2.89 \times 10^{-3} \pm 8 \times 10^{-5}$	0.578 ± 0.028
8.9	$1.86 \times 10^{-3} \pm 3 \times 10^{-5}$	0.372 ± 0.016

The value of k_b can be approximated to the limiting value of k_{obs} / $[C_6H_5CH_2N(CH_3)(CH_2SO_3^-)]_{stoich}$. Therefore k_b is approximately 0.58 s^{-1}. Calculated K_a and corresponding pK_a values using this value of k_b are shown in Table 7.16. Values cannot be calculated for pH values above pH 6 as above this pH the $k_{obs}/[C_6H_5CH_2N(CH_3)(CH_2SO_3^-)]_{stoich}$ values become constant.

Table 7.16: Calculated K_a and pK_a values at each pH

pH	K_a	pK_a
4.0	$1.5 \times 10^{-5} \pm 1 \times 10^{-6}$	4.8
4.4	$1.4 \times 10^{-5} \pm 7 \times 10^{-7}$	4.9
4.7	$9.1 \times 10^{-6} \pm 1.1 \times 10^{-6}$	5.0
5.1	$1.1 \times 10^{-5} \pm 3 \times 10^{-7}$	5.0
5.3	$1.2 \times 10^{-5} \pm 5 \times 10^{-7}$	4.9
6.1	$1.7 \times 10^{-5} \pm 4 \times 10^{-7}$	4.8

The average K_a is 1.2×10^{-5} corresponding to a pK_a of 4.9. Figure 7.14 shows a plot of $\log[(k_{obs} / [C_6H_5CH_2N(CH_3)(CH_2SO_3^-)]_{stoich}) / s^{-1}]$ against pH for the experimental data with a calculated plot using a pK_a of 4.9 superimposed.

The calculated plot shows a good fit for the data. The pK_a of *N*-methylbenzylamine is 9.59, therefore the presence of the $-CH_2SO_3^-$ group, an electron withdrawing group, reduces the pK_a by approximately five pH units.

Figure 7.14: Log[(k_{obs}/[$C_6H_5CH_2N(CH_3)(CH_2SO_3^-)$]$_{stoich}$) / s^{-1}] against pH with a calculated plot using a pK_a of 4.9 superimposed

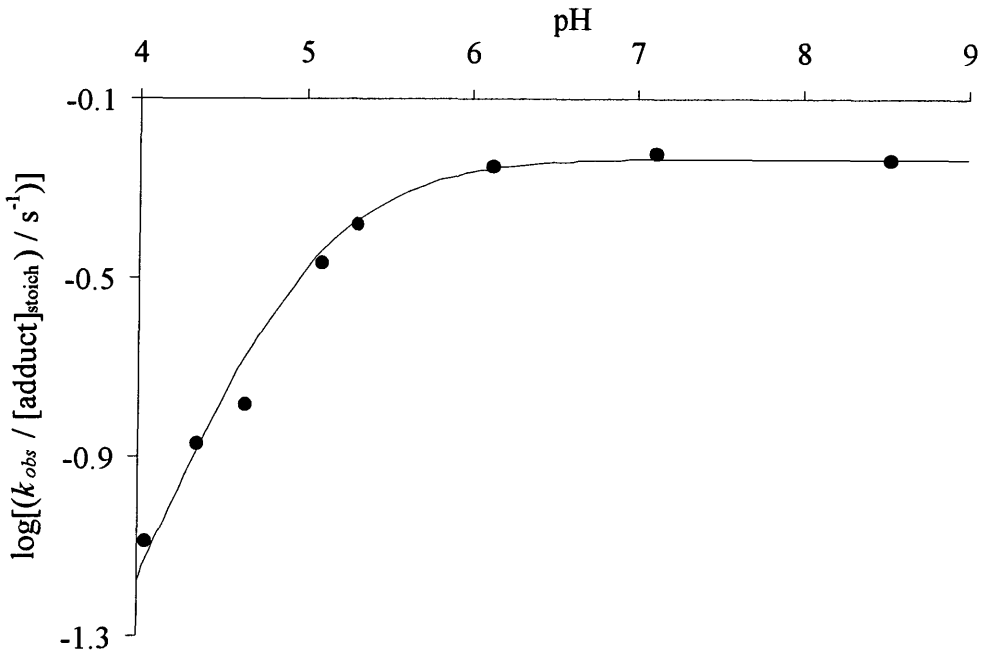

7.2.2.5 Summary

The first order rate constants, k_b, for the decomposition of $RCH_2NR'CH_2SO_3^-$ to the iminium ion $[RCH_2NR'=CH_2]^+$ and the pK_a values obtained for the $RCH_2N^+HR'CH_2SO_3^-$ adducts are summarised in Table 7.17.

Table 7.17: Summary of k_b / s^{-1} values and pK_a values obtained at 25 °C

adduct	k_b / s^{-1}	pK_a[†]
$C_6H_5CH_2NHCH_2SO_3^-$	8.0×10^{-3}	5.4
4-$CH_3OC_6H_4CH_2NHCH_2SO_3^-$	1.1×10^{-2}	5.6
4-$CH_3C_6H_4CH_2NHCH_2SO_3^-$	1.1×10^{-2}	5.5
$C_6H_5CH_2N(CH_3)(CH_2SO_3^-)$	0.58	4.9

[†] pK_a values correspond to dissociation of the protonated adducts

The k_b values for the benzylamine, 4-methoxybenzylamine and 4-methylbenzylamine adducts are all similar but the value for the *N*-methylbenzylamine adduct is around 100 times larger. This can be explained in terms of the electron donating effect of the methyl group which will stabilise the positive charge on the nitrogen in the developing iminium ion.

The pK_a values of the benzylamine, 4-methoxybenzylamine and 4-methylbenzylamine adducts are all around 5.4 to 5.6. However the pK_a of the *N*-methylbenzylamine adduct is lower at 4.9. This may be attributed to the steric effect of the methyl group which will prevent solvation to a greater degree and so make the *N*-methylbenzylamine adduct a weaker base.

The effect of the $-CH_2SO_3^-$ substituent is to increase the acidity of the benzylammonium ions by approximately 4 pH units. This may be attributed partly to electronic effects and partly to solvation effects.

It has previously been shown that the effect of the $-CH_2OH$ substituent on nitrogen lowers the pK_a of protonated amines by 2 to 3 pH units.[1] This effect was attributed largely to the reduction in solvation of the protonated species. In the protonated species $RCH_2N^+H(CH_3)(CH_2SO_3^-)$, the $-CH_2SO_3^-$ group will be expected to increase acidity due to its electron withdrawing ability. However the main effect is likely to be steric hindrance to solvation. Hence the energy will be raised and the acidity increases relative to the benzylammonium ion.

7.3 CONCLUSION

The decomposition of $RCH_2NR'CH_2SO_3^-$ adducts was followed in buffered solution. The adduct decomposes back to the starting materials. The rate of decomposition increases with increasing pH. The rate of decomposition was faster for the adduct formed from *N*-methylbenzylamine, $C_6H_5CH_2N(CH_3)(CH_2SO_3^-)$, than that formed from benzylamine, $C_6H_5CH_2NHCH_2SO_3^-$.

The addition of aqueous formaldehyde solution increased the rate of decomposition: sulfite ions released when the adduct decomposes to the iminium ion will react with the aqueous formaldehyde solution to produce $CH_2(OH)(SO_3^-)$.

The addition of sulfite ions decreases the rate of decomposition as the equilibrium is pushed back towards formation of the adduct.

The first order rate constants, k_b, obtained for the decomposition of $RCH_2NR'CH_2SO_3^-$ to the iminium ion $[RCH_2NR'=CH_2]^+$ are equal to 1×10^{-2} s^{-1} for the benzylamine, 4-methoxybenzylamine and 4-methylbenzylamine adducts where R' = H and R = H, 4-OCH_3 and 4-CH_3 respectively, and 0.58 s^{-1} for the *N*-methylbenzylamine adduct where R = H and R' = -CH_3. The k_b value for the *N*-methylbenzylamine adduct is larger due to the electron donating effect of the methyl group which will stabilise the positive charge on the nitrogen in the developing iminium ion.

The pK_a values of the benzylamine, 4-methoxybenzylamine and 4-methylbenzylamine adducts were determined to between 5.4 and 5.6. The pK_a of the *N*-methylbenzylamine adduct is lower, 4.9, due to the steric effect of the methyl group which will prevent solvation to a greater degree.

7.4 EXPERIMENTAL

7.4.1 Decomposition of $RCH_2NHCH_2SO_3^-$ to the starting materials

The decomposition of the adducts formed from benzylamine and *N*-methylbenzylamine was studied by pre-forming the adducts then obtaining absorbance against wavelength and absorbance against time plots for diluted samples at a range of pH values.

The adducts were prepared using approximately equimolar concentrations of amine and $CH_2(OH)(SO_3Na)$ to prevent formation of the 1 : 2 adduct. High concentrations of amine and $CH_2(OH)(SO_3Na)$ were used to ensure formation of the 1 : 1 adduct. The $CH_2(OH)(SO_3Na)$ solid was dissolved in distilled water and placed in a 100 cm^3 flask. The amine was then added and the solution made to the line using distilled water. In cases where an amine was used which was not soluble in water, a concentrated stock solution of the amine in methanol was prepared. The final solvent composition in the reaction mixture was < 1 % methanol / > 99 % water by volume.

The stock adduct solution was left for 3 to 5 minutes to ensure adduct production. If the solution was left too long it became cloudy. Therefore the time the solution was left was determined from considering the time taken for adduct formation in the ^1H NMR spectra (Chapter 6) and the time taken for the solution to become cloudy.

The concentrations of adduct quoted assume that the minor reagent reacts quantitatively to give the adduct: this assumption is valid considering the ^1H NMR experiments described in Chapter 6 which generally show complete conversion of the minor reagent.

Absorbance against wavelength spectra were obtained for the decomposition of 2×10^{-3} mol dm^{-3} benzylamine adduct at pH 6 and 7 and 1×10^{-3} mol dm^{-3} *N*-methylbenzylamine adduct at pH 5 to 9 and in the presence of 0.010 to 0.10 M added aqueous formaldehyde solution at pH 6 and 7. Spectra were recorded using a Perkin – Elmer Lambda 2 or Lambda 12 uv / vis spectrometer at 25 °C with 1 cm stoppered quartz cuvettes, taking scans every 1 to 10 minutes for up to 10 hours using a scan speed of 480 nm min^{-1}.

Absorbance against time plots were obtained for the decomposition of the adducts at pH 5 to 9 and in the presence of 0.010 to 0.10 M added aqueous formaldehyde solution at pH 6 and 7 and in the presence of 6.0×10^{-4} to 2.0×10^{-3} M aqueous sulfite solution at pH 6 and 7.

Sulfite ions absorb in the region studied: spectra of 0.01, 0.05 and 0.10 M aqueous sodium sulfite solution show high absorbance around 250 nm and to shorter wavelength. For example the extinction coefficient of sulfite ions at 245 nm was found to be 50 $dm^3\ mol^{-1}\ cm^{-1}$. Therefore the appropriate concentration of sulfite ions was added to the reference in order to subtract the absorbance due to the presence of sulfite from the absorbance against time plots.

Where $[sulfite]_{stoich}$ is quoted this refers to the total concentration of aqueous sodium sulfite added externally to the system and does not include the concentration of sulfite ions present due to dissociation of the adduct.

The aqueous formaldehyde solutions were prepared by diluting, with distilled water, the purchased 37 % by weight aqueous formaldehyde solution. These solutions were left to stand at room temperature for at least 2½ hours, more usually 4 – 4½ hours, to ensure depolymerisation.

Spectra were recorded using a Perkin – Elmer Lambda 2 or Lambda 12 uv / vis spectrometer at 25 °C with 1 cm stoppered quartz cuvettes, taking readings every 5 to 90 seconds for between 5 minutes and 3 hours. First order rate constants were obtained using the Perkin Elmer Computerised Spectroscopy Software (PECSS) program installed on the Perkin – Elmer Lambda 2 spectrometer or by plotting $\ln(A_\infty - A)$ against time / s using Microsoft Excel and performing linear regression.

For the reaction of the *N*-methylbenzylamine adduct with added aqueous formaldehyde solution the plots were recorded at 25.0 – 25.2 °C using an Applied Photophysics DX.17MV BioSequential Stopped – flow ASVD Spectrometer with a 1 cm path length. Five averages were obtained, each the average of three runs of 50 seconds. The appropriate adduct solution was placed in one syringe and the aqueous formaldehyde solution with the appropriate buffer solution in the other. The solutions were made just

prior to use. The disappearance of the adduct was followed at 230 nm. First order kinetics were observed. The averages were fitted using the single exponential equation on the !SX.17MV program installed on the spectrometer.

The buffers employed and the corresponding stoichiometric buffer concentrations in the final reaction mixture are shown in Table 7.18.

Table 7.18: Final buffer concentrations, in aqueous solution

pH	component A†	$[A]_{stoich}$ / M	component B‡	$[B]_{stoich}$ / M
5	CH_3COONa	0.08	CH_3COOH	0.03
6	KH_2PO_4	0.19	NaOH	0..022
7	KH_2PO_4	0.19	NaOH	0.108
8	KH_2PO_4	0.19	NaOH	0.177
8	$Na_2B_4O_7.10\ H_2O$	0.03	HCl	0.012

† CH_3COONa = sodium acetate; KH_2PO_4 = potassium dihydrogen phosphate; $Na_2B_4O_7.10\ H_2O$ = borax

‡ CH_3COOH = acetic acid; NaOH = sodium hydroxide; HCl = hydrogen chloride

The pH values of all solutions were determined using a Jenway 3020 pH meter calibrated using pH 7 and pH 10 (for alkaline solutions) or pH 4 (for acidic solutions) buffers. pH values are quoted to one decimal place.

7.4.2 Decomposition of $RCH_2NHCH_2SO_3^-$ to the iminium ion

Initially the reaction of each amine with aqueous iodine solution was investigated: the absorbance against wavelength spectrum of 1×10^{-3} M amine in the presence of 4×10^{-4} M aqueous iodine solution at pH 5.1 was followed over time. 4-Methylbenzylamine and *N*-methylbenzylamine are not soluble in water. Therefore a stock solution in methanol was prepared. A final solvent composition of 2 % methanol / 98 % water by volume was used. Spectra were recorded using a UV-2101 PC Shimadzu Corporation or Perkin – Elmer Lambda 2 uv / vis spectrometer at 25 °C with 1 cm

stoppered quartz cuvettes, taking scans every 10 minutes using a scan speed of 480 nm min^{-1}.

Plots of absorbance against time for the reaction of adduct with 4×10^{-4} M aqueous iodine solution were obtained at pH 5.1 using four adduct concentrations from 2.5×10^{-3} to 0.010 M or 1.0×10^{-3} to 5.0×10^{-3} M in the case of the *N*-methylbenzylamine adduct, then at pH 4 to 9 using a constant adduct concentration of 5.0×10^{-3} M. Plots were recorded at 24.8 – 25.1 °C using an Applied Photophysics DX.17MV BioSequential Stopped – flow ASVD Spectrometer with a 1 cm path length. The experiments for each adduct were carried out in a random order to minimise errors due to environmental changes.

Ten averages were obtained, each the average of three runs of 0.05 to 200 seconds depending on the amine, the adduct concentration and the pH used, except where the timescale was 50 seconds or more when only 3 or 5 averages were obtained. The appropriate adduct solution was placed in one syringe and the aqueous iodine solution with the appropriate buffer solution in the other. The solutions were made just prior to use. The disappearance of the aqueous iodine solution peak at 350 nm was followed. Zero order kinetics were observed. The averages were fitted using linear regression using the !SX.17MV program installed on the spectrometer.

The adducts were prepared using approximately equimolar concentrations of amine and $CH_2(OH)(SO_3Na)$ to prevent formation of the 1 : 2 adduct, except for the one experiment where the solutions were made with one reagent in excess. The method used was the same as that described in Section 7.4.1. The stock adduct solution was left for 2 to 8 minutes to ensure adduct production.

KI was added to the stock aqueous iodine solution in great excess to ensure formation of the absorbing species (Appendix 2). For absorbance against time plots where the initial absorbance of the aqueous iodine solution was above 2 due to the high extinction coefficient of iodine, the initial data was not included in the linear fit.

k_{obs} / mol dm^{-3} s^{-1} values were determined by dividing the gradient of the linear fit by the extinction coefficient, ε, of aqueous iodine solution at 350 nm, 13400 ±

300 dm^3 mol^{-1} cm^{-1} (Appendix 2). The errors in the k_{obs} values were determined by applying Equation 7.10.

$$\% \text{ error in } k_{obs} = \sqrt{[(\% \text{ error in } \varepsilon)^2 + (\% \text{ error in gradient})^2]} \qquad \textbf{(7.10)}$$

The errors in the k_{obs} / $[adduct]_{stoich}$ and K_a values were calculated by determining the percentage error in the k_{obs} value and converting this into an absolute value of k_{obs} / $[adduct]_{stoich}$ or K_a.

k_{obs} values are quoted to three significant figures, k_{obs} / $[adduct]_{stoich}$ to two, or three significant figures in the case of the *N*-methylbenzylamine adduct, and K_a values to two significant figures.

The pH 8.9 data point for the *N*-methylbenzylamine adduct gave an anomalously low result and therefore was not included in the $\log[(k_{obs} / [adduct]_{stoich}]) / s^{-1}]$ against pH plot. A pH 10 borax / hydrochloric acid buffer was prepared but could not be used as the aqueous iodine solution immediately decolourised when added to the buffer: the pH 9 buffer was also prepared from borax, with sodium hydroxide, therefore this may account for the lower than expected values obtained at this pH.

The buffers employed and the corresponding stoichiometric buffer concentrations in the final reaction mixture are shown in Table 7.19.

The pH values of all solutions were determined using a Jenway 3020 pH meter calibrated using pH 7 and pH 10 (for alkaline solutions) or pH 4 (for acidic solutions) buffers. pH values are quoted to one decimal place.

Table 7.19: Final buffer concentrations, in aqueous solution

pH	component A	$[A]_{stoich}$ / M	component B	$[B]_{stoich}$ / M
4.0	CH_3COONa	0.24	CH_3COOH	1.08
4.4	CH_3COONa	0.24	CH_3COOH	0.54
4.7	CH_3COONa	0.24	CH_3COOH	0.26
5.1	CH_3COONa	0.24	CH_3COOH	0.10
5.3	CH_3COONa	0.36	CH_3COOH	0.10
6	KH_2PO_4	0.10	NaOH	0.011
7	KH_2PO_4	0.10	NaOH	0.058
8	KH_2PO_4	0.10	NaOH	0.093
9	$Na_2B_4O_7.10\ H_2O$	0.017	HCl	6×10^{-3}

7.5 REFERENCES

1. R. G. Kallen and W. P. Jencks, *J. Biol. Chem.*, 1966, **241**, 5864

CHAPTER 8

Conclusion

CHAPTER 8: Conclusion

8.1 SUMMARY OF RESULTS

The kinetics and mechanisms of the reaction of formaldehyde and an amine in the presence of sulfite have not previously been studied in detail. Only one study in the literature has briefly examined the reaction, using ammonia as the amine.[1] The reactions using anilines as the amine are known to yield aminomethanesulfonates, $RNHCH_2SO_3^-$, which are industrially important in the azo dye industry and are of interest in medical applications.

The reaction of formaldehyde with amines, with and without sulfite, has been studied here using anilines ($RC_6H_4NH_2$) and benzylamines ($RC_6H_4CH_2NH_2$) as the amine. Individual steps as well as the overall reaction have been investigated to gain a better understanding of the kinetics and mechanisms involved.

The mechanism of $RNHCH_2SO_3^-$ formation is shown in Scheme 8.1. For the reaction with benzylamines the experiments were generally performed at pH values lower than the pK_a values of the amines. The equilibrium between the protonated amine and the reactive unprotonated amine is therefore included in the mechanism.

Scheme 8.1:

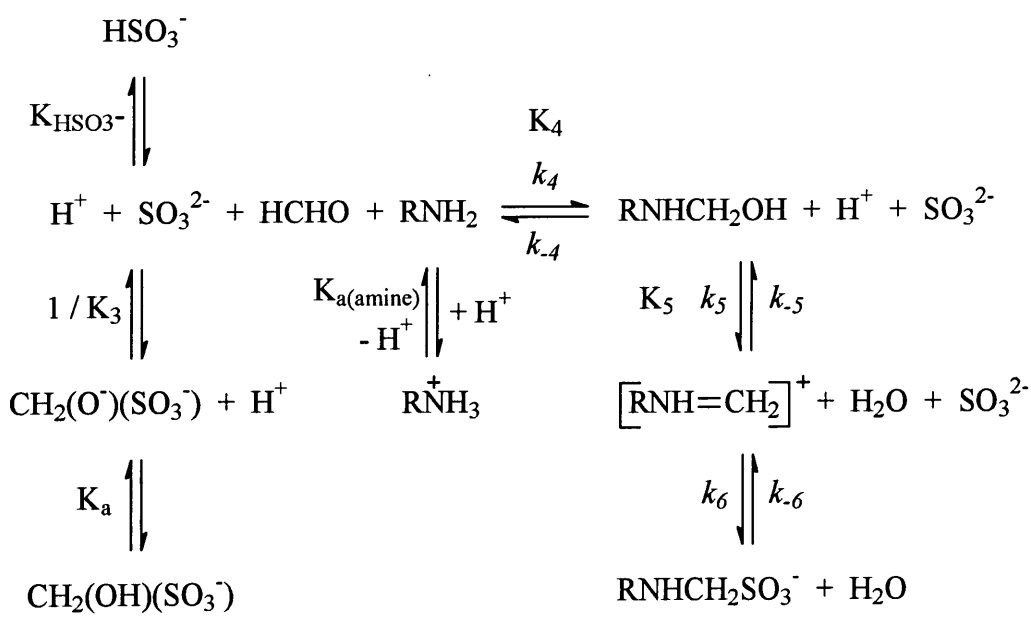

Hydroxymethanesulfonate, $CH_2(OH)(SO_3Na)$, was used to introduce formaldehyde and sulfite into the reaction. This eliminates the need to include the kinetics of dehydration of aqueous formaldehyde in the overall reaction. Decomposition of $CH_2(OH)(SO_3^-)$ must occur initially to produce reactive free formaldehyde, HCHO. Results show that above pH 3 decomposition occurs mainly through the dianion $CH_2(O^-)(SO_3^-)$. Below this pH, decomposition through the monoanion $CH_2(OH)(SO_3^-)$ forms the major pathway. Rate constants of 24 ± 5 s^{-1} and 2.3 × 10^{-8} s^{-1} respectively have been determined for these two decomposition pathways. Values of K_a and K_3 equal to 2.0 × 10^{-12} mol dm^{-3} and 2.2 × 10^5 mol^{-1} dm^3 are already reported in the literature.[2] The presence of additional sulfite ions in the system reduces the rate of formation of the product $RNHCH_2SO_3^-$ due to competition of the reaction of HCHO with sulfite ions to regenerate $CH_2(OH)(SO_3^-)$ rather than reaction with the amine.

After dissociation of $CH_2(OH)(SO_3^-)$, the free formaldehyde reacts with RNH_2 to form an *N*-(hydroxymethyl)amine, $RNHCH_2OH$. *N*-(Hydroxymethyl)amines have been observed using uv / vis and ^1H NMR spectroscopy. The reaction is subject to general acid and base catalysis. Values of k_4, k_{-4}, and K_4 of 8.0 × 10^3 to 2.4 × 10^5 dm^3 mol^{-1} s^{-1}, 0.13 to 6.6 s^{-1}, and 3.3 × 10^4 to 7.1 × 10^4 dm^3 mol^{-1} respectively have been determined using aniline and 3-, 4- and *N*- substituted anilines. The values of k_4, k_{-4}, and K_4 depend on the pK_a of the amine. The reaction occurs via a zwitterionic intermediate as shown in Scheme 8.2.

Scheme 8.2: $RNH_2 + HCHO \rightleftharpoons R\overset{+}{N}H_2CH_2O^- \rightleftharpoons RNHCH_2OH$

Values of k_4 equal to 2.3 × 10^5 and 4.3 × 10^6 dm^3 mol^{-1} s^{-1} have been calculated for benzylamines.

The *N*-(hydroxymethyl)amine dehydrates in acid conditions or loses hydroxyl ion to form an iminium ion, $[RNH{=}CH_2]^+$. This reaction has been examined indirectly by combining results obtained for the overall reaction with results for individual steps. A value of k_5 equal to 3.0 × 10^7 dm^3 mol^{-1} s^{-1} has been deduced for the reaction with anilines. This value represents the proton catalysed reaction.

The iminium ion reacts with sulfite ions, probably in a diffusion controlled reaction, to form $RNHCH_2SO_3^-$. Formation of $RNHCH_2SO_3^-$ and $RN(CH_3)(CH_2SO_3^-)$, from *N*-methylbenzylamine, have been observed using uv / vis and ^1H NMR spectroscopy. Equilibrium constants of 410 and 780 dm^3 mol^{-1} were obtained for the formation of $RNHCH_2SO_3^-$ from anilines.

Polymerisation of imines has also been studied. A cyclic trimer or a 1 : 2 formaldehyde amine adduct can form in the reaction of formaldehyde with anilines in equimolar amounts. The cyclic imine trimer formed with aniline is known to react with bisulfite.[3] However the reactions here were studied with $CH_2(OH)(SO_3Na)$ or formaldehyde in excess therefore no imine polymer will be present under these conditions. Other reactions of imines such as hydrolysis and reaction with amines will also not compete as the reaction of the iminium ion with sulfite will be more rapid under the conditions used.

The rate determining step of the mechanism shown in Scheme 8.1 depends on the pH of the system. At low and neutral pH the reaction of HCHO with RNH_2 is thought to be the rate determining step. Below pH 3, decomposition of $CH_2(OH)(SO_3^-)$ may become rate limiting. At high pH the rate determining step is likely to be dehydration of the *N*-(hydroxymethyl)amine to form the iminium ion. This reaction is acid catalysed therefore at high pH can become rate limiting.

Decomposition of the products $RNHCH_2SO_3^-$ and $RN(CH_3)CH_2SO_3^-$ formed from benzylamines has been studied. The rate of decomposition is faster for the adduct formed from *N*-methylbenzylamine, $RN(CH_3)CH_2SO_3^-$, than that of $RNHCH_2SO_3^-$ due to the electron donating effect of the methyl group which will stabilise the positive charge on the nitrogen in the developing iminium ion. The addition of aqueous formaldehyde solution increases the rate of decomposition: sulfite ions released when the adduct decomposes to the iminium ion will react with the aqueous formaldehyde solution to produce $CH_2(OH)(SO_3^-)$. The addition of sulfite ions decreases the rate of decomposition as the equilibrium is pushed back towards formation of the adduct.

pK_a values of 5.4 to 5.6 were obtained for $RN^+H_2CH_2SO_3^-$ products formed from benzylamines, apart from $RN^+H(CH_3)(CH_2SO_3^-)$ formed from *N*-methylbenzylamine

which was found to have a pK_a of 4.9. The steric effect of the methyl group will prevent solvation to a greater degree and hence lower the pK_a.

Benzylamines are more nucleophilic than anilines therefore with these amines the $RNHCH_2SO_3^-$ product can react with another molecule of $CH_2(OH)(SO_3^-)$ to give $RN(CH_2SO_3^-)_2$. The mechanism of formation of $RN(CH_2SO_3^-)_2$ is shown in Scheme 8.3. However, the major product of reaction with benzylamines is still the 1 : 1 adduct $RNHCH_2SO_3^-$.

Scheme 8.3:

$$RNHCH_2SO_3^- + HCHO \underset{k'_{-4}}{\overset{k'_4}{\rightleftharpoons}} RN(CH_2SO_3^-)(CH_2OH)$$

$$+ H^+ \; k'_5 \Big\uparrow\Big\downarrow k'_{-5}$$

$$[(R)(CH_2SO_3^-)N{=}CH_2]^+ + H_2O$$

$$+ SO_3^{2-} \; k_6 \Big\uparrow\Big\downarrow k_{-6}$$

$$RN(CH_2SO_3^-)_2 + H_2O$$

It was found that 1 : 2 adducts do not form if there is an electron withdrawing group present on the benzylamine. The nucleophilicity of the benzylamine nitrogen is lowered therefore reducing the tendency to add a second $CH_2(OH)(SO_3^-)$ molecule.

The work here has provided a better understanding of the kinetics and mechanisms of the reaction of formaldehyde with amines in the presence of sulfite. The overall reaction and the individual steps have been studied. Primary and secondary amines have been examined: substituent, pK_a and pH effects have also been investigated. Results obtained here could be beneficial for optimising industrial processes in, for example, the azo dye industry. The rate determining step under a range of conditions has been determined. The potential of using $CH_2(OH)(SO_3^-)$ as a way of producing HCHO in situ has also been highlighted.

8.2 REFERENCES

1. P. Le Hénaff, *Compt. Rend. Acad. Sci.*, 1963, **256**, 3090

2. P. E. Sørensen and V. S. Andersen, *Acta. Chem. Scand*, 1970, **24**, 1301

3. Badische Anilin and Soda Fabrik, Germ. Patent, 1902, 132621

CHAPTER 9

Experimental

CHAPTER 9: Experimental

9.1 MATERIALS

Materials of the highest grades were purchased commercially from Aldrich and used without purification, apart from the imine polymers which were synthesised as described in the text. A Sonomatic sonic bath was used to dissolve compounds with low solubility.

A 37 % by weight aqueous formaldehyde solution with 10 % methanol stabiliser was used: this was diluted and left to stand for at least 2½ hours, more usually 4 – 4½ hours, prior to use to ensure depolymerisation of higher molecular weight polyoxymethylene glycols to methylene glycol. For NMR work, 99.6 to 99.9 atom % D solvents in 1 cm^3 prescored ampules were used.

General purpose methanol was used for washing all apparatus.

9.2 EXPERIMENTAL MEASUREMENTS

Volumes were measured generally using glass pipettes for volumes greater than 0.5 cm^3 and Gilson Pipettman dispensing pipettes with disposable tips for smaller volumes. The Gilson Pipettman pipettes were calibrated prior to use by weighing the volume of water dispensed at a particular setting, assuming a density of water of 1 g cm^{-3}, and adjusting the volume setting accordingly.

Melting points were determined using a digital Gallenkamp melting apparatus.

9.3 CONVENTIONAL UV / VIS SPECTROMETRY

Absorbance against time spectra and absorbance against time plots were recorded using a UV-2101 PC Shimadzu Corporation or a Perkin – Elmer Lambda 2 or Lambda 12 uv / vis spectrometer at 25 °C using 1 cm path length stoppered quartz cuvettes. The

cuvettes were left in the spectrometer for at least 10 minutes prior to use to allow the temperature to equilibrate to 25 °C. Absorbance against time spectra were generally recorded using a scan speed of 480 nm min^{-1}. Spectra were obtained to determine an appropriate wavelength to follow absorbance against time plots.

Water was generally used as the solvent: mixed solvent systems were used where the compounds were only sparingly soluble in water at the concentration required. Reactions were carried out under pseudo first order or zero order conditions.

Where solutions were buffered, buffer was also added to the reference cuvette.

9.4 STOPPED FLOW SPECTROPHOTOMETRY

Reactions too fast to study on conventional spectrometers were followed using stopped flow spectrophotometry. Plots of absorbance against time were recorded using an Applied Photophysics DX.17MV BioSequential Stopped – flow ASVD Spectrometer at 24.8 – 25.2 °C with a cell of 2 mm or 1 cm path length. Scheme 9.1 shows a schematic of the stopped flow spectrometer.

Scheme 9.1:

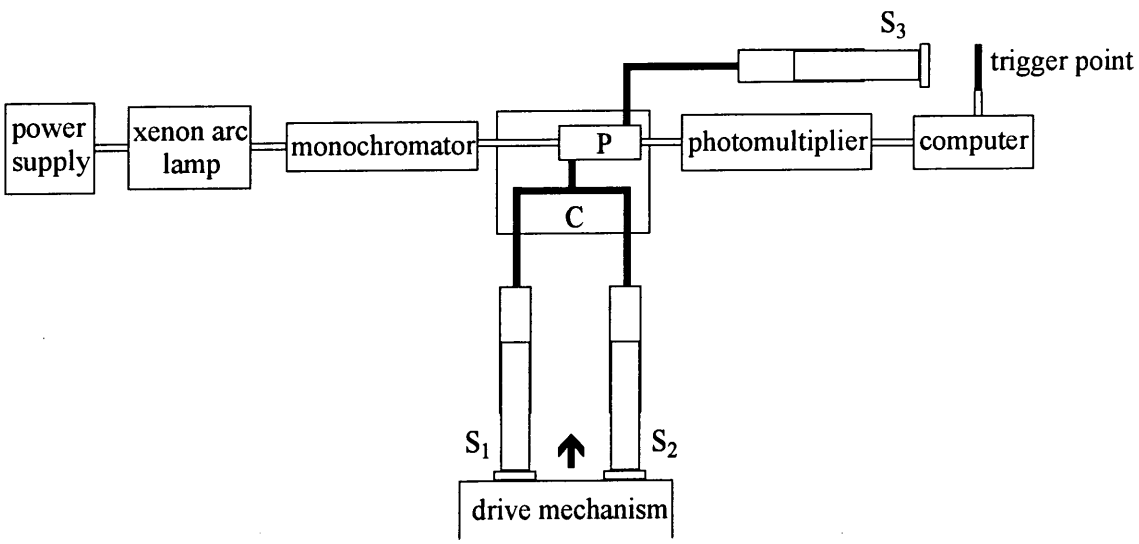

The two syringes, S_1 and S_2, are filled with their respective solutions. To start the reaction, equal volumes of solution are pneumatically forced out of the two syringes,

through a mixing cell, C, and along an observation tube to the collector syringe, S_3. The recording of the plot and the stopping of the flow of solution are triggered by the plunger of syringe S_3 reaching the trigger point.

The amount of light passing through a fixed point, P, just downstream of the mixing cell will change as the reaction proceeds. The monochromator fixes the light at the desired wavelength. The photomultiplier converts the light passing through point P into an electric current and a voltage is generated proportional to the light intensity. This signal is sampled by the computer at pre-selected intervals over an appropriate time range: the computer software transforms this change in voltage against time data into absorbance against time data by applying Equation 9.1, where A = absorbance, V_o = initial voltage and ΔV = change in voltage.

$$A = \log_{10}\left(\frac{V_o}{V_o - \Delta V}\right) \qquad \textbf{(9.1)}$$

The dead time of the spectrometer is approximately 5 ms therefore reactions with half lives smaller than this cannot be measured using stopped flow techniques.

The apparatus was washed through with distilled water and the appropriate solutions prior to use. Approximately five short runs were performed prior to obtaining results to ensure efficient mixing. Water was generally used as the solvent: mixed solvent systems were used where the compounds were only sparingly soluble in water at the concentration required. Reactions were carried out under pseudo first order or zero order conditions. Runs were often carried out in a random order rather than in increasing / decreasing concentration to minimise errors due to environmental changes.

9.5 DATA FITTING AND ERRORS IN MEASUREMENT

For results obtained using conventional spectroscopy methods, first order kinetics were fitted using the Perkin Elmer Computerised Spectroscopy Software (PECSS) program installed on the Perkin – Elmer Lambda 2 spectrometer or by plotting $\ln(A_\infty - A)$ against time / s using Microsoft Excel and performing linear regression. Good

correlation was obtained between the two methods. Zero order plots were fitted using linear regression on Microsoft Excel. First order rate constants obtained using stopped flow spectrophotometry were fitted using the single exponential fit function and zero order plots fitted using linear regression on the !SX.17MV program installed on the spectrometer.

All fitting methods used to obtain first order rate constants are based on the following equations for deriving a rate expression for a first order reaction. For a reaction of the type A $\rightarrow$ B, the rate of formation of B, or the rate of decomposition of A, can be expressed in terms of Equation 9.2.

$$\frac{d[B]}{dt} = -\frac{d[A]}{dt} = k_{obs}[A] \qquad \textbf{(9.2)}$$

Integrating this equation gives:

$$-\int_{[A]_o}^{[A]_t} \frac{1}{[A]}\, d[A] = \int_{0}^{t} k_{obs}\, dt \qquad \textbf{(9.3)}$$

$$\ln[A]_t - \ln[A]_o = -k_{obs}\, t \qquad \textbf{(9.4)}$$

$$k_{obs} = -\frac{1}{t} \ln \frac{[A]_t}{[A]_o} \qquad \textbf{(9.5)}$$

where $[A]_o$ and $[A]_t$ are concentrations of A at time t = 0 and t respectively.

The Beer Lambert Law states that A = εcl, where ε is the extinction coefficient, c the concentration and l the cell pathlength. If the pathlength is assumed to be 1 cm then Equations 9.6 to 9.14 apply.

$$A_o = \varepsilon_A[A]_o \qquad \textbf{(9.6)}$$

$$A_t = \varepsilon_A[A]_t + \varepsilon_B[B]_t \qquad \textbf{(9.7)}$$

$$\text{Since} \quad [B]_t = [A]_o - [A]_t \qquad \textbf{(9.8)}$$

$$\Rightarrow \quad A_t = \varepsilon_A[A]_t + \varepsilon_B[A]_o - \varepsilon_B[A]_t \qquad \textbf{(9.9)}$$

$$A_\infty = \varepsilon_B[B]_\infty = \varepsilon_B[A]_o \quad \text{since } [B]_\infty = [A]_o \qquad \textbf{(9.10)}$$

$$\text{Therefore} \quad (A_\infty - A_t) = \varepsilon_B[A]_t - \varepsilon_A[A]_t \qquad \textbf{(9.11)}$$

$$\text{Hence} \quad [A]_t = \frac{(A_\infty - A_t)}{(\varepsilon_B - \varepsilon_A)} \qquad \textbf{(9.12)}$$

$$\text{Similarly} \quad (A_\infty - A_o) = \varepsilon_B[A]_o - \varepsilon_A[A]_o \qquad \textbf{(9.13)}$$

$$\text{Hence} \quad [A]_o = \frac{(A_\infty - A_o)}{(\varepsilon_B - \varepsilon_A)} \qquad \textbf{(9.14)}$$

Substituting Equations 9.12 and 9.14 into Equation 9.5 gives:

$$k_{obs} = -\frac{1}{t} \ln \frac{(A_\infty - A_t)}{(A_\infty - A_o)} \qquad \textbf{(9.15)}$$

$$\Rightarrow \quad \ln(A_\infty - A_t) = -k_{obs}\, t + \ln(A_\infty - A_o) \qquad \textbf{(9.16)}$$

Therefore plotting $\ln(A_\infty - A_t)$ against time should give a linear plot with a gradient equal to $-k_{obs}$. Infinity values, A_∞, were determined over at least ten half lives and the data fitted over approximately 80 % of the reaction.

The MicroMath Scientist package for Microsoft Windows, Version 2.0 was also used to fit data. Linear regression on Microsoft Excel was used to calculate gradients and intercepts of linear plots and the errors in these values.

9.6 ^{1}H NMR SPECTROSCOPY

^{1}H NMR spectra were recorded using a 200 MHz Varian Mercury-200 or Varian VXR-200, or a 400 MHz Varian Gemini-400 spectrometer. The solvent present in the highest proportion was used for locking purposes and as the reference peak for spectra.

Mixed solvents were used where the compounds were not soluble in water at the concentrations required.

Spectra were recorded immediately and continued until there was no further change in the spectrum. The time of mixing refers to the time at which the reaction initiator was added to the NMR tube. The time of each spectrum was taken as the time when the spectrometer started to acquire the spectrum.

For the reactions involving an amine and $CH_2(OH)(SO_3Na)$, the volumes of amine and $CH_2(OH)(SO_3Na)$ needed to obtain the required final concentrations using 1 cm^3 D_2O solvent were calculated using Equation 9.17 or 9.18, depending on whether the amine used was a liquid or a solid respectively, and Equation 9.19.

$$c_1 = \frac{yd}{MW} \times \frac{1000}{1+y+x} \qquad \textbf{(9.17)}$$

$$c_1 = \frac{y}{1+y+x} \times [\text{amine}]_{\text{stock}} \qquad \textbf{(9.18)}$$

$$c_2 = \frac{x}{1+y+x} \times [CH_2(OH)(SO_3Na)]_{\text{stock}} \qquad \textbf{(9.19)}$$

y = volume of neat amine / cm^3; x = volume of $CH_2(OH)(SO_3Na)$ solution / cm^3; d = density of the amine; MW = molecular weight of the amine; c_1 = final concentration of amine in the NMR tube / mol dm^{-3}; c_2 = final concentration of $CH_2(OH)(SO_3Na)$ in the NMR tube / mol dm^{-3}; $[\text{amine}]_{\text{stock}}$ = concentration of the stock amine solution in D_2O / mol dm^{-3}; $[CH_2(OH)(SO_3Na)]_{\text{stock}}$ = concentration of the stock $CH_2(OH)(SO_3Na)$ solution in D_2O / mol dm^{-3}.

Where the amine was insoluble in D_2O, mixed solvent systems were used. A stock amine solution was prepared in a mixed solvent: this was then added to the NMR tube. The mixed solvent required to prepare the amine was determined using Equation 9.20.

$$\frac{\%}{100} = \frac{y}{1+y+x} \times \frac{z}{1} \qquad \textbf{(9.20)}$$

% = final percentage of the minor solvent required in the NMR tube; z = volume of minor solvent / cm^3; 1 – z = volume of D_2O / cm^3.

9.7 pH MEASUREMENTS

The pH values of solutions were determined using a Jenway 3020 pH meter calibrated using pH 7 and pH 10 (for alkaline solutions) or pH 4 (for acidic solutions) buffers at 25 °C. The sample was thermostatted at 25 °C prior to taking a pH measurement. The pH meter temperature probe was also inserted into the sample solution to measure the temperature.

APPENDICES

APPENDIX 1: Derivation of standard rate equations

A1.1 RATE EQUATION USED TO OBTAIN k_f AND k_b

For a reaction of the type shown in Scheme A1.1, if the reaction is performed under conditions where [B] >> [A], the reaction becomes pseudo first order and the rate is given by Equation A1.1.

Scheme A1.1:

$$A + B \underset{k_b}{\overset{k_f}{\rightleftharpoons}} C$$

$$-\frac{d[A]}{dt} = k_f'[A] - k_b[C] \quad \text{where } k_f' = k_f[B] \qquad \textbf{(A1.1)}$$

If $[A]_e$ and $[C]_e$ are the concentrations of A and C at equilibrium and x is the distance of the concentrations from equilibrium, then:

$$x = [A] - [A]_e = [C]_e - [C] \qquad \textbf{(A1.2)}$$

$$\text{Therefore } [A] = [A]_e + x \qquad \textbf{(A1.3)}$$

$$\text{and } [C] = [C]_e - x \qquad \textbf{(A1.4)}$$

Substituting Equations A1.3 and A1.4 into Equation A1.1 gives:

$$-\frac{d[A]}{dt} = (k_f' + k_b)x + (k_f'[A]_e - k_b[C]_e) \qquad \textbf{(A1.5)}$$

However $k_f'[A]_e = k_b[C]_e$ as at equilibrium the rates of the forward and reverse reactions are equal. Therefore Equation A1.5 reduces to:

$$-\frac{d[A]}{dt} = (k_f' + k_b)x \qquad \textbf{(A1.6)}$$

Therefore the observed pseudo first order rate constant, k_{obs}, is given by:

$$k_{obs} = k_f' + k_b \qquad \textbf{(A1.7)}$$

Therefore $k_{obs} = k_f[B] + k_b$ **(A1.8)**

Therefore plotting k_{obs} / s^{-1} against [B] / M should give a linear plot with a gradient equal to k_f and an intercept equal to k_b.

APPENDIX 2: Standardisation of the aqueous iodine solution and determination of the extinction coefficients

A2.1 STANDARDISATION OF THE AQUEOUS IODINE SOLUTION

A method based on that described[1] in Vogel's 'Textbook of Quantitative Inorganic Analysis' involving standard sodium thiosulfate solution was used to standardise an approximately 1M aqueous iodine solution to determine the exact concentration.

First an aqueous solution of approximately 1 M sodium thiosulfate was standardised using potassium iodate.[1] 3.568g potassium iodate was dissolved in 1 dm^3 distilled water. 25 cm^3 of this solution was placed in a conical flask and 1.00 g iodate – free potassium iodide[†] added, followed by 3 cm^3 1 M sulfuric acid. The solution became brown in colour due to liberation of iodine. This iodine was titrated against the aqueous sodium thiosulfate solution with constant shaking. When the solution had become pale yellow in colour, the mixture was diluted to about 200 cm^3 and 0.5 g BDH iodine indicator, a starch substitute, was added. The titration was continued until the colour changed from blue to colourless. This procedure was repeated twice more. The average volume of aqueous sodium thiosulfate solution added was 2.53 ± 0.06 cm^3.

Potassium iodate reacts with potassium iodide in acid solution to liberate iodine according to the reaction shown in Scheme A2.1.

Scheme A2.1: $IO_3^- + 5I^- + 6H^+ \longrightarrow 3I_2 + 3H_2O$

When thiosulfate solution is added to a solution containing iodine, a colourless intermediate, $S_2O_3I^-$, is formed by a rapid reversible reaction. This then reacts with thiosulfate ions to give the main pathway of the overall reaction (Scheme A2.2).

[†] The absence of iodate was indicated when no immediate yellow colouration was obtained when dilute sulfuric acid was added. Also when a starch – substitute indicator was added to a separate portion, no blue coloration was produced.

Scheme A2.2:

$$S_2O_3^{2-} + I_2 \rightleftharpoons S_2O_3I^- + I^-$$

$$S_2O_3I^- + S_2O_3^{2-} \longrightarrow S_4O_6^{2-} + I^-$$

$$2S_2O_3^{2-} + I_2 \longrightarrow S_4O_6^{2-} + 2I^-$$

Potassium iodide was added in excess therefore the limiting reagent is potassium iodate. 4.17×10^{-4} moles of potassium iodate reacted therefore 2.50×10^{-3} moles of $Na_2S_2O_3$ were present in 25 cm^3. Hence the concentration of aqueous sodium thiosulfate solution is 0.99 M.

This standardised 0.99 M aqueous sodium thiosulfate solution was then used to standardise the aqueous iodine solution. 25 cm^3 of the aqueous iodine solution was placed in a conical flask and diluted to approximately 100 cm^3 with distilled water. This was titrated against the standardised aqueous sodium thiosulfate solution until the solution was pale yellow in colour. 0.5 g of BDH Iodine Indicator was then added and the titration continued until the colour changed from blue to colourless. This procedure was repeated twice more.

The average volume of sodium thiosulfate solution required was 41.90 ± 0.20 cm^3. The reactions in Scheme A2.2 apply here also. 0.042 moles of $Na_2S_2O_3$ reacted therefore 0.021 moles of iodine reacted. Hence 0.021 moles of iodine are present in 25 cm^3 therefore the concentration of the aqueous iodine solution is 0.83 M.

A2.2 EXTINCTION COEFFICIENTS OF THE AQUEOUS IODINE SOLUTION

The extinction coefficient, ε, of the aqueous iodine solution is necessary to calculate rate constants for reactions that are zero order with respect to aqueous iodine solution concentration. The absorbance of the aqueous iodine solution was found to increase considerably in the presence of potassium iodide, KI. Addition of KI will push the equilibrium shown in Scheme A2.3 over to the triiodide species I_3^-.

Scheme A2.3:

$$I_2 + I^- \rightleftharpoons I_3^-$$

As addition of KI increases the absorbance, this suggests that I_3^- is the main absorbing species rather than I_2.

Six concentrations of aqueous iodine solution ranging from 1.7×10^{-5} to 1.0×10^{-4} M with 1.0×10^{-3} M aqueous KI solution added were used to obtain absorbance against wavelength spectra. Spectra were recorded using a UV-2101 PC Shimadzu Corporation at 25 °C with 1 cm stoppered quartz cuvettes, using a scan speed of 480 nm min^{-1}. The absorbance of the highest aqueous iodine solution concentration was not used for the 287 nm peak as the absorbance was greater then 2 and so was greater than the limit of the machine.

Two main peaks were observed at 287 and 350 nm. Using the Beer – Lambert relationship $A = \varepsilon cl$, where c is the concentration and l the cell pathlength, ε may be determined by plotting A against the aqueous iodine solution concentration. The value of ε is equal to the gradient of the line (Figure A2.1).

Figure A2.1: Plot to determine the extinction coefficients of the aqueous iodine solution with added KI

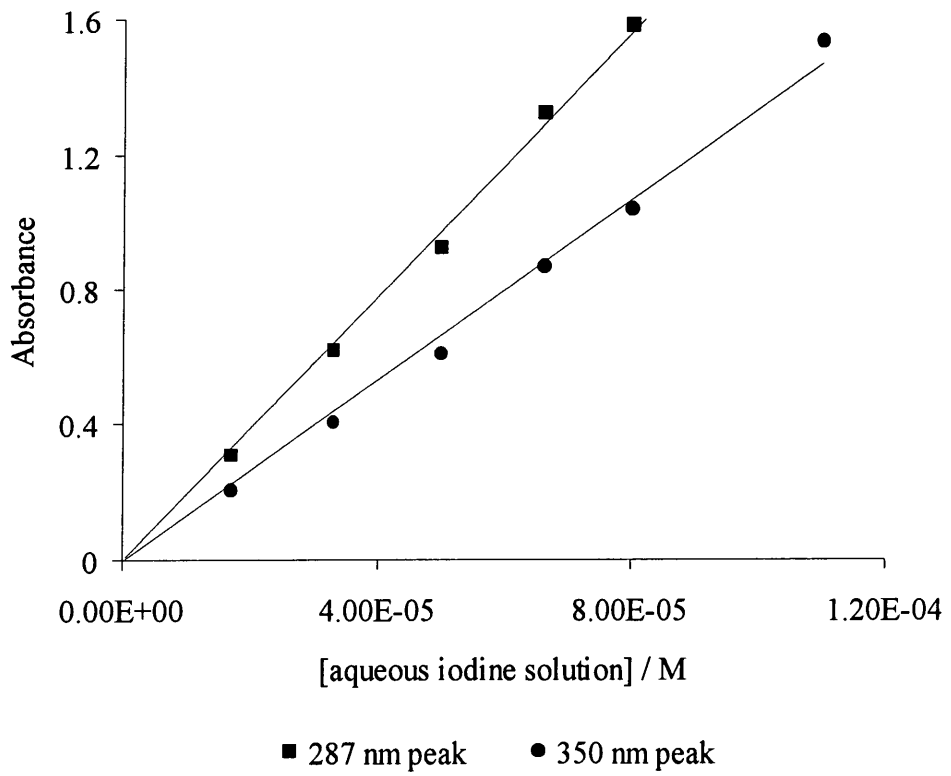

Values of ε equal to 19600 ± 300 and 13400 ± 300 dm^3 mol^{-1} cm^{-1} for the 287 and 350 nm peaks respectively are obtained. Linear regression yielded correlation coefficients of 0.995 and 0.990 respectively.

To ensure the presence of the absorbing species, I_3^-, KI was usually added in great excess to the aqueous iodine solution when used experimentally.

A2.3 REFERENCES

1. A. Vogel, 'A Textbook of Quantitative Inorganic Analysis', 4th Ed., Longman Inc., 1978, New York, pp. 375 - 379

APPENDIX 3: Seminars and conferences attended

A3.1 SEMINARS ATTENDED

23.10.96 Professor H. Ringsdorf, Johannes Gutenberg – Universitat, Germany
Function Based on Organisation

30.10.96 Dr. P. Mountford, Nottingham University
Recent Developments in Group IV Imido Chemistry

06.11.96 Dr. M. Duer, Cambridge University
Solid State NMR Studies of Organic Solid to Liquid – Crystalline Phase Transitions

18.11.96 Professor G. Olah, University of Southern California
Crossing Conventional Lines in My Chemistry of the Elements

27.11.96 Dr. R. Templer, Imperial College, London
Molecular Tubes and Sponges

15.01.97 Dr. V. K. Aggarwal, University of Sheffield
Sulfur Mediated Asymmetric Synthesis

29.01.97 Professor A. Kirby, University of Cambridge, Ingold Lecturer
Molecular Recognition of Transition States

05.02.97 Dr. A. Haynes, University of Sheffield
Mechanism in Homogeneous Catalytic Carbonylation

19.02.97 Professor B. Hayden, Southampton University
The Dynamics of Dissociation at Surfaces and Fuel Cell Catalysts

19.03.97 Dr. K. Reid, University of Nottingham
Probing Dynamical Processes with Photoelectronics

29.10.97 Professor B. Peacock, University of Glasgow, RSC Endowed Lecture
Probing Chirality with Circular Dichroism

05.11.97 Dr. M. Hii, Oxford University
Studies of the Heck Reaction

03.12.97 Professor A. P. Davis, Trinity College Dublin
Steroid – Based Frameworks for Supramolecular Chemistry

10.12.97 Professor M. Page, University of Huddersfield
The Mechanism and Inhibition of Beta – Lactamases

28.01.98 Dr. S. Rannard, Coutaulds Coatings, Coventry
Synthesis of Dendrimers using Highly Selective Chemical Reactions

18.02.98 Professor G. Hancock, Oxford University
Surprises in the Photochemistry of Tropospheric Ozone

11.03.98 Professor M. J. Cook, University of East Anglia
How to Make Phthalocyanine Films and What to Do With Them

23.10.98 Professor J. Scaiano, University of Ottawa, Canada, RSC Endowed Lecture
In Search of Hypervalent Free Radicals

18.11.98 Dr. R. Cameron, Cambridge University
Biodegradable Polymers: Morphology and Controlled Release

02.12.98 Dr. M. Jaspers, University of Aberdeen
Bioactive Compounds Isolated from Marine Invertebrates and Cyanobacteria: Drugs from the Deep

27.01.99 Professor K. Wade, University of Durham
Foresight or Hindsight? Some Borane Lessons and Loose Ends

03.02.99 Dr. C. Schofield, University of Oxford
Studies on the Stereoelectronics of Enzyme Catalysis

17.02.99 Dr. B. Horrocks, Newcastle University
Microelectrode Techniques for the Study of Immobilised Enzymes and Nucleic Acids

A3.2 CONFERENCES ATTENDED

22.12.97 Graduate Poster Competition, University of Durham
Sponsored by ICI
Poster presented entitled 'Mechanism of Amine / Formaldehyde and Nucleophile Reactions'

09.01.98 to 17.01.98 International Winter School on Organic Reactivity, Bressanone, Italy
Sponsored by EU
Poster presented entitled 'Mechanism of Amine / Formaldehyde and Nucleophile Reactions'

18.09.98 Organic Reaction Mechanisms Group Conference, Zeneca, Huddersfield
Poster presented entitled 'Mechanism of Amine / Formaldehyde / Nucleophile Reactions'

21.12.98 Graduate Poster Competition, University of Durham
Sponsored by ICI
Poster presented entitled 'Condensation Reactions of Formaldehyde and Amines with addition of Sulfite'

23.06.99 University of Durham Graduate Symposium, University of Durham
Oral presentation entitled 'Reaction of Formaldehyde with Amines in the presence of Sulfite'

22.08.99 to 27.08.99 7th European Symposium on Organic Reactivity (ESOR), Ulm, Germany
Poster presented entitled 'Condensation Reactions of Formaldehyde and Amines with and without the presence of Sulfite'

17.09.99 Organic Reaction Mechanisms Group Conference, Roche Discovery, Welwyn Garden City
Poster presented entitled 'Condensation Reactions of Formaldehyde and Amines with and without the presence of Sulfite'